LEABHARLANN CHOLÁISTE NA TRÍONÓIDE, BAILE ÁTHA CLIATH | TRINITY COLLEGE LIBRARY DUBLIN
Ollscoil Átha Cliath | The University of Dublin

Terms and Conditions of Use of Digitised Theses from Trinity College Library Dublin

Copyright statement

All material supplied by Trinity College Library is protected by copyright (under the Copyright and Related Rights Act, 2000 as amended) and other relevant Intellectual Property Rights. By accessing and using a Digitised Thesis from Trinity College Library you acknowledge that all Intellectual Property Rights in any Works supplied are the sole and exclusive property of the copyright and/or other IPR holder. Specific copyright holders may not be explicitly identified. Use of materials from other sources within a thesis should not be construed as a claim over them.

A non-exclusive, non-transferable licence is hereby granted to those using or reproducing, in whole or in part, the material for valid purposes, providing the copyright owners are acknowledged using the normal conventions. Where specific permission to use material is required, this is identified and such permission must be sought from the copyright holder or agency cited.

Liability statement

By using a Digitised Thesis, I accept that Trinity College Dublin bears no legal responsibility for the accuracy, legality or comprehensiveness of materials contained within the thesis, and that Trinity College Dublin accepts no liability for indirect, consequential, or incidental, damages or losses arising from use of the thesis for whatever reason. Information located in a thesis may be subject to specific use constraints, details of which may not be explicitly described. It is the responsibility of potential and actual users to be aware of such constraints and to abide by them. By making use of material from a digitised thesis, you accept these copyright and disclaimer provisions. Where it is brought to the attention of Trinity College Library that there may be a breach of copyright or other restraint, it is the policy to withdraw or take down access to a thesis while the issue is being resolved.

Access Agreement

By using a Digitised Thesis from Trinity College Library you are bound by the following Terms & Conditions. Please read them carefully.

I have read and I understand the following statement: All material supplied via a Digitised Thesis from Trinity College Library is protected by copyright and other intellectual property rights, and duplication or sale of all or part of any of a thesis is not permitted, except that material may be duplicated by you for your research use or for educational purposes in electronic or print form providing the copyright owners are acknowledged using the normal conventions. You must obtain permission for any other use. Electronic or print copies may not be offered, whether for sale or otherwise to anyone. This copy has been supplied on the understanding that it is copyright material and that no quotation from the thesis may be published without proper acknowledgement.

Investigations of mechanisms of drug-resistance and associated biomarkers in HER2-overexpressing breast cancer

A thesis submitted to the University of Dublin, Trinity College

towards a degree of Doctor of Philosophy

by

Susan Breslin MSc.

Based on research carried out under the supervision of

Assoc. Prof. Lorraine O'Driscoll

School of Pharmacy & Pharmaceutical Sciences,

Trinity Biomedical Sciences Institute,

Trinity College Dublin

September 2015

TRINITY COLLEGE DUBLIN
11 MAY 2016
ACADEMIC REGISTRY

PhD
Pharmacy & Pharmaceutical Sciences

50691051
50691051

THESIS
11215

Declaration

I declare that this thesis has not been submitted as an exercise for a degree at this or any other university and it is entirely my own work. For research that has been carried out jointly or includes the published or unpublished work of others is duly acknowledged within the text of my work. I agree that the Trinity College Library may lend or copy this thesis upon request.

Signed:

TRINITY LIBRARY
0 8 MAR 2017
DUBLIN

Thesis 11215

Acknowledgements

I would like to say a huge and sincere thank you to Lorraine for giving me the opportunity to take on this research project and for your guidance, support and encouragement throughout, for which I am very grateful.

I would also like to thank all the members of the LOD research group past and present. I would like to say thanks Sweta, Claire and Keith for showing me the ropes when I first started. Big thanks to Sadhbh, Melissa, Martina, Vanesa and Michelle for your help in the lab, all the help with proof-reading and being a great group to work with. Also, I would like to thank all the other post-graduate students, both past and present, for having made the last few years both enjoyable and memorable.

To all my friends who always had kind words of support over the past few years while I was being a lab hermit, a massive thank you.

Special thanks to Gary for all the support while doing this project and for the copious amounts of chocolate when I needed it most!

Finally, to Mum, Dad and Seona, thank you for your support and encouragement over the past few years. I couldn't have done it without you!

1. Table of Contents

Figures x

Tables xiii

Summary 1

Abbreviations 2

Chapter 1: Introduction 4

1.1 Cancer 5

1.1.1 Hallmarks of cancer 5

1.1.2 Breast cancer 10

1.2 Disease management and current therapies for breast cancer 11

1.2.1 Surgery 12

1.2.2 Radiation therapy 12

1.2.3 Hormone therapy 13

1.2.4 Drug therapy 13

1.3 Drug-resistance 20

1.3.1 Increased drug efflux 20

1.3.2 Altered drug metabolism 21

1.3.3 Altered drug targets 21

1.3.4 Increased DNA repair 22

1.3.5 Evasion of apoptosis 23

1.3.6 Activation of pro-survival pathways 25

1.3.7 Tumour microenvironment, heterogeneity and stem cells 27

1.4 Extracellular Vesicles 30

1.4.1 EV formation 30

1.4.2 EV composition 31

1.4.3 EV function 33

1.4.4 EVs as biomarkers in cancer 35

1.5 Three-dimensional cell culture and drug discovery 37

1.5.1 Trends in drug discovery 37

1.5.2 Cell culture 38

1.5.3 3D cell culture methods 41

1.5.4 Supporting evidence for the importance of including 3D cultures in drug development 44

1.6 Project aims 48

Chapter 2: Acquired neratinib-resistance induces cross-resistance to HER-targeting drugs and increased cell aggression in HER2-overexpressing breast cancer cells 49

2. Abstract 50

2.1 Introduction 51
2.2 Materials and methods 53
2.2.1 Cell culture 53
2.2.2 Toxicity assays 53
2.2.3 Proliferation assays 54
2.2.4 Migration assays 55
2.2.5 Invasion assays 55
2.2.6 *Anoikis* assays 56
2.2.7 Immunoblots 56
2.2.8 qPCR miR-210 57
2.2.9 Quantification of cellular ATP 58
2.2.10 Flow cytometry analysis of cells with stem cell-like properties 59
2.2.11 NmU 59
2.2.12 Cytochrome p450 assay 59
2.2.13 Statistical analysis 60
2.3 Results 61
2.3.1 Establishment of HCC1954-NR and EFM192A-NR variants 61
2.3.2 Cross-resistance to other anti-cancer drugs due to neratinib-resistance 62
2.3.3 Cross-resistance to neratinib due to LR and TR 62
2.3.3 Reduced cell proliferation due to neratinib-resistance 63
2.3.4 Increased cell migration in neratinib-resistant cells 64
2.3.5 Increased cell invasion in neratinib-resistant cells 65
2.3.6 Neratinib-resistant cells demonstrate an increased resistance to anchorage-independent cell death i.e. *anoikis* 66
2.3.7 Effects of neratinib-resistance on drug targets and PGP 67
2.3.8. Neratinib-resistance does not significantly alter miR-210 expression 69
2.3.9. Neratinib-resistance is not induced by altered levels of ATP 70
2.3.10. Neratinib-resistance increases a stem cell-like sub-population in HCC1954-NR cells, but not EFM192A-NR cells 71
2.3.11. NmU mediates neratinib-resistance 72

2.3.12. CYP3A4 mediates neratinib-resistance 73
2.4 Discussion 75
2.4.1 Neratinib-resistance is associated with cross-resistance to other HER2-targeting agents 75
2.4.2 Neratinib-resistance induces increased cell aggression 76
2.4.3. Mechanism of neratinib-resistance 77
2.5 Conclusion 80
Chapter 3: The relevance of extracellular vesicles as diagnostic and predictive biomarkers in HER2-overexpressing breast cancer patients 81
3. Abstract 82
3.1 Introduction 84
3.1.1 Personalised medicine 84
3.1.2 Liquid biopsy and EVs 87
3.1.3. Aims 88
3.2 Materials and methods 89
3.2.1 Clinical trial design 89
3.2.2 EV isolation 91
3.2.3 Immunoblots 92
3.2.4 Transmission Electron Microscopy of EVs 93
3.2.5 Nanoparticle tracking analysis (NTA) 93
3.2.6 ELISAs 94
3.2.7 Total RNA isolation and quantification 94
3.2.8 Preparation of cDNA for NmU analysis by qPCR 95
3.2.9 Preparation of cDNA for miR-210 analysis by qPCR 95
3.2.10 qPCR: NmU and miR-210 96
3.2.11 Statistical analysis 96
3.3 Results 97
3.3.1 Patient outcome from clinical trial 97
3.3.2 Successful isolation of EVs from serum specimens 98
3.3.3 Quantification of EVs 99
3.3.4. EV HER2 and serum HER2 104
3.3.5 EV NmU and serum NmU 109
3.3.6 Survivin 119
3.3.7 miR-210 124

3.4 Discussion 126
3.4.1 ICORG trial 10-05 126
3.4.2. Successful EV isolation 127
3.4.3. EV Quantities 128
3.4.4. EV HER2 and serum soluble HER2 129
3.4.5. EV NmU and serum NmU 131
3.4.6. Survivin 132
3.4.7. miR-210 132
3.5 Conclusion 133

Chapter 4: Innate levels of drug resistance differs between cells grown as monolayers compared to 3D cell cultures 134

4. Abstract 135

4.1 Introduction 136
4.2 Methods 138
4.2.1 2D and 3D cell culture 138
4.2.2 Optical microscopy 138
4.2.3 Scanning electron microscopy (SEM) imaging 138
4.2.4 Immunoblotting 139
4.2.5 2D and 3D cell viability 140
4.2.6 2D and 3D cell response to drug treatment 140
4.2.7 EV isolation 141
4.2.8 CYP3A4 activity in 2D and 3D cells and their EVs 141
4.2.9. Statistical analysis 142
4.3 Results 143
4.3.1 Different morphology of cells grown in 2D versus 3D 143
4.3.2 Cell survival pathways in 2D and 3D cell culture 145
4.3.3. HER-family drug target expression in 2D and 3D cell culture 146
4.3.4. Drug efflux pump expression in cells grown using 2D and 3D culture methods 148
4.3.5 Altered cell viability in 2D and 3D cell culture 149
4.3.6 Altered drug toxicity in 2D and 3D cell culture 150
4.3.7 Isolation of EVs from 2D and 3D cells 153
4.3.8 CYP3A4 activity 156
4.4 Discussion 160

4.4.1 Altered morphology of cells grown in 2D and 3D cultures 160
4.4.2 Growing cells in 3D as opposed to 2D can alter protein expression 160
4.4.3 Cells grown in 3D have reduced viability compare to 2D cultures 162
4.4.4 Drugs have reduced efficacy in 3D cells compared to 2D cells 163
4.4.5 Growing cells in 3D alters secretion of EVs 164
4.4.6 3D cell cultures have higher CYP3A4 activity than 2D cells 164
4.4.7 Consistency of trends observed 165
4.5 Conclusion 166
Chapter 5: Discussion, conclusion and future work 167
5.1 Discussion 168
5.2 Conclusion 171
5.3 Future work 172
5.3.1 Is CYP3A4 activity functionally involved in acquired neratinib-resistance? 172
5.3.2 Does the increase in CYP3A4 activity in NR cells increase the rate of neratinib metabolism in these cells? 172
5.3.3 Does FGFR play a role in neratinib-resistance? 172
5.3.4 Are the trends associated with neratinib-resistance observed here also seen in patients? 173
5.3.5 Do the trends for the association of EV quantity with cancer and patient response to therapy observed here validate when tested over a larger patient cohort? 173
5.3.6 Is NmU expression in HER2-overexpressing tumours indicative of patient response to therapy? 173
5.3.7 Longer term follow up of trends observed for EV quantities in relation to patient response 173
5.3.8 Complete characterisation of EVs isolated from 2D and 3D cultured cells 174
5.3.9 Expand 2D and 3D culture comparisons to include parent versus resistant cell comparisons 174
Chapter 6: References 175
Appendix I: 188
Appendix II 190

Appendix III.....191

Appendix IV: 192

Appendix V.....195

Figures

Figure 1.1: Mechanism of action of targeted therapies for HER2 breast cancer 19
Figure 1.2. Mechanisms of drug-resistance 23
Figure 1.3. Intrinsic and extrinsic pathways of apoptosis 25
Figure 1.4. Pro-survival pathways involved in drug-resistance 27
Figure 1.5. The heterogeneity of tumours can cause drug-resistance 29
Figure 1.6. The biogenesis of exosomes and microvesicles 31
Figure 1.7. The drug development process 38
Figure 1.8. Methods for 3D cell spheroid production 44
Figure 2.1. Proliferation assays of NR compared to Par cells 63
Figure 2.2 Migration and wound healing assays of NR compared to Par cells 64
Figure 2.3. Invasion assays of NR compared to Par cells 65
Figure 2.4. *Anoikis* assays of NR compared to Par cells 66
Figure 2.5. Effects of NR on EGFR family members and drug transporter expression 68
Figure 2.6. Expression of miR-210 in NR and Par cells 69
Figure 2.7. ATP levels in NR compared to Par cells 70
Figure 2.8. Stem-cell like populations in NR compared to Par cells 71
Figure 2.9. NmU expression in NR compared to Par cells 72
Figure 2.10. CYP3A4 activity in NR compared to Par cells 73
Figure 3.1. Diagnostic, prognostic and predictive biomarkers are essential for personalised medicine 85
Figure 3.2. Schematic illustration of ultracentrifugation technique used to isolate EVs from serum specimens 91
Figure 3.3. Patients' outcome from clinical trial 97
Figure 3.4. Characterisation of EVs isolated from serum 98
Figure 3.5. EV quantities of normal control and cancer patients 100
Figure 3.6. EV quantities for patients grouped for response to treatment 101
Figure 3.7. Pre- and post-treatment EV quantities for patients grouped based on their response to therapy 102
Figure 3.8. EV quantities shows trend for predicting response to treatment. 103
Figure 3.9. EV HER2 content 104
Figure 3.10. Serum soluble HER2 concentration pre, during and post-treatment 105

Figure 3.11. Serum soluble HER2 concentration in response to treatment 106
Figure 3.12. Serum soluble HER2 for patients grouped for response, pre- and post-treatment 107
Figure 3.13. EV HER2 compared to serum soluble HER2 108
Figure 3.14. EV NmU concentration during treatment 110
Figure 3.15. EV NmU concentration for patients in response to treatment 111
Figure 3.16. EV NmU concentration in patients grouped for response, pre- and post-treatment 112
Figure 3.17. EV NmU mRNA pre-and post-treatment 113
Figure 3.18. EV NmU mRNA grouped for response 114
Figure 3.19. EV NmU concentration showed a trend for predicting response to treatment 114
Figure 3.20. Serum NmU concentration during treatment 115
Figure 3.21. Serum NmU at pre- and post-treatment with patients grouped for response 116
Figure 3.22. Serum NmU concentrations for patients grouped for CR, PR and NR 117
Figure 3.23. EV NmU compared to serum NmU concentrations pre-treatment. 118
Figure 3.24. EV survivin concentrations during treatment 120
Figure 3.25. EV survivin concentrations for patients grouped for response pre- and post-treatment 121
Figure 3.26. EV survivin concentrations for patients grouped for response 122
Figure 3.27. EV survivin concentrations show a trend for predicting response to treatment 123
Figure 3.28. EV miR-210 CT values for patients grouped for complete response, partial response and NR 124
Figure 3.29. Fold change in EV miR-210 as measured by qPCR for patients grouped for complete response, partial response and NR 124
Figure 4.1. Phase contrast images of 2D (i) and 3D (ii) cell cultures 143
Figure 4.2. SEM images of HCC1954 cells grown in 2D and 3D cultures 144
Figure 4.3. Immunoblots of 2D and 3D pAkt, Akt, pErk and Erk expression 145
Figure 4.4. Expression of EGFR family receptors in cells grown in 3D compared to 2D cells 147
Figure 4.5. Expression of drug transporters in 3D compared to 2D cells 148
Figure 4.6. Viability of cells grown in 3D compared to 2D cultures 149
Figure 4.7. Efficacy of neratinib in 3D compared to 2D cells 150

Figure 4.8. Efficacy of trastuzumab in 3D compared to 2D cells 151
Figure 4.9. Efficacy of docetaxel in 3D compared to 2D cells 152
Figure 4.10. Characterisation of EVs isolated from 2D and 3D cells 153
Figure 4.11. EV quantities released from 3D compared to 2D cells 155
Figure 4.12. CYP3A4 activity in 3D compared to 2D cells 156
Figure 4.13. EV CYP3A4 activity from EVs released from 2D and 3D cells 158

Tables

Table 1.1. Pro- and anti-apoptotic factors 8

Table 1.2. Pro- and anti-angiogenic factors 10

Table 1.3. Proposed advantages and disadvantages of different 3D cell culture methods 40

Table 2.1. Preparation of sodium acetate buffer. 54

Table 2.2. Preparation of master mix for miR-210 cDNA synthesis 57

Table 2.3. Incubation times and temperatures used to prepare miR-210 cDNA 58

Table 2.4. Preparation of master mix for qPCR 58

Table 2.5. Incubation times and temperatures used to perform qPCR 58

Table 2.6. IC_{50} and fold difference values for HCC1954 and EFM192A parent and resistant cells 61

Table 2.7. Average IC_{50} values for neratinib in HCC1954-Par and -LR, SKBR3-Par, -LR and -TR cells with corresponding fold difference values 62

Table 2.8. Summary of characteristics of neratinib-resistant cells compared to their parents control cells for both HCC1954 and EFM192A cells 74

Table 3.1. Patients enrolled into ICORG clinical trial 10-05 90

Table 3.2. Ages of patients and healthy control specimens 90

Table 3.3. Reagents for master mix for NmU cDNA synthesis 95

Table 3.4. Preparation of master mix for miR-210 cDNA synthesis 95

Table 3.5. Incubation times and temperatures used to prepare miR-210 cDNA 95

Table 3.6. Preparation of master mix for qPCR 96

Table 3.7 Incubation times and temperatures used to perform qPCR 96

Table 3.8. Summary of the relevance of EVs as biomarkers for HER2-overexpressing breast cancer detection and prediction of response to therapy 125

Table 3.9 Different categories of proteins and their expected presence in EV isolates, including some examples (non-exclusive) 127

Table 4.1. Summary of the characterisation of BT474 3D, HCC1954 3D and EFM192A 3D cells compared to their 2D counterparts 159

Summary

Breast cancer is the most commonly diagnosed cancer amongst women in Ireland. HER2-overexpressing breast cancer accounts for 25-30% of all breast cancer cases and was the focus of this project. While treatment options for breast cancer are continuously improving, the main issue with effective patient therapy is the development of drug-resistance. Consequently, it is critical that the mechanisms that mediate resistance are understood. This was a major focus of this work. Additionally, identifying biomarkers that will successfully diagnose and predict patient response to therapy are also essential to improve disease management, an issue which was also addressed in this project.

Novel neratinib-resistant HER2-overexpressing breast cancer cell lines were developed as a model of drug-resistance. The mechanism of this acquired-resistance to neratinib appeared to be mediated, in part, by an increase in NmU expression and CYP3A4 activity. These cells demonstrated strong cross-resistance to other HER-targeting agents and increased cell aggression in terms of increased migration, invasion and resistance to *anoikis*. Studies on EVs secreted from breast cancer patients and healthy controls revealed that EV quantities may be used to diagnose breast cancer, as EV quantities from patients were found to be significantly higher than the quantities of healthy controls. EV NmU and survivin were found not to be predictive of patient response to therapy, while lower levels of serum HER2 prior to treatment appears to be predictive of complete response to therapy. Patient specimen numbers were limited for this work and so findings require validation. Finally, we investigated differences between 2D and 3D cultures and found that cells grown using these methods differ substantially. Specifically, we found that cells grown in 3D appear to have a higher innate resistance to the effects of drugs. This increased innate drug-resistance appears to be mediated, at least in part, by altered expression of proteins involved in cell growth and survival, drug transporters and drug targets and also increased CYP3A4 activity.

In conclusion, the research presented here revealed that acquired neratinib-resistance is associated with resistance to other HER-targeting agents, an increase in cell aggression and is mediated, at least in part, through increased NmU expression and CYP3A4 activity. EV quantities isolated from breast cancer patient serum specimens may be useful as a diagnostic tool to detect the disease. The basic biological information represented by cells grown in 2D and 3D is substantially different and it appears that the innate resistance of cells to drug treatment may be higher than that which is represented in 2D cell culture models.

Abbreviations

5-FU	5-fluorouracil
ABC	ATP Binding Cassette
ABCB1	ATP-Binding cassette, subfamily B, member 1
ABCG2	ATP-BINDING cassette, subfamily C, member 2
ADCC	Antibody-dependent cell-mediated cytotoxicity
AFM	Atomic force microscope
Akt	Protein Kinase B
ALT	Alanine aminotransferase
APAF1	Apoptotic Peptidase Activating Factor 1
APC	Allophycocyanin
ATP	Adenosine triphosphate
BCRP	Breast cancer resistance protein
BRCA1	Breast Cancer 1, early onset
BSA	Bovine serum albumin
CD24	Cluster of differentiation 24
CD44	Cluster of differentiation 44
cDNA	Complementary cDNA
CR	Complete response
CT	Cycle threshold
CYP1A1	Cytochrome P450 enzyme, Family 1, member A1
CYP1A2	Cytochrome P450 enzyme, Family 1, member A2
CYP3A4	Cytochrome P450 enzyme, Family 3, member A4
DNA	Deoxyribonucleic acid
dNTP	Deoxynucleotide triphosphate
DR 4	Death receptor 4
DR5	Death receptor 5
E2F	E2F transcription factor
ECM	Extracellular matrix
EGFR	Epidermal growth factor receptor
EGFRvIII	Epidermal growth factor receptor variant III
ELISA	Enzyme linked immunosorbent assay
ER	Estrogen receptor
ESCRT	Endosomal sorting complexes required for transport
EVs	Extracellular vesicles
FACS	Fluorescence-activated cell sorting
FADD	FAS cell surface death receptor
FAS	Fas-associated protein with Death Domain
FBS	Fetal bovine serum
FGFR	Fibroblast growth factor receptor
FITC	Fluorescein isothiocyanate
GnRH	Gonadotropin-releasing hormone
HER2	Human epidermal growth factor receptor 2
HER3	Human epidermal growth factor receptor 3
HER4	Human epidermal growth factor receptor 4
IC50	Half maximal inhibitory concentration
ICORG	All -Ireland Cooperative Oncology Research Group
IL1β	Interleukin 1β
IL32	Interleukin 32

IL-8	Interleukin 8
IPA	Isopropyl acetal
kDa	Kilo Dalton
LLC	Lewis lung carcinoma
LR	Lapatinib-resistant
miRNA	MicroRNA
MMPs	Matrix metalloproteinases
mRNA	Messenger RNA
MUC4	Mucin 4
MVB	Multivesicular body
NmU	Neuromedin U
NR	Neratinib-resistant
NR	No response
NTA	Nanoparticle tracking analysis
Par	Parent
PARP	Poly (ADP-ribose) polymerase
PBS	Phosphate buffered saline
PCA3	Prostate cancer antigen 3
pCR	Pathological complete response
PDK1	Phosphoinositide-dependent protein kinase-1
PGP	P-glycoprotein
PI3K	Phosphatidylinositol 3-kinase
Poly-HEMA	Poly(2-hydroxyethyl methacrylate)
PR	Partial response
PR	Progesterone
PTEN	Phosphatase and tensin homolog
PVDF	Polyvinylidene difluoride
qPCR	Quantitative polymerase chain reaction
Rb	Retinoblastoma protein
RNA	Ribonucleic acid
RPMI	Roswell Park Memorial Institute medium
RT	Reverse transcription
SDS-PAGE	Sodium dodecyl sulfate polyacrylamide gel electrophoresis
SMAC	Second Mitochondria-derived Activator of Caspases
snRNA	Small nuclear RNA
TCH	Docetaxel, carboplatin and trastuzumab
TCHL	Docetaxel, carboplatin, trastuzumab and lapatinib
TCL	Docetaxel, carboplatin and lapatinib
T-DM1	Trastuzumab emtansine
TEM	Transmission electron microscopy
TMPRSS2	Transmembrane protease, serine 2
TNFAIP1	Tumor necrosis factor alpha-induced protein 1
TNFAIP3	Tumor necrosis factor alpha-induced protein 3
TNFR1	Tumor necrosis factor receptor 1
TNFα	Tumor necrosis factor alpha
TR	Trastuzumab-resistant
TRAIL-R1	TNF-related apoptosis-inducing ligand-receptor 1
TRAIL-R2	TNF-related apoptosis-inducing ligand-receptor 1
VEGF	Vascular endothelial growth factor

Chapter 1: Introduction

1.1 Cancer

1.1.1 Hallmarks of cancer

Each normal cell in the body has a function and a life span, and form tissues by growing, dividing and undergoing apoptosis, as appropriate. The cell cycle process involves an intricate balance of signals between those that support cell replication and those that suppress it. An array of cell membrane receptors, extracellular matrix molecules, cell adhesion molecules and other soluble growth factors, all have roles in the control of cell division; a process that is strictly regulated in order to maintain normal tissue homeostasis. However, in cancer this balance is not maintained as cells mutate and no longer effectively respond to the control signals that typically sustain usual growth. Through numerous mutations, cancer cells accumulate certain traits that enable them to grow independently and uncontrollably, to avoid cell death, maintain cancerous masses supported by angiogenesis and invade into other tissue sites during metastasis. These traits, named the 'Hallmarks of Cancer', by Hanahan and Weinberg are the deviations that make cancer cells so different and aggressive compared to normally controlled cells [1] and will be discussed below.

1.1.1.1 Independent cell growth

Normal cells require stimulation from their environment in order to facilitate cell growth. Conversely, cancer cells acquire the ability to kick-start the cell cycle without the aid of external growth cues, by becoming self-sufficient in terms of cell growth factors [1]. This is executed by a number of processes, all of which aim to enable proliferation without the help of normal signalling. For example, cancer cells can reduce their reliance on paracrine and endocrine signalling as they can induce autologous production of growth factors to facilitate their growth. Typically, the growth factors released are ligands of functional mitogenic receptors that are expressed by the cell. This means that these cancer cells can stimulate mitosis by producing growth factors that will activate the relevant mitogenic receptors that are also self-expressed, resulting in activation of the receptors and initiation of the mitotic process. Cuttitta *et al.* 1985, demonstrate this cancer cell self-sufficiency in growth factors where bombesin is produced by human small-cell lung cancer cell lines NCI-N592 and NCI-N417 and that it can stimulate growth in these cells [2]. They found that the addition of 2A11, an anti-bombesin antibody, prevented cell growth by 100% and 99%, respectively, in NCI-N592 and NCI-N417 cells. This indicates that these cells rely on bombesin, which they

can produce, for proliferation and survival, thus further indicating that bombesin can act as an autocrine growth factor in human small-cell lung cancer.

In addition to an increase in levels of growth factors, cancer cell proliferation can be enhanced by an increase in expression of growth factor receptors. This overexpression of receptors can lead to excessive receptor activation and response. For example, EGFR levels were found to be 10.6 ± 4.5 fold higher in pancreatic cancer patient tumours compared to normal pancreatic tissue, implicating overexpression of EGFR in tumour cells in the pathogenesis of this cancer [3].

Furthermore, growth signalling pathways can be activated when receptor activation occurs independently of their ligands. For example, androgen-independent activation of the androgen receptor is commonly associated with prostate cancer relapse following androgen-depravation therapy. Lyons *et al.* found that in these cases, Vav3, another growth factor, is simultaneously activated and increased in prostate cancer [4]. This active Vav3 causes androgen-independent transcription of the androgen receptor *via* Rac1 signalling, resulting progression of androgen-independent prostate cancer.

1.1.1.2 Insensitive to suppressive growth signals

Normal cells respond to inhibitory growth signals, which synchronise with growth stimulatory signals to maintain tissue homeostasis. Conversely, tumours thrive due to the acquired the ability of cancer cells to avoid these anti-proliferative signals, thus leading to uncontrolled proliferation. This can be facilitated by the inhibition of tumour suppressor genes. The cell cycle is tightly regulated and won't allow cell progression to the next phase of replication until the present phase is perfectly completed. Cancer cells with mutated or malfunctioning tumour suppressor genes may not stop the replication process at these checkpoints, which can lead to unregulated cell growth and tumour formation [1].

Retinoblastoma protein (Rb) is a tumour suppressor gene that is involved in cell cycle regulation. Rb binds to and controls the release of E2F transcription factors that allow the progression of a cell from G1 to S phase in the cell cycle. Cancer cells can disrupt this pathway and enable release of the E2F transcription factors required for proliferation, independently of Rb regulation. Mutation of Rb can also result in uncontrolled cell growth as in its mutated form, Rb cannot bind and control release E2F, resulting in uncontrolled cell division.

p53 is another cell cycle regulating tumour suppressor gene. Presence of wild-type p53 in normal cells regulates the cell cycle by checking for DNA damage before a

progression from G1 to S phase during mitosis [5]. If p53 detects DNA damage it will stall cell division and activate DNA repair. As a result, only healthy cells with complete and undamaged DNA will continue to proliferate. In cancer cells, however, p53 is often found mutated causing loss of function; and it is estimated that approximately 50% of human cancers have mutated p53 [6].

1.1.1.3 Evasion of apoptosis

Apoptosis is a form of programmed cell death that is characterised by either intrinsic or extrinsic activation of apoptosis of a cell, followed by the release of DNAse and subsequent breakdown of DNA. The nucleus and cytoplasm condense and the cell breaks up into membrane-bound fragments. Finally, these cell fragments are phagocytosed and degraded in the lysosome of phagocytes (e.g., macrophages) [7, 8]. Apoptosis enables the body to rid itself of unhealthy or unnecessary cells during embryonic development or following cellular stress; and is one of the mechanisms that helps maintain tissue homeostasis. However, in cancer it is manipulated and reduced in order to allow a tumour to flourish [1]. Cancer cells can alter levels of apoptosis using several mechanisms: the balance between pro- and anti-apoptotic proteins can be disrupted; caspase function can be impaired and death receptor signalling can be reduced.

A balanced ratio of pro- and anti-apoptotic proteins is essential for maintaining appropriate levels of apoptosis, see Table 1.1. However, in cancer this ratio is skewed and the ratio slips in favour of less apoptosis. For example, anti-apoptotic protein Mcl-1 has been found to be overexpressed in patients suffering from multiple myeloma in comparison to levels in healthy control bone marrow [9]. The increase in Mcl-1 expression also correlated with shorter survival and relapse of disease. Whereas levels of pro-apoptotic Bax have been found to be decreased in breast cancer tumours in comparison to healthy breast tissue, where this decrease in Bax was associated with shorter overall survival and a failure to respond to therapy [10]. Caspases are integral to initiating and executing apoptosis and reduced caspase activity has been associated with carcinogenesis. Shen *et al.* found caspase-9 levels were significantly decreased in tumours of patients with stage II colorectal cancer when compared with levels in healthy control colon specimens [11]. They also found that this downregulation of caspase-9 correlated with worse overall survival. Death receptors activate the extrinsic pathway of apoptosis; examples include TNFR1, FAS, TRAIL-R1 and TRAIL-R2 [8]. Alterations in expression of these receptors and their ligands can facilitate a reduction in apoptosis

in cancer cells. A study of cervical carcinogenesis revealed that reduced expression of FAS and reduced function of TRAIL-R1 and TRAIL-R2, through mutations, lead to reduced apoptosis in cells and correlated with progression of cervical cancer [12].

Pro-apoptotic factors	Anti-apoptotic factors
Death receptors (activated by TRAIL)	Bcl2
FAS	Survivin
FADD/caspase 8 complex	Mcl-1
Caspases 3, 7 and 9	
BAK	
BAX	
Cytochrome c	
SMAC	
APAF1	

Table 1.1. Pro- and anti-apoptotic factors

1.1.1.4 Potential for indefinite cell growth

Normal cells have a finite capacity to divide that is controlled by a cellular process that allows a strict number of cell divisions before induction of cell death, thereby maintaining tissue homeostasis. Telomeres are positioned at the end of chromosomes and contain thousands of repeats of a 6kb base pair sequence which can be used as a 'counting device' for the numbers of cell cycles that have occurred. This is due to the fact that 50-100 base pairs are lost from the telomeres with each cell cycle. The progressive shortening of telomeres ultimately results in complete erosion of this protective string of base pairs and, eventually, once it is exhausted the ability to protect chromosomal DNA is lost. This results in the fusion of chromosomal ends and the eventual death of the affected cell [1].

It follows that telomeres play a role in cancer. In normal cells where the presence and progressive shortening of telomeres dictate the definite amount of cell cycles possible, in cancer cells (or immortalised cells) the telomeres are maintained. Two mechanisms can be employed to do this: the upregulation of telomerase and the alternative lengthening of telomeres (ALT) process [1]. Telomerase has the ability to lengthen telomeres, thus circumventing the issue telomere loss that occurs in normal cells. Kim *et al.* demonstrated this by discovering that 90% of 12 different tumour types tested were positive for telomerase activity, while no normal tissues tested positive for the enzyme [13]. Telomeres can be maintained in the absence of telomerase by the ALT process. Here, it has been proposed that telomerase-independent maintenance of telomeres occurs when the end of a telomeric strand of an ALT cell anneals to a

complimentary strand of another telomeric strand, using this as a template to synthesise new telomeric double stranded DNA from here [14]. ALT is characterised by the presence of circular extra-chromosomal telomeric DNA (e.g., C-circles) [15] and is detectible by measuring C-circle levels in the blood of cancer patients by rolling circle amplification [16].

1.1.1.5 Establishing and maintaining angiogenesis

Access to oxygen and nutrients is essential for cell growth, survival and the removal of waste products. To facilitate this, all cells in the human body must exist within 100-200μm of a blood vessel [17]. Angiogenesis is the process by which new blood vessels are formed and it is controlled in normal tissue by a balance of pro- and anti-angiogenic molecules, see Table 1.2. For a cancerous mass to flourish it, too, needs a vascular network to feed its cells; thus to enable this, cancer cells acquire the ability to establish and maintain angiogenesis.

Hypoxia is a key inducing factor of angiogenesis. Hypoxia (i.e., low oxygen levels) within the tumour is caused by the increasing distance between tumour cells and blood vessels due to cancer cell proliferation, an immune or inflammatory response, or mutation of genes involved in angiogenesis regulation [17]. Angiogenesis can be induced when cancer cells produce angiogenic activators, e.g., vascular endothelial growth factor (VEGF), angiogenin, transforming growth factors 1 and 2, and tumour necrosis factor α. For example, endothelial cells nearby a cancer cell producing VEGF can become activated and produce matrix metalloproteinases (MMPs), which breaks down the extracellular matrix between cells, thereby enabling endothelial cell migration. The endothelial cells divide and migrate through the surrounding tissue and organise themselves into hollow tubes. The new blood vessels mature and form a basement membrane and the resulting network of blood vessels provides the surrounding tumour tissue with adequate oxygen and nutrients for survival [18].

The necessity for sustained angiogenesis in tumour survival and the role VEGF plays in it was described by Kim *et al.*, where they injected nude mice with human A673 rhabdomyosarcoma, SKLMS-1 leiomyosarcoma or G55 glioblastoma cells and treated the mice with anti-VEGF monoclonal antibodies [19]. Treatment proved extremely successful, with up to 96% reduction in tumour burden, compared to control mice treated with a control antibody or PBS. This indicates that tumour rely on angiogenesis for progression and that this progression is mediated, in part, *via* VEGF.

Pro- angiogenesis factors	Anti-angiogenesis factors
VEGF	Anti-VEGF antibodies
Angiogenin	Thrombospondins
Transforming growth factor 1/2	Angiostatin
Tumour necrosis factor α	Endostatin

Table 1.2. Pro- and anti-angiogenic factors.

1.1.1.6 Capacity for invasion and metastasis

Metastasis is a unique capability acquired by cancer cells whereby cells can break away from a primary tumour and settle in another part of the body resulting in a secondary, metastatic tumour. Metastatic cancers tend to be more resistant to therapy and are the cause of 90% of cancer deaths [20]. The metastatic process comprises of a number of sequential steps. As a tumour grows it must attract a blood supply *via* angiogenesis to maintain its survival and so it induces the infiltration of blood vessels. Cancer cells also have the ability to detach from a primary tumour and invade through the basal membrane into the blood-stream through these infiltrating blood vessels. Once in the circulation it can travel anywhere in the body and can become trapped in capillary beds of distant organs and tissues. Here they can adhere to the blood vessel wall, extravasate into the surrounding tissue and proliferate, establishing a secondary metastatic tumour [21]. The nature of metastatic sites is not a random one and cells from primary tumours from certain organs are more likely to metastasise to specific distant organs. For example, breast cancers are most likely to form bone, liver, lung or brain metastases; lung adenocarcinomas are most likely to result in bone, liver, adrenal gland and brain metastases; and pancreatic cancers are likely to metastasis to the liver or lungs [22].

1.1.2 Breast cancer

1.1.2.1 Statistics

According to the National Cancer Registry Ireland (statistics correct as of March, 2015), the number of new cancer cases annually in Ireland is 20,063, with more males (10,751 cases) being diagnosed with the disease than females (9,312 cases). The number of deaths from cancer was 8,781 cases in 2012, where more males die from cancer (4,677 deaths) than females (4,104 deaths). Of these, there are 2,844 breast cancer cases each year, 2,816 female and 28 male, which accounts for 30.2% of all female cancers and just 0.3% of all male cancers; making breast cancer the second most commonly diagnosed cancer in Irish women. Survival rates are high and a trend of increasing percentage survival has been observed from 1994 (74.3%) to 2012 (84.7%). Breast

cancer incidence in Ireland tend to reflect those seen globally, as according to the World Health Organisation, breast cancer is the most common cancer affecting women worldwide. Survival rates in Ireland (84.7%) are similar to those observed on average in other developed countries (>80%); and are higher than survival rates in middle-income (~60%) and low-income (~40%) countries.

1.1.2.2 Breast cancer subtypes

Breast cancer is complex disease and displays heterogeneity in tumour histology, aggression, patient response to treatment and overall outcome between patients. As a consequence of the observed heterogeneity of breast cancer tumours, global gene expression analysis of samples has resulted in the stratification of breast cancers into five separate disease subtypes. These subtypes of breast cancer are clinically relevant and allow for more personalised and targeted therapy for patients. They are as follows: luminal A, luminal B, HER2-overexpressing, basal-like and normal-like [23].

The HER2-overexpressing breast cancer subgroup will be the main focus of this project. Patients with HER2-overexpressing breast cancer exhibit amplification and/or overexpression of the HER2 oncogene in their tumours. This overexpression is found in 25-30% of breast cancer cases. HER2 regulates cell growth and survival, this its overexpression facilitate tumour growth. In addition, the HER2-overexression is associated with aggressive disease and poor prognosis as patients with amplified HER2 tend to relapse sooner and have shorter overall survival than those who do not overexpress this oncogene [24].

1.2 Disease management and current therapies for breast cancer

Once cancer has been diagnosed, decisions regarding appropriate treatment strategies can begin. Therapeutic options include surgery, radiation therapy and drug therapy, where different combinations of these can be used together for more effective treatment, as appropriate. The use of combination drug-therapy typically involves co-administration of multiple drugs with different mechanisms of action with the aim of killing more cancer cells, while reducing the likelihood of the cancer becoming resistant to any one particular drug.

1.2.1 Surgery

Most patients diagnosed with breast cancer will undergo some form of surgery to remove the tumour and check lymph nodes for the presence of cancer cells. Patients can undergo a lumpectomy, where the tumour and some normal tissue from the surrounding areas are removed. If no cancer cells are found at the edge of the removed tissue, margins are said to be negative [25]. However, in the case where cancer cells are detected in the edges of these tissues (positive margins) [25], further surgery may be required to remove more tissue or in some cases where negative margins cannot be achieved, a full mastectomy may be necessary. In a full mastectomy, the entire breast tissue, possibly with some additional adjacent tissues and/or lymph nodes, are removed. In cases where a second cancer in the other breast is likely, e.g., patients with a BRCA mutation, a prophylactic double mastectomy may be performed [26].

Surgical removal of lymph nodes may be performed to check for the presence of cancer cells. The presence of cancer cells in the lymph nodes indicates a strong possibility for metastasis. Consequently, the examination of the nodes plays an integral role in staging of cancers. The stage of disease can be determined by taking into consideration the size of the primary tumour, the size and/or number of cancer cell containing lymph nodes [27], position of the tumour in the breast and whether or not metastasis has already occurred. Detection of cancer cells in the nodes also plays a role in the decision of whether further treatment is required following surgery. Therapy administered before surgery is termed neoadjuvant and typically aims to shrink tumours before surgery, while further treatment after surgery is known as adjuvant and aims to kill any cancer cells that may remain following surgery [28].

1.2.2 Radiation therapy

Radiation therapy uses a high-energy beam to induce cell death in a specific area by causing high levels of DNA damage. Radiation therapy can be delivered externally, by focussing beams on cancerous tissue, or can be delivered internally by inserting radioactive beads into a tumour site (brachytherapy), which are then removed after a certain amount of time, once a suitable dose of radiation has been delivered [29]. Radiotherapy is commonly used following surgery. While the main tumour bulk can be surgically removed, every cancerous cell may not have been removed in the process, leading to a risk of cancer reoccurrence; thus, radiotherapy often follows surgery in order to kill any cancer cells that may have been left behind. Houghton *et al.* found that

breast cancer patients who undergo radiotherapy as part of their disease management have up to 60% reduced risk of cancer reoccurrence [30].

1.2.3 Hormone therapy

Some breast cancer patients are diagnosed as estrogen receptor (ER) and/or progesterone receptor (PR) positive. In these cases, the respective hormones can drive tumour growth. It follows that inhibition of these hormones can form a part of therapy for these patients to stop or slow down the progression of hormone sensitive tumours. This can be done directly by inhibiting the ovaries *via* an oophorectomy [31] or the use of drugs that suppress ovarian function, for example gonadotrophin-releasing hormone (GnRH) agonists like Zoladex [32]. Alternatively, aromatase inhibitors (e.g. anastrozole, exemestane) can be used to prevent estrogen production [33] or selective estrogen receptor modulators (e.g. tamoxifen) may be used to block the effects of estrogen [34].

1.2.4 Drug therapy

1.2.4.1 Chemotherapy

Chemotherapy is an umbrella term that includes different drug families that aim to damage or kill rapidly growing cancer cells. Different drug families are segregated according to their mechanisms of action. While an exhaustive description of all chemotherapeutic agents is outside the scope of this work, some currently available chemotherapeutic drug types along with their mechanisms of action are described below.

Alkylating agents

Alkylating agents inflict DNA damage to cells by covalently transferring an alkyl, platinum or chloroethyl groups to cellular biomolecules, which results in changes in their structure [35]. This structural modification of DNA leads to disruption of function in fundamental cellular processes such as DNA replication and protein synthesis, which can lead to cell death. Monofuntional alkylating agents act at one DNA site and include dacarbazine and nimustine. Alkylating agents that act at two DNA sites can induce cytotoxicity through DNA-crosslinking [36]. Drugs that act at two separate sites are known as bifunctional and include chlorambucil, mitomycin C and thiotepa.

Antimetabolites

Cellular metabolism is extremely complex and involves numerous enzymes in the pathways that produce purines and pyrimidines, the building blocks of DNA and RNA. Anti-metabolite drugs interfere with normal cell metabolism. Purine and pyrimidine antimetabolite drugs are converted into nucleotide analogues by enzymes involved in metabolism. The metabolites produced inhibit enzymes essential for DNA synthesis, resulting in DNA damage and apoptosis [37]. Examples of these antimetabolites include 6-mercaptopurine, 5-fluorouracil and capacetabine. Folate-antagonists are another type of antimetabolite drug that act by inhibiting the central role that folates have in cell metabolism. Methotrexate is a folate-antagonist and acts by inhibiting dihydrofolate reductase, an enzyme essential for nucleotide production [38].

Anthracyclines

Anthracycline anti-cancer drugs include doxorubicin and daunorubicin. These drugs exert their cytostatic and cytotoxic effects through a number of proposed mechanisms. They interfere with DNA in a number of ways, through DNA intercalation thereby preventing macromolecule synthesis, free-radical production which damages DNA, DNA binding, alkylating and cross-linking, and through topoisomerase II inhibition, which leads to DNA damage and apoptosis [39]. While the anthracyclines have been shown to be effective as anti-cancer agents, their clinical usefulness has been hindered due to the development of cardiotoxicity associated with its use [40].

Vinca Alkaloids

Vinca alkaloid drugs are mitotic inhibitors and include vincristine, vinblastine, vindesine, vinepidine and vinrosidine. These drugs exert anti-proliferative effects by inhibiting mitotic spindle function during mitosis. This is done by interfering with addition and loss of tubulin during microtubule formation, thereby preventing appropriate spindle formation. This in turn results in loss of appropriate chromosome movement for successful cell mitosis, which is catastrophic for the cells and inhibits proliferation [41, 42].

Taxanes

The taxanes are also mitotic inhibitors and include docetaxel and paclitaxel. These drugs interfere with cell cycle progression by binding to the β-subunit of tubulin [43]. This results in the stabilisation of microtubules, rendering them non-functional for mitosis due to the fundamental need for reorganising of microtubules during cell division [44, 45]. In addition to inhibiting mitosis, paclitaxel can induce apoptosis by blocking the anti-apoptotic activity of Bcl-2 [46].

1.2.4.2 Anti-angiogenic drugs

Angiogenesis is the essential to the proliferation of primary tumours and their subsequent metastases [18]. As discussed in Section 1.1, the angiogenic process relies on the stimulation of vascular endothelial growth factor (VEGF) receptors expressed on vascular endothelial cells by pro-angiogenic VEGF ligands [47]. The most established drug that targets angiogenesis is bevacizumab, a humanised monoclonal antibody that targets and neutralises the VEGF-A ligand and thereby prevents VEGF receptor activation [48]. Angiogenesis can also be inhibited by small molecule tyrosine kinase inhibitors such as sunitinib, sorafinib and vatalanib; which exert their effects by inhibiting VEGF receptors [49-51].

1.2.4.3 Targeted therapy

While drugs from the above categories are effective in cancer treatment, their use in the clinic can be limited by their generic toxicity, in that the cytotoxic effects of most chemotherapeutic drugs is not cancer-specific and they can, and do, also kill normal cells. Continued efforts to improve cancer therapeutics have led to the development of 'targeted therapies' that act on molecular targets that are overexpressed by cancer cells in comparison to healthy normal cells and that have a critical role in the development and growth of tumours. This results in more specific treatment being delivered to the tumour, while also being less toxic to non-cancerous tissue [52].

HER2 is a member of the epidermal growth factor receptor (EGFR) family of receptors that comprise of EGFR/HER1, HER2, HER3 and HER4. Dimerisation (both hetero- and homodimerisation) of these receptors can be induced by ligand binding, receptor mutation and receptor overexpression, and results in receptor activation [53]. Activation of these tyrosine kinase receptors results in a signalling cascade that promotes cell growth and survival, thus their inhibition by targeted therapy prevents HER2-dependent tumour growth and survival. In addition to the full receptor, HER2 can exist in soluble forms including a truncated intracellular receptor of 95kDa and as herstatin, the product of an alternatively spliced HER2 transcript [54]. Some targeted therapies approved for the treatment of HER2-overexpressing breast cancer are described below and in Figure 1.2.

Monoclonal antibodies

Trastuzumab is a HER2-targeting humanised monoclonal antibody and was the first therapy approved for use in the treatment of HER2-overexpressing breast cancer.

Trastuzumab binds to the extracellular portion of the HER2 receptor and a number of mechanisms by which HER2 signal transduction is inhibited by trastuzumab have been suggested [53]:

i. Binding of trastuzumab to HER2 prevents receptor dimerisation, thereby preventing receptor activation
ii. Trastuzumab binding can prevent shedding of the extracellular portion of HER2 which, when occurs, leaves a p95-HER2 portion that retains tyrosine kinase activity
iii. Trastuzumab binding increases HER2 endocytosis and subsequent degradation
iv. The humanised Fc portion of trastuzumab may result in an immune response, termed antibody-dependent cell-mediated cytotoxicity (ADCC), resulting in tumour cell death

Pertuzumab is also a HER2-specific humanised monoclonal antibody. It binds to domain II of the HER2 receptor, which is specifically responsible for dimerisation of HER2 with the other receptors, thus it prevents receptor activation and downstream signalling [55, 56]. Furthermore, it has been found that pertuzumab is more effective than trastuzumab at blocking EGFR/HER2 and HER2/HER3 dimerisation. Due to the differences in mechanism of action of these two therapies, the potential synergism of co-administration of both drugs has been suggested. Nahta *et al.* found that co-administration of both trastuzumab and pertuzumab is more efficient at inhibiting HER2-overexpressing BT474 breast cancer cell growth *in vitro* than treatment with either drug on its own, indicating the potential benefits of this combination therapy [57]. Additionally, a phase II clinical trial investigating the efficacy of dual pertuzumab and trastuzumab treatment found that the combined treatment of both drugs is effective in treating patients who had previously experienced disease progression on trastuzumab monotherapy, indicating that the combined therapy can overcome trastuzumab resistance in the clinic [58].

Trastuzumab-DM1 (T-DM1; trastuzumab-emtansine) is an antibody-cytotoxic drug conjugate that uses the antibody-specific nature of trastuzumab to deliver a cytotoxic agent, DM1, to HER2-overexpressing cells [59]. Here, the HER2 receptor/T-DM1 conjugate is internalised and the DM1 portion is released into the cell [60]. DM1 is a maytansinoid, which are a group of anti-mitotic cytotoxic agents that exert their effects by binding to microtubules and, thereby, prevent mitosis. *In vitro* assays showed that T-DM1 is potent and selectively kills HER2-overexpressing cells (BT474, HCC1954 and KPL-4 cell lines) while not having an effect on normal cells (HMEC and NHEK cell lines). Other pre-clinical testing indicated that T-DM1 is effective in killing SKBR3

lapatinib-resistant cell lines that were also cross-resistant to trastuzumab [61]. Furthermore, *in vivo* experiments were performed where trastuzumab-resistant tumour tissue from Fo5 HER2 transgenic mice, were transplanted into the mammary fat pad of female nude mice. Results indicated that T-DM1 may be effective in trastuzumab-resistant tumours as mice treated with T-DM1 responded well where tumour volume did not increase for over 20 days, compared to an immediate increase in tumour volume in trastuzumab-treated mice [61]. T-DM1 is not being tested clinically. Welslau *et al.* [62] found that patients with advanced HER2-overexpressing breast cancer treated with T-DM1 had longer progression-free survival compared to those treated with lapatinib plus capecitabine, indicating T-DM1 has good clinical efficacy. Additionally, T-DM1 has shown efficacy in a phase III clinical trial where patients who have progressed on other HER2-targeted therapies respond to T-DM1; and where T-DM1 has been recommended as a new standard therapy for these patients [63].

Small molecule inhibitors

Lapatinib is a dual EGFR and HER2 tyrosine kinase inhibitor. More specifically, lapatinib is a reversible inhibitor of the ATP-binding sites of EGFR and HER2 tyrosine kinases, which prevents phosphorylation and thus activation of these receptors [64]. Suggested advantages of lapatinib over trastuzumab include the fact that lapatinib inhibits both EGFR and HER2, which may be more effective than trastuzumab which exerts effects on HER2 only. Additionally, lapatinib may be more effective on truncated receptors, as in these cases receptors have lost their extracellular domain that trastuzumab binds to, which can result in the antibody not recognising its receptor. Lastly, patients that develop resistance to trastuzumab may benefit from lapatinib treatment, due to their different mechanisms of action [65].

Afatinib is an irreversible EGFR, HER2 and HER4 tyrosine kinase inhibitor currently being investigated for efficacy in HER2-overexpressing breast cancer [66, 67]. Similarly to lapatinib, afatinib prevents receptor activation by blocking ATP-binding sites and thus blocking receptor phosphorylation. Rimawi *et al.* described results from a phase II trial in which afatinib, lapatinib and trastuzumab were each administered to drug-naïve patients as monotherapies for 6 weeks [68]. At the end of this course of treatment, patients treated with afatinib showed higher overall response rates than those treated with either lapatinib or trastuzumab, indicating potential use for afatinib in the clinic for HER2-overexpressing breast cancer.

Neratinib is also an irreversible EGFR, HER2 and HER4 small molecule inhibitor being investigated for efficacy HER2-overexpressing breast cancer [69, 70]. It prevents target receptor activation by covalently binding their ATP-binding sites, thereby preventing receptor phosphorylation [71]. In a phase II clinical trial investigating the clinical activity of neratinib, it was found that progression-free survival rates in drug naïve patients receiving neratinib monotherapy was 78%, where the median onset of progression was at 39.6 weeks [72]. Additionally, Awada *et al.* [73] observed anti-tumour activity in patients treated with neratinib and vinorelbine, where patient responses to dual therapy showed a higher progression free survival rate than with neratinib monotherapy. Puma technology, the developers of neratinib, have reported that a New Drug Application will be submitted for neratinib in early 2016 based on promising clinical trial results [74].

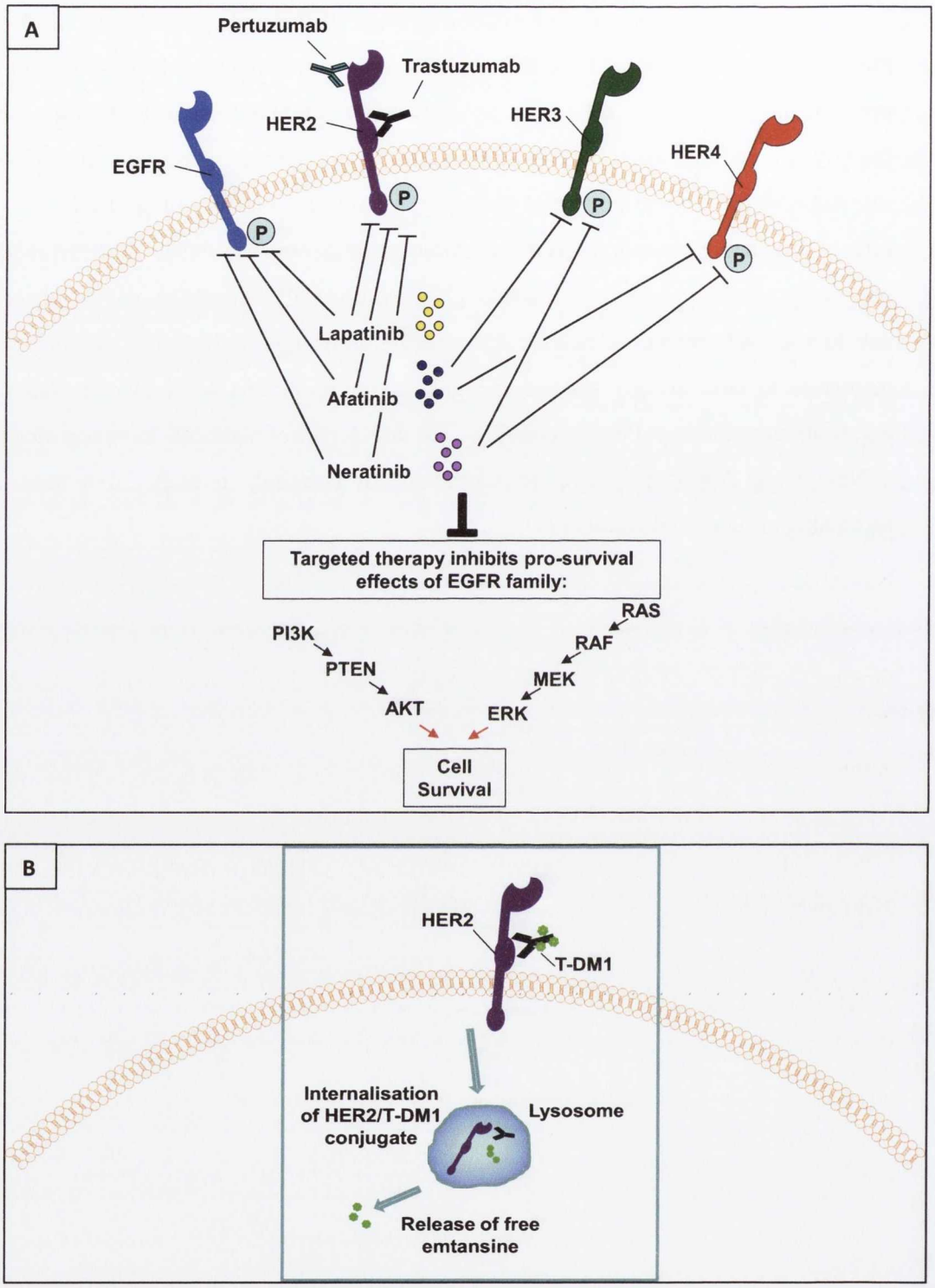

Figure 1.1. Mechanism of action of targeted therapies for HER2 breast cancer. A. Pertuzumab and trastuzumab target the extracellular portion of HER2. Lapatinib targets the intracellular tyrosine kinase portion of EGFR and HER2. Afatinib and neratinib target EGFR, HER2 and HER4 at their intracellular tyrosine kinase domains. B. T-DM1 uses the specificity of trastuzumab to target HER2-overexpressing cells; once receptor-T-DM1 conjugate is internalised, DM1 is released and executes anti-mitotic activity.

1.3 Drug-resistance

Despite the numerous therapies available for breast cancer treatment, drug-resistance is a major issue in the management of the disease and is one of the primary causes of failure for effective treatment in the clinic [75]. Drug-resistance can manifest in 2 ways; patients can be innately resistant to a treatment, meaning that they do not respond to their therapy from the beginning or they can initially respond to a treatment, but over time develop resistance to the effects of a drug and eventually their tumour begins to progress again. This second form of resistance is considered acquired drug-resistance and will be the focus of the drug-resistance section. Here, the resistance is not limited to the original drug administered and cross-resistance can develop, whereby a patient's acquired resistance to their primary therapy can also result in resistance to drugs to which they have not yet been exposed [76]. Cancer cells can elude the effects of drug therapy by a number of complex mechanisms, some of which are discussed below.

While drug-resistance remains as a prominent limitation to efficient cancer therapy, constant efforts are being made into elucidating the mechanisms that drive drug-resistance. The idea is to use this information to potentially target integral components of drug resistant pathways in order to circumvent the issue of drug-resistance and reinstate activity of cancer drugs that are often lost during patient therapy. Cancer cells can elude the effects of drug therapy by a number of complex mechanisms, some of which are discussed in Sections 1.3.1 – 1.3.7.

1.3.1 Increased drug efflux

Failure of anti-cancer therapy can arise due to an increase in efflux of drugs from the target cells, which results in sub-optimal levels of drug in the cell leading to a lack of drug efficacy. This can result from an increase in levels of drug efflux pumps in the cell. Examples include members of the ATP-binding cassette (ABC) transporter superfamily; P-glycoprotein (PGP) and breast cancer resistance protein (BCRP), which are coded by ABCB1 and ABCG2, respectively [76, 77]. The association of ABC transporter mediated drug-resistance in breast cancer has been observed in a number of studies. Mechetner *et al.* found that increased levels of PGP is associated with drug-resistance in breast cancer both *in vitro* and *in vivo* [78]. It was found that doxorubicin-resistant MCF-7 cells expressed more PGP than their drug-naïve wild-type control cells. Furthermore, elevated PGP levels were found to be associated with taxol resistance in breast cancer patients [78]. Additionally, BCRP overexpression has been associated

with resistance to methotrexate [79] and doxorubicin [80] in drug their respective drug-resistance MCF7 breast cancer cells.

1.3.2 Altered drug metabolism

In order to avoid the effects of anti-cancer therapy, cancer cells can increase levels of the enzymes that metabolise drugs so as to increase the speed in which the drug is metabolised and decrease the amount of time that the active drug is present in the cell and able to exert its effects. It has been shown that the genes for drug metabolising enzymes CYP1A1 and CYP1A2, from the drug metabolising cytochrome P450 family, were upregulated by 206 and 96 fold, respectively, in MCF7-doxorubicin resistant cells compared to their wild-type controls [81]. Similarly, CYP3A4, from the same drug metabolising enzyme family, was found to be associated with vinblastine resistance. While CYP3A4 has been shown to metabolise vinblastine in Chinese hamster ovary cells, an overexpression of CYP3A4 protein has also been associated with resistance to vinblastine, where Yao *et al.* observed that CYP3A4 overexpressing cells survived vinblastine treatment better than cells with lower CYP3A4 levels [82]. Other drug metabolising enzymes implicated in facilitating drug-resistance to anti-cancer drugs include glutathione S-transferases [83] and thymidine phosphorylase [84].

1.3.3 Altered drug targets

Response to targeted drug therapies can be hampered due to alterations in the target of interest. In these cases, drug-resistance develops as expression levels of a target can increase/decrease relative expression or the target in question can mutate, thus preventing a drug from recognising it and exert its effects on the intended cancer cells. For example, we have previously shown that acquired lapatinib resistance is associated with increased levels of HER2 in lapatinib resistant HCC1954 and SKBR3 cells in comparison to drug naïve control cells [85]. This can mediate drug-resistance as the effectiveness of the drug is reduced because more target molecules are present and need to be inhibited in order for the drug to execute anti-cancer effects [84]. Additionally, in the case of trastuzumab resistance, membrane-associated glycoprotein mucin-4 (MUC4) can bind to HER2, thereby blocking trastuzumab from binding to its intended target, preventing drug action at that site; and resulting in drug-resistance. This was demonstrated by Nagy *et al.* who found that the binding capacity of trastuzumab in drug-resistant JIMT-1 cells (that were isolated by pleural effusion from a trastuzumab-

resistant patient and subsequently cultured) was reduced, compared to trastuzumab sensitive SKBR3 cells [86].

1.3.4 Increased DNA repair

Cancer cells can avoid cell death by harnessing cell's ability to repair DNA damage, in the case of cancer treatment it is DNA damage induced by anti-cancer drugs that directly or indirectly damage DNA as their mechanism of action. There are numerous mechanisms used by cancer cells to reverse drug induced damage including: repair of single strand breaks and base damage by base excision repair, repair of DNA cross-linking, mismatches and loop insertion/deletion by DNA mismatch repair and repair of double strand breaks by homologous recombination and non-homologous end joining [87]. Poly(ADP-ribose) polymerase 1 (PARP1) and p53 are examples of DNA repair proteins that play a role in drug-resistance. For example, lung cancer patients with low levels of PARP1, a DNA repair protein that mediates repair of single-strand breaks [88], are more likely to respond to chemotherapy than those with higher levels [89]. Additionally, increased levels of mutated p53 have found to be associated with doxorubicin resistance, where HT29 colon cancer cells have higher p53 expression and are more resistant to the effects of doxorubicin than HCT116 colon cancer cells that had less p53 and were more sensitive to doxorubicin [90].

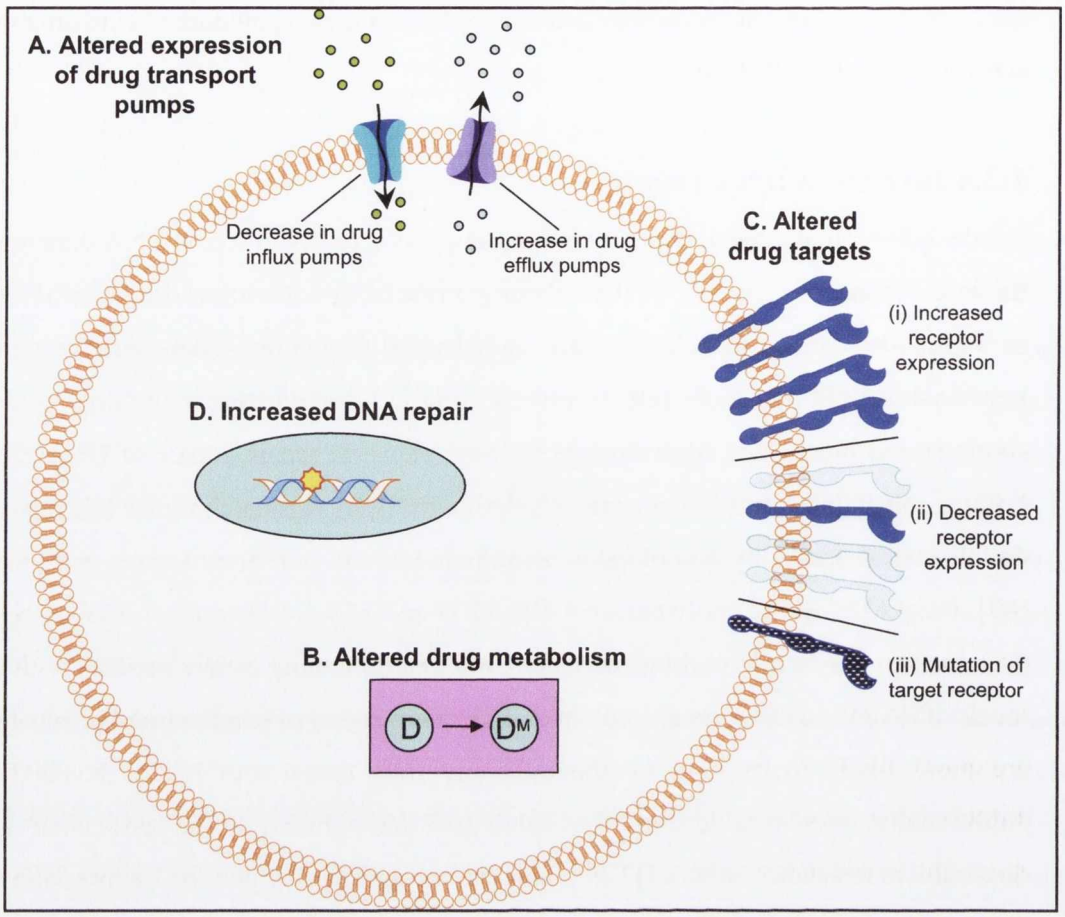

Figure 1.2. Mechanisms of drug-resistance. A. Altered expression of drug transport pumps: Increased drug efflux pumps and/or decreased drug influx pumps reduces levels of availability of drug in cancer cell; **B.** Altered drug metabolism results in decreased levels of active drug being available in the cell; **C.** Altered drug target: (i) Increased expression of target, (ii) decreased expression of target, and (iii) mutation of target, can alter drug efficacy; **D.** Increased DNA repair reverses drug induced DNA damage in target cells.

1.3.5 Evasion of apoptosis

The link between cancer cells and their ability to evade apoptosis to enable their survival has been described previously in Section 1.1. However, the relationship between cancer and apoptosis evasion goes further, in that cancer cells can harness their ability to avoid drug-induced apoptotic death as a mechanism for resistance to anti-cancer therapy. Drug resistant cells can avoid apoptotic death *via* intrinsic pathways where there is deregulation of the mitochondrial pathways of apoptosis; and/or *via* extrinsic pathways which rely on ligand/receptor binding to mediate apoptosis [91]. The caspase family of

proteolytic enzymes play a central role in apoptosis, initiating and executing apoptosis in both intrinsic and extrinsic apoptotic pathways [91].

Apoptotic signalling *via* the extrinsic pathway can be mediated through death receptors CD95, also called FAS, death receptor 4 (DR4) and death receptor 5 (DR5) that initiate apoptosis when bound by their ligands. When tumour necrosis factor-related apoptosis-inducing ligand (TRAIL) binds to any of these death receptors, the activated receptor recruits FAS-associated protein with death domain (FADD) and caspase-8 into a cell death-inducing signalling complex. Upon its recruitment into this complex, caspase-8 becomes activated, which further activates downstream executioner caspases 3 and 7; resulting in apoptosis [84, 92]. An example of how cells can manipulate the extrinsic apoptotic pathway for acquired drug-resistance is demonstrated by lapatinib resistant SKBR3 HER2-overexpressing breast cancer cells, which were found to be less responsive to TRAIL-induced apoptosis compared to drug naïve control cells [93].

The intrinsic pathway or mitochondria-mediated apoptosis is initiated by oligomerisation of BAX and BAK, pro-apoptotic proteins that form pores in mitochondria once they have interacted. The resulting 'leaky' mitochondria allow pro-apoptotic molecules such as cytochrome c and second mitochondria-derived activator of caspases (SMAC) enter into the cytoplasm. This is enables the formation of the apoptosome, a complex of cytochrome c, caspase 9 and apoptotic protease-activating factor 1 (APAF1); upon formation of this complex caspase 9 is activated, which subsequently activates executioner caspases 3 and 7; resulting in apoptosis [84, 91]. Cancer cells can evade apoptosis by blocking parts of these pro-apoptotic pathways as a mechanism of drug-resistance. For example, Bcl2 is an anti-apoptotic protein that controls BAX and BAK oligomerisation, thus it can control the initiation of the mitochondrial apoptosis pathway. Levels of Bcl2 have been found to be increased in drug resistant cells, for example UACC-812 lapatinib-resistant breast cancer cells expressed higher levels of Bcl2 compared to sensitive control cells [94]. Similarly, BT474 lapatinib-resistant breast cancer cells expressed higher levels of survivin, an anti-apoptotic protein that inhibits pro-apoptotic proteins in the mitochondria [95], compared to drug sensitive control cells [94].

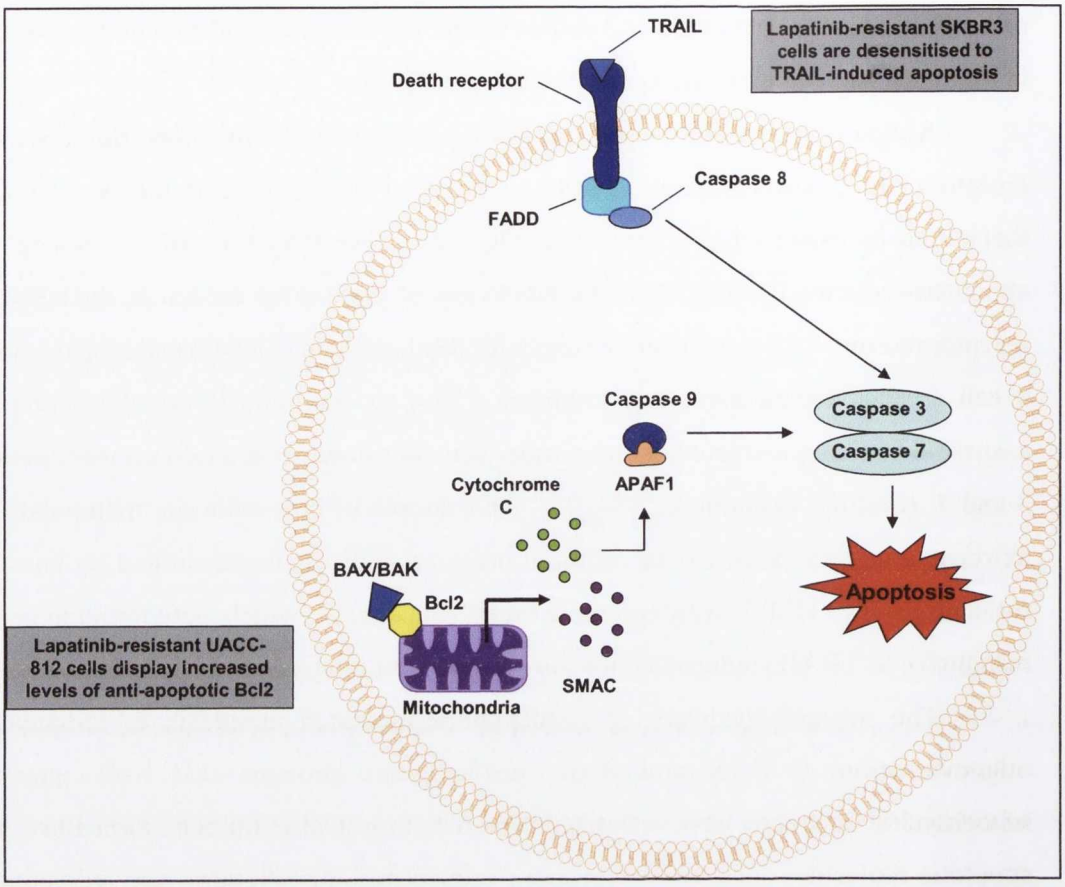

Figure 1.3. Intrinsic and extrinsic pathways of apoptosis. TRAIL induced apoptosis is executed by effector caspases 3 and 7. Cancer cells can become desensitised to TRAIL-induced cell death as a mechanism of drug-resistance. The mitochondrial apoptotic cascade also ends with caspase-induced apoptosis but can be avoided by drug resistant cancer cells that over-express the anti-apoptotic protein Bcl2.

1.3.6 Activation of pro-survival pathways

Another resistance mechanism to various anti-cancer therapies is the activation or up-regulation of pro-survival pathways. For example, the RAS/RAF/MEK/ERK and PI3K/PTEN/AKT pathways are typically associated with regulating cell growth and survival. However, when unregulated these pathways have roles in cancer progression and the development of drug-resistance [96]. Typically in the PI3K/PTEN/AKT pathway the activation of receptor tyrosine kinases can result in intracellular binding and activation of PI3K. This in turn phosphorylates PIP_2 to PIP_3. PTEN, a tumour suppressor protein can dephosphorylate PIP_3 to PIP_2 and so is a regulator of the PI3K/PTEN/AKT pathway. The formation of PIP_3 instigates further intracellular signalling by binding both PDK1 and AKT. As a results, this brings both proteins into close proximity and allows AKT to become phosphorylated by PDK1 [97]. In turn,

activated AKT can then phosphorylate a number of substrates involved in proliferation, cell growth and survival. The PI3K/PTEN/AKT can be hijacked during drug-resistance, whereby cells can alter the expression levels of some or all of the components of the pathway (e.g., inhibition of pro-apoptotic proteins like BAX) in order to survive drug insult during therapy. For example, in SKBR3-trastuzumab resistant cells, levels of PTEN are decreased compared with drug naïve cells. In this case, activated AKT is subsequently increased in the drug-resistant cells as a means of evading the anti-tumour effects of trastuzumab [98].

In the RAS/RAF/MEK/ERK pathway, the activation of RAS propagates a cascade of signals resulting in cell growth and survival Activated RAS in turn activates RAF, which goes on to activate MEK and activated MEK follows on to activate ERK. At the end of this pathway phosphorylated ERK can subsequently activate a number of substrates including c-Jun, c-Myc and ribosomal S6 kinase, which are all involved in proliferation and apoptosis [96]. Similarly to the PI3K/PTEN/AKT pathway, cells can adapt expression levels of proteins in the pro-survival RAS/RAF/MEK/ERK pathway to counter toxic effects of anti-cancer drugs. For example, Lee *et al.*, 2013 found that human gastric carcinoma cells, SNU216, resistant to lapatinib displayed an increased level of phosphorylated ERK when compared to drug naïve control cells, indicating that this pathway plays a part in resistance to lapatinib in these cells [99].

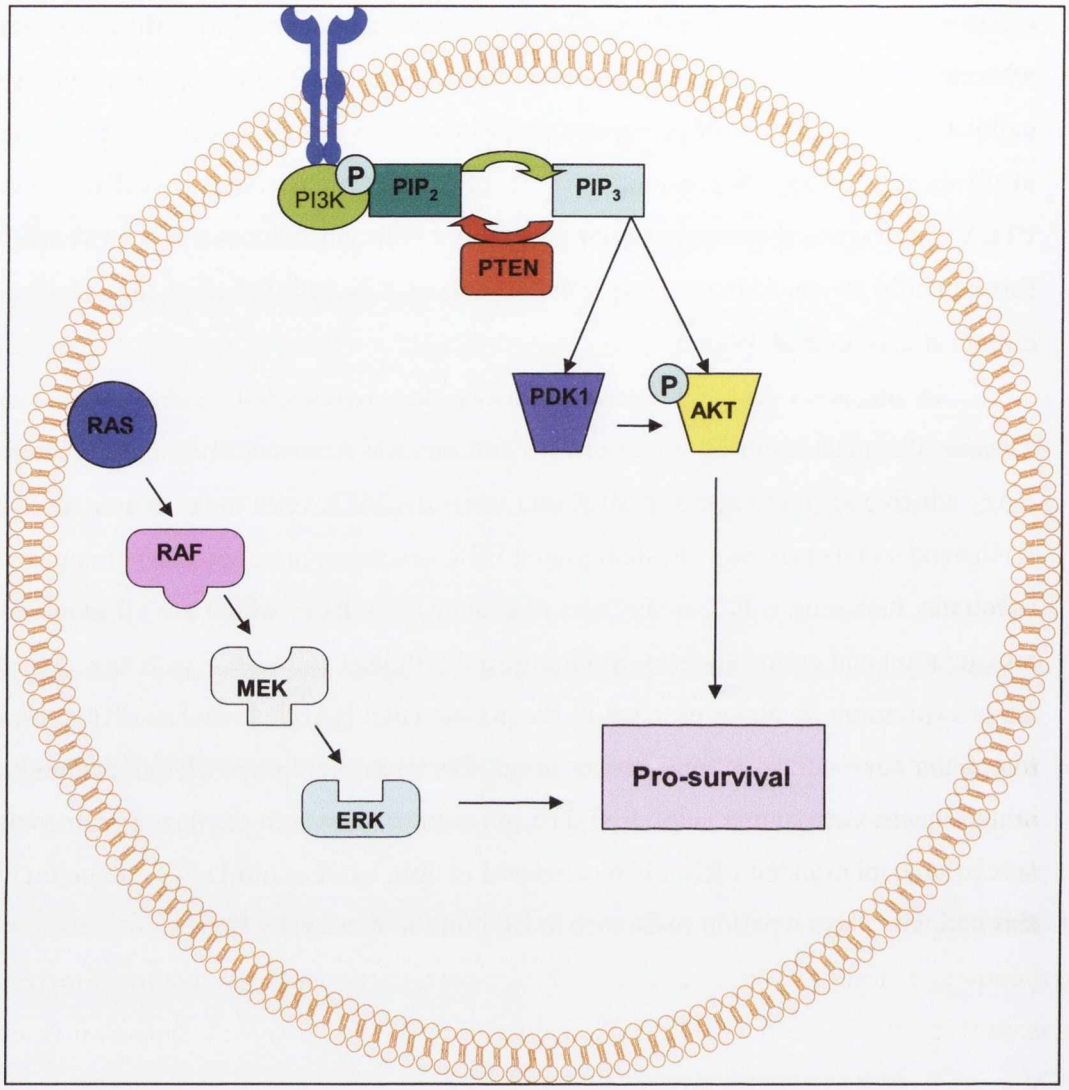

Figure 1.4. Pro-survival pathways involved in drug-resistance. Expression of components of both the PI3K/PTEN/AKT and the RAS/RAF/MEK/ERK pathways can be altered in drug-resistance cells in order to circumvent effects of toxic anti-cancer therapies.

1.3.7 Tumour microenvironment, heterogeneity and stem cells

Solid cancers have been identified as having extensive intratumour heterogeneity in terms of receptor expression and biomarker mutation, which plays a part in the failure of drugs in the clinic and can contribute to drug-resistance. This heterogeneity of the tumour microenvironment was observed and described by Gerlinger *et al.*, where they found that single tumour core biopsies, which are commonly used for cancer diagnosis and therapy-based decisions, are likely not representative of the tumour as a whole [100]. It was found that analysis from 9 individual biopsies from different areas of the

same renal tumour yielded different cancer staging information ranging from grade 1 to grade 4. Additionally, their analysis showed that RNA expression signatures indicative of both poor and positive prognosis being detected in different biopsies of the same tumour. This alarming level of variability could lead to gross under- or overestimation of the level of a patient's disease.

The relevance of tumour heterogeneity to drug-resistance is demonstrated in Figure 1.5. It is increasingly accepted that tumours have a heterogeneous, rather than homogenous, cell type conformation. As a result, effective therapy can be hampered by the development of drug-resistance through a therapy-induced selection of a drug-resistant sub-population within the original tumour. Following anti-cancer treatment, drug-sensitive cells within a tumour die resulting in shrinkage of the mass, however this can cause the selection out of a minor drug-resistant sub-population that remain following treatment. It is these cells that have the capacity to support the regrowth of a tumour that consequently is resistant to therapy [101].

Additionally, the presence of cancer stem cells has been suggested as having a role in tumour heterogeneity and drug-resistance. It has been proposed that the presence of these cells, which are considered innately resistant to anti-cancer therapy due to their lack of proliferation, elevated expression of drug transporters and ability to repair DNA damage, can mediate drug-resistance in a similar manner to the drug-resistant sub-population described above. Here, a heterogeneous tumour may comprise of drug-sensitive cells and cancer stem cells. However, following treatment the sensitive cells die off, leaving cancer stem cells behind that survive therapy and can support the development of drug resistant tumours [101].

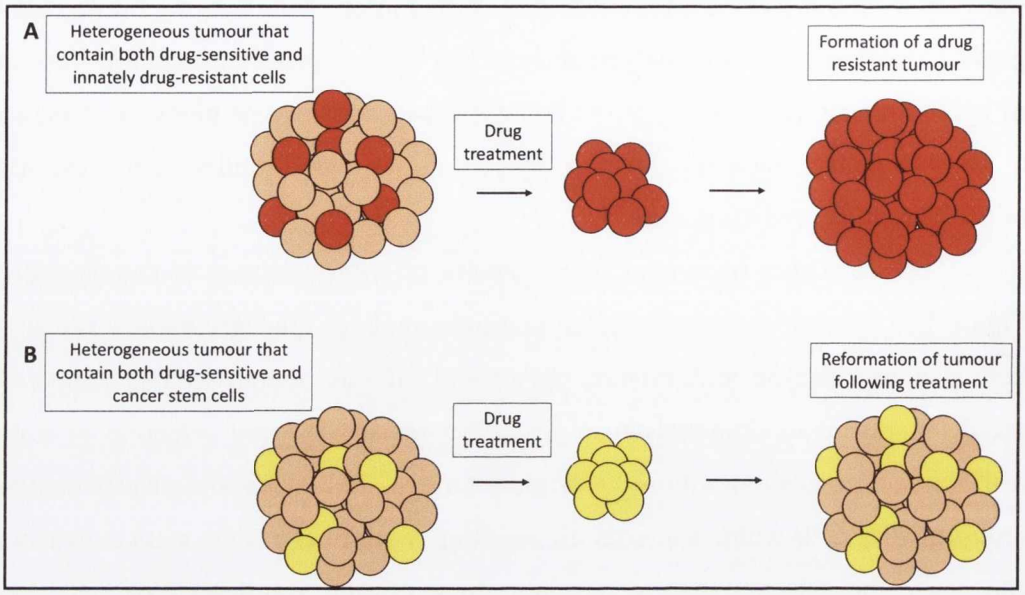

Figure 1.5. The heterogeneity of tumours can cause drug-resistance. A. Heterogeneously populated tumours can result in drug-resistance when only innately resistant cells remain following treatment and subsequently proliferate into a drug resistant tumour (pink cells=innately drug-sensitive); red cells=innately drug-resistant); B. Cancer stem cell sub-populations are resistant to treatment and can repopulate a tumour following treatment (pink cells=drug-sensitive; yellow cells=cancer stem cells).

1.4 Extracellular Vesicles

The ability of cells to mediate intercellular signalling *via* direct cell-cell signalling or by secretion of biomolecules is well established. However, over the past few decades, it has been found that cells secrete extracellular vesicles (EVs) into extracellular space, and that these EVs can also facilitate intercellular signalling. These EVs are released from cells and contain a molecular 'fingerprint' of the cells from which they are released and have been found to contain proteins, receptors and RNA that match their cell of origin. Secreted EVs have been detected in a range of bodily fluids including blood, saliva, urine, cerebrospinal fluid, breast milk, amniotic fluid, semen and ascites [102].

1.4.1 EV formation

EVs can be formed *via* two different mechanisms, where the products of each mechanism results in the formation of different types of EVs, e.g., exosomes and microvesicles (also known as ectosomes). Exosomes are 30-130nm EV that are produced when endosomes are formed by endocytosis at the cell membrane. The membrane of these early endosomes then buds inwards forming mature endosomes, which are also known as multivesicular bodies (MVB). During their formation, MVBs acquire lipids, proteins and other biomolecules from the cytosol that are sorted specifically into the MVB vesicles by a number of proteins. The endosomal sorting complex required for transport (ESCRT) group of proteins, the tetraspanin family of proteins and lipids can all facilitate the specific sorting of biomolecules into the vesicles of MVBs. Formed MVBs then have one of two fates, either they fuse with lysosomes and become degraded by the lysosomal hydrolases or fuse with the cell membrane and in doing so release exosomes into extracellular space. This is not a random occurrence, however, as it has been shown that only MVBs low in cholesterol are targeted for lysosomal degradation, while cholesterol rich MVBs are preferred for fusing with the cell membrane and releasing their vesicles into the extracellular space. The exosome secretion process can be regulated by Rab proteins [102].

Microvesicles are ~120-1000nm sized EVs that are formed by a completely separate process to exosomes. They are formed by small cytoplasmic protrusion budding at the edge of a cell. Cholesterol-rich plasma microdomains are essential for this process. These buds contain specifically accumulated membrane and cytosolic proteins and shedding occurs by fission at the stalk of the buds, releasing microvesicles in to the extracellular space [103].

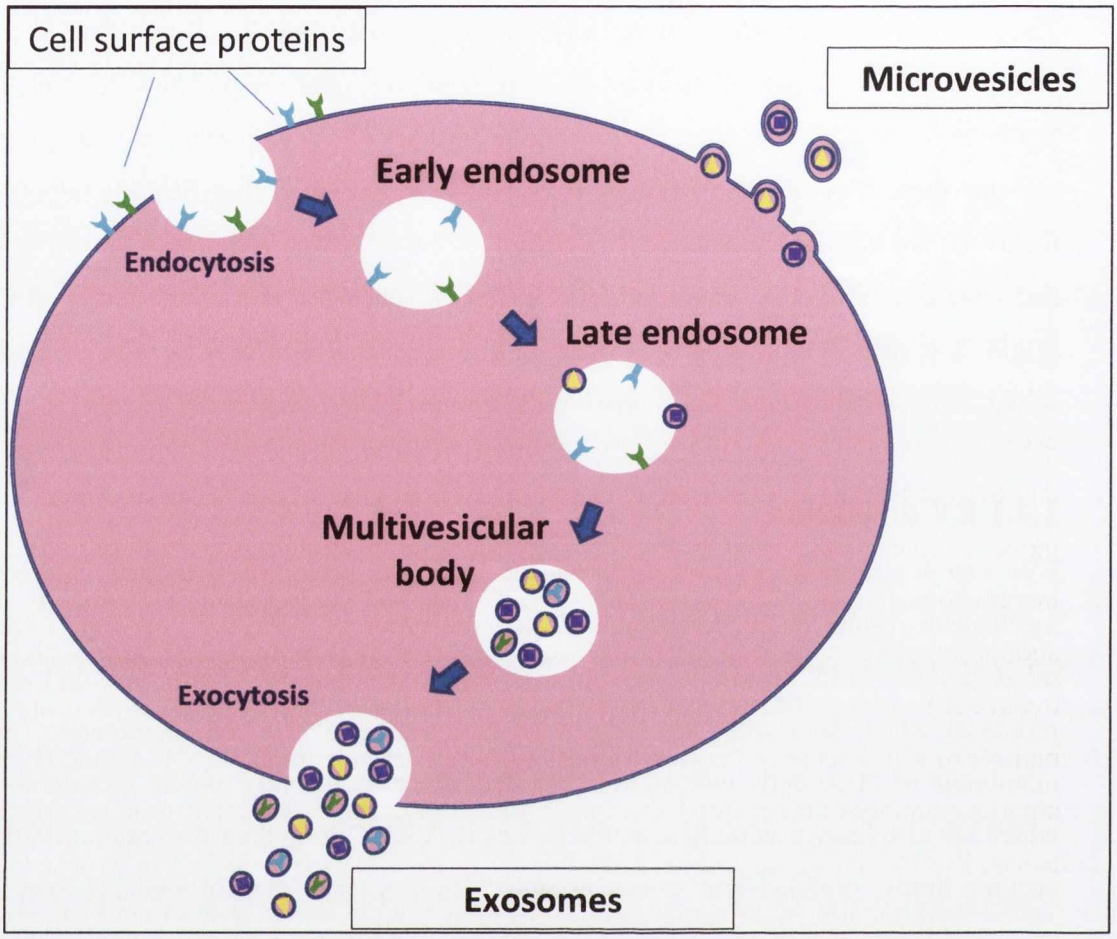

Figure 1.6. The biogenesis of exosomes and microvesicles. A. Exosomes are formed by endocytosis at the membrane, followed by MVB formation and exosome release from MVBs by fusion to the cell membrane. B. Microvesicles are formed by budding directly off of the cell membrane.

1.4.2 EV composition

The composition of EVs has been researched extensively and has revealed that these secreted particles contain a wide range of bio-molecules including proteins, lipids and nucleic acids. Proteomic analysis of EV content revealed that they contain two subsets of proteins, some that are dependent on and specific to the cell type from which they were secreted, while others are detectable in the majority of exosomes irrespective of their cell of origin [102]. The enrichment of the aforementioned exosome-specific proteins (e.g., ALIX, TSG101 and CD9) are involved in the endocytic process and demonstrate that exosomes are formed specifically and are not just cellular fragments. EV proteins include both membrane-bound (e.g., adhesion molecules and antigen-presenting molecules) and cytosolic (e.g., ESCRT proteins and signalling proteins)

proteins. Analysis of lipid-content has shown that cholesterol, ceramide and sphingomyelin are enriched in the membranes of EVs. The presence of nucleic acids in EVs has been reported, with absent or low levels of ribosomal 18s and 28s RNA being characteristic. RNA, mRNA, miRNA have all been detected in EVs [102].

The packaging of content into EVs can be influenced by the microenvironment of the cells from which they are secreted. Inflammation has been shown to have an effect on RNA and protein content of endothelial cells. De Jong *et al.* reported that exosomes isolated from human microvascular endothelial cells exposed to the TNFα, an inflammation mediator, resulted in alterations in RNA and protein content of the exosomes when compared to exosomes isolated from untreated cells [104]. They found that tumour necrosis factor α-induced protein 1 (TNFAIP1), tumour necrosis factor α-induced protein 3 (TNFAIP3), intracellular adhesion molecule 1, were all upregulated in exosomes from TNFα-stimulated cells, while complement component 5, apolipoprotein M and collagen type XVIII-α-1 were all downregulated due to TNFα treatment in comparison to control exosomes. Similarly, the levels of RNA from a number of genes detected in the exosomes was altered, for example, IL8, IL1β and IL32, among a number of other genes were upregulated in exosomes isolated from exosomes isolated from TNFα exposed cells, compared to exosomes from cells not exposed to TNFα. Additionally, in the same study it was found that hypoxic environments can also affect protein and RNA levels in these endothelial cell-derived exosomes. Exposure of cells to hypoxic conditions resulted in secretion of exosomes with increased levels of proteins: semenogelin 1, complement component 4A and lysyl oxidase-like 2, while collagen-1-α1 and epsin 1 were decreased in comparison to exosomes from control cells. Furthermore, the hypoxic conditions also resulted in altered exosomal RNA content, where N-Myc downstream regulated 1 protein and BCL2/adenovirus E1B 19kDa interacting protein 3 were upregulated and cold inducible RNA binding protein was downregulated, in comparison to control exosomes derived from cells grown in normoxia [104].

The ability of the microenvironment to influence EV biogenesis was also observed by Parolini *et al.*, who found alterations in the protein and lipid composition of EVs released from cells grown in an acidic environment that is meant to mimic the low pH core of a tumour [105]. Melanoma cells, Mel-1, were grown in a normal buffered medium (pH 7.4) and in acidic medium (pH 6.0), and it was found that when the same concentration of exosomes were analysed using SDS-PAGE analysis, those derived from cells grown in the acidic environments had a higher content of both lamp-2 and

Rab 5B, in comparison to exosomes derived from cells grown at a normal pH. Additionally, approximately 4 times more exosomes were released by cells grown in the acidic medium compared to those released in medium of a normal pH. In these same conditions, exosomes derived in acidic medium were enriched with lipids, sphingomyelin and ganglioside GM3 [105].

1.4.3 EV function

Cell-cell communication is essential for proper tissue function. EVs participate in this intercellular communication by interacting with secondary cells and have the ability to transfer their nucleic acids and proteins as part of this process that can impact the physiology and pathophysiology of the recipient cell. Different mechanisms are employed by exosomes to mediate cell communication; (i) ligand-receptor signalling between EV and recipient cell surfaces can be used to activate intracellular signalling in the recipient cells; (ii) proteases in the extracellular space can cleave membrane-bound proteins from EVs, resulting in soluble ligands that can activate cell surface receptors; (iii) EVs can fuse with the cell surface and enable the release of exosomal proteins within the recipient cell; and (iv) the entire EV can be endocytosed or phagocytosed by the recipient cell and once internalised EV proteins and nucleic acids can affect recipient cell physiology [106].

EVs have been associated with a number of physiological and pathological processes, including inflammation, immunity and cancer. EVs have been shown to play a role in inflammation; for example EVs derived from neutrophils can stimulate anti-inflammatory cytokines, while EVs released by fibroblasts can induce pro-inflammatory IL6 and metalloproteinase release [107]. Furthermore, EVs are involved in the antigen presentation process during immune reactions, where EVs released by pathogen-infected cells can contain pathogen antigens. For example, Walker *et al.* discovered that EVs derived from patient endothelial cells infected with the cytomegalovirus, transfer cytomegalovirus antigens to antigen presenting cells, which in turn can activate $CD4^+$ T cells [108].

EVs have also been proven as having a numerous roles in cancer. Janowska-Wieczorek *et al.* investigated the role of EVs in lung cancer [109]. They found that using platelet-derived EVs from healthy volunteer donors as a chemoattractant resulted in an increase in cell migration of A549, HTB 177, HTB 183 and CRL 2062 lung cancer cells, *in vitro*. In addition to increasing cell migration, they found that these EVs can stimulate MMP expression by A549 and HTB 177 cells, which also corresponded to an increase

in invasive capacity of these cells when treated with EVs and in comparison to untreated controls. To investigate the effects of EVs on metastasis, they covered Lewis lung carcinoma cells (LLC) with murine platelet-derived EVs from healthy C57BL/6 mice and injected them intravenously into mice. Several weeks later, the number of metastatic foci was measured and there were significantly more in mice injected with EV-coated LLCs than control cells. Additionally, mice injected with EV coated cells had more cancer cells detected in their bone marrow, when compared to controls, indicating that the presence of platelet-derived EVs play a functional role in the metastatic process [109]. Harris *et al.* also reported similar findings regarding the relevance of EVs in cancer cell migration using breast cancer cells [110]. They applied EVs isolated from breast cancer cell lines of increasing migratory capacity; MCF7, Rab27b-MCF7 (a modified MCF7 cell line that has increased invasive capacity), and MDA-MB-231 cells. The EVs from each cell line were added to MCF7 cells in culture and a wound-closure migration assay was subsequently performed. It was found that EVs from the more aggressive cell lines, Rab27b-MCF7 and MDA-MB-231 cells, caused greater would closure, indicating that EVs play a role in cell migration [110].

Breast cancer derived EVs have also been shown to play a role in angiogenesis. Using a triple negative breast cancer cell line, Hs578t, and its more invasive variant, Hs578T(i)$_8$, O'Brien *et al.* isolated EVs from both cell lines and applied them to endothelial cells [111]. They found that EVs isolated from the more aggressive Hs578T(i)$_8$ cell line were able to induce a 2.67-fold increase in angiogenesis compared to EVs derived from the Hs578t cells. This data indicates that EVs may have a role in the angiogenesis process during tumour formation and growth.

Breast cancer EVs have also been shown to transfer miRNAs that they contain from their cell of origin to recipient cells, where they can alter the protein levels of their target gene. Singh *et al.* demonstrated the ability of EVs containing miRNA to transfer this biological information to recipient cells through the uptake of the EVs [112]. They isolated EVs from MDA-MB-231 breast cancer cells that express miR-10b at a high level and found that these EVs also contain miR-10b at a high level. When these EVs were applied to non-malignant HMLE control cells, they found a 5-fold increase in miR-10b levels in the HMLE EV treated cells compared to the non-treated controls. Additionally, it was found that miR-10b maintained functional capabilities inside the recipient HMLE cells, where levels of Homeobox D10 protein, the target of miR-10b, is reduced in cells treated with miR-10b containing EVs [112].

EVs have also been linked to a role in drug-resistance. EVs isolated from HER2-overexpressing cells (SKBR3 and BT474) were found to have the ability to bind to trastuzumab *in vitro,* thereby limiting the amount of free-trastuzumab that can exert effects on cells [113]. When these cells were treated with just their autologous EVs, no alteration in proliferation was observed; when these cells were treated with trastuzumab, a significant reduction in proliferation was observed due to the drug treatment; however, cells co-treated with both their autologous EVs and trastuzumab displayed a significant resistance to the anti-proliferative effects of trastuzumab. Here the role of EVs in drug-resistance is evident as the HER2-positive EVs 'mop up' trastuzumab, leaving less drug available to act on cells, thereby conferring drug-resistance through a decoy system [113].

1.4.4 EVs as biomarkers in cancer

The molecular content of EVs, where they incorporate and are enriched for proteins and nucleic acids of their cell of origin, combined with their ability to be detected in a number of accessible body fluids make EVs an appealing tool for biomedicine. As they are released during a number of pathological conditions, the potential is there to use EVs as diagnostic and predictive biomarkers in a range of diseases; however, only their relevance as biomarkers in cancer will be focused on here. Cancer biomarkers have been detected in blood and urine-derived EVs, which can be obtained with minimal invasiveness, with some examples being explained below.

It appears that cancer cells secrete large amounts of EVs and the amount releases can give insight into the disease state of a patient. EV quantities from plasma taken from gastric cancer patients were measured and revealed that plasma EV levels were higher in cancer patients when compared to healthy control plasma levels. In addition, levels of EVs in plasma appears to correlate to disease stage, where EV levels in patients with stage IV disease were significantly higher than those with stage I disease [114].

Prostate cancer has clinically relevant biomarkers (e.g., prostate specific antigen) that can be used to some extent to diagnose disease and predict and monitor response to treatment. However, these solid tumours tend to have a heterogeneous composure where a biopsy from one portion may not be representative of the tumour as a whole. In this case, it may be advantageous to analyse urine EVs which can be released by prostate cancer cells as a means to detect biomarkers to give clinicians a balanced view of a patient's disease state, as EVs secreted into urine would be from the tumour as a whole; and may be more representative of a patients disease state [115]. An example

of this is the mRNA for PCA-3 and TMPRSS2, proposed prostate cancer biomarkers that were detected in the urine-derived EVs of prostate cancer patient. Here, the biomarker levels detected in the patient EVs provides an alternative means to obtain information regarding patient diagnosis, as opposed to relying solely on information from biopsies [115].

Glioblastomas are aggressive brain cancers that are associated with a poor prognosis. Skog *et al.* analysed EVs isolated from the serum of glioblastoma patients and found that mRNA for EGFRvIII, a mutant form of EGFR associated with a clinical subgroup of glioma, is detectable in vesicles [116]. miR-21, which may be overexpressed in glioblastoma tumours, was found in elevated levels in patient EVs in comparison to control serum EVs. This data indicates that the mRNA and miRNA profile of EVs isolated from glioblastoma patient serum is representative of the levels of these biomarkers in corresponding tumours, which potentially allows for biomarker observation through serum without the need for dangerous and invasive brain surgery. As EGFRvIII-positive patients respond significantly better to EGFR inhibitors than EGFRvIII-negative patients, characterising cancer patient EVs for nucleic acid content may provide a less invasive method for disease management and therapeutic choices in these cases [116].

Ovarian cancer often presents in the clinic at an advanced stage. Long term survival of ovarian cancer is particularly low with advanced disease having 5-year survival rates of just 21% [117]. Consequently, early diagnosis is imperative for improving ovarian cancer survival rates. While a panel of miRNA biomarkers has been proposed for ovarian cancer diagnosis (miR-21, miR-141, miR- 200a, miR-200c, miR-200b, miR-203, miR-205 and miR-214), it is limited by the need of tumour tissue to test for these miRNAs [117]. Taylor and Taylor reported that when they compared expression levels of these miRNAs between ovarian tumour tissue specimens and patient serum-derived EVs, levels in both specimen types showed similar trends in levels of the biomarker miRNA signature. Following this discovery they suggest screening serum EVs for this miRNA biomarker panel to detect ovarian cancer in the hopes that it would enable earlier detection and could also be used for monitoring for disease recurrence [117].

1.5 Three-dimensional cell culture and drug discovery

1.5.1 Trends in drug discovery

Cells naturally grow in a 3D environment. The spatial arrangement of cells within this environment, including the extra cellular matrix (ECM), affects how they interact with each other and their microenvironment. In turn, these signals affect cell processes including proliferation, differentiation, morphology and a range of cellular functions [118, 119]. Therefore, when drug candidates are being tested using cell-based assays, the culture methods used should mimic the *in vivo* form as closely as possible. The most natural, tissue-mimicking method of cell growth for drug discovery applications is, arguably, 3D. Here, the drug discovery process and the roles that monolayer (2D cell culture) and 3D cell culture play in this process are discussed.

The design and development of new drugs, for the most part, follow a similar trend of progression. Typically a potentially druggable target is identified and, often with the aid of *in silico* modelling, lead compounds are designed, developed and optimised to act on this target. *In vitro* and *in vivo* preclinical testing is then performed with compound libraries to establish which, if any, exhibit efficacy towards the target in question. Clinical testing of suitable compounds through various stages of clinical trials is then performed in humans, which is essential to evaluate the ultimate usefulness of the drug.

The number of potential anti-cancer products that progress successfully through clinical development is low, at approximately 10% [120]. Lack of clinical efficacy and/or unacceptable toxicity are two of the main causes of drug failures during development [121, 122]. Because of the high costs (typically ~1 billion US dollars) in getting new drugs approved and the fact that many oncology drugs fail during clinical testing, especially during phase III – the most expensive phase of clinical development [123, 124], it is imperative that compounds that are potentially ineffective or have an unacceptable toxicity profile are dismissed as early in the evaluation process as possible. This would preferably be before clinical trials and ideally before animal testing has begun. Failing early in the developmental stages enables the cost of failed molecules to remain relatively low, that is, the further into the development process a compound fails, understandably the more money a company has invested and so stands to lose, see Figure 1.5.1 [125]. It is, therefore, necessary to improve *in vitro* cell-based testing methods for a more informed prediction of drug candidate efficacy and safety, and

thereby sieve out poorly functioning compounds while prioritising promising drug candidates [124].

The ability of an *in vitro* assay to produce reliable biomedically-relevant information is essential in drug development; therefore, it is necessary that the cells used in this testing mimic the phenotype of cells within the target tissue [125, 126]. 2D cell culture is conventionally used in *in vitro* drug candidate testing; however, limitations of 2D culture suggest that an alternative method should be considered. These limitations include the lack of cell–cell and cell–ECM signalling that occurs in the 3D *in vitro* environment where such signals are essential to cell differentiation, proliferation and a range of cellular functions [118, 119]. For example, integrins, which are cell surface receptors, anchor cells to the ECM and are also involved in the cells' interpretation of biochemical cues from their local environment [127]. It is probable, therefore, that 3D cellular assays would be more analogous to – and so predictive of – *in vivo* events compared to more simplified 2D cultures in which essential signalling pathways may have been lost or, at least, compromised [128]. The use of 3D *in vitro* systems in drug research and development has, therefore, been suggested as a potential link to bridge the gap between monolayer cultures and animal model studies [129].

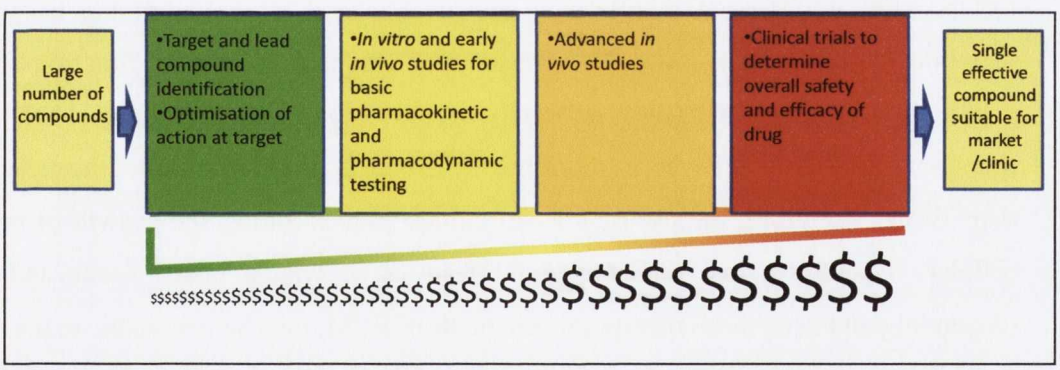
Large number of compounds
•Target and lead compound identification
•Optimisation of action at target
•In vitro and early in vivo studies for basic pharmacokinetic and pharmacodynamic testing
•Advanced in vivo studies
•Clinical trials to determine overall safety and efficacy of drug
Single effective compound suitable for market /clinic
$$$

to be continually observed [131]; demonstrating a means by which cells of interest could be maintained outside the body of origin and observed over time. Substantial improvements have been made on the 2D cell culture technique initially developed by Harrison in terms of availability of sterile cell culture plastics, synthetic medium, antibiotics and anti-fungal agents. While continued development of this technique over the past century has been of fundamental importance, developments in the form of 3D cultures have highlighted some of the shortcomings of 2D monolayers. The correlation of results from 2D cultures to real-life *in vivo* scenarios has been questioned. Differences in cell morphology, polarity, receptor expression, oncogene expression, interaction with the ECM (including the basement membrane) and overall cellular architecture have been noted between cells grown as 2D monolayers and what is observed *in vivo*. As a result, more attention is shifting to 3D culture methods as it has been suggested and, indeed, verified in many reports, that cells grown in 3D are more representative of what occurs naturally *in vivo*.

To improve drug development using 3D culture, the functional unit of tissues must be considered rather than single cells. Mammary tissue comprises of epithelial cells that have a distinguished cellular architecture. These cells have specialised cell–cell contacts, a polarised morphology and are attached to an underlying basement membrane. The maintenance of these features is essential for normal function of the tissue, including proliferation, differentiation, survival and secretion [132]. The functional unit in breast tissue, as described by Bissell *et al.* [118] includes the cells plus their ECM. Therefore, the use of 3D cell culture, which allows the growth of multi-cellular 3D cultures that retain essential features of typical breast tissue and can (depending on the method) incorporate elements of ECM, may be invaluable to the drug development process. While the perfect method for 3D cell structures may not yet have been determined, methods have been developed based on current knowledge of cellular/tissue architecture, in efforts to produce the most *in vivo*-like structures possible. The more commonly used 3D culture methods are detailed below, while some newer methods are also discussed. Advantages and disadvantages associated with these methods are highlighted in Table 1.3.

Method Type	Advantages	Disadvantages
Forced-floating	relatively simple inexpensive suitable for high-throughput testing spheroids produced are easily accessible	variability in cell size and shape if not as fixed cell no./well DIY plate-coating is relatively labour intensive
Hanging drop	inexpensive if using standard 96-well plate homogenous spheroids suitable for high-throughput testing spheroids produced are easily accessible	more expensive if using specialised plates labour intensive if preparing plates in-house small culture volume makes medium exchange, without disturbing cells, difficult (proposed easier handling with commercially-available formats)
Agitation-based approaches	simple to culture cells large-scale production relatively easily achievable motion of culture assists nutrient transport spheroids produced are easily accessible	specialised equipment required no control over cell no./ size of spheroid (can be overcome by additional culture step; see *Forced-Floating Methods*) time consuming for HTS due to extra step required for homogenous spheroids cells possibly exposed to shear force in spinner flasks (may be problematic for sensitive cells)
Matrices and Scaffolds	provide 3D support that mimics *in vivo* some incorporate growth factors	can be expensive for large-scale production can have difficulty in retrieving cells following 3D culture formation
Microfluidic cell culture platforms	described as suitable for high-throughput testing	specialised equipment required adding expense Further analysis of 3D cultures produced may be difficult

Table 1.3. Proposed advantages and disadvantages of different 3D cell culture methods.

1.5.3 3D cell culture methods

1.5.3.1 Forced-floating methods

A relatively simple method for generating 3D spheroids is to prevent their attachment to the vessel surface by modifying the surface, resulting in forced-floating of cells. This promotes cell–cell contacts which, in turn, promotes multi-cellular sphere formation [133]. In brief, for this method plates are coated with poly-2-hydroxyethyl methacrylate (poly-HEMA) and dried before the addition of cells. The poly-HEMA prevents cells from attaching to the surface of the wells. Using this approach, Ivascu and Kubbies [134] developed a method for producing 3D spheroids from cancerous and non-cancerous cells which enables the rapid production of spheroids in round or conical bottomed 96-well plates. Additionally, low-adherance round-bottomed plates can be purchased commercially, where plates are coated with 2-ethacryloyloxtethyl phosphorylcholine, a polymer that prevents cell attachment to the plate and encourages 3D spheroid formation [135].

On the basis of the same principle of simply preventing cell attachment to the culture vessel, 3D cultures can be formed by using 1.5% agarose in culture medium to form a thin coating over the culture dish surface. The agar prevents cell adhesion to the surface, thus resulting in the establishment of 3D spheroids [136]. The forced-floating method using agar is simple and inexpensive, and is proposed to allow for long-term culture of cells (more than 20 days) [136].

1.5.3.2 Hanging drop method

The hanging drop method of 3D spheroid production is an adaption of the method used by Harrison. When originally performed by Kelm *et al.* [137] this method used a small aliquot (typically 20μL) of a single cell suspension which was pipetted into the wells of a 60-well MicroWell MiniTray (Nunc). Following cell seeding, the tray was subsequently inverted and aliquots of cell suspension turn into hanging drops that are kept in place due to surface tension. Cells accumulate at the tip of the drop, at the liquid–air interface, and are allowed to proliferate. Moisture levels are maintained using bioassay dishes which act as moisture chambers and cells are incubated as per standard cell culture procedures of 37°C and 5% CO_2. Originally, cell culture plates were used for this method, however, companies, including 3D Biomatrix and InSphero, now provide hanging-drop plates, which makes using this method more user-friendly and reproducible; and are becoming popular for *in vitro* cell analysis for researchers [138, 139].

1.5.3.3 Agitation-based approaches

Agitation-based approaches for the production of 3D spheroids can be loosely placed into two categories as (i) spinner flask bioreactors that contain a stirring element to ensure that the cell suspension is continuously mixed [133] [140] and (ii) rotational culture systems which function by rotating the container of cells itself, rather than using a stirrer to maintain a cell suspension [141, 142]. The general principle behind these methods is that a cell suspension is placed into a container and the suspension is kept in motion, that is, either it is gently stirred or the container is rotated. The continuous motion of the suspended cells means that cells do not adhere to the container walls, but instead form cell–cell interactions, thus forming spheroids.

1.5.3.4 Matrices

As mentioned above, the make-up of mammary glands is complex and includes an organised branched network of ducts from epithelial cells [143]. Epithelial cells that make up mammary tissue develop in this highly organised manner by interacting with neighbouring cells and their ECM, including the basement membrane to which they are attached. Signals between these breast tissue components enable cells to arrange themselves in an appropriately organised way within the tissue. As ECM affects cellular organisation and cell function, 3D culture methods that incorporate ECM arguably help to better mimic *in vivo* situations, as they allow for cell–ECM interactions. Matrigel (BD Biosciences) is an example of a commercially-available ECM that can be used to support 3D culture [144]. Cells grown on, or in, ECM interact with each other in 3D and, as they continue to grow, they develop into structures similar to those found in the tissue from which the cells originated [145]. There are two commonly used methods for spheroid generation in ECM. In the first, cells are embedded and grown within the gel; in the second, the cells are grown on top of the gel [146].

1.5.3.5 Scaffolds

Prefabricated scaffolds can alternatively be used to aid 3D culture. Cells seeded into such scaffolds can migrate between fibres of the scaffolds and attach to them. The interstitial space between fibres is filled by cells as they grow and divide, forming 3D cellular structures [147]. Collagen, laminin, alginate [148] and other biodegradable materials are commonly used for this purpose [149]. These products can be processed to form hydrogels for use as 3D cell culture scaffolds. Gels that incorporate ECM molecules can apparently communicate *in vivo*-like cues to cells to enable *in vivo*-like

cell behaviour [150]. Hydrogels used in this manner are often porous. This allows oxygen, nutrients and drugs to reach the proliferating cells and also facilitates removal of waste molecules; thus providing appropriate cell culture conditions [151]. The size of pores in a hydrogel can be manipulated as necessary during production [152], enabling hydrogels to be engineered to suit experimental requirements, for example, for hypoxia or drug-based studies [153].

1.5.3.6 Microfluidic cell culture platforms

Toh *et al.* [154] described a microfluidic system that supports 3D culture. This system comprises a main microfluidic channel within which there is an array of micropillars through which a cell suspension is passed. The micropillar array is designed to immobilise passing cells within the pillars and supports their growth, thus enabling cell–cell interactions. A collagen matrix is then passed through the system and forms a thin layer over the cells, conforming to their shapes and allowing for cell–matrix interactions. Lei *et al.* also described a 3D cell culture microfluidic chip, however, an addition to this system is that enables impedance to be measured, thereby allowing real-time proliferation to be measured [155]. The MiCA plate (CellASIC) and the iuvo Microconduit Array Platform (BellBrook Labs) are 2 other examples of such commercially available products.

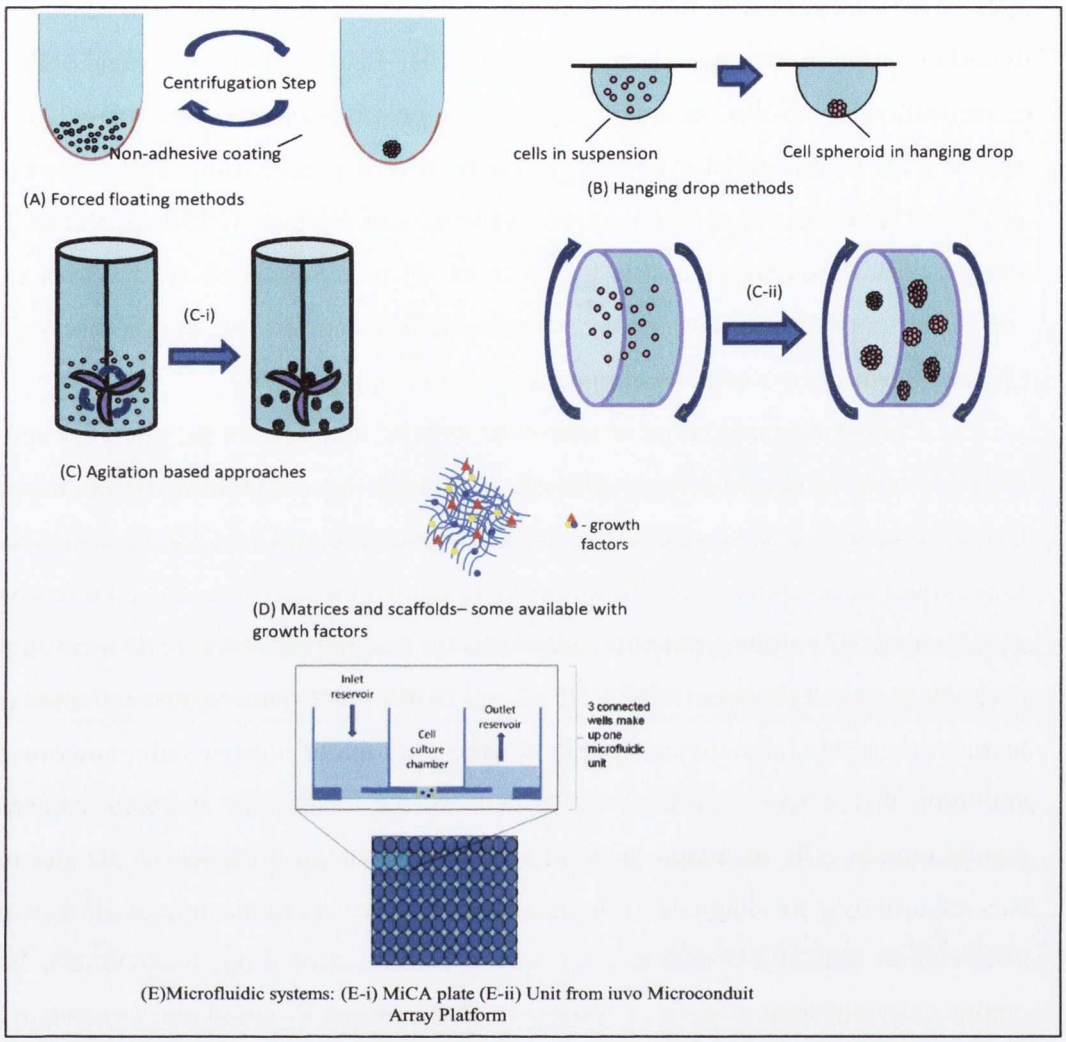

Figure 1.8. Methods for 3D cell spheroid production. (A) forced-floating; (B) hanging drop; (C) agitation methods; (D) matrices and scaffolds; (E) microfluidic platforms that support 3D cell growth.

1.5.4 Supporting evidence for the importance of including 3D cultures in drug development

Apart from the differences in the spatial arrangement of cells when grown in 2D or 3D, there are a number of biological differences that contribute to how the cells are exposed and thus react to therapeutic agents. The substantial effects that the microenvironment of a cell can have on its behaviour are well documented [118, 119]. For example, in a study by Weaver *et al.* [119], non-malignant HMT-3522 breast cells and malignant HMT-3522 type cells were grown in 3D using Matrigel. The normal cells formed organised, polarised acini, similar to those found in healthy breast tissue. The cancerous cells, however, formed disorganised, loose aggregates. Both normal and cancerous cell

types were treated with antibodies against β1-integrin, the surface receptor of which was found to be overexpressed on the cancerous cells. Treatment of the normal cells with these antibodies resulted in apoptosis, but treatment of cancerous cells resulted in an apparent reversal of phenotype back to the normal cell type, where cells appeared to lose their abnormal shape and growth patterns and become indistinguishable from normal cells. A similar result was not observed when the same cells were grown in 2D; indicating that extracellular cues can affect cellular phenotype and, in this case, cellular phenotype was proposed to be dominant over genotype [148].

Another example of an alteration of cellular architecture between 2D and 3D cells was observed in the growth of SKBR-3 cells that overexpress the HER2 oncogene. Cells grown as 3D spheroids using p-HEMA-coated plates had HER2 homodimers form; while in 2D cultures, HER2 formed heterodimers with HER3 [156]. Furthermore, in 3D versus 2D culture, epidermal growth factor receptor (EGFR) levels were slightly reduced; phosphorylation of HER2, HER3 and EGFR was enhanced; and activated AKT was downregulated. Finally, when a fixed concentration of trastuzumab (a monoclonal antibody that targets HER2) was added to the cells, 2D cultures underwent approximately 16% reduction in proliferation, whereas proliferation in 3D spheroids was reduced by a considerable 48%. This indicates that the architecture of 3D spheroids differs from that in 2D and that the targeted anti-cancer drug, trastuzumab, has a dramatically different effect on cells grown in monolayer as compared to those in 3D, due to differences in the cell surface molecules and thus intracellular signalling events. Pickl and Ries concluded the 3D cultures to be more representative of the HER2 signalling pathway in tumours *in vivo* [156].

This difference with sensitivity to drug exposure between cells grown in 2D and 3D has also been shown with classical chemotherapy drugs. Using the hanging drop method to generate 3D spheroids, Tung *et al.* presented data indicating that A431.H9 cells grown in 2D and 3D show differences in viability when treated with the same concentrations of 5-fluorouracil (5-FU) and tirapazamine (TPZ) [157]. In the case of 5-FU, 2D cultures were reduced to approximately 5% viability following a 96 hour treatment (5-FU; 10 μm), whereas 3D cells treated with the same concentration and duration remained at 75% viability; indicating that these 3D spheroids were more resistant to the antiproliferative effects of 5-FU. Conversely, cells treated for 96 hours with TPZ (10 μm) in 2D exhibit cell viability of 72%, whereas corresponding 3D cultures had a viability of just 40%. In this case, the 2D cells were more resistant to the effects of TPZ. This was reasoned to have occurred due to the mechanism of TPZ which,

as a hypoxia-activated cytotoxin, was activated more so in the 3D scenario as the core of the spheroids are hypoxic due to the limited ability of oxygen to diffuse to the centre of the spheroid. Consequently, TPZ was further activated in 3D cells due to the higher levels of hypoxic cells than in 2D, resulting in 3D cells being more sensitive to the effects of the drug.

These data show that the manner in which cells are cultured (i.e. 2D or 3D) can substantially alter the effect of a drug on the cells. Also, this research highlights the fact that cells in 3D do not necessarily exhibit a higher drug-resistance, but that it is a combination of the specific drug and the cellular environment that influence the cells' reaction. The hypoxic core described by Tung *et al.* mimics the hypoxic core found in solid tumours that occurs due to poor oxygen diffusion into cells at the centre of a cancerous mass, as oxygen cannot diffuse past an approximate 200μm limit [158]. Up to 60% of solid tumours have hypoxic regions within their structure [159]. This further supports the 3D spheroid tumour models as relevant for investigating effects of drugs intended for use on solid tumours, as hypoxia has many effects in tumour biology, some of which can affect drug responses. For example, hypoxia can enhance receptor tyrosine kinase-mediated signalling, it can cause pro-survival alterations in expression of genes that suppress apoptosis, and it can affect DNA repair pathways [158].

The hypothesis that differences in culture environment can affect how cells will respond to drug treatment is supported by findings that cells grown as spheroids exhibiting polarised 3D architecture and show difference in resistance to apoptosis and chemotherapeutic drugs (in addition to those mentioned above) when compared to 2D controls [160]. For example Li *et al.* showed that MCF10A cell variants in 3D exhibit a higher resistance to doxorubicin compared to 2D controls [161]; SA87, NCI-H460 and H460M cells grown in 3D have higher resistance to 5-FU and doxorubicin than those in 2D [162]; and MCF-7 cells grown in 3D and then treated with tamoxifen are less susceptible to the cytotoxic effects of the drug than cells grown in the same tamoxifen concentrations, but in 2D [163].

In vivo, tumours can develop drug gradients, due to poor drug uptake by a tumour or poor distribution of drugs within a tumour. This phenomenon can reduce therapeutic effects of a drug at the target site [164]. The rate at which drugs diffuse into a cancerous mass effects the efficiency of treatment with that drug; therefore, it is an important pharmacokinetic feature that should be replicated in cell-based *in vitro* drug development assays. Thurber and Wittrup discuss the distribution of drugs in tumours compared to 3D spheroids [164]. While the variabilities noted as contributing to drug

penetration of a tumour *in vivo* were found to be a function of concentration and exposure time, variabilities that effect drug penetration into multi-cellular spheroid included drug dose, antigen density (for antibody-based therapy), incubation time and spheroid size. Spheroids used for this study were generated using the hanging drop method and were found to closely replicate drug diffusion observed in the *in vivo* scenario. This indicated that 3D spheroids would be useful for pre-*in vivo* drug screening during development. Similarly, others have reported that drug diffusion through cells is reduced in 3D spheroid [165].

1.6 Project aims

Overall, the aim of this project was to investigate drug-resistance in HER2-overexpressing breast cancer using cell lines (in both 2D and 3D cell cultures) and also the relevance of EVs as biomarkers for response to therapy in breast cancer.

- Acquired resistance to neratinib was investigated using two HER2-overexpressing breast cancer cell lines, HCC1954 and EFM192A. Once neratinib-resistant cell lines were established, the effects of the acquired-resistance on these cells were determined by assessing any cross-resistance to other drugs; the effects of drug-resistance on cell aggression; and subsequently we aimed to elucidate the mechanism that facilitated resistance to neratinib *in vitro*.

- Evaluating serum specimens procured from breast cancer patients with HER2-overexpressing breast tumours and control serum specimens, EVs were isolated and the relevance of their quantities towards cancer diagnosis and patient response to therapy were investigated. Additionally, the content and relative expression of NmU, HER2 and survivin in EVs was investigated for their potential use as companion biomarkers for predicting response to therapy.

- Finally, three HER2-overexpressing breast cancer cell lines, BT474, HCC1954 and EFM192A, were grown using 2D and 3D cell culture methods. In order to characterise any differences between the two culture methods, expression levels of proteins involved in cell growth and survival, drug targets and drug transporters were measured. In addition, the efficacy of drugs on cells grown in 2D and 3D was compared in order to see if innate levels of drug response/resistance is altered between the cell culture methods used. Effects of growing cells in 2D and 3D on EV secretion were also investigated.

Chapter 2: Acquired neratinib-resistance induces cross-resistance to HER-targeting drugs and increased cell aggression in HER2-overexpressing breast cancer cells

2. Abstract

Introduction: Neratinib is an EGFR, HER2 and HER4 tyrosine kinase inhibitor that is being investigated in Phase III clinical trials for its efficacy in treating HER2-overexpressing breast cancer patients. Here, we provide an insight into the effects and potential mechanisms of acquired neratinib-resistance using two novel cell line models.

Methods: Neratinib-resistant cells were generated by long-term exposure of the cells to neratinib. Development of neratinib-resistant cell lines and cross-resistance of neratinib-resistant cells to HER-targeting agents was determined using proliferation/*in vitro* cytotoxicity assays. Similarly, the cross-resistance of trastuzumab-resistant and lapatinib-resistant cells to neratinib was determined in this way. Cell characterisation studies included migration, invasion and *anoikis* assays. The mechanism of acquired neratinib-resistance was investigated using immunoblotting, ELISA and CYP3A4 activity assays.

Results: In this study, we show that cells with acquired neratinib-resistance are also cross-resistant to other HER-targeting agents tested, *i.e.* lapatinib and afatinib. Efficacy of neratinib was reduced in trastuzumab- and lapatinib-resistant cells. Cell characterisation studies indicated that these neratinib-resistant cells are significantly more aggressive than their drug-sensitive parent cell lines. Neratinib-resistant cells were shown to have decreased expression of its target members of the EGFR family. Additionally, Neuromedin U (NmU) was significantly increased in neratinib-resistant cells and so appears to form part of the mechanism of neratinib-resistance. Furthermore, a novel mechanism of HER2-targeting drug resistance was identified, which involves increased CYP3A4 activity.

Conclusion: The development of neratinib-resistance is associated with increased cell aggression and cross-resistance to other HER-targeting drugs *in vitro*, indicating that the development of neratinib-resistance may interfere with effective anti-cancer therapy, including other HER-targeting drugs, in the clinic. Both NmU and CYP3A4 appear to be at least partially responsible for neratinib-resistance in these breast cancer cells.

2.1 Introduction

The increased understanding of molecular oncology has enabled the development of a range of targeted therapies for breast cancer, including HER2-targeting trastuzumab, lapatinib and pertuzumab, which have all been approved for breast cancer treatment. However, despite the fact that these drugs are effective anti-cancer agents, their use is limited by the development of drug resistance, due to the highly-adaptive nature of tumour cells. It follows that elucidating mechanisms of resistance to anti-cancer drugs is of utmost importance to ensuring effective patient therapy. The most common ways of doing this are to either model the development of drug-resistance using a drug-sensitive cell line by exposing these cells to the drug of choice over time until they are resistant to its effects or to analyse tumour biopsies from patients in order to identify genes and/or proteins that could be mechanistically involved in resistance to therapy.

Successful identification of mechanisms of resistance to particular drugs may lead to the prevention of drug resistance from developing or may lead to the development of inhibitors for mediators of drug-resistance, which could allow drug efficacy to be reinstated and improve patient disease management. In addition to having an understanding of cellular mechanisms that mediate drug-resistance, it is also useful to know which drugs are likely still effective in a patient that has developed resistance to their first type of treatment. In this way, clinicians may have viable alternative treatment options once drug-resistance to a primary therapy occurs.

Neratinib is an irreversible EGFR, HER2 and HER4 tyrosine kinase inhibitor being investigated in clinical trials for HER2-overexpressing breast cancer treatment [69, 70, 166]. It is an irreversible inhibitor of both EGFR and HER2 tyrosine kinases and acts by covalently interacting with Cys-773 and Cys-805, which are conserved cysteine residues found in EGFR and HER2 kinase domains, respectively [167]. Neratinib was developed by modifying pelitinib (EKB-569), a compound that exhibited inhibitory effects on HER2 and EGFR kinases, but whose effects on HER2 were less potent than those being exhibited by neratinib. A Phase 1 clinical study of neratinib found it to have an acceptable safety profile with anti-tumour activity observed with once daily oral administration of the drug to patients with advanced solid tumours [168]. Phase 2 data reported that neratinib resulted in substantial clinical activity in advanced HER2-overexpressing cancer in terms of progression-free survival and reduction of tumour burden treatment [169]. Early clinical data from Swaby *et al.* [170] indicates that dual administration of neratinib with trastuzumab is well tolerated in patients with

advanced HER2-overexpressing breast cancer and produces a clinical response. Additionally, Awada *et al.* [171] observed anti-tumour activity in patients with HER2-overexpressing metastatic breast cancer treated with neratinib and vinorelbine, where patient responses to dual therapy show a higher progression free survival rate than neratinib monotherapy. Multiple other clinical trials investigating neratinib efficacy are also underway [70, 172-174].

To the best of our knowledge, there is very limited published data detailing the ability of breast cancer cells to acquire neratinib resistance *in vitro* and the effects that this acquired resistance has on cell behaviour. Seyhan *et al.* [175] found that the expression of a number of genes involved in oncogenesis, transcription factors and cellular ion transport are altered due to neratinib-resistance. However, this group did not show any functional effects that this acquired-resistance had on cells.

In this study, following the development of neratinib-resistant cells using HER2-overexpressing breast cancer cell lines, HCC1954 and EFM192A, we aimed to determine if neratinib-resistant cells were cross-resistant to other drugs typically used in breast cancer treatment; to investigate phenotypic changes that may have developed with neratinib-resistance; and to elucidate the mechanism that may, at least in part, be responsible for acquired neratinib-resistance by comparing protein expression and metabolic enzyme activity in neratinib-sensitive and neratinib-resistant cells.

2.2 Materials and methods

2.2.1 Cell culture

HCC1954 (derived from ductal carcinoma) and EFM192A (derived from adenocarcinoma) cell lines were obtained from the American Tissue Culture Collection and Leibniz-Institut DSMZ, respectively. Cells were cultured in RPMI-1640 (Sigma-Aldrich; Cat. #: R0883) supplemented with 10% FBS (Gibco; Cat. #: 10270-106) and 1% L-glutamine (Sigma-Aldrich; Cat. #: G7513). HCC1954 neratinib-resistant (HCC1954-NR) and EFM192A neratinib-resistant (EFM192A-NR) cell line variants were established by continuous exposure to increasing concentrations of neratinib (up to 250nM for HCC1954-NR cells; up to 80nM for EFM192A-NR cells) for approximately 4 months. Age-matched controls for both cell lines – HCC1954-Par and EFM192A-Par cells, were also maintained. Lapatinib-resistant HCC1954 and SKBR3 (derived from adenocarcinoma at metastatic site) cells (SKBR3-LR, HCC1954-LR) were established by exposing cells to increasing concentrations of lapatinib (up to 250nM) over 6 months. Trastuzumab-resistant SKBR3 (SKBR3-TR) cells were established by continuous exposure to 100μg/mL trastuzumab for 9 months [176]. Neratinib (Cat. #: SRP06000n), lapatinib (Cat. #: SRP01211l) and afatinib (Cat. #: SRP04670c) were obtained from Sequoia Research Products Ltd, while docetaxel was purchased from Sigma Aldrich (Cat. #: D2650). Trastuzumab (Herceptin, Roche) was obtained from St. James' Hospital.

2.2.2 Toxicity assays

The IC_{50} values of HCC1954-Par, HCC1954-NR, EFM192A-Par and EFM192A-NR for neratinib, afatinib, lapatinib, trastuzumab and docetaxel were determined using *in vitro* cytotoxic proliferation assays. Afatinib, neratinib, lapatinib and docetaxel stocks were diluted in DMSO. HCC1954-Par and HCC1954-NR cells were seeded at $3x10^3$cells/well and EFM192A-Par and EFM192A-NR cells were seeded at $5x10^3$cells/well, in a 96 well plate (Sigma-Aldrich; Cat. #: 3595). All drugs were prepared in RPMI (10% FBS, 1% L-glutamine) and 24 hours after seeding cells, drugs were added at 2x of the final treatment concentration in 100μL complete RPMI to make a 1x final concentration once added to the 100μL RPMI used to seed cells. Concentrations were as follows: neratinib (0-100nM for HCC1954-Par; 0-900nM for HCC1954-NR; 0-125nM for EFM192A-Par and 0-1μM for EFM192A-NR), afatinib (0-900nM for HCC1954-Par; 0-7μM for HCC1954-NR; 0-5μM for EFM192A-Par and 0-

10μM for EFM192A-NR), lapatinib (0-1.4μM for HCC1954-Par; 0-10μM for HCC1954-NR; 0-2.5μM for EFM192A-Par and 0-10μM for EFM192A-NR), trastuzumab (0-500μg/mL for EFM192A-Par and 0-500μg/mL for EFM192A-NR), docetaxel (0-7nM for HCC1954-Par; 0-7nM for HCC1954-NR; 0-125nM for EFM192A-Par and 0-125nM for EFM192A-NR). Sensitivity of HCC1954-LR, SKBR3-LR and SKBR3-TR to neratinib was also determined and compared to HCC1954-Par and SKBR3-Par values, respectively. HCC1954-LR cells were seeded at $3x10^3$cells/well and SKBR3-LR and SKBR3-TR cells were seeded at $1x10^4$cells/well, in a 96 well plate. As above, 24 hours after seeding cells were exposed to increasing concentrations of neratinib (0-100nM for HCC1954-LR; 0-20nM for SKBR3-LR and 0-20nM for SKBR3-TR).

After 5 days growth in the presence of drugs, cell viability was measured using the acid phosphatase assay method [177]. Briefly, culture medium was removed from wells and plates were washed twice with 100μL PBS (Sigma-Aldrich, Cat. #: D8537) per well. After the second wash, plate was blotted on tissue paper to ensure all PBS was removed. 100μL of freshly prepared phosphatase substrate (10mM p-nitrophenol phosphate (VWR; Cat. #: 27963.101) in pre-prepared 1 M sodium acetate buffer (Table 2.1)) was added to each well. Plates were covered in tin foil and placed in the incubator at 37°C/5% CO_2, for 1.5 hours. The reaction was stopped by adding 50μL 1 M NaOH to each well. Absorbance was read at 405nm, using a FlouStar Optima microplate reader (BMG Labtech).

Reagent	Amount
Sodium Acetate (Sigma-Aldrich, Cat. #: S2889)	4.1g
TritonX-100 (Sigma-Aldrich, Cat. #: T8787)	500μL
dH_2O	500mL
Adjust pH to 5.5	

Table 2.1. Preparation of sodium acetate buffer.

2.2.3 Proliferation assays

HCC1954 cell variants were seeded in 96-well plates (Sigma-Aldrich; Cat. #: 3595) at a density of $3x10^3$ cells/200μL/well, while EFM192A cell variants were seeded at $5x10^3$ cells/200μL/well. Cell proliferation was measured at 24, 48, 72 and 96 hours after seeding using the acid phosphatase assay method as described in Section 2.2.2.

2.2.4 Migration assays

Migration assays for HCC1954 cells were performed using 8μm pore cell culture inserts. HCC1954-Par and HCC1954-NR cells were seeded at $1x10^5$ cells/well in a 24 well plate in RPMI (1% FBS) within cell culture inserts (Unitech; Cat. #: 353097). 400μL of RPMI (10% FBS) was placed in the wells under inserts. Cells were allowed to migrate through the 8μm pores of the inserts over 24 hours. Cells that did not migrate were removed with a PBS soaked swab. Inserts were washed with PBS and migrated cells were stained with crystal violet (Sigma-Aldrich; Cat. #: C3886). Photographs of migrated cells were taken before crystal violet was solubilised with 10% acetic acid (Sigma-Aldrich; Cat. #: 27225). Solubilised crystal violet absorbance was read at 595 nm [178].

Migration assays for EFM192A-Par and EFM192A-NR cells were performed using a wound healing assay as these cells were found not to pass through a cell culture insert. These cells were seeded at $5x10^5$ cells/well in a 24-well plate (Sigma-Aldrich; Cat. #: 3524). Cells were allowed to attach and form a monolayer. Medium was removed from wells and the monolayer of cells was scratched using a p200 tip. 1% FBS-supplemented RPMI medium was carefully placed in each well and the wound size was captured by phase contrast microscopy using AxioVision Release 4.7 software and measured using NIH Image J software at 0, 24 and 48 hours. Note: 1% FBS supplemented medium was used in order to reduce any effects of proliferation on the measurement of cell migration during this assay.

2.2.5 Invasion assays

Cell culture inserts were coated with 200μL ECM (Sigma-Aldrich; Cat. #: E1270), placed in a 24-well plate and left at 4°C for 4 hours in order to allow the ECM to gel [178]. HCC1954-Par and HCC1954-NR cells were seeded at $1x10^5$ cells/400μL/well. Cells were seeded in 1% FBS supplemented RPMI and 400μL of regular 10% FBS supplemented RPMI was placed in the wells below the insert, in order to make a cell nutrient gradient to encourage cells to invade through the pores of the insert. HCC1954 cell variants were allowed to invade through ECM and pores for 48 hours. Following this, cells that had invaded through to the other side of their inserts were quantified as per migration assay described in Section 2.2.4.

2.2.6 *Anoikis* assays

24-well plates were prepared for *anoikis* assays by coating wells with 200µL of poly(2-hydroxyethyl methacrylate) (poly-HEMA) (Sigma-Aldrich; Cat. #: P3932) solution - 12mg/mL poly-HEMA prepared in 95% ethanol. Poly-HEMA was allowed to completely evaporate and the coating process was performed a second time. 95% ethanol coated wells served as controls. HCC1954-Par, HCC1954-NR, EFM192A-Par and EFM192A-NR cells were all seeded at a cell density of $5x10^4$cells/mL/well. 48 hours after seeding, 100µL of alamar blue (Invitrogen; Cat. #: DAL1100) solution was added to each well, plates were covered in tin-foil and placed in an incubator for 5 hours. After this incubation absorbance was read at 570 nm using a FluoStar Optima microplate reader.

2.2.7 Immunoblots

Cells were scraped using cell scrapers (Fisher Scientific, Cat. #: 08-100-241) and centrifuged at 13,000*g*. Pellets were washed with 1mL PBS and centrifuged again. PBS was removed and pellets were lysed using Cell Extraction Buffer (Invitrogen, Cat. #: FNN0011) supplemented with protease inhibitor cocktail (Roche, Cat. #: 05892970001) on ice for 30 minutes and vortexed for 10 seconds every 10 minutes during this time. Following this, lysates were centrifuged at 13,000g for 10 minutes at 4°C and lysates were transferred to fresh Eppendorf tube.

Protein was quantified using BioRad protein assay dye reagent (BioRad, Cat. #: 500-0006). Protein from each sample was diluted 1:10 (1µL sample + 9µL dH_20) in duplicate in a 96 well plate. Protein standards (10µL) (from same BioRad, Cat. #: 500-0006 kit) were also prepared in duplicate (0µg/mL, 12.5 µg/mL, 25µg/mL, 50µg/mL, 100µg/mL, 200µg/mL, 400µg/mL). Bio-Rad protein assay reagent was diluted 1:5 with dH_20 and 200µL of this solution was added to each sample and standard. Plate was incubated in the dark for 5 minutes and absorbance was read at 595nm using a FluoStar Optima Microplate Reader (BMG Labtech). Linear regression was applied to absorbance readings obtained using GraphPad Prism and the unknown concentrations of samples were extrapolated from the standard curve. Loading buffer was added to a final concentration of 1x and samples were heated at 95°C for 5 minutes.

30µg total cellular sample protein was used for EGFR, HER2 and HER3, while 50µg total cellular sample protein was used for HER4, PGP and BCRP immunoblots. 7.5% sodium dodecyl sulphate gels were used to resolve sample proteins along with a

molecular weight marker, SeeBlue Plus2 Pre-Stained standard (Invitrogen; Cat. #: LC5925). Separated proteins were transferred to polyvinylindene fluoride (PVDF) membranes (Bio-Rad; Cat. #: 162-0177) using semi-dry transfer. Ponceau (Sigma-Aldrich; Cat. #: P7170) was used to ensure successful transfer of proteins onto the membrane. Blots were then washed 3 times for 5 minutes in PBS-tween (0.1%) and blocked in 5% bovine serum albumin (BSA) in PBS-tween for 1 hour at room temperature. Blots were washed again and incubated overnight at 4°C in primary antibodies: HER2 (Calbiochem; Cat. #: OP15; 1:500), EGFR (Cell Signalling; Cat. #: D38131; 1:1000), HER3 (Cell Signalling; Cat. #: 4754; 1:1000), HER4 (Cell Signalling; Cat. #: 4795; 1:1000), PGP (Santa Cruz; Cat. #: SC55510; 1:200), BCRP (Santa Cruz; Cat. #: sc-58224; 1:200) and β-actin (Sigma-Aldrich; Cat. #: A5316; 1:1000). Horseradish peroxidase-conjugated secondary antibodies were used as appropriate: Anti-rabbit (Cell Signalling; Cat. #: 7076; 1:1000) and Anti-mouse (Cell Signalling; Cat. #: 7074; 1:1000) and Anti-Rat (Santa Cruz; Cat. #: sc-2006; 1:1000). Blots were washed again and protein bands were visualised by chemiluminescence (ThermoFisher; Cat. #: 34080) using a Chemidoc exposure system (BioRad laboratories). Densitometry was performed on the bands of protein detected by immunoblot using ImageJ software and normalised to β-actin which served as a loading control.

2.2.8 qPCR miR-210

2.2.8.1 Preparation of cDNA for miR-210

cDNA was prepared for qPCR to measure miR-210 levels in cell samples. 4μL total RNA (10ng) per sample was used for cDNA synthesis. The RNA was added to 11μL of a master mix per sample, as outlined in Table 2.2, to produce a total of 15μL cDNA. Once reagents were prepared, cDNA was made using incubation times and temperatures as outlined in Table 2.3.

Reagent	Volume (per sample)
100mM dNTP (Life Technologies; Cat. #: 18427013)	0.15μL
Multiscribe reverse transcriptase (Life Technologies; Cat. #: 18427013)	1μL
10x RT buffer (Life Technologies; Cat. #: 18427013)	1.5μL
Rnase inhibitor (Life Technologies; Cat. #: 18427013)	0.19μL
Nuclease free water (Life Technologies; Cat. #: AM9920)	5.16μL
5x primer (Life Technologies; Assay ID 000512)	3μL
Total RNA	4μL

Table 2.2. Preparation of master mix for miR-210 cDNA synthesis.

Steps	Temperature	Duration
Step 1	16°C	30 mins
Step 2	42°C	30 mins
Step 3	85°C	5 mins
Step 4	4°C	∞

Table 2.3. Incubation times and temperatures used to prepare miR-210 cDNA.

2.2.8.2 qPCR miR-210

qPCR was performed for miR-210 using 1.33µL cDNA per technical repeat for each sample. Taqman assays were used (miR-210: Assay ID: 000512) and purchased from Life Technologies. Reagents for qPCR were prepared as outlined in Table 2.4 and qPCR was run under conditions outlined in Table 2.5. miR-210 was quantified using the cycle threshold (C_T) adjusting to the levels of U6 snRNA (Assay ID #: 001973), which was used as an endogenous control.

Reagent	Volume (per sample)
20x primer	1µL
Nuclease free water (Life Technologies; Cat. #: AM9920	7.67µL
Taqman 2x Universal PCR master mix, no Amperase UNG	10µL
Prepared cDNA	1.33µL
Total reaction volume	**20µL**

Table 2.4. Preparation of master mix for qPCR.

Steps	Temperature	Duration
Step 1	95°C	10mins
Step 2:	95°C	15secs
40 cycles	60°C	60secs

Table 2.5. Incubation times and temperatures used to perform qPCR.

2.2.9 Quantification of cellular ATP

HCC1954-Par and HCC1954-NR cells were seeded at $1x10^4$ cells/100µL/well and EFM192A-Par and EFM192A-NR cells were seeded at $1x10^4$ cells/100µL/well, in 96-well plates. 48 hours after seeding, ATP assay was performed using CellTitre-Glo (Promega; Cat. #: G9681), where medium was removed from wells, 70µL medium was replaced with fresh medium and 70µL CellTitre-Glo substrate was added. Cells were incubated at room temperature for 20 minutes and assay solution from each well was transferred to a white, opaque 96-well plate for luminescence reading. Plates were read

using a Luminoskan luminescence plate reader (Thermo Scientific). Note: white plates were kept in the dark prior to use to prevent their auto-luminescence in the plate-reader.

2.2.10 Flow cytometry analysis of cells with stem cell-like properties

[Performed with the help of Dr. Vanesa Martinez]

HCC1954-Par, HCC1954-NR, EFM192A-Par and EFM192A-NR cells were seeded at $1x10^5$ cells/2mL/well of a 6-well plate and were allowed to attach overnight. Cells were trypsinised, washed in PBS and blocked with 10% FBS diluted in PBS at 4°C for 15 minutes. Cells were then washed again with PBS and stained with APC-conjugated anti-CD24 (eBioscience; Cat. #:17-0247-41) (1:75 in 10% FBS diluted in PBS) and FITC-conjugated anti-CD44 (eBioscience; Cat. #: 11-0441-82) (1:800 10% FBS diluted in PBS) for 30 min at 4°C in the dark. Cells were washed again and resuspended in 200µL 10% FBS diluted in PBS. Cell staining for CD24 and CD44 was measured using a FACSCanto II flow cytometer (BD Biosciences) and analysed using BD FACSDiva software.

2.2.11 NmU

NmU was quantified from cell lysates by ELISA (Peninsula Laboratories International; Cat. #: S-1253.0001) which was performed according to manufacturer's instructions using 2.5µg (HCC1954-Par and HCC1954-NR cells) and 10µg (EFM192A-Par and EFM192A-NR cells) of total cellular protein diluted in 50µL enzyme immunoassay buffer, which was provided in the ELISA kit.

2.2.12 Cytochrome p450 assay

HCC1954-Par and HCC1954-NR cells were seeded at $3x10^3$ cells/100µL/well and EFM192A-Par and EFM192A-NR cells were seeded at $5x10^3$ cells/100µL/well, in a 96-well plate. 48 hours after seeding, P450-Glo CYP3A4 (Promega; Cat. #: V9001) assay was performed by removing medium from wells with a pipette and adding 50µL of 3µM Luciferin-IPA solution (1:1000 dilution of Luciferin-IPA solution provided in kit, diluted in base RPMI medium) per well. Plate was returned to 37°C incubator for 1 hour and, following this, 50µL of the Luciferin detection reagent (provided in P450-Glo CYP3A4 kit) was added. Assay solution was allowed to incubate at room temperature for 20 minutes and solution in each well was transferred to a white opaque 96-well plate

for luminescence reading. Plates were read using a Mithras LB 940 (Berthold Technologies) luminescence plate reader using no filter.

2.2.13 Statistical analysis

Statistical analysis of data was performed using Excel. *P*-values were generated using Student's t-tests, where $p<0.05$ was considered as statistically significant. Results are displayed as n=3± standard error of mean (SEM). Graphs were generated using GraphPad software.

2.3 Results

2.3.1 Establishment of HCC1954-NR and EFM192A-NR variants

Two neratinib-resistant breast cancer cell line variants, HCC1954-NR and EFM192A-NR, were generated by culturing HCC1954 and EFM192A cells with increasing concentrations of neratinib (see Section 2.2.1). Once established, HCC1954-NR cells proliferated well in 250nM neratinib, while EFM192A-NR cells proliferated well in 80nM neratinib. The age-matched drug-naïve control cells of HCC1954 (HCC1954-Par) and EFM192A (EFM192A-Par) are sensitive to neratinib and were maintained in culture while the resistant-variants were being established. HCC1954-NR cells were found to have an approximate 6.5±0.4 fold increase in resistance compared to the HCC1954-Par cells ($p=1.08x10^{-4}$), while EFM192A-NR cells have an approximate 6.8±0.3 fold increase in resistance to neratinib when compared to EFM192A-Par cells ($p=5.1x10^{-5}$) (Table 2.6).

IC_{50} and fold difference values for HCC1954 and EFM192A parent and neratinib-resistance cell variants				
Drug	**HCC1954-Par**	**HCC1954-NR**	**Fold Difference**	**p-value**
Neratinib	49 nM	325 nM	6.5 ± 0.4	$1.08x10^{-4}$
Afatinib	103 nM	3.6 μM	37 ± 7.2	0.008
Lapatinib	273 nM	2.7 μM	10 ± 0.8	$3.7x10^{-7}$
Trastuzumab	Innate resistance	Innate resistance	N/A	N/A
Docetaxel	0.6 nM	0.65 nM	1.08 ± 0.04	0.15
Drug	**EFM192A-Par**	**EFM192A-NR**	**Fold Difference**	**p-value**
Neratinib	6.8 nM	46.7 nM	6.8 ± 0.3	$5.1x10^{-5}$
Afatinib	151.3	5.1 μM	34.6 ± 4.4	0.002
Lapatinib	50 nM	7.97 μM	162.9±22	$4x10^{-6}$
Trastuzumab	>500μg/mL	>500μg/mL	N/A	N/A
Docetaxel	2.6	2.7	1.03±0.07	0.692

Table 2.6. IC_{50} and fold difference values for HCC1954 and EFM192A parent and resistant cells. Average IC_{50} values for neratinib, afatinib, lapatinib, trastuzumab and docetaxel in HCC1954-Par, HCC1954-NR, EFM192A-Par and EFM192A-NR cells with corresponding fold difference values. Values indicate that neratinib-resistant cells are also cross-resistant to afatinib, lapatinib and trastuzumab, but not docetaxel (n=3±SEM).

2.3.2 Cross-resistance to other anti-cancer drugs due to neratinib-resistance

Both HCC1954-NR and EFM192A-NR cell variants demonstrated cross-resistance to HER-targeting agents, afatinib and lapatinib, compared to their age-matched controls. Specifically, HCC1954-NR cells are 37±7.2 and 10±0.8 fold more resistant to afatinib and lapatinib, respectively, than HCC1954-Par cells. EFM192A-NR cells are 34.6±4.4 and 162.9±22 fold more resistant to afatinib and lapatinib compared to EFM192A-Par cells, respectively. EFM192A-Par and EFM192A-NR cells do not appear to be sensitive to the effects of trastuzumab as both cell variants maintained over 80% cell viability following treatment with 500μg/mL trastuzumab for 5 days. IC_{50} values for HCC1954-Par and HCC1954-NR cells for docetaxel were 0.6nM and 0.65nM; values for EFM192A-Par and EFM192A-NR cells were 2.6nM and 2.7nM, respectively, which indicate that cross-resistance to docetaxel does not occur with neratinib-resistance (Table 2.3.1).

2.3.3 Cross-resistance to neratinib due to LR and TR

HCC1954-LR cells demonstrated cross-resistance to neratinib, with a 1.7±0.1 fold increase in resistance to neratinib compared to HCC1954-Par cells. Similarly, SKBR3-LR cells had a 15.3±3.2 fold increase in resistance to neratinib compared to sensitive control cells. SKBR3-TR cells exhibited a 3.3±0.2 fold increase in resistance to neratinib compared to SKBR3 parent cells (Table 2.7).

Sensitivity of lapatinib and trastuzumab-resistant cells to neratinib			
IC50 neratinib		**Fold difference**	**p-value**
HCC1954-Par	**HCC1954-LR**		
53 nM	91 nM	1.7±0.1	0.001
SKBR3-Par	**SKBR3-LR**		
4.7 nM	69.3 nM	15.3±3.2	0.002
SKBR3-Par	**SKBR3-TR**		
4 nM	15 nM	3.3±0.2	$2.4x10^{-4}$

Table 2.7. Average IC_{50} values for neratinib in HCC1954-Par and -LR, SKBR3-Par, -LR and -TR cells with corresponding fold difference values. Data indicates that cells with acquired-resistance to lapatinib and trastuzumab are also cross-resistant to neratinib (n=3±SEM).

2.3.3 Reduced cell proliferation due to neratinib-resistance

Proliferation assays (see Section 2.2.3) were performed over 4 days to evaluate the effect of long-term exposure to neratinib on cells (Figure 2.1). At days 2, 3 and 4, for both cell lines, there was a trend for slower growth in the neratinib-resistant cell line variants compared to parent-control cell variants. By day 4 of the assay, HCC1954-NR cells proliferated 1.4±0.1 fold slower than HCC1954-Par cells ($p=0.015$) and EFM192A-NR cells proliferated 1.5±0.14 fold slower than EFM192A-Par cells ($p=0.025$).

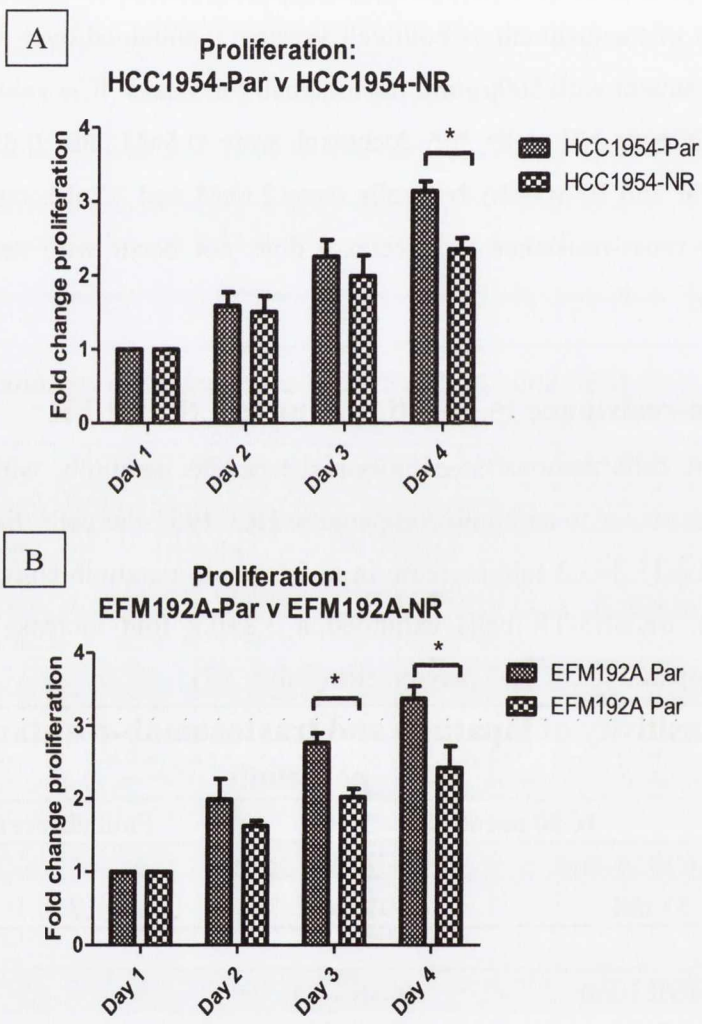

Figure 2.1. Proliferation assays of NR compared to Par cells. Proliferation was significantly decreased in (A) HCC1954-NR cells and (B) EFM192A-NR cells in comparison to control cells (n=3±SEM), where *$p<0.05$.

2.3.4 Increased cell migration in neratinib-resistant cells

Cell migration was measured using cell-culture insert migration assays for HCC1954 cell variants while wound-healing assays were performed on EFM192A cell variants (see Section 2.2.4), as EFM192A cells seemed not to pass through cell culture inserts. Results observed indicate that neratinib-resistance enhances the ability of cells to migrate (Figure 2.2.A), where HCC1954-NR cells migrated 1.25±0.03 fold more than HCC1954-Par cells (p=0.002). Similarly, but using the wound-healing assay, EFM192A-NR cells were found to be more migratory compared to EFM192A-Par cells (Figure 2.3.2.B). Specifically, 24 hours after the 'wound' was scratched in the cell monolayers, wound closure was 18.8±3.8% for EFM192A-Par cells and 23.3±4.9% for EFM192A-NR cells. At this time point, the % wound closure for neratinib-resistant cells was higher than control cells, but not significantly (p=0.513). However, after 48 hours, wound closure was 29.1±3.74% for EFM192A-Par cells and 46.1±3.86% for EFM192A-NR cells (p=0.034).

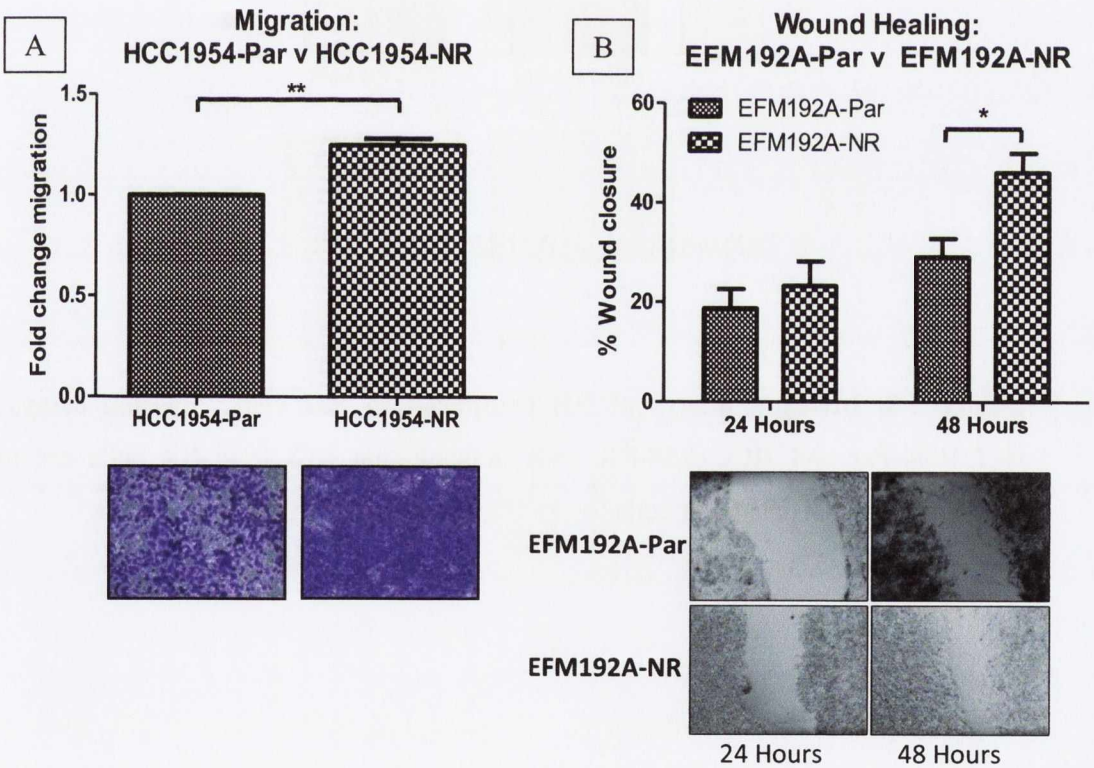

Figure 2.2 Migration and wound healing assays of NR compared to Par cells. Migration assays indicate that (A) HCC1954-NR cells are more migratory than HCC19954-Par cells and (B) EFM192A-NR cells are more migratory than EFM192A-Par cells (n=3±SEM), where *p<0.05 and **p<0.01.

2.3.5 Increased cell invasion in neratinib-resistant cells

Neratinib-resistance also influences cell invasion, as seen in Figure 2.3. Cell invasion was assessed using an ECM-coated insert and revealed that HCC1954-NR cells are 1.31±0.04 fold more invasive than HCC1954-Par cells (p=0.001). Data for invasion assays performed on the EFM192A cell variants is not shown as these cells do not seem to pass through the ECM-coated insert, therefore this assay is not possible to perform using these cells.

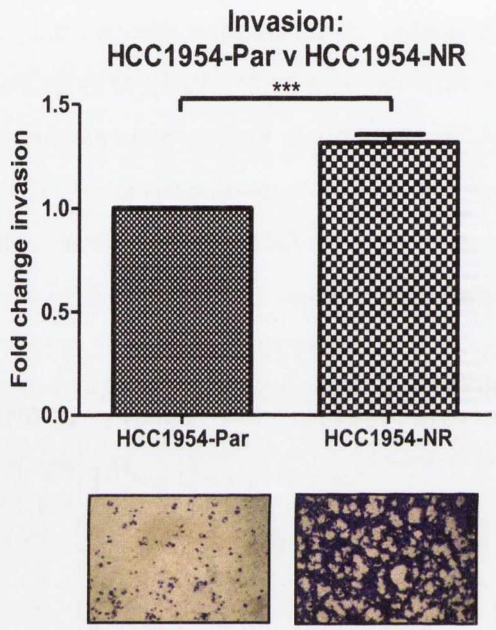

Figure 2.3. Invasion assays of NR compared to Par cells. Invasion assays for HCC1954-Par and HCC1954-NR cells indicate that HCC1954-NR cells are more invasive than HCC1954-Par cells (n=3±SEM), where ***p<0.001.

2.3.6 Neratinib-resistant cells demonstrate an increased resistance to anchorage-independent cell death i.e. *anoikis*

Anoikis assays were performed in order to measure any effects that acquired neratinib-resistance may have on the ability of cells to resist anchorage-independent cell death (Figure 2.4). We observed that HCC1954-NR cells were more resistant to anchorage-independent induced cell death, where only 2.8±0.2% of HCC1954-NR cells died under forced floating conditions during the 48 hour assay period, compared to 12±1.7% of HCC1954-Par cells ($p=0.003$) under the same conditions. Similarly, EFM192A-NR cells were also more resistant to *anoikis*, where only 24.7±1.1% of EFM192A-NR cells died during the assay period compared to 33.7±0.8% of EFM192A-Par cells ($p=7.0\times10^{-4}$).

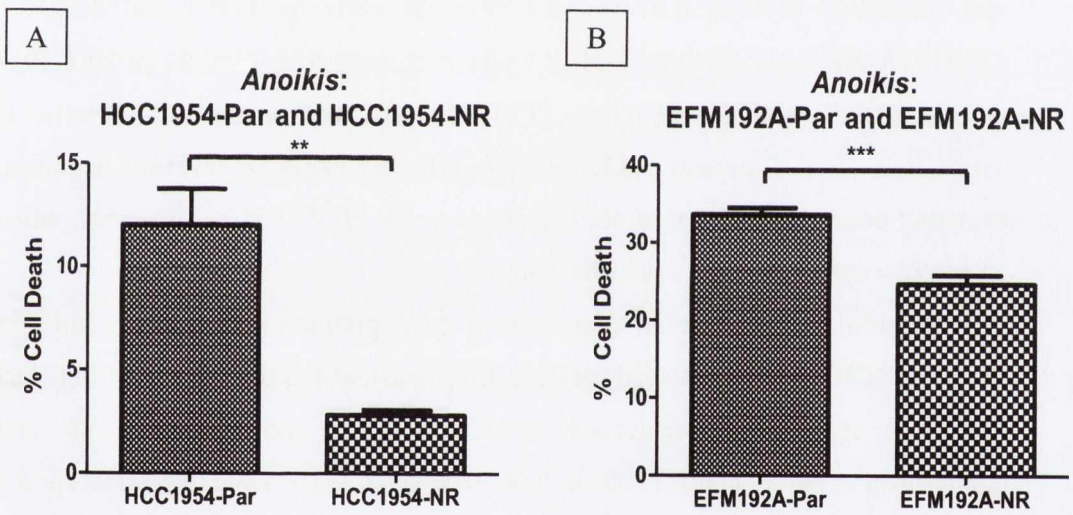

Figure 2.4. *Anoikis* assays of NR compared to Par cells. *Anoikis* assays indicate that (A) HCC1954-NR and (B) EFM192A-NR cells are more resistant to anchorage-independent cell death (n=3±SEM), where **$p<0.01$ and ***$p<0.001$.

2.3.7 Effects of neratinib-resistance on drug targets and PGP

Expression of drug targets and drug transporters are often altered in drug-resistant cells (see Sections 1.3.3 and 1.3.1, respectively). To investigate if acquiring neratinib-resistance had any effects on neratinib targets EGFR, HER2 and HER4, immunoblots were performed on total protein lysates from parent and neratinib-resistant cell variants (Figure 2.5). While HER3 is not a target of neratinib, the association between neratinib-resistance and HER3 expression in cells was also considered due to the tendency for it to dimerise with HER2 and HER4 [179].

We found that the entire EGFR-family of receptors was reduced in both neratinib-resistant cell lines in comparison to parent cells. EGFR was decreased in HCC1954-NR cells to 0.66±0.05 ($p=0.003$), while EGFR is not detected in EFM192A cells. This was confirmed by using SKBR3 cells as a positive control. HER2 expression was decreased to 0.45±0.07 in HCC1954-NR cells ($p=0.001$) and 0.59±0.14 in EFM192A-NR cells ($p=0.041$). HER3 was decreased to 0.75±0.04 in HCC1954-NR cells ($p=0.003$) and 0.71±0.03 in EFM192A-NR cells ($p=5x10^{-4}$). Finally, HER4 expression was decreased to 0.52±0.08 ($p=0.005$) in EFM192A-NR cells in comparison to parent controls. HER4 was not detectable in the HCC1954 cell variants, where the EFM192A cells served as a positive control.

Additionally, potential alterations in the expression of two drug efflux pumps, PGP and BCRP, were measured between drug-resistant and drug-sensitive cell variants. PGP was significantly decreased in HCC1954-NR and EFM192A-NR cells in comparison to parent control cells to 0.36±0.07 ($p=1.3x10^{-4}$) and 0.42±0.04 ($p=8.5x10^{-4}$), respectively. Similarly, BCRP expression was decreased in HCC1954-NR and EFM192A-NR cells in comparison to parent control cells to 0.72±0.05 ($p=0.006$) and 0.74±0.04 ($p=0.004$), respectively. β-actin was used as a loading control for all immunoblots and the corresponding densitometry graphs for these immunoblots are displayed in Appendix I.

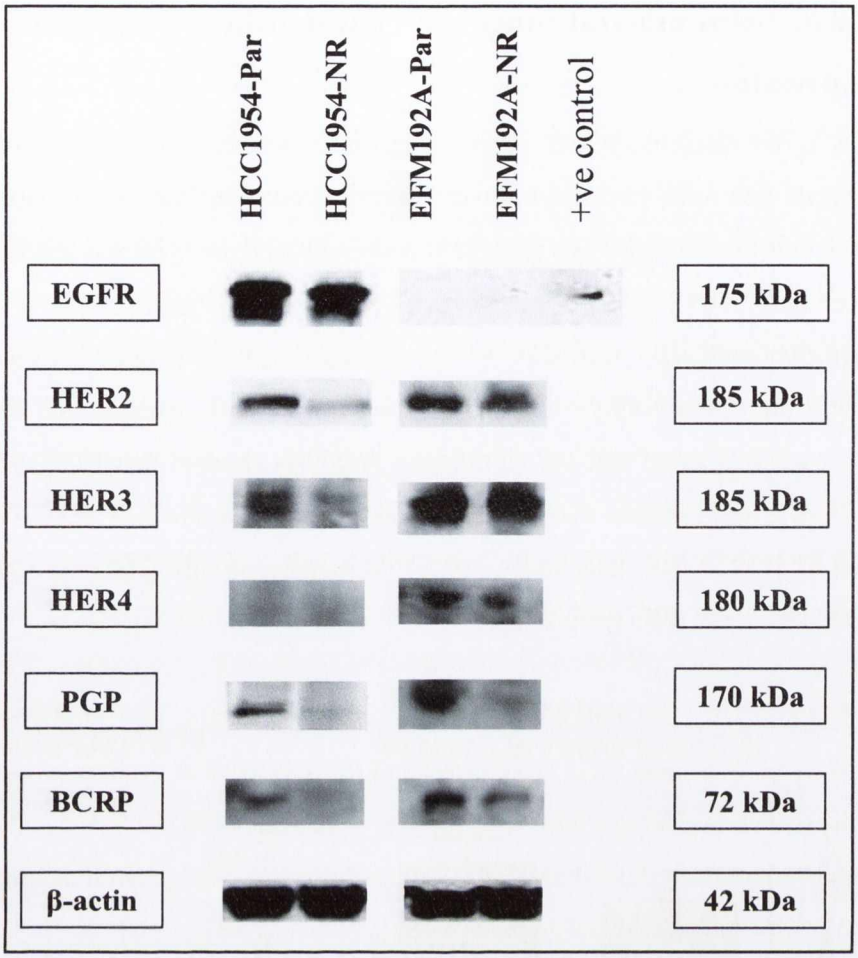

Figure 2.5. Effects of NR on EGFR family members and drug transporter expression. Association between neratinib-resistance and expression of the EGFR family of receptors and drug efflux pumps PGP and BCRP. SKBR3 cells served as positive control in EGFR blot for EFM192A cell variants. Blots are representative images of n=3.

2.3.8. Neratinib-resistance does not significantly alter miR-210 expression

Next, the mechanism that drives acquired resistance to neratinib was investigated. Several potential mechanisms were investigated. First, cell expression of miR-210 in both cell line variants was measured and compared as increased levels of miR-210 has been associated with breast cancer, including trastuzumab resistance in breast cancer (see Section 2.4.3). miR-210 was measured by qPCR (Figure 2.6) and revealed that while there was a slight increase in miR-210 in both resistant cell line variants; this increase was small and not significant. Analysis showed that HCC1954-NR cells had 1.18±0.2 fold increase in miR-210 expression compared to HCC1954-Par cells (p=0.29) and EFM192A-NR cells had 1.7±0.5 fold increase in miR-210 expression compared to EFM192A-Par cells (p=0.28).

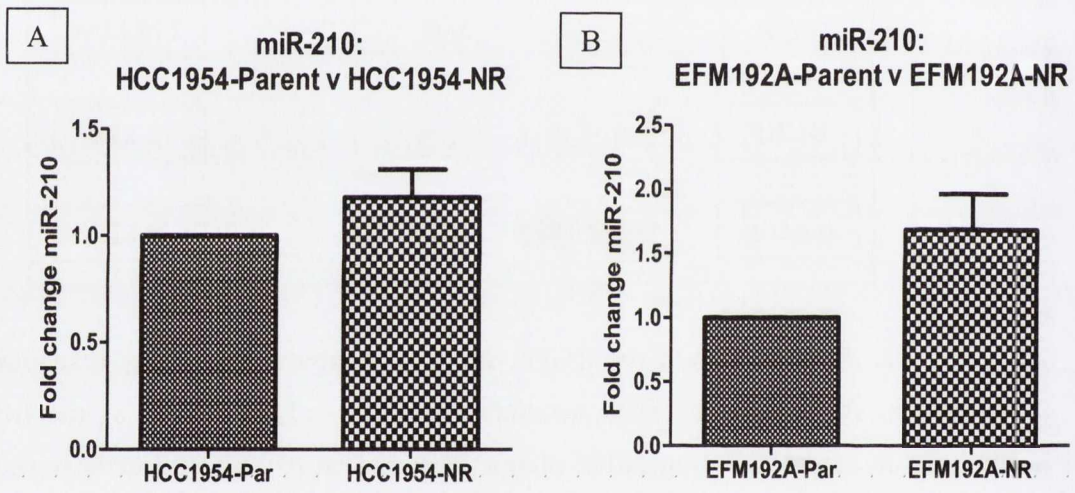

Figure 2.6. Expression of miR-210 in NR and Par cells. miR-210 was increased slightly, but not significantly, in neratinib-resistant cells in comparison with parent control cells (n=3±SEM).

2.3.9. Neratinib-resistance is not induced by altered levels of ATP

Altered activity of ATP has been associated with drug-resistance (see Section 2.4.3). It follows that a luciferase-IPA assay was performed to investigate if neratinib-resistance was accommodated through an increase in amount of cellular ATP (Figure 2.7). Here, HCC1954-NR cells were found to contain a small but significant increase in ATP, with 1.13±0.04 fold more ATP than their parent control counterparts ($p=0.032$). Conversely, the EFM192A-NR cells had slightly less intracellular ATP, with the EFM192A-NR cells decreasing to 0.85±0.05 compared with the parent control cells ($p=0.042$).

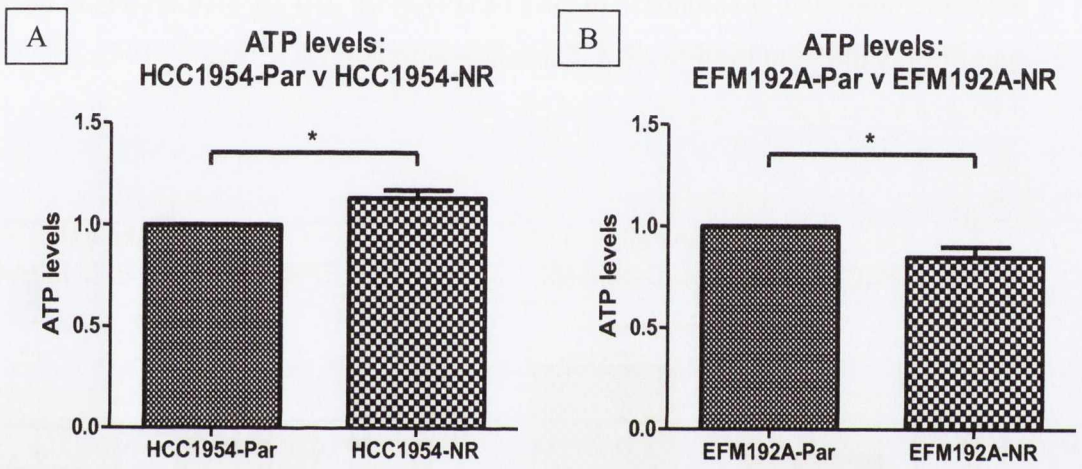

Figure 2.7. ATP levels in NR compared to Par cells. ATP levels in (A) HCC1954-NR cells are slightly higher than HCC1954-Par cells (B) ATP levels in EFM192A-NR cells are slightly lower than in EFM192A-Par cells (n=3±SEM), where *$p<0.05$.

2.3.10. Neratinib-resistance increases a stem cell-like sub-population in HCC1954-NR cells, but not EFM192A-NR cells

Stem cells have been shown to play a role in cancer cell drug-resistance (see Section 1.3.7). Here, cells were analysed and compared for expression of breast cancer stem cell markers CD44 and CD24 by flow cytometry (Figure 2.8). It was found that while HCC1954-Par cells contained, on average, 17.6±3.3% of CD44-positive/CD24-negative cells, this population had increased significantly to 25.6±1.2% in the HCC1954-NR cells ($p=0.027$). In contrast, the EFM192A-Par cells had a much smaller native CD44-positive/CD24-negative sub-population at only 0.17±0.03%. This figure decreased slightly to 0.13±0.03% in the EFM192A-NR cell population, which was not significantly different to EFM192A-Par cells ($p=0.519$).

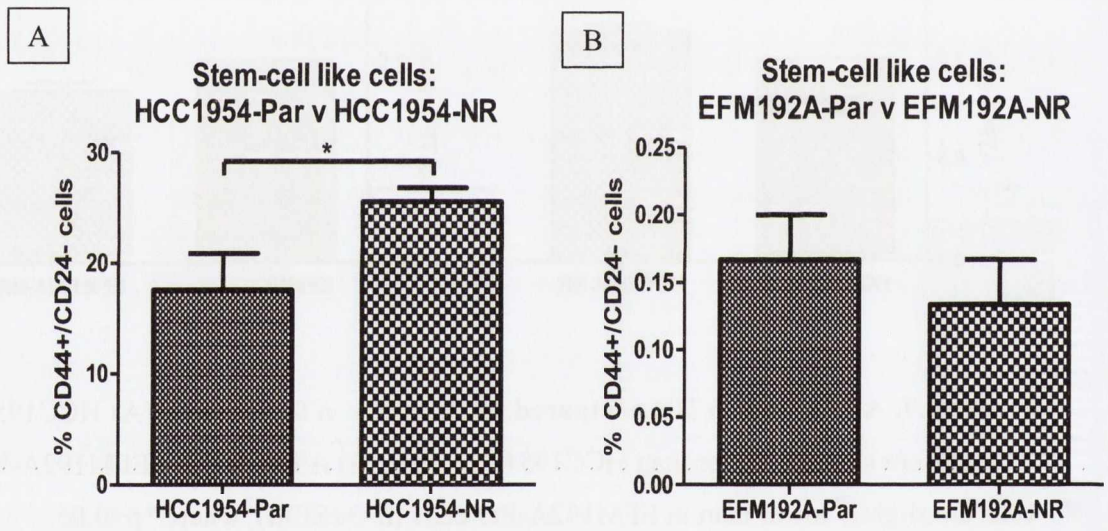

Figure 2.8. Stem-cell like populations in NR compared to Par cells. There was an increase in the CD44-positive/CD24-negative stem cell-like sub-population in (A) HCC1954-NR cells compared to HCC1954-Par cells. (B) There was no significant difference in the stem cell-like sub-population in EFM192A-NR cells compared to EFM192A-Par cells (n=3±SEM), where *$p<0.05$.

2.3.11. NmU expression upregulated with neratinib-resistance

Increased levels of NmU expression has been associated with acquired-resistance to HER-targeted therapy in breast cancer (see Section 2.4.3), and so, here, the amount of NmU contained within drug-resistant and drug-sensitive cells was measured by ELISA (Figure 2.9). Analysis indicated that HCC1954-NR cells had 1.31±0.1 fold more NmU expression than their HCC1954-Par control cells ($p=0.034$). Likewise, EFM192A-NR cells were found to show a 1.6±0.06 fold increase in NmU expression in comparison to the EFM192A-Par cell variants ($p=5.1x10^{-4}$).

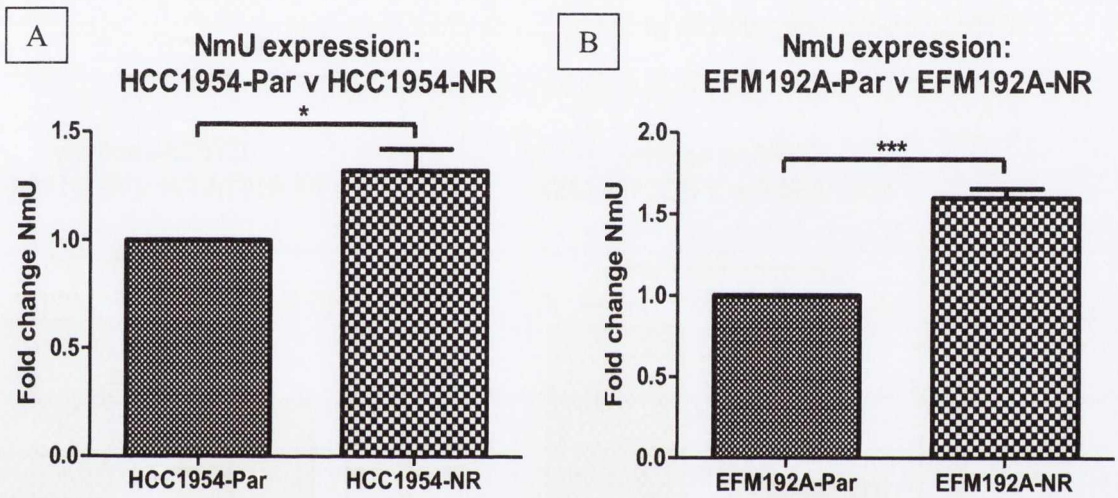

Figure 2.9. NmU expression in NR compared to Par cells. NmU in (A) HCC1954-NR cells is significantly higher than HCC1954-Par cells (B) EFM192A-NR cell NmU levels are also significantly higher than EFM192A-Par cells (n=3±SEM), where *$p<0.05$ and ***$p<0.001$.

2.3.12. CYP3A4 mediates neratinib-resistance

Altered activity of enzymes involved in drug metabolism has been associated with drug-resistance (see Section 1.3.2). Consequently, CYP3A4 enzyme activity was measured using a P450-Glo CYP3A4 Assay with Luciferin-IPA and these activity levels were compared for neratinib-resistant and parent control cells (Figure 2.10). It was found that there was higher CYP3A4 activity in both neratinib-resistant cell lines, compared to controls. More specifically, the HCC1954-NR cells showed a 2.93±0.3 fold increase in CYP3A4 activity when compared to HCC1954-Par cells ($p=0.002$). Similarly, EFM192A-NR cells displayed a 1.5±0.2 fold increase in CYP3A4 activity compared to EFM192A-Par control cells ($p=0.03$).

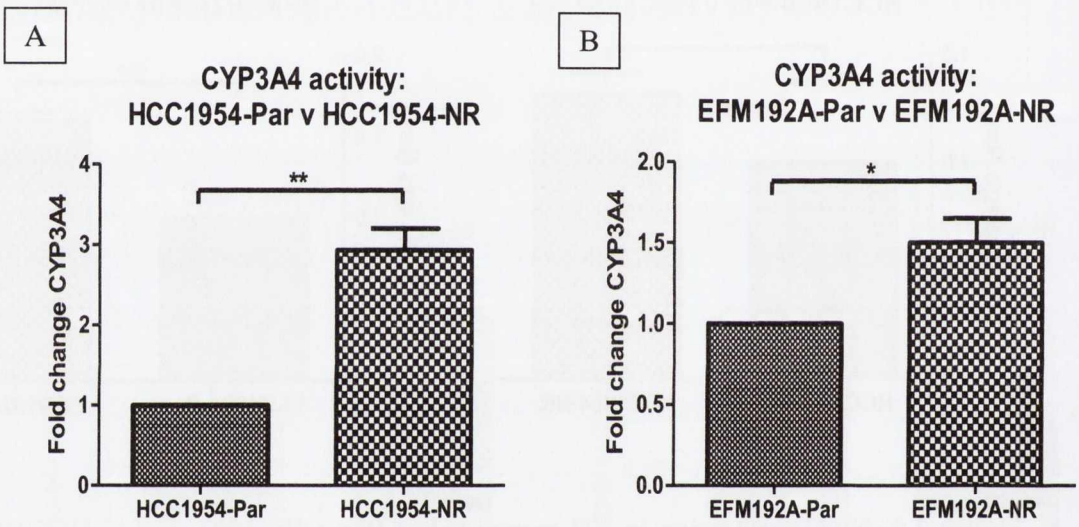

Figure 2.10. CYP3A4 activity in NR compared to Par cells. CYP3A4 activity is substantially and significantly higher in both (A) HCC1954-NR and (B) EFM192A-NR cells in comparison to their respective control cells (n=3±SEM), where *$p<0.05$ and **$p<0.01$.

Characteristic	HCC1954-NR v HCC1954-Par	EFM192A-NR vs EFM192A-Par
Proliferation rate	↓	↓
Migration	↑	↑
Invasion	↑	Not assessable
Anoikis resistance	↑	↑
EGFR expression	↓	Not expressed
HER2 expression	↓	↓
HER3 expression	↓	↓
HER4 expression	Not detected	↓
PGP expression	↓	↓
BCRP expression	↓	↓
miR-210 expression	No significant difference	No significant difference
ATP levels	↑	↓
Stem cell-like population	↑	No significant difference
NmU expression	↑	↑
CYP3A4 activity	↑	↑

Table 2.8. Summary of characteristics of neratinib-resistant cells compared to their parents control cells for both HCC1954 and EFM192A cell lines.

2.4 Discussion

2.4.1 Neratinib-resistance is associated with cross-resistance to other HER2-targeting agents

Neratinib is a tyrosine kinase inhibitor being investigated in clinical trials for its efficacy in treating HER2-overexpressing breast cancer patients. While data from these trials are indicating that the drug is having the desired anti-cancer effects in some patients, there is a gap in available information on the effects of neratinib-resistance in cells, when it develops. This study provides an insight into the effects of developing neratinib-resistance on HER2-overexpressing cells, which may serve as a model of eventual acquired neratinib-resistance in patients in the clinic.

Neratinib is similar to other HER2-targeting drugs, lapatinib and trastuzumab, in that chronic exposure resulted in the development of drug-resistance. Here, chronic exposure of HCC1954 and EFM192A cells to neratinib induced drug-resistant cell line variants, HCC1954-NR and EFM192A-NR, as demonstrated by the increase in IC_{50} for neratinib of the neratinib-resistant cell variants compared to their parent control cells. However, in addition to the development of neratinib-resistance in response to long-term neratinib exposure, we observed that cross-resistance to other HER-targeting agents (lapatinib and afatinib) also developed. Interestingly, this cross-resistance occurs in both directions of resistance as both lapatinib and trastuzumab-resistant cell lines were also found to be cross-resistant to neratinib.

A similar trend of cross-resistance has been observed *in vitro* by Wang *et al.* [180] who generated SKBR3 lapatinib-resistant cells. They treated these cells with neratinib and found that their SKBR3-LR cells were 26.8 fold more resistant to neratinib than the SKBR3 parent cells. Furthermore, the trends seen here where lapatinib and trastuzumab-resistant cells demonstrate cross resistance to neratinib, have also been observed *in vivo* in clinical trials. Specifically, Burstein *et al.* [169] found that drug-naïve patients responded better to neratinib than patients previously treated with trastuzumab; furthermore, patients with prior trastuzumab treatment had a progression-free survival time of on average 22.3 weeks, while patients without prior exposure to trastuzumab had a much longer progression-free survival time of on average 39.6 weeks. Similarly, Awada *et al.* [171] reported that patients with prior exposure to lapatinib did not respond to neratinib as well as patients that had no prior lapatinib exposure, where average progression-free survival for lapatinib-naïve patients was 48 weeks, which compared favourably to the average 22.7 weeks progression-free survival experienced

by patients who had previously been treated with lapatinib. Likewise, Saura *et al.* [70] found that patients who had previous lapatinib exposure had a lower (57%) overall response rate in comparison to patients with no prior lapatinib exposure (64%).

The extensive cross-resistance between HER2-targeting agents seen in this study does not appear to occur between lapatinib-resistant cells and trastuzumab, nor is it seen with trastuzumab-resistant cells and lapatinib. Many groups have demonstrated the sensitivity of lapatinib resistant cells to trastuzumab [181] and the sensitivity of trastuzumab-resistant cells to lapatinib [182], indicating that resistance to either of these drugs apparently does not make patient tumours resistant to the effects of the other. However, based on cell-line data, unfortunately, it would appear that in the case of neratinib-resistance, if a patient were to suffer disease progression while being treated with neratinib, no other HER2-targeting agent would be successful in their treatment or, at least, the efficacy of other HER2-targeting drugs would be impaired by the previous exposure to neratinib.

2.4.2 Neratinib-resistance induces increased cell aggression

Migration, invasion and *anoikis* assays were performed to evaluate any phenotypic changes that may have occurred in cells with acquired neratinib-resistance, in terms of altered cell aggression. These assays mimic different processes that occur *in vivo* during the metastatic process (see Section 1.1.1.6), which relies on cells obtaining traits that enable them to migrate and invade into and out of the circulatory system, and also survive while in circulation [183]. For example, cell migration assays measure the ability of cells to migrate from one location to another; here, two types of migration assay were used that allow measurement of these phenomena, the first used a cell culture insert containing 8μm pores for cells to migrate through, the second involved a scratch being made on a cell monolayer and closure of this cell 'wound' enables migration quantification [184]. The invasion assay used here is an extension of the insert migration assay, whereby the insert is coated with ECM, and for cells to pass through they must first invade through the ECM before they can pass through the pores of the insert for quantification. Finally, the *anoikis* assay imitates the ability of cells to survive while unattached in the circulatory system. *In vivo*, detachment of cells from the ECM results in programmed cell death via apoptosis in a process known as *anoikis* [185]. It follows that a form of *anoikis* is utilised by the body to prevent detached cells from colonising secondary tissues. However, in cancer this process is dysregulated and cells can become resistant to *anoikis*, which can in turn facilitate metastasis [186]. In this study, we

artificially imitate this scenario whereby cells were forced to float by coating culture plastic with poly-HEMA. Cells seeded were then measured for their ability to resist *anoikis*-induced cell death. Those that are resistant were considered to mimic cells that are more likely to survive in the circulatory system during metastasis. Together this selection of assays gives us important information regarding phenotypic changes in the cells, in terms of increased metastatic potential and thus cell aggression.

Using these assays, we found that both neratinib-resistant cell variants (HCC1954-NR and EFM192A-NR cells) had developed a more aggressive phenotype than their sensitive counterparts in terms of being more migratory (HCC1954-NR and EFM192A-NR cells) and invasive (HCC1954-NR cells); and also improving their ability to avoid *anoikis* induced cell death. In agreement with this observation of increased cell aggression in association with acquired-drug resistance, Formisano *et al.* [187] found that breast cancer MDA-MB-361 lapatinib-resistant cells were more migratory and invasive in comparison to their drug-sensitive control cells. Considering other cancer types, La Monica *et al.* [188] found that their gefitinib-resistant non-small cell lung cancer cells, HCC827 GR5-G, were more aggressive in terms of migration and invasion than control cells. Finally, Corcoran *et al.* [178] found that two docetaxel-resistant prostate cancer cell line variants of DU145 and 22Rv cells were more invasive, migratory and resistant to *anoikis*-induced cell death when compared to control cells.

2.4.3. Mechanism of neratinib-resistance

Following observations of drug cross-resistance and increased cell aggression in association with acquired neratinib-resistance in our cells, we aimed to elucidate the mechanism that facilitates this drug-resistance. Firstly, we looked at the associations between neratinib-resistance and the targets of neratinib. We found that expression of all three members of the EGFR family that are targeted by neratinib, EGFR, HER2 and HER4, was reduced in the drug resistant cell-variants compared to control cells. Additionally, HER3, which is not targeted by neratinib but heterodimerises with HER2 [179], was also reduced as a result of neratinib-resistance. These observations are contrary to typical HER2-drug resistance, where EGFR and HER2 are often increased in association with lapatinib [85, 189] and trastuzumab-resistance [190]. The decrease in drug targets is potentially due to the irreversible binding nature of neratinib. This theory is backed up by findings of Azuma *et al.* [191] who generated PC9 lung cancer cells resistant to afatinib, which is also an irreversible EGFR, HER2 and HER4 inhibitor. They found that expression of EGFR, HER2 and HER3 was downregulated

in the afatinib-resistant cell variants in comparison to their drug naïve control cells. In addition, they found that fibroblast growth factor receptor (FGFR) is increased in afatinib-resistant cells and that this increase compensates for cell growth and survival in resistant cells where the EGFR family has been downregulated. Judging by the similarities between our neratinib-resistant cells and their afatinib-resistant cells, future work on this project should include analysis of FGFR in neratinib-resistant cells in comparison to control cells.

Additionally, we looked at levels of drug efflux pumps, PGP and BCRP, in drug-resistant cells. PGP is widely cited as one of the most common mediators of drug resistance in cancer and is often found to be overexpressed in drug-resistant cells [76, 192-195]. In contrast to classical drug-resistance, we found that our neratinib-resistant cells show downregulation of PGP. Zhao *et al.* [196] found similar trends, finding that neratinib inhibits PGP activity and describe the ability of neratinib treatment to reverse multidrug resistance in PGP overexpressing cells including MCF7 and KBv200 cells. This trend has also been observed with another tyrosine kinase inhibitor, lapatinib [197], which was also found to reduce PGP activity. BCRP is also a drug efflux pump whose overexpression is associated with breast cancer drug-resistance [80]. However, similarly to PGP, we found levels of BCRP to be reduced in neratinib-resistant cells, suggesting that it does not have a functional role in the mediation of neratinib-resistance.

miRNAs are small single-stranded non-coding RNAs that comprise approximately 1% of the genome [198]. Data is emerging that suggests miRNAs as valuable biomarkers for cancer diagnosis [199-201] and prognosis [202, 203]. These miRNAs are detectable in both blood and urine and so have potential as a non-invasive diagnostic tool. Advantages of using these miRNAs for cancer diagnosis include their stability during sample processing, low cost and ease of use for PCR-based analysis [204]. We investigated the relative expression of miR-210 in our cells as overexpression of miR-210 has been shown to be associated with breast cancer and drug resistance. Specifically, Jung *et al* [205] found that plasma levels of miR-210 was higher in breast cancer patients compared to healthy controls, miR-210 levels are lower in patients following surgery and additionally, they found that miR-210 was higher in trastuzumab-resistant BT474 breast cancer cells following treatment with trastuzumab compared to control cells. Similarly, Hong *et al.* showed that miR-210 overexpression is associated with a poor prognosis in breast cancer patients [206]. Here, results showed a trend towards increased levels of miR-210 in association with neratinib-resistance, although this was not significant. Our neratinib-resistant cells are cross-resistant to other HER2-

targeting agents and are also more invasive than control cells. With this in mind and the result of a slight increase in miR-210 in neratinib-resistance, our observations are in agreement with the findings of Hong *et al.* [206].

Altered energy metabolism in the form of increased aerobic glycolysis has been observed in cancer in comparison to healthy tissue [207]. ATP is a molecule essential to cellular metabolism and so can be used as a measure of this process. Zhou *et al.* [208] reported a link between altered cellular metabolism and drug-resistance, where they found that ATP levels are altered in response to chemoresistance. More specifically, they demonstrated that oxaliplatin-resistant HT29 and HCT116 colon cancer cells have higher levels of intracellular ATP. They showed that this increase in ATP is functionally relevant to the development of chemoresistance as the introduction of ATP to drug sensitive-cells induced drug-resistance, while ATP depletion rendered chemoresistant cells sensitive to drug treatment. While we found a significant increase in HCC1954-NR ATP levels compared to that in control cells, this increase was not substantial at just 1.13±0.04 fold compared to the approximate 2 fold and 2.5 fold increase in ATP observed by Zhou *et al* in their oxaliplatin-resistant HT29 and HCT116 cells, respectively. Meanwhile, here, no significant difference in ATP levels between drug-sensitive and drug-resistant EFM12A cells was observed. This suggests that ATP does not form a key part of the mechanism of neratinib-resistance in these cells.

Recently, we have published data showing that levels of Neuromedin U (NmU) are increased in cells resistant to HER2-targeting agents [209]. Our results showed that NmU was increased in cells resistant to lapatinib, trastuzumab and neratinib (neratinib data included HCC1954-NR and HCC1954-Par cell data displayed in this chapter). In addition, NmU was found to be functionally involved in drug-resistance as when SKBR3 and HCC1954 drug-sensitive cells were transfected with NmU they became resistant to lapatinib, trastuzumab, neratinib and afatinib. Additionally, the knock-down of NmU in SKBR3-LR and HCC1954-LR cells resulted in an increase of the anti-proliferative effects of lapatinib, neratinib, afatinib and trastuzumab. Consequently, we measured the levels of NmU in EFM192A-NR cells and compared them to EFM192A-Par cells, with the results indicating significantly elevated NmU levels in the neratinib-resistant cell variant. This data indicates that acquired neratinib-resistance is mediated, at least in part, by increased levels of NmU in both HCC1954-NR and EFM192A-NR cells.

CYP3A4 is an enzyme of the cytochrome P-450 enzyme family. This enzyme plays a role in the metabolism of approximately half of all drugs currently used in the

clinic [210], including neratinib [211]. While CYP3A4 is predominantly expressed in the liver [212], it is also found in breast tissue [213]. Abbas *et al.* [211] demonstrated that co-administration of ketoconazole, a CYP3A4 inhibitor, with neratinib increases peak plasma concentrations of neratinib by 3.2 fold. This suggests that alterations of CYP3A4 levels in the body will also alter the availability of neratinib. From this, it follows that we investigated the potential of role of CYP3A4 in neratinib-resistance. Measurements of CYP3A4 activity in both neratinib-resistant cell lines revealed an increase in enzyme activity, suggesting that the increased amounts of CYP3A4 in neratinib-resistant cells enhance neratinib metabolism and thereby drives neratinib-resistance in these drug-resistant cell models.

2.5 Conclusion

In conclusion, the data here indicates that, similarly to other drugs, chronic treatment of cell lines with neratinib will result in acquired drug-resistance. We show that this acquired neratinib-resistance is also associated with cross-resistance to other HER2-targeting agents; specifically, neratinib-resistant cells are cross-resistant to other HER2-targeting agents (lapatinib and afatinib) and also that cells resistant to other HER2-targeting agents (lapatinib and trastuzumab) are cross-resistant to the effects of neratinib. Furthermore, this cross-resistance in neratinib-resistant cells is coupled with an increase in cell aggression. Additionally, targets of neratinib were found to be decreased in resistant cells, potentially due to the irreversible-binding nature of neratinib. We demonstrated that the mechanism of acquired neratinib-resistance is likely to be multifaceted and one in which both increased levels of NmU and increased CYP3A4 activity play roles.

Chapter 3: The relevance of extracellular vesicles as diagnostic and predictive biomarkers in HER2-overexpressing breast cancer patients

3. Abstract

Introduction: Tissue biopsies are commonly used to evaluate a patient's disease pathology, however this method is very invasive for the patient. Extracellular vesicles (EVs) are released from cells and their contents have been shown to be representative of their cell of origin. Consequently, it has been proposed that the isolation and analysis of patient EVs may be useful for minimally-invasive detection of blood-based biomarkers for the diagnosis and prediction of patient response to therapy. So, the relevance of circulating EVs as biomarkers was investigated.

Methods: EVs were isolated from 250µl of serum from patients with HER2-overexpressing breast tumours and from age-matched healthy control serum specimens, using filtration and ultracentrifugation techniques. EVs were characterised by TEM, NanoSight analysis and immunoblotting for EV markers. EV quantities were determined by lysing EVs and quantifying the protein content of the lysate. EV and serum Neuromedin U (NmU) and HER2 were measured by ELISA. EV survivin was also measured by ELISA. EV NmU mRNA and EV miR-210 levels were detected by qPCR.

Results: EVs were successfully isolated from serum. We show that EV quantities from breast cancer patients' sera were significantly higher than healthy control EV quantities. We also found that an increase in EV quantities was associated with reduced patient response to carboplatin and docetaxel (plus trastuzumab or lapatinib) treatment. HER2 was not detected in EVs; however, soluble HER2 levels in serum correlated with response to treatment, where HER2 levels of patients who achieved a complete response decreased significantly with therapy, whereas patients who achieved partial or no response showed a decrease in soluble HER2 with therapy, but this was not significant. Cancer patients were found to have decreased EV NmU compared to healthy controls and serum NmU and EV NmU levels were found not to be predictive of patient response to therapy. Patient EV survivin levels were found to be slightly, but not significantly, higher than healthy control EV survivin levels. miR-210 was not predictive of patient response to therapy.

Conclusion: EV quantities may potentially be used to diagnose HER2-overexpressing breast cancer and also predict patient response to therapy. While EVs contain NmU and survivin, these proteins were not found to be of use for prediction of response to therapy. HER2 was not detected in EVs, however, soluble HER2 in serum may have a role in prediction of patient response to therapy.

3.1 Introduction

3.1.1 Personalised medicine

Breast cancer diagnosis and treatment options have improved greatly over the past number of decades (see Section 1.2). Personalised medicine is now the goal which is strived for to improve patient care, where patients are to be treated more as individuals, as opposed to all patients receiving the same therapy regardless of the unique profile of their disease. Traditionally certain aspects of a patient's personal profile e.g. age, family history and gender, are taken into consideration while therapy options are being considered. However, more in-depth genetic profiling of a patient's disease is likely to give further detailed information that can be used to diagnose and treat patients in a manner where patients can be streamlined into groups that are more or less likely to respond to certain treatment regimens.

This personalised medicine approach to patient care may enable more specific, successful and tolerable cancer treatment, while reducing unnecessary systemic side effects. To facilitate the personalised medicine approach, researchers aim to find biomarkers that are diagnostic of disease, can aid in prognosis and predict patient sub-group who are more or less likely to respond to particular treatments (see Figure 3.1). Typically, these biomarkers will be proteins, genes, enzymes or other biological molecules that can be tested in patient specimens.

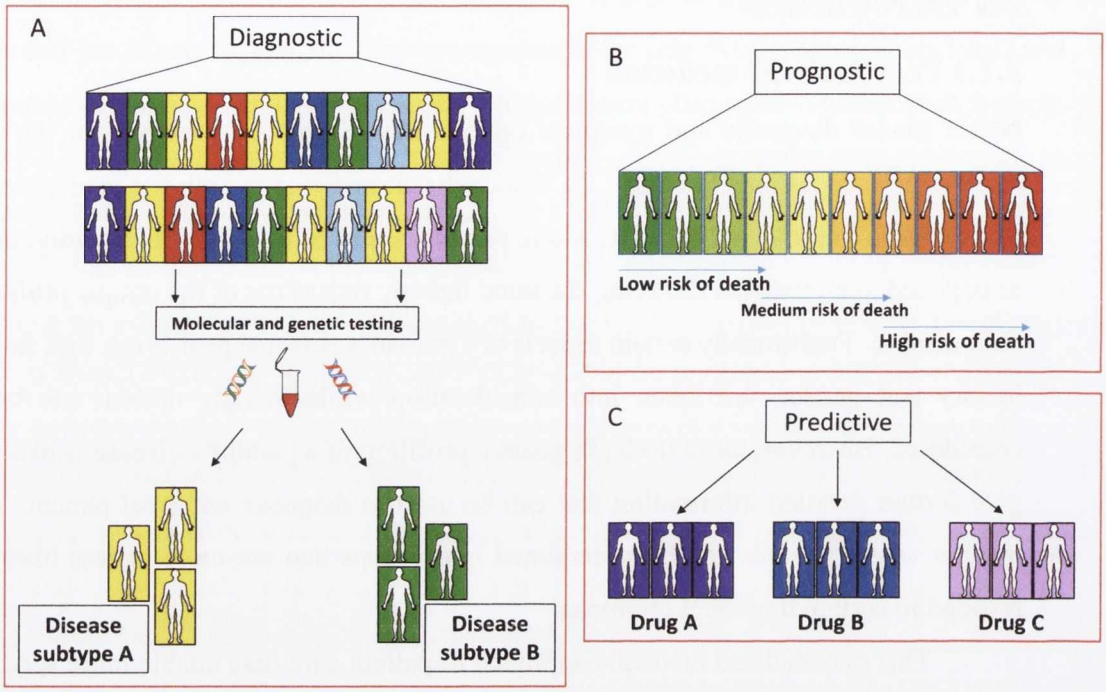

Figure 3.1. Diagnostic, prognostic and predictive biomarkers are essential for personalised medicine. A. Diagnostic biomarkers can identify patients suffering from a disease and can be used to classify which disease subtype, if any, a patient may have. B. Prognostic biomarkers can identify subsets of people who are more or less likely to have a poorer outcome due to disease. C. Predictive biomarkers are useful for identifying patients most likely to respond to a particular type of drug therapy.

A classic example of personalised medicine is the discovery of HER2 and the subsequent development of trastuzumab, the monoclonal antibody that blocks its function. As per mentioned in Section 1.1.2., HER2 is overexpressed in a subtype of breast cancer and so measuring levels of this protein in cancer patients allows for a more specific diagnosis and prognosis of disease. Also, patients having tested positive for HER2 also have a poorer prognosis than those with lower HER2 levels, as HER2-overexpressing breast cancer is associated with cancer aggression. Finally, those presenting with high levels of HER2 are candidates for treatment with the anti-HER2 monoclonal antibody, trastuzumab, which is a targeted therapy specific for this disease subtype. Accordingly, the measurement of tumour tissue HER2 levels reveals vital information on the patient's disease state. Use of trastuzumab has shown to be very successful where patients treated with this drug tend to have a reduced likelihood of cancer reoccurrence by 50% [214]. Another example of patient specific therapy is demonstrated by targeting of the BRAF mutation in melanoma cells. It is estimated that

approximately 50% of all melanoma patients develop mutations in the BRAF protein that stimulates cancer cell growth in these cases. To counter this issue BRAF inhibitors, including vemurafenib and dabrafenib, have been developed that specifically target the mutated form of BRAF [215].

While treatment options available to patients can be tailored due to altered levels of protein biomarker expression in their respective tumour, genetic screening of patient mRNA may offer a more in-depth view of the genetic signature of individual patient disease states. Van't Veer *et al.*, describe how they screened 117 breast cancer patients for over 5,000 gene transcripts that are involved in the regulation of cell invasion, signal transduction, the cell cycle, angiogenesis and metastasis [216]. Data from this screen was analysed and aided with stratification of patients into groups of good prognosis and bad prognosis, where poor prognosis identification correlated to a short time to the development of metastatic disease. This screening also identified patients more likely to respond to adjuvant systemic anti-cancer therapy. They found that by using this screen, patients with a good prognosis were identifiable and most were found not to develop metastasis within 5 years of diagnosis and therefore would not benefit from treatment, but if treated could still suffer from drug induced side effects. Those patients with poor prognosis are very likely to develop metastatic disease within 5 years of diagnosis and therefore are good candidates for therapy. This means that the use of this screen may enable patient specific tailoring of treatment resulting in better patient care.

The efficacy of this genetic screen to identify patients with a poor prognosis was validated by Van de Vijver, whereby they used 70 genes found to be most effective for patient prognosis from the previous study and tested this screen on 295 breast cancer patients [217]. Again, this wide genetic screening of tumours identified patients who were most at risk of developing distant metastases within 5 years of diagnosis. In addition to this essential prognostic information, the ability to identify these patients is an asset to designing patient treatment options as those patients assigned as having a poor prognosis by this screen are also the patients who are most likely to respond to adjuvant therapy.

Oncotype DX is an example of a commercially available genetic screen for cancer that measures aggressiveness and therapeutic responsiveness [218]. It analyses activity of 21 genes, 16 of which are involved in tumour progression and the other 5 are used for normalisation of patient variability. The test offers a 'Recurrence Score' of between 0 and 100, which indicates the likelihood a patient has of their cancer returning within 10 years of their diagnosis and also indicates which patients are most likely to

benefit from chemotherapy. Patients with low Recurrence Scores are less likely to see their cancer return and are less likely to benefit from chemotherapy, whereas patients with higher Recurrence Scores are more likely to see their cancer return, but are also more likely to reap benefit from chemotherapy treatment.

3.1.2 Liquid biopsy and EVs

Tissue biopsies and blood specimens are commonly used to evaluate a patient's disease pathology; however, these specimen sources have their limitations. Tissue biopsies only represent the tumour at the point which the biopsy is taken and would be far too invasive as a specimen source for effective monitoring of the success of therapy; overall it is not ideal for real-time patient observation. Also, due to tumour heterogeneity, basing medical decisions on a single biopsy could be risky and inadequate due to the fact that the tissue taken from a biopsy likely does not represent the tumour as a whole. Blood specimens are a far less invasive option for patient observation and have been used to monitor protein-based disease biomarker levels in patient blood (e.g. prostate specific antigen). It is known that cell-free nucleic acids are released from tumours and are detectable in the blood of cancer patients; and so are useful as biomarkers that could be used as a 'liquid biopsy' to avoid the need for tissue biopsies. It has been proposed that EVs (see Section 1.4) be isolated from patient blood and act be used as a liquid biopsy. It has the advantage of routine blood testing, in that it is minimally-invasive, but as the encapsulation and protection of both proteins and nucleic acids has been demonstrated in EVs it may be a superior choice for biomarker detection and analysis and could be used in the clinic to diagnose disease and monitor patient response to therapy.

3.1.3. Aims

In this study, we aimed to isolate EVs from ICORG trial 10-05 patient and healthy control serum specimens, and to characterise the vesicles isolated. Using these EVs we aimed to investigate if EV quantities differ between breast cancer patients and healthy controls, and also if EV quantities measured correlates with patient response to therapy. EV NmU, HER2 and survivin and serum NmU and soluble HER2 were also measured for their ability to detect breast cancer and predict patient response to therapy. Finally, we aimed to investigate if EV miR-210 levels were indicative of patient response to therapy.

3.2 Materials and methods

3.2.1 Clinical trial design

Clinical trial titled 'A Phase II Neo-adjuvant Study Assessing TCH (Docetaxel, Carboplatin and Trastuzumab), TCL (Docetaxel, Carboplatin and Lapatinib) and TCHL (Docetaxel, Carboplatin, Trastuzumab and Lapatinib) in HER-2 Positive Breast Cancer Patients' (clinicaltrial.gov identifier - NCT01485926), was sponsored by All Ireland Cooperative Oncology Research Group (ICORG). The primary objective of this trial was to assess the efficacy of TCH, TCHL and TCL as neo-adjuvant treatment of HER-2 positive breast cancer, using pathological complete response (pCR) as the primary endpoint, which was established following 6 cycles of treatment. Complete Response (CR) is defined by the absence of invasive carcinoma in the breast and lymph nodes. Partial Response (PR) is defined as a decrease in either or both the tumour or lymph nodes compared to the pre-treatment tumour or lymph nodes, while having no increase in either the tumour or lymph nodes. No Response (NR) is defined as no apparent change in either the tumour or lymph nodes compared to the clinical (pre-treatment) assignment or an increase in the tumour or lymph nodes at the time of post-treatment pathologic evaluation.

Serum specimens were obtained from patients accrued to this trial for translational studies. Medications permitted to be taken by patients during the trial included anti-emetics, steroid prophylaxis, growth factors, loperamide for diarrhoea, diuretics for fluid retention and common immunizations, such as influenza vaccine, while amifostine, dexrazoxane, any other investigational agent or any other non-protocol anti-tumour therapy while on study neo-adjuvant treatment medicines were not permitted during the trial. Specimens were taken over the course of neo-adjuvant treatment, more specifically serum specimens were taken pre-treatment, pre-cycles 2, 3, 4, 5 and 6; and post-treatment. In total, 88 patients were accrued. 33 of these patients gave their consent for blood specimens to be taken and were able to be used in our studies. Table 3.1 gives a breakdown of patients accrued for the trial, patients that completed the trial, gave their consent to serum specimens being taken and had a specimen profile that was of use in our studies (i.e. patients for which specimens from all time points were available or patients for whom pre- and post-treatment specimens were available). Additionally, age-matched healthy control serum specimens were obtained from University Hospital Galway. A detailed breakdown of serum specimens from this trial and the healthy control specimens are outlined in Tables 3.2.

Patients	Total	TCH	TCHL	TCL
# Patients recruited into trial	88	38	40	10
# Patients completed trial	65	36	23	6
# Patients consented to samples being taken	44	21	17	6
# Patients available to us (i.e., full set of samples per patient **or** pre & post matched)	33	13	14	6
% of samples available for testing	38	34	35	60

Table 3.1. Patients enrolled into ICORG clinical trial 10-05. Breakdown of patients who took part in the trial into treatment arms and availability of specimens. T = docetaxel; C = carboplatin; H= trastuzumab; L = lapatinib.

Cancer patients from trial 10-05								Healthy controls	
No	Arm	AGE	pCR	Primary Tumour	Regional Lymph Nodes	Distant Metastases	Overall Staging	Healthy Control	Age (years)
3	TCL	42.1	PR	T2	N0	MX	Stage IIA	B08-0399	33
4	TCHL	50.8	PR	T2	N0	M0	Stage IIA	B14-1613	35
6	TCH	42.8	PR	T2	N0	M0	Stage IIA	B11-0262	37
7	TCL	43.4	PR	T2	N1	M0	Stage IIB	B14-1615	39
8	TCL	79.7	PR	T2	N0	M0	Stage IIA	B14-1659	39
9	TCH	38.9	CR	T2	N1	M0	Stage IIB	B09-0667	45
11	TCHL	47.3	PR	T1	N1	M0	Stage IIA	B09-1234	50
12	TCL	69.7	No response	T1	N1	M0	Stage IIA	B11-0864	51
14	TCH	42.9	CR	T3	N1	M0	Stage IIIA	B10-0756	57
15	TCL	53.4	CR	T4d	N1	M0	Stage IIIB	B09-1275	57
18	TCHL	50.5	PR	T2	N1	M0	Stage IIB	B14-2019	57
20	TCHL	67.9	CR	T2	N0	M0	Stage IIA	B09-1235	60
26	TCH	51.6	CR	T3	N2	M0	Stage IIIA	B14-2040	63
29	TCL	45.8	CR	T4d	N1	M0	Stage IIIB	B06-0293	65
32	TCH	49.9	PR	T3	N0	M0	Stage IIB	B09-1592	32
34	TCH	49.0	CR	T2	N1	M0	Stage IIB	B14-2043	70
39	TCH	59.5	PR	T2	N1	M0	Stage IIB	B14-2008	73
42	TCHL	49.2	PR	T2	N1	M0	Stage IIB	B13-0223	34
45	TCH	45.4	CR	T2	N0	M0	Stage IIA	B14-1621	35
46	TCH	45.8	PR	T2	N1	M0	Stage IIB	B06-0291	36
49	TCHL	40.0	PR	T3	N0	M0	Stage IIB	B13-0226	37
50	TCH	45.7	CR	T2	N0	M0	Stage IIA	B10-0753	39
53	TCHL	38.0	N/A discontued lapatinib	T2	N1	M0	Stage IIB	B11-0675	41
54	TCHL	44.7	PR	T2	N0	M0	Stage IIA	B07-1167	48
59	TCH	49.2	CR	T2	N1	M0	Stage IIB	B09-1278	50
61	TCHL	40.8	CR	T2	N0	M0	Stage IIA	B09-1232	52
64	TCHL	57.9	CR	T1	N1	M0	Stage IIA	B13-0262	54
66	TCHL	52.6	CR	T2	N0	M0	Stage IIA	B06-0290	55
72	TCH	68.6	No response	T1	N1	M0	Stage IIA	B09-1276	55
78	TCH	65.6	CR	T2	N1	M0	Stage IIB	B06-0347	59
82	TCHL	57.3	PR	T2	N0	M0	Stage IIA	B10-1668	61
84	TCHL	46.1	PR	T2	N0	M0	Stage IIA	B14-2046	62
88	TCHL	65.3	PR	T1	N0	M0	Stage IA	B09-0743	82

Table 3.2. Ages of patients and healthy control specimens.

3.2.2 EV isolation

Patient serum was isolated and stored according to ICORG instructions (see Appendix II). EVs were isolated using a filtration and ultracentrifugation technique (Figure 3.2.1). 250µL serum specimens were diluted in 5mL PBS. Using a syringe (Sigma-Aldrich; Cat. #: Z248029), BD Precisionglide syringe needle (Sigma-Aldrich; Cat. #:118044) and 0.2µm Acrodisc 32mm syringe filter (VWR; Cat. #: 514-4131), the diluted specimen was filtered into a fresh tube which was then transferred to 8.3mL Quickseal polyallomer ultracentrifuge tubes (Beckman Coulter; Cat. #: 344621), filled with PBS and sealed. Tubes were ultracentrifuged at 110,000*g* for 1 hour 15 minutes at 4°C using a SW32.1Ti swinging bucket rotor. Supernatant was removed, leaving 1mL in the bottom of the tube to resuspend EV pellet. Specimens were transferred to fresh ultracentrifuge tubes, filled with PBS and ultracentrifugation step was repeated. Supernatant was removed, leaving just 100µL in the bottom of the tube to resuspend EV pellet, which was transferred to an Eppendorf. Another 100µL of PBS was used to wash any remaining EVs on the base of the ultracentrifuge tube and was added to the rest of the EV specimen. Specimens were stored at -80°C until required for analysis. Analysis of EVs was displayed in Section 3.3 as per mL of EVs. EV quantities were evaluated whereby EVs were lysed and quantified as described in Section 2.2.7, where equal volumes of EVs and lysis buffer were used to lyse the EVs.

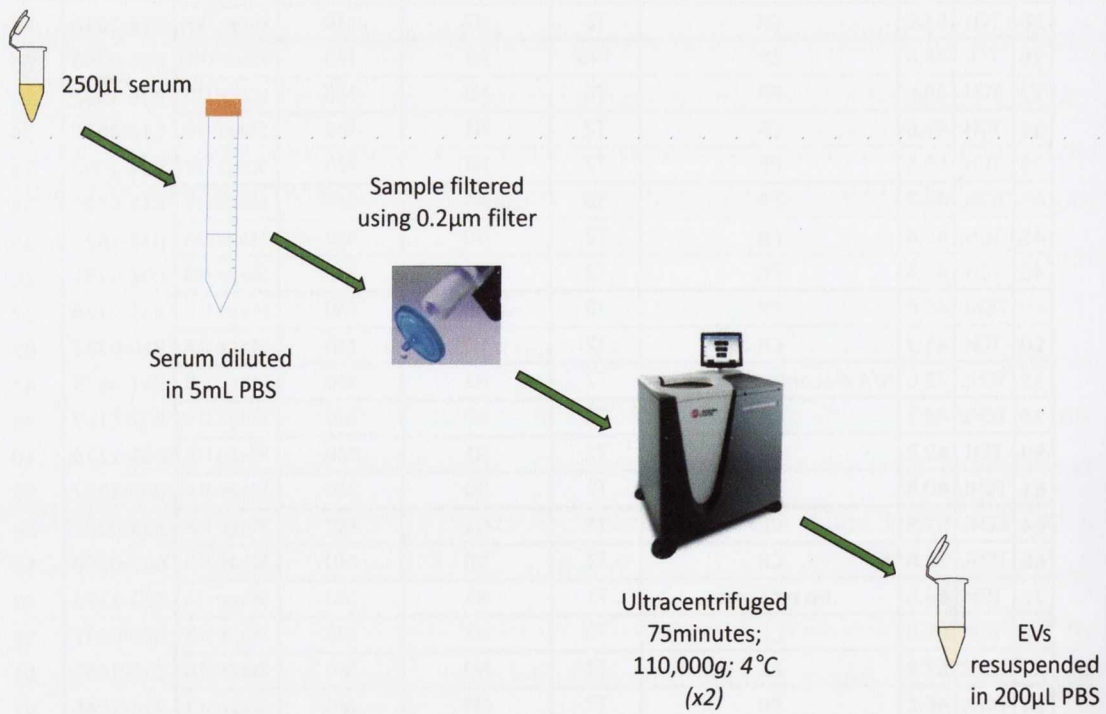

Figure 3.2. Schematic illustration of ultracentrifugation technique used to isolate EVs from serum specimens.

3.2.3 Immunoblots

To extract total protein from EVs, at the end of the isolation process as outlined in Section 3.2.2, however, here, specimens were resuspended in 30μL cell extraction buffer (Invitrogen; Cat. #: FNN0011) supplemented with protease inhibitors (Roche; Cat. #: 05892970001) as opposed to being resuspended with 200μL PBS. Specimens were kept on ice for 30 minutes and vortexed for 10 seconds every 10 minutes during this time. Lysates were centrifuged at 13,000*g* for 10 minutes at 4°C and EV lysate was transferred to a fresh Eppendorf.

Protein concentrations were measured using a Bio-Rad protein assay (Bio-Rad; Cat. #: 5000006). Protein from each specimen was diluted 1:5 (2μL specimen + 8μL dH_20) in duplicate in a 96 well plate. Protein standards (10μL) were also prepared in duplicate (3.125μg/mL, 6.25μg/mL, 12.5μg/mL, 25μg/mL, 50μg/mL, 100μg/mL, 200μg/mL). Bio-Rad protein assay reagent was diluted 1:5 with dH_20 and 200μL of this solution was added to each specimen and standard. Plate was incubated in the dark for 5 minutes and absorbance was read at 595nm using a FluoStar Optima Microplate Reader (BMG Labtech). Linear regression was applied to absorbance readings obtained using GraphPad Prism and the unknown concentrations of specimens were extrapolated from the standard curve. 15μg of each specimen was placed into an Eppendorf and loading buffer was added to at a final concentration of 1x. Specimens were heated at 95°C for 5 minutes and centrifuged briefly to bring all contents to the bottom of the Eppendorf. 10μg of pooled specimens of cancer patients and healthy controls was prepared and loaded for HER2 blot (see Section 3.3.4).

Specimens were loaded into a 10% sodium dodecyl sulphate gels along with a molecular weight marker, SeeBlue Plus2 Pre-Stained standard (Invitrogen; Cat. #: LC5925). Protein was transferred to polyvinylindene fluoride (PVDF) membranes (Bio-Rad; Cat. #: 162-0177) using semi-dry transfer. Ponceau (Sigma-Aldrich; Cat. #: P7170) was used to ensure successful transfer of proteins onto the membrane. Blots were then washed 3 times for 5 minutes in PBS-tween (0.1%) and blocked in 5% bovine serum alumin (BSA) for 1 hour at room temperature. Blots were washed again with PBS-tween (0.1%) and incubated overnight at 4°C, in primary antibodies: PDC61/ALIX (anti-rabbit; 1:1000), CD81 (Santa Cruz; Cat. #: SC-9158), CD82 (anti (Abcam; Cat. #: ab83), Grp94 (anti-Rabbit; 1:1000) (Cell signalling; Cat. #: 2104) and HER2 (anti-mouse; 1:1000) (Calbiochem; Cat. #: OP15; 1:500). Note: SKBR3 and HCC1954 cell protein was used as a positive control for the Grp94 and HER2 blots, respectively. Cells for these specimens were prepared as described in Section 2.2.7). The following day blots

were washed 3 times for 5 minutes in PBS-tween (0.1%) and incubated in appropriate secondary antibody for 1 hour at room temperature (anti-Rabbit; 1:1000) (Cell Signalling; Cat. #: 7076); (anti-Mouse; 1:1000) (Cell Signalling; Cat. #:7074). Blots were washed again and protein bands were visualised by chemiluminescence (ThermoFisher: Cat. #: 34080) using a Chemidoc exposure system (BioRad laboratories).

3.2.4 Transmission Electron Microscopy of EVs

[TEM imaging of EVs was performed in the Centre for Microscopy and Analysis in Trinity College Dublin, with the help of Neal Leddy, Chief Technical Officer]

Following EV isolation protocol outlined above in Figure 3.1, a 10μL aliquot of EV specimen was placed onto Parafilm (Sigma-Aldrich; Cat. #: P7793). A formvar carbon coated nickel grid was placed on the drop, ensuring that the coated side of the grid faces the drop. Grid was left for 30-60 minutes. Grid was washed by placing 30μL drops PBS on the Parafilm and placing grid on each drop for 5 minutes, using absorbent paper between each drop. A drop of paraformaldehyde (2%) was placed on Parafilm and grid placed on top to fix specimen for 10 minutes. Washing step was repeated as above. Grid was contrasted in 2% uranyl acetate (BDH, Cat. #: 30550) and images taken using a JEOL JEM-2100 transmission electron microscope at 100kV.

3.2.5 Nanoparticle tracking analysis (NTA)

The size of EVs isolated from serum was measured using NTA NS500 system (NanoSight, Amesbury, UK). This technology measures the rate of Brownian motion of the nanoparticles using a light scattering system that enables accurate size characterisation of the EV within the range of 10nm to 2000nm. Filtered PBS (0.2μm) was run as a negative control. EV specimens were diluted 1:10-1:100 in filtered PBS, were run at 24°C and had a viscosity of 0.909cP. Six 60 second videos were run for each specimen where the software identifies, tracks and measures Brownian motion of each particle in a specimen from frame to frame of each video. Videos were analysed using NTA software to determine the size of EVs.

3.2.6 ELISAs

ELISA kits for NmU (Peninsula Laboratories International; Cat. #: S-1253.0001), HER2 (Merck Chemicals Limited; Cat. #: QIA10-1EA) and Survivin (Enzo Life Sciences; Cat. #: ADI-900-111) were used according to manufacturer's instructions. A set volume of 50µl per specimen of lysed EVs was used.

3.2.7 Total RNA isolation and quantification

RNA was isolated from serum derived EVs using TRI Reagent (Sigma-Aldrich; Cat. #: T9424). 90µL EV specimen, 160µL PBS (Sigma-Aldrich; Cat. #: D8537) and 750µL TRI Reagent were added to an RNase-free Eppendorf (Ambion: Cat. #: AM12400) and incubated at room temperature for 10 minutes. 200µL chloroform (Sigma-Aldrich; Cat. #: C2432) was added and solution was shaken vigorously for 15 seconds and left to incubate at room temperature for 15 minutes. Specimens were then centrifuged at $13.2x10^4$r.p.m for 15 minutes at 4°C, which separates the specimen into a pink bottom layer containing protein, a white middle layer containing DNA and a clear upper layer containing RNA. The clear upper layer was carefully removed and placed in a fresh Eppendorf. 1.2µL glycogen (derived from oyster) (Sigma-Aldrich; Cat. #: G8751) was added and solution inverted to mix. Then 500µL isopropanol (Sigma-Aldrich; Cat. #: I9516) was added and solution inverted to mix. RNA solutions were placed at -20°C overnight. Specimens were then left at room temperature for 10 minutes and then centrifuged at 13,000*g* for 30 minutes at 4°C. Supernatant was decanted and RNA pellet was washed with 750µL 75% ethanol (Sigma-Aldrich; Cat. #: E7148). Wash step was repeated. Following second wash, supernatant was completely removed and the RNA pellet was allowed to air dry on bench. 10µL RNase-free water (Ambion; Cat. #: AM9930) was added and pellet was allowed to dissolve in this while sitting on ice for 30 minutes. RNA was stored at -80°C. RNA concentration was quantified using 1µL of each specimen with a Nanodrop spectrophotometer ND-1000. See Appendix III for RNA quantifications.

3.2.8 Preparation of cDNA for NmU analysis by qPCR

Following total RNA extraction, cDNA was prepared for qPCR to measure NmU levels in EV specimens. A set volume of 4μL total RNA per specimen was used. 1μL of oligo dT primers (500ng/μL) (Eurofins MWG Operon) was added to 4μL RNA and specimens were incubated at 72°C for 10 minutes, then cooled on ice. A master mix was prepared in as outlined in Table 3.3., and 15μL was added to each specimen. cDNA was then prepared by incubating specimens at 37°C for 60 minutes.

Reagent	Volume (per sample)
10x buffer (Sigma-Aldrich; Cat. #: B8559)	2μL
RNasin (40U/μL) (Sigma-Aldrich; Cat. #: R2520)	1μL
dNTP (100mM) (Sigma-Aldrich; Cat. #: DNTP100)	1μL
Nuclease free water (Life Technologies; Cat. #: AM9920)	10μL
MMLV-RT (200U/μL) (Sigma-Aldrich; Cat. #: M1302)	1μL

Table 3.3. Reagents for master mix for NmU cDNA synthesis.

3.2.9 Preparation of cDNA for miR-210 analysis by qPCR

cDNA was also prepared for qPCR to measure miR-210 levels in serum specimens. A set volume of 4μL total RNA per specimen was used for cDNA synthesis. The RNA was added to 11μL of a master mix per specimen, as outlined in Table 3.4, for a total of 15μL cDNA. Once reagents were prepared, cDNA was made using incubation times and temperatures as outlined in Table 3.5.

Reagent	Volume (per sample)
100mM dNTP (Life Technologies; Cat. #: 18427013)	0.15μL
Multiscribe reverse transcriptase (Life Technologies; Cat. #: 18427013)	1μL
10x RT buffer (Life Technologies; Cat. #: 18427013)	1.5μL
Rnase inhibitor (Life Technologies; Cat. #: 18427013)	0.19μL
Nuclease free water (Life Technologies; Cat. #: AM9920)	5.16μL
5x primer (Life Technologies; Assay ID 000512)	3μL
Total RNA	4μL

Table 3.4. Preparation of master mix for miR-210 cDNA synthesis.

Steps	Temperature	Duration
Step 1	16°C	30 mins
Step 2	42°C	30 mins
Step 3	85°C	5 mins
Step 4	4°C	∞

Table 3.5. Incubation times and temperatures used to prepare miR-210 cDNA.

3.2.10 qPCR: NmU and miR-210

qPCR was performed for NmU and miR-210 using a fixed volume of cDNA, 4μL cDNA per specimen. Taqman assays were used (miR-210: Assay ID: 000512; NmU: Assay ID: 4351370), and purchased from Life Technologies. Reagents for qPCR were prepared as outlined in Table 3.6 and qPCR was run under conditions outlined in Table 3.7.

Reagent	Volume (per sample)
20x primer	1μL
Nuclease free water (Life Technologies; Cat. #: AM9920	5μL
Taqman 2x Universal PCR master mix, no Amperase UNG (Life Technologies; Cat. #: 4440048)	10μL
Prepared cDNA	4μL
Total reaction volume	**20μL**

Table 3.6. Preparation of master mix for qPCR.

Steps	Temperature	Duration
Step 1	95°C	10mins
Step 2: 40 cycles	95°C	15secs
	60°C	60secs

Table 3.7 Incubation times and temperatures used to perform qPCR.

3.2.11 Statistical analysis

[Performed in collaboration with statistician Ricardo Segurado]

Statistical analysis was performed using GraphPad Prism 5. *P*-values were generated using Student's t-tests and ANOVA, where $p<0.05$ was considered as statistically significant. With the help of Ricardo Segurado, binary logistic regression was applied to data to predict CR relative to PR or NR. Predictors were EV quantities, EV NmU and EV survivin concentrations at pre-treatment, after cycles 2, 3, 4, 5 and 6 and at post-treatment. Analyses were adjusted for treatment arm by including two dummy variables: for trastuzumab treatment and for trastuzumab and lapatinib treatment, where lapatinib alone served as the reference group. Graphs for patterns over time of the probability of CR as predicted by EV quantities, EV NmU or EV survivin were generated.

3.3 Results

3.3.1 Patient outcome from clinical trial

Specimens from 32 patients were available for testing. Following 6 cycles of anti-cancer treatment, patients were assessed for the success of their neo-adjuvant treatment and were determined as having achieved a CR, PR or NR (see Section 3.2.1). Overall outcome of patients along with a breakdown of which treatment group patients belong to is summarised in Figure 3.3., where the assessment of patient outcome was analysed several weeks after the last cycle of treatment was administered and is referred to here as post-treatment. 43.75% of patients achieved a CR, 50% achieved a PR and 6.25% of patients displayed NR to treatment.

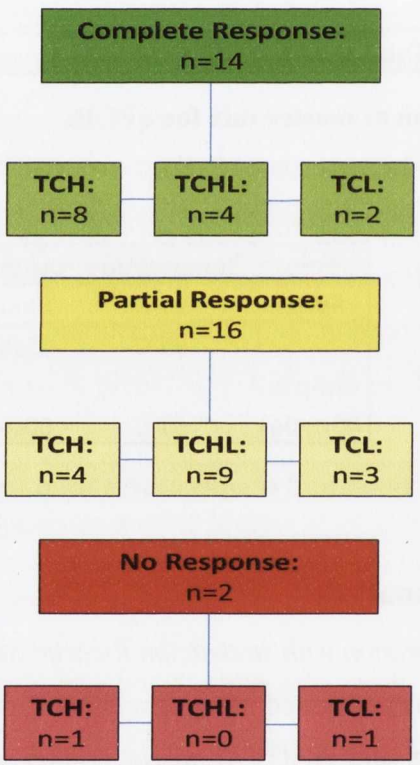

Figure 3.3. Patients' outcome from clinical trial. 43.75% of patients achieved CR, 50% of patients achieved PR and 6.25% achieved NR. (CR = complete response; PR = partial response) (T = docetaxel; C = carboplatin; H= trastuzumab; L = lapatinib).

3.3.2 Successful isolation of EVs from serum specimens

EVs were successfully isolated from patient serum specimens using the filtration and ultracentrifugation technique described in Section 3.2.2. Nanoparticle tracking analysis was performed using a NanoSight and revealed that the vesicles isolated using this method were, on average, 67–86nm in diameter (Figure 3.4.A). TEM images indicate that the vesicles isolated have the appropriate spherical shape typically associated with EVs (Figure 3.4.B). Immunoblots were also performed in the characterisation of the EVs in order to establish if the vesicles isolated contain typical EV-markers (see Section 1.4.2), ALIX/PDC6I and CD81. Presence of EVs was confirmed by the positive detection of both ALIX/PDC6I and CD81, while specimens were found to be negative for the negative control Grp94 (Figure 3.4.C).

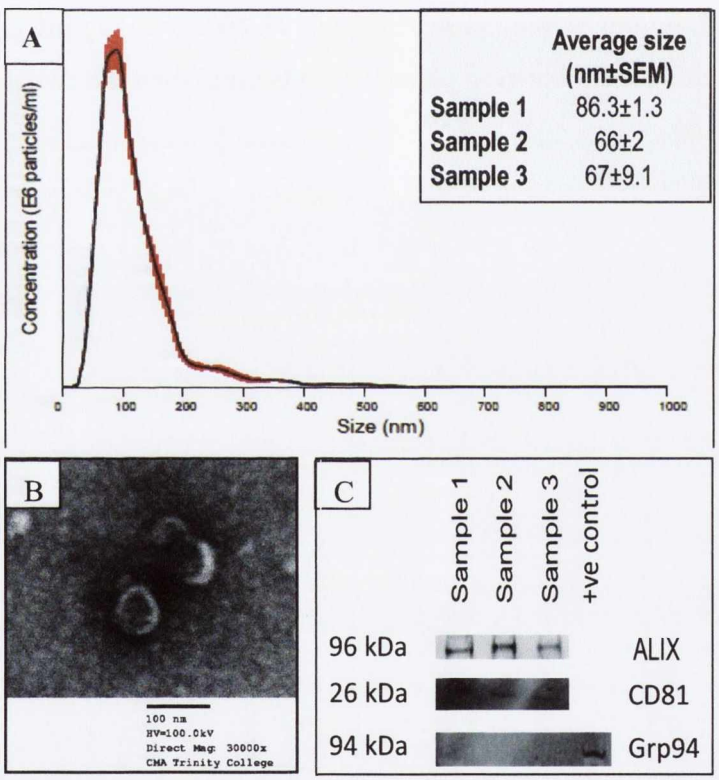

Figure 3.4. Characterisation of EVs isolated from serum. A. NanoSight analysis indicated that EVs isolated were nanosized particles (67–86nm in diameter, on average); B. TEM analysis confirmed that the vesicles were nanosized and that they display the spherical shape associated with EVs; C. Immunoblotting of EVs confirmed the presence of exosomal markers ALIX/PDC6I and CD81, and the absence of negative control Grp94.

3.3.3 Quantification of EVs

Protein quantification using a BCA assay (see Section 3.2.2) was performed as a surrogate measurement of the quantity of EVs isolated from healthy control and cancer patient serum specimens. The EV quantities of healthy controls was (607.4±15.3μg/mL) compared to the levels EV quantities of cancer patients' pre-treatment (1,290.0±58.0μg/mL). Quantification of these specimens revealed that healthy control specimens contained significantly ($p=5.04x10^{-17}$) less EVs i.e. 2.2±0.1 fold less, compared to the cancer patients prior to treatment per mL of EVs (Figure 3.5.A).

EV quantities were also measured at all stages of treatment i.e., pre-treatment, pre-cycle 2 (1,158.6±91.3μg/mL), pre-cycle 3 (1,105.2±88.7μg/mL), pre-cycle 4 (1,111.2±88.1μg/mL), pre-cycle 5 (1,144.9±90.3μg/mL) and pre-cycle 6 (1,104.5±85.4μg/mL) and post-treatment (1,260.3±48.7μg/mL). There were no significant differences between patient EV quantities over the course of their treatment (Figure 3.5.B).

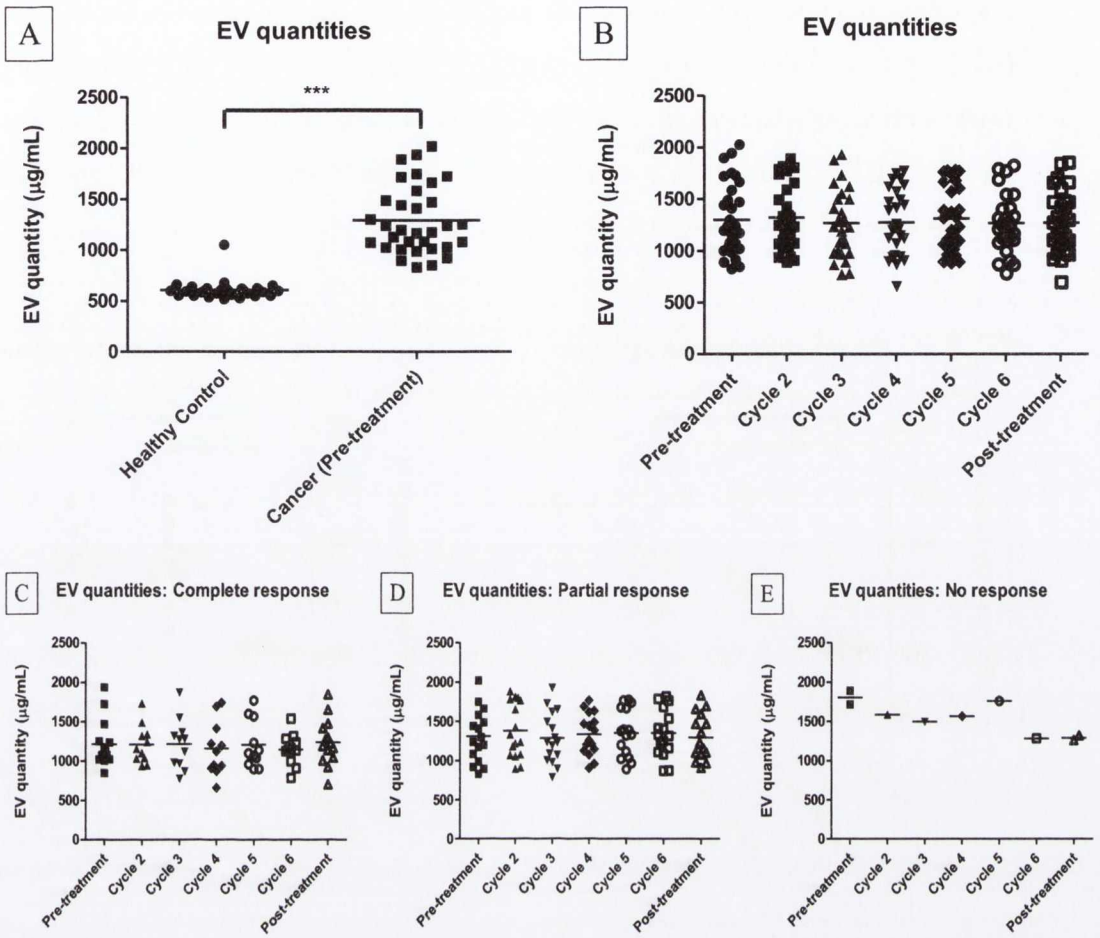

Figure 3.5. EV quantities of normal control and cancer patients. A. Cancer patients had 2.2 fold higher EV concentrations compared to healthy controls. B. There was no significant variation in EV quantity between patients when compared pre-, during and post-treatment. C-E. No significant variation in EV quantity between patients was detected during the course of treatment when patients are grouped as achieving CR, PR or NR.

When patient EVs were grouped according to response i.e. CR, PR or NR, at pre-treatment, a trend was observed (Figure 3.6.A). Here a stepwise increase in EV quantities (displayed per mL of EVs) is seen beginning at the lowest for normal controls at 607.4±15.3µg/mL, increasing to 1,215.94±79.9µg/mL for those who achieved CR, increasing further to 1,308.4±84.0µg/mL for those who achieved a PR and reaching 1,801.44±88.0µg/mL on average for non-responders. While the increase in EV quantity is statistically significant ($p=3.78\times10^{-7}$) between healthy controls and CR; and healthy controls and PR ($p=8.16\times10^{-11}$), the difference in EVs between CR and PR grouped patients was not significant (p=0.435). The stepwise increase in EV quantities observed

at pre-treatment plateaus at post-treatment (Figure 3.6.B), where values for CR, PR and NR were 1,238.3±78.7µg/mL, 1,294.7±72.2µg/mL and 1,290.3±30.0µg/mL respectively. Again, here the CR ($p=1.61x10^{-7}$) and PR ($p=8.18x10^{-11}$) groups are significantly different from healthy controls, but were not found to be significantly (p=0.601) different from each other.

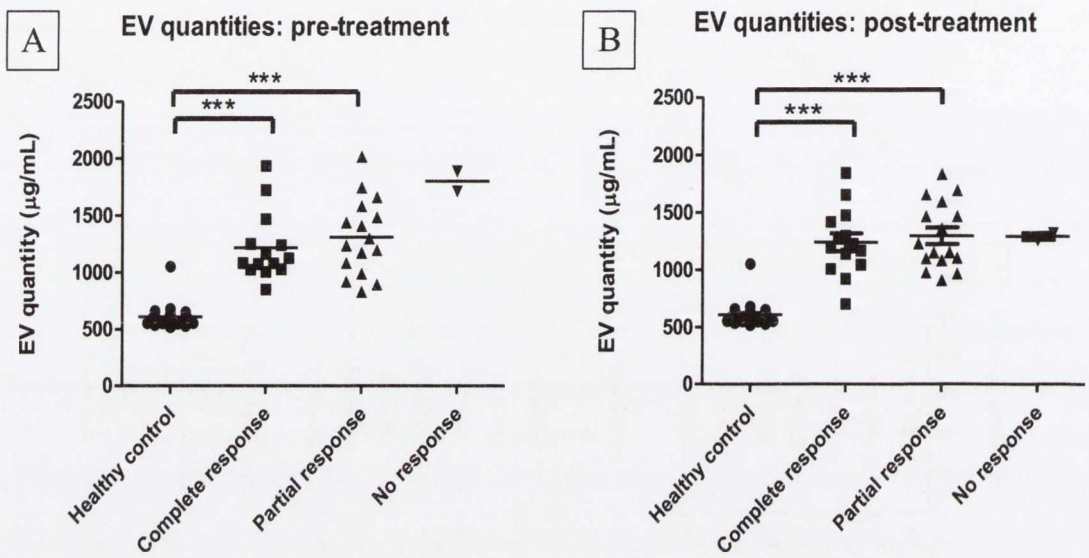

Figure 3.6. EV quantities for patients grouped for response to treatment. A. Incremental increases in EV concentration was seen pre-treatment when comparing normal control specimens to patients that experienced a CR, PR or NR to anti-cancer treatment; B. This trend remained at post-treatment, which was taken several weeks after the last cycle of drug treatment.

Patients grouped for response to treatment were then compared for EV quantification pre- and post-treatment (Figure 3.7). The average values for CR were 1,215.9±79.9µg/mL at pre-treatment and 1,238.3±78.7µg/mL post-treatment, which do not differ significantly (p=0.844) from each other. Similarly, for PR patients, average EV quantities at pre-treatment were 1,308.4±84.0µg/mL, which was not significantly (p=0.903) different from 1,294.7±72.2µg/mL, post-treatment values. Pre-treatment EV quantities for patients with NR were 1,801.4±88.0µg/mL, which decreased to 1,290.3±30.0µg/mL on average post-treatment.

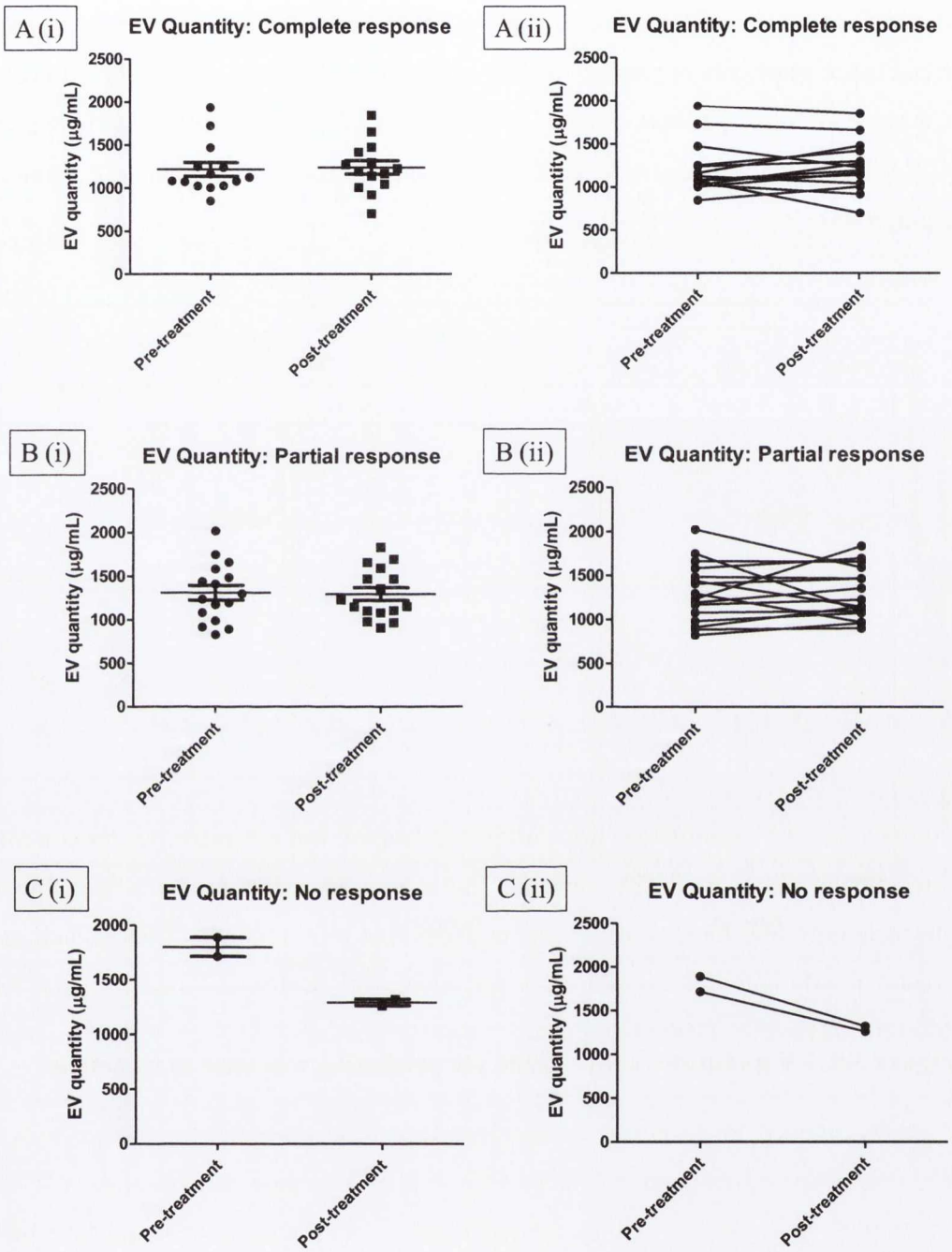

Figure 3.7. Pre- and post-treatment EV quantities for patients grouped based on their response to therapy. A-C. There was no significant difference in EV quantities between pre- and post- treatment time-points for patients who achieved CR, PR or NR.

To evaluate the potential for using EV quantities for prediction of response to treatment binary logistic regression (see Section 3.2.11) was applied to the EV data, which was then adjusted for each treatment arm in the clinical trial. Across each treatment arm the trend is the same, where patients with lower levels of EVs were more likely to achieve CR response while patients with higher levels of EV quantity were less likely to achieve CR. While these observed differences do not reach statistical significance, the trends are clear, Figure 3.8.

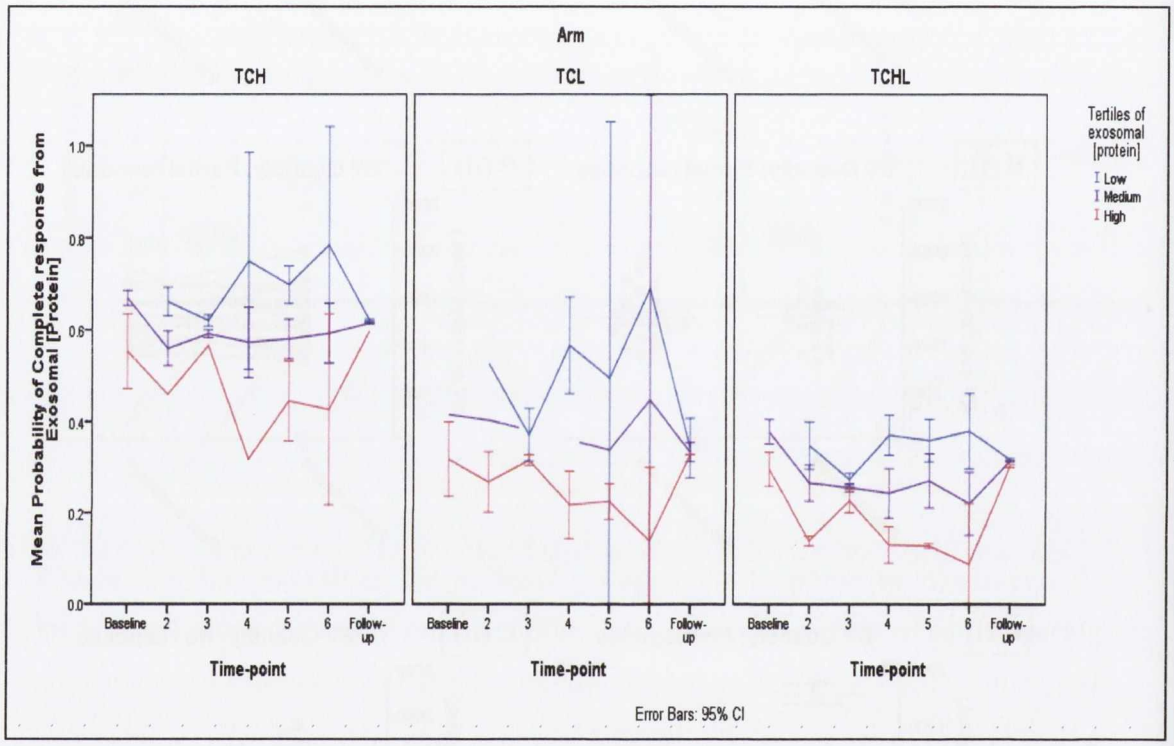

Figure 3.8. EV quantities shows trend for predicting response to treatment.

3.3.4. EV HER2 and serum HER2

3.3.4.1 EV HER2

Levels of EV HER2 content were measured by ELISA and it was found that levels of HER2 detectable in these EV specimens were negligible (0 – 0.029 ng/mL) (Figure 3.9.A). As most specimens did not have detectable HER2, statistical analysis could not be performed. To validate this finding, cancer patients' and healthy control EVs were pooled and analysed using immunoblotting for HER2, using HCC1954 cell lysate as a positive control. The blot image in Figure 3.3.4.B confirms the absence of HER2 from these EV specimens, where no band was detected at 185kDa.

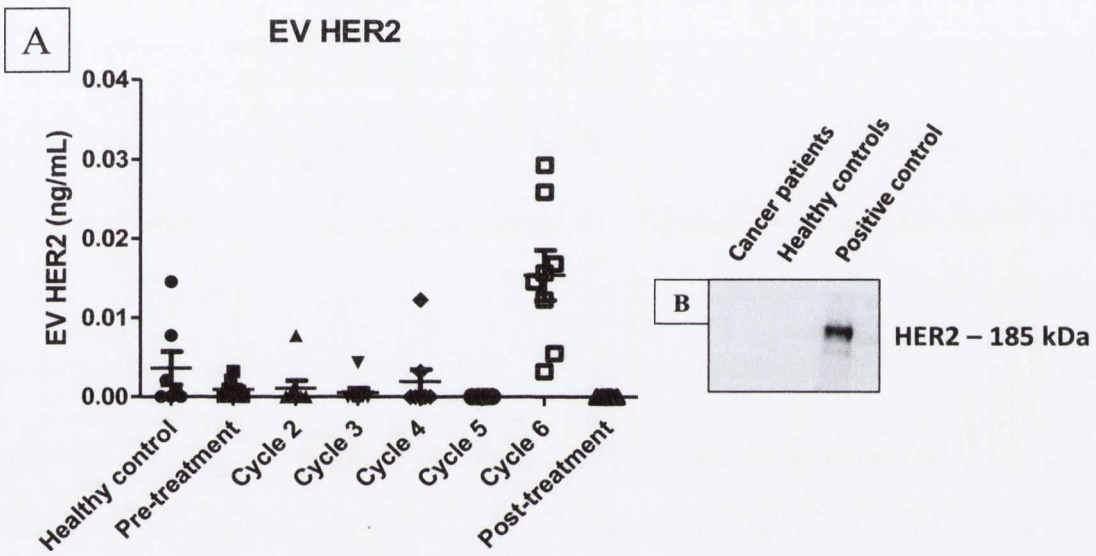

Figure 3.9. EV HER2 content. A. EV HER2 content as measured by ELISA reveals little to no HER2 detection in specimens. B. EV HER2 content as measured by immunoblot validates the absence of detectable HER2 in EV specimens.

3.3.4.2 Serum soluble HER2

Serum levels of non-membrane bound, soluble HER2 were also measured by ELISA. Average values for soluble HER2 over the course of treatment for all patients were 0.547±0.12ng/mL (pre-treatment), 0.105±0.04ng/mL (cycle 2), 0.107±0.04ng/mL (cycle 3), 0.093±0.03ng/mL (cycle 4), 0.09±0.04 (cycle 5), 0.104±0.03ng/mL (cycle 6) and 0.068±0.03ng/mL (post-treatment) (Figure 3.10.A). Soluble HER2 was detected at all treatment cycles and post-treatment. These were significantly reduced when compared to pre-treatment.

This trend was also seen when data was analysed for patient response (Figure 3.10.B-D). For patients with CR, soluble HER2 values for treatment cycles and post-

treatment were significantly decreased when compared to pre-treatment values. A similar trend was also seen for patients with PR and NR, however, here, soluble HER2 values for treatment cycles and post-treatment did not decrease significantly when compared to pre-treatment values.

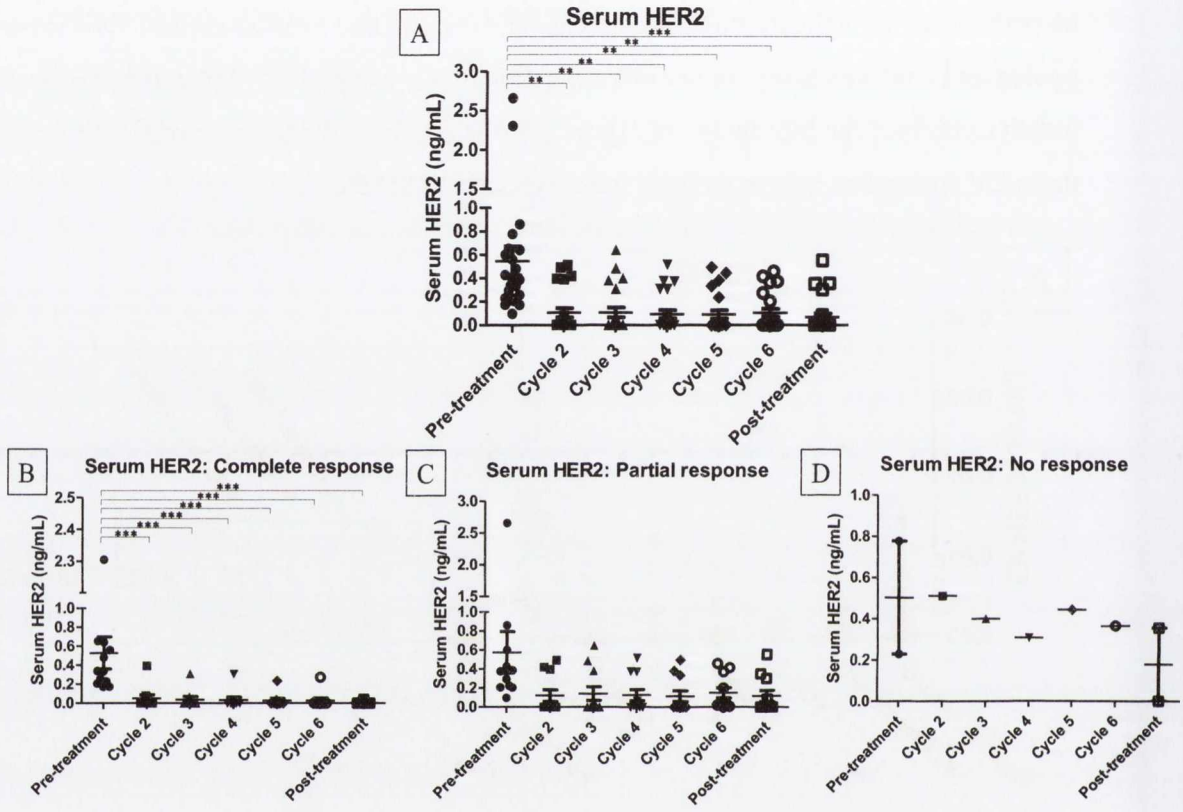

Figure 3.10. Serum soluble HER2 concentration pre, during and post-treatment. A. Serum levels of soluble HER2 were measured prior to, during and after treatment and were found to decrease overall during the course of therapy. B. Serum soluble HER2 levels in patients with CR. C. Serum soluble HER2 levels in patients with PR. D. Serum soluble HER2 levels for patients with NR to treatment.

Average serum soluble HER2 levels did not differ significantly when grouped patients who achieved CR, PR and NR patients (Figure 3.11). Average HER2 at pre-treatment was 0.529±0.17ng/mL, 0.576±0.22ng/mL and 0.503±0.27ng/mL for patients who achieved CR, PR and NR, respectively. At pre-treatment, CR soluble HER2 was not significantly (p=0.366) different from PR concentrations. Average soluble HER2 concentrations had decreased by post-treatment to 0.005±0.004ng/mL, 0.117±0.06ng/mL and 0.178±0.18ng/mL, respectively. A trend was observed here where soluble HER2 for those who achieve PR is higher on average than levels for those who achieve CR, however this increase is not significant (p=0.057). This trend continued with higher HER2 levels in patients with NR than with PR.

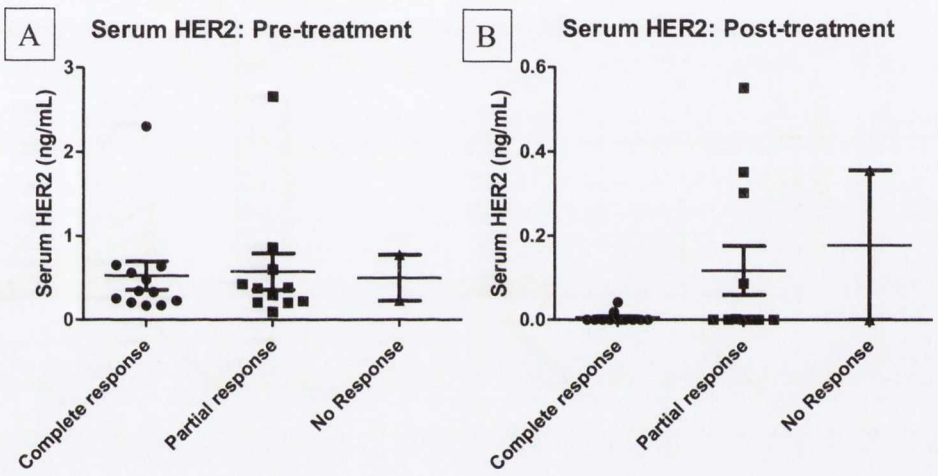

Figure 3.11. Serum soluble HER2 concentration in response to treatment. A. Serum soluble HER2 levels did not differ between CR, PR and non-responders before treatment. B. At post-treatment patients with CR had very low levels of HER2, patients with PR had higher concentrations of HER2 on average and those showing NR to treatment had the highest average HER2 levels measured in serum.

Patients grouped based on their response to treatment were then compared for serum soluble HER2 levels pre- and post-treatment (Figure 3.12). The average value for CR was 0.529±0.17ng/mL pre-treatment, which decreased significantly (p=0.005) to 0.005±0.004ng/mL post-treatment. Similarly, for PR patients, HER2 decreased from a pre-treatment level of 0.576±0.22ng/mL to 0.117±0.06ng/mL at post-treatment, however, this difference was not significant (p=0.903). Pre-treatment EV quantities for patients with NR were 0.503±0.27μg/mL, which decreased to 0.178±0.18μg/mL, on average, at post-treatment.

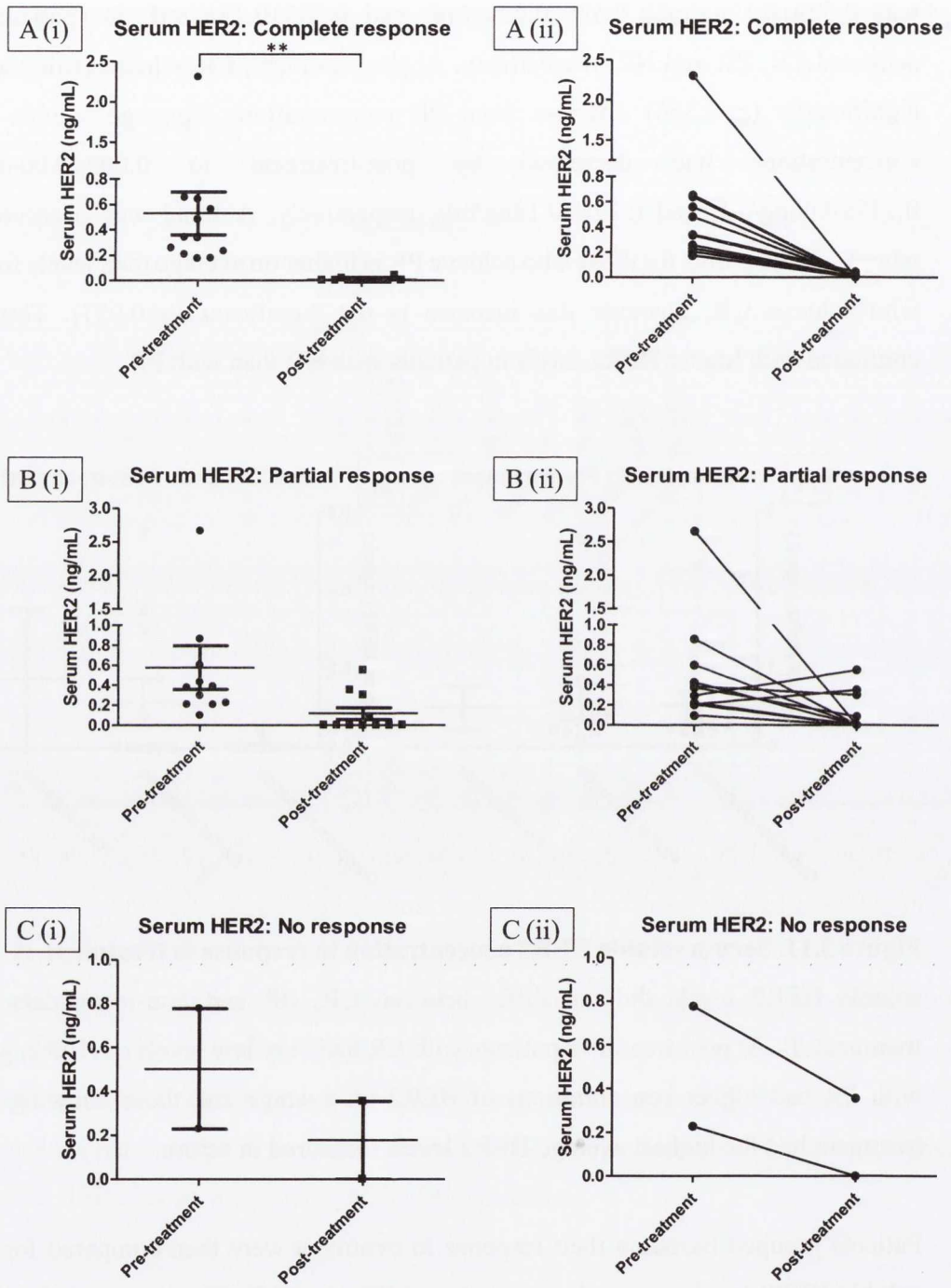

Figure 3.12. Serum soluble HER2 for patients grouped for response, pre- and post-treatment. Serum soluble HER2 decreased significantly at post-treatment compared to pre-treatment for patients who achieved CR. The same trend was observed for patients who achieved PR and NR, but this was not significant.

HER2 was measured both in patient EVs and serum; and were compared (Figure 3.13). Average HER2 was measured as $9.0x10^{-4}\pm4.2x10^{-4}$ng/mL and 0.4719±0.09ng/mL for EVs and serum at pre-treatment, respectively. This average 523.5 fold increase in detectible HER2 in serum was significantly ($p=1.64x10^{-5}$) higher than that measured in EVs.

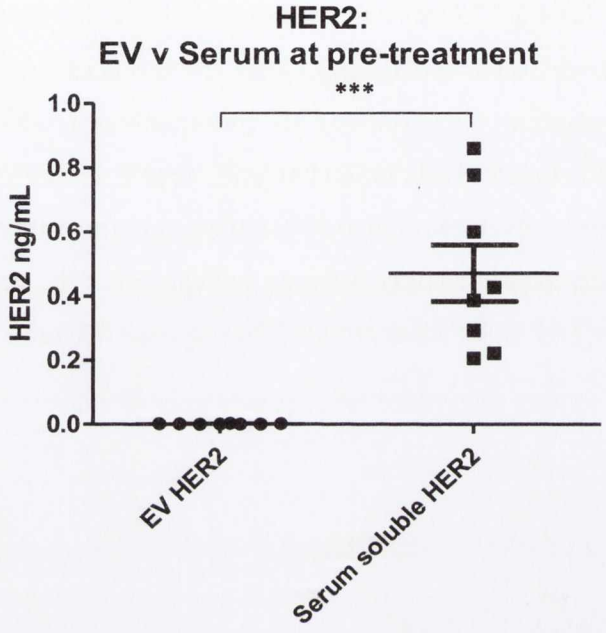

Figure 3.13. EV HER2 compared to serum soluble HER2. Significantly higher amounts of HER2 was detected in serum compared to that detected in EVs.

3.3.5 EV NmU and serum NmU

3.3.5.1. EV NmU

EV NmU concentration was measured by ELISA (see Section 3.2.6) and levels were compared between amounts present in healthy control EVs and cancer patient EVs. Healthy control EVs were found to contain 1.305±0.02ng/mL NmU, while cancer patients had 0.933±0.04ng/mL NmU prior to treatment. As such, cancer patients' EVs were found to have a 1.33±0.04 fold decrease in NmU levels in comparison to healthy control EVs ($p=6.87x10^{-13}$) (Figure 3.14.A). EV levels of NmU were also measured at all stages of treatment: 0.933±0.04ng/mL (pre-treatment), 0.908±0.03ng/mL (cycle 2), 0.94±0.04ng/mL (cycle 3), 0.965±0.04ng/mL (cycle 4), 0.960±0.04ng/mL (cycle 5), 0.914±0.04ng/mL (cycle 6) and 0.974±0.03ng/mL (post-treatment). There were no significant differences in NmU between patients over the course of their treatment overall (Figure 3.14.B) or when grouped for response (Figure 3.14.C-E).

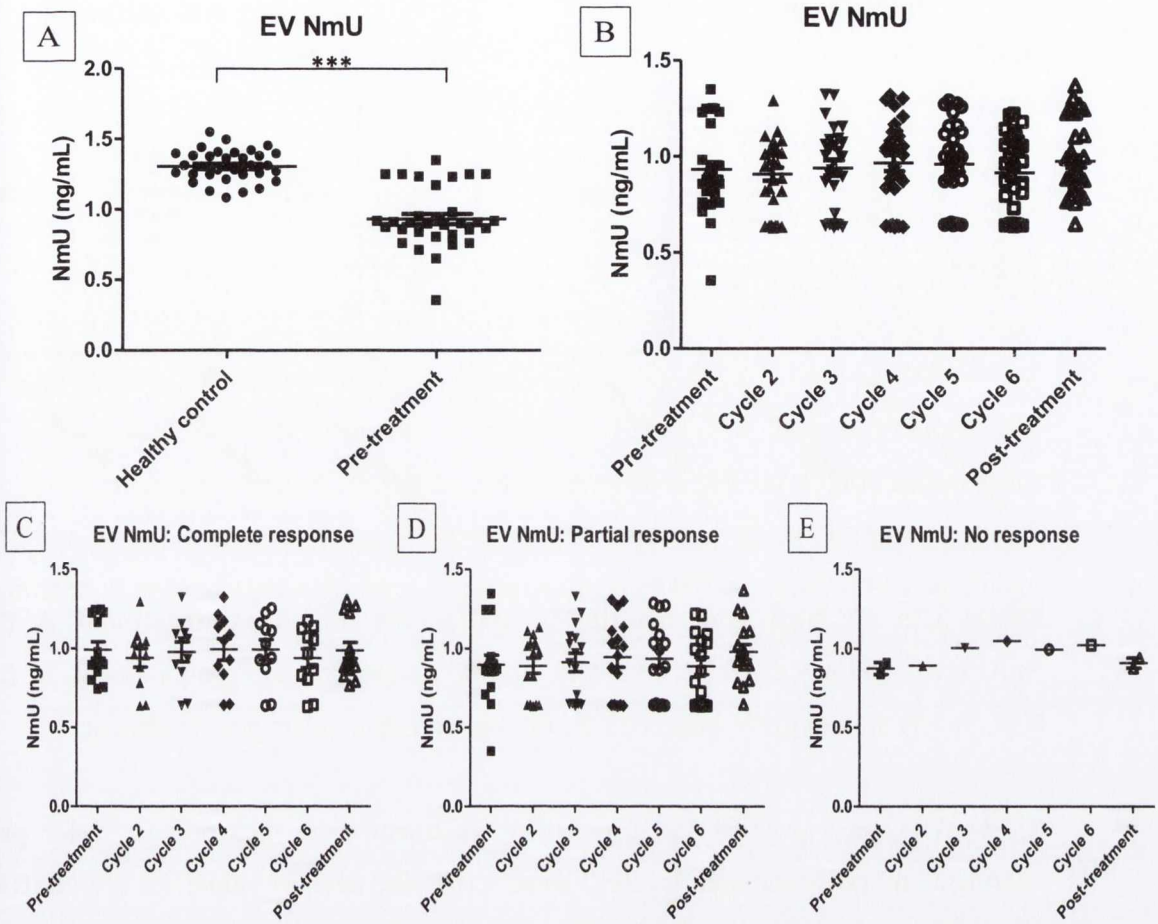

Figure 3.14. EV NmU concentration during treatment. A. There was 1.4 fold more NmU detected in healthy control EVs than in cancer patient EVs B. There was no significant variation in EV NmU concentration between patients when compared pre-, during and post-treatment. C-E. No significant variation in EV NmU levels between patients was detected during the course of treatment when patients were grouped for response.

Similarly, when EV NmU was grouped according to response at pre-treatment, no significant difference was observed between patient who achieved CR and PR ($p=0.300$), where EV NmU was 0.991±0.05ng/mL, 0.897±0.06ng/mL and 0.874±0.04ng/mL for those who achieved CR, PR and NR, respectively (Figure 3.15.A). Likewise, there was no significant difference in patient EV NmU between CR and PR patients at post-treatment ($p=0.878$), where EV NmU concentrations were 0.987±0.05ng/mL, 0.979±0.05ng/mL and 0.909±0.03ng/mL for patients that achieved CR, PR and NR (Figure 3.15.B).

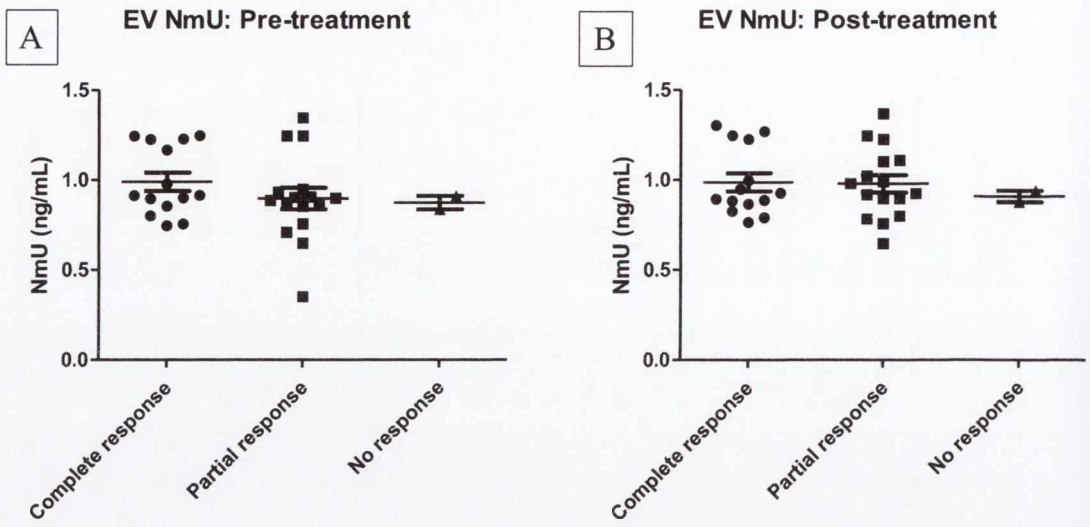

Figure 3.15. EV NmU concentration for patients in response to treatment. A. EV NmU levels did not differ between CR, PR and non-responders pre-treatment. B. EV NmU levels did not differ between CR, PR and non-responders post-treatment.

EV NmU values grouped for response to treatment were then compared for pre-treatment and post-treatment levels (Figure 3.16). The average values for EV NmU at pre-treatment for CR was 0.991±0.05ng/mL and 0.987±0.05ng/mL at post-treatment ($p=0.965$). Average EV NmU at pre-treatment for PR was 0.897±0.06ng/mL and 0.979±0.05ng/mL at post-treatment ($p=0.299$), while average EV NmU at pre-treatment for non-responders at pre-treatment was 0.874±0.04ng/mL and 0.909±0.03ng/mL at post-treatment.

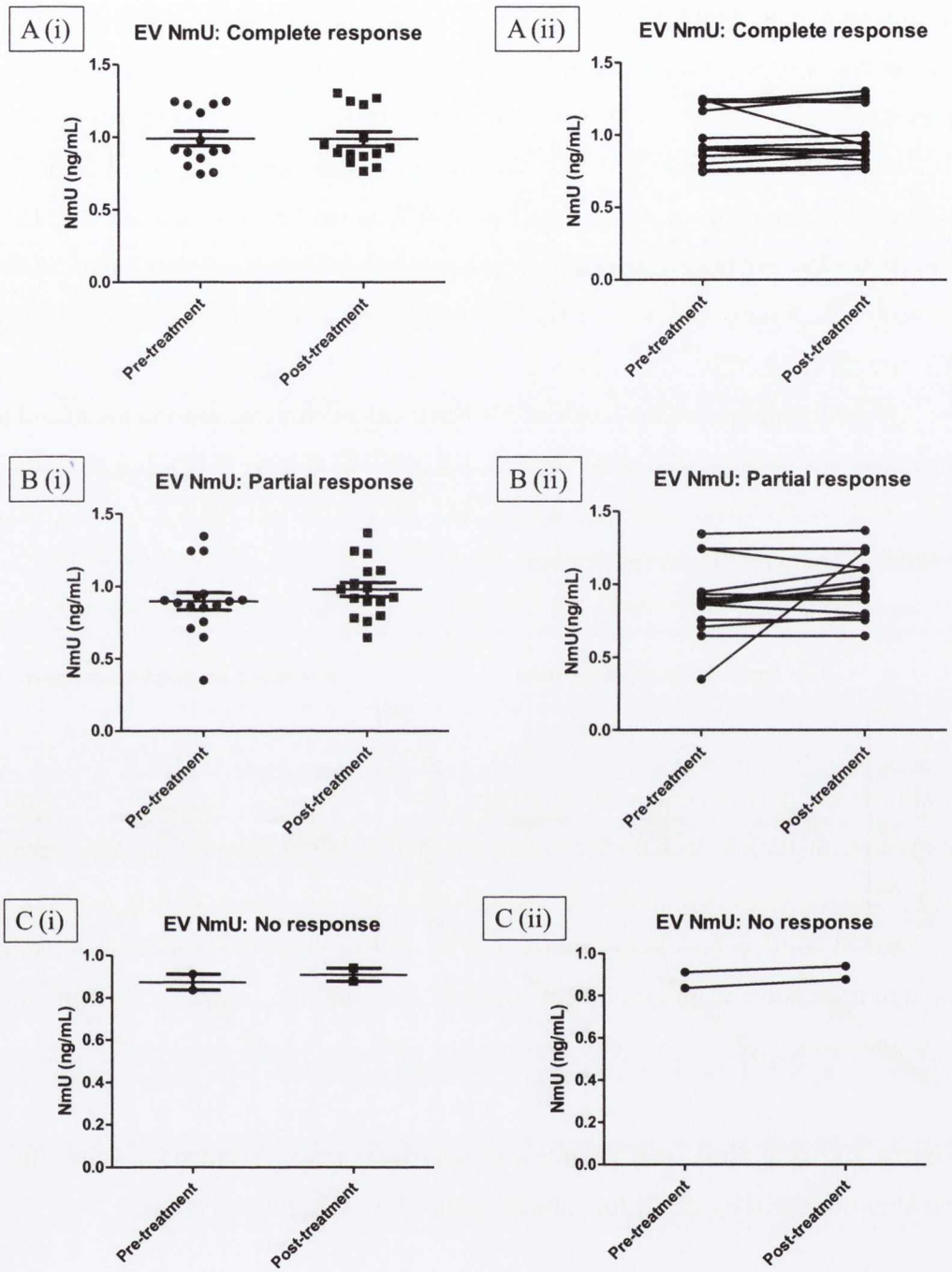

Figure 3.16. EV NmU concentration in patients grouped for response, pre- and post-treatment. There was no significant difference in EV NmU concentration at pre-treatment compared to post-treatment for patients who achieved (A) CR, (B) PR or (C) NR to therapy.

To measure EV NmU at the mRNA level, qPCR was performed on patient EV specimens, where results were grouped for response to therapy at pre-treatment and post-treatment (Figure 3.17). C_T values for NmU mRNA at pre-treatment were 36.2±0.1, 36.1±0.2 and 36.3±0.1 for patients who achieved CR, PR and NR, respectively, where there was no significant differences between patients with CR and PR (p=0.738). At post-treatment, C_T values were 36.4±0.4, 35.7±0.3 and 36.0±0.5, respectively. Again, there was no significant difference observed between patients with CR and PR (p=0.205).

Additionally, mRNA levels of EV NmU were compared pre-treatment and post-treatment for patients who achieved CR, PR and NR (Figure 3.18). For patients with CR, NmU mRNA was increased by 1.8 fold, PR by 1.3 and NR by 2.4 fold, at post-treatment compared to pre-treatment.

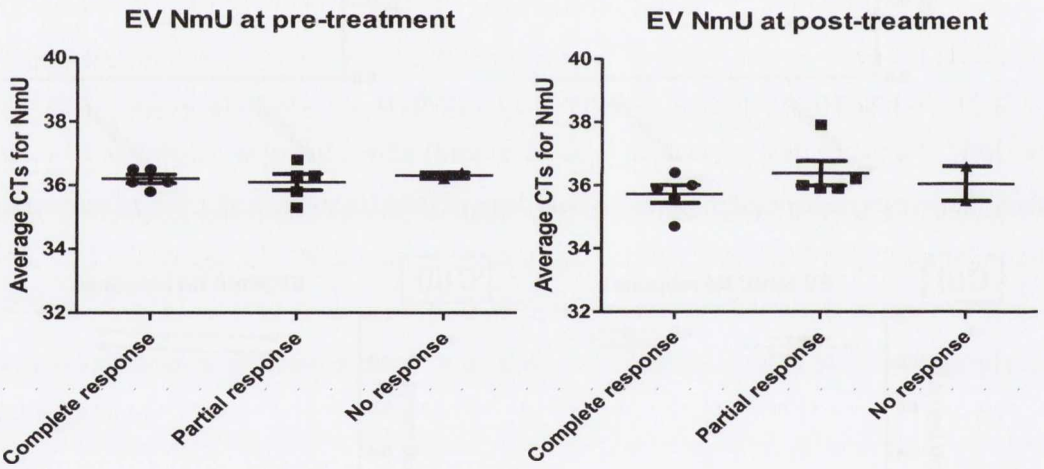

Figure 3.17. EV NmU mRNA pre-and post-treatment. Average C_T values for EV NmU as measured by qPCR for patients grouped for CR, PR and NR.

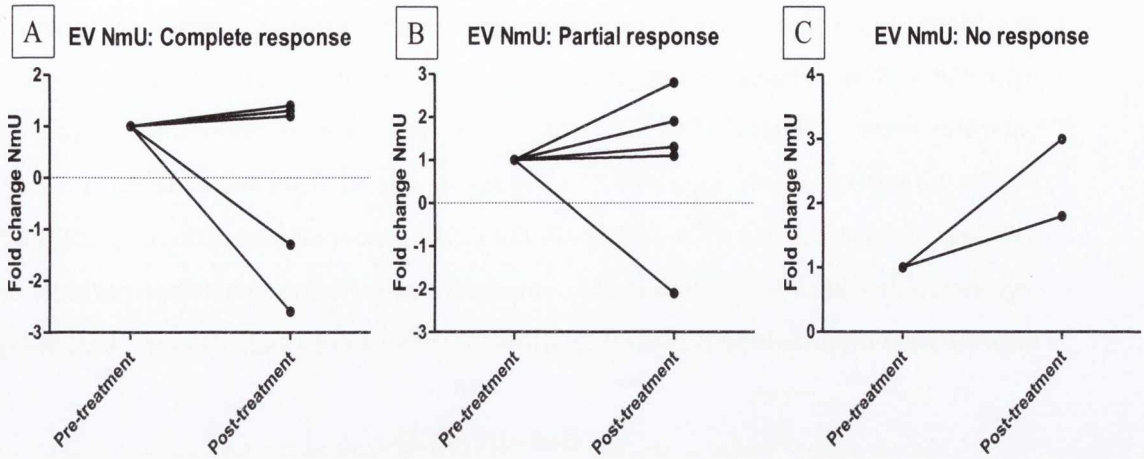

Figure 3.18. EV NmU mRNA grouped for response. Fold change in EV NmU as measured by qPCR for patients grouped for complete response, partial response and NR.

To assess the potential for using EV NmU protein concentration as a tool for predicting response to treatment, binary logistic regression was applied to the data (see Section 3.2.11). The data was grouped for the three treatment arms in the clinical trial (TCH, TCL and TCHL). Although no significant differences were observed, a trend can be seen across the three treatment arms whereby patients that were found to have high levels of EV NmU were more likely to achieve a complete response and patients with low levels of EV NmU were less likely to respond to treatment (Figure 3.19).

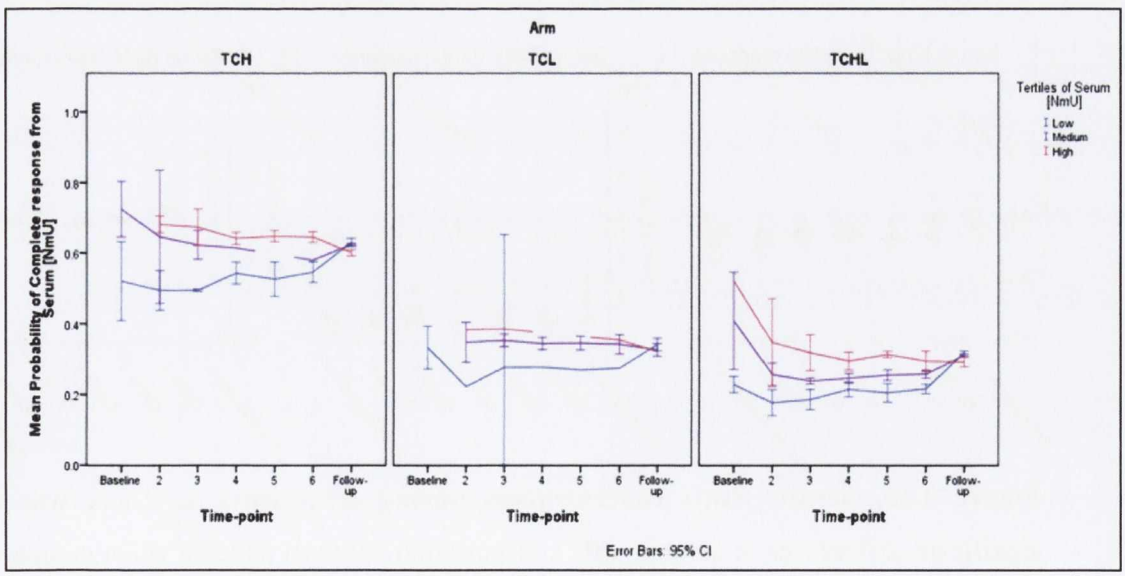

Figure 3.19. EV NmU concentration showed a trend for predicting response to treatment. Patients with high EV NmU were more likely to achieve CR than patients with lower levels of EV NmU.

3.3.5.2 Serum NmU

In addition to measuring EV NmU content, serum levels of NmU were also quantified by ELISA. The average values of serum NmU over the course of treatment for all patients were 1.862±0.75ng/mL (pre-treatment), 0.965±0.06ng/mL (cycle 2), 0.990±0.12ng/mL (cycle 3), 2.488±1.12ng/mL (cycle 4), 1.043±0.17ng/mL (cycle 5), 0.845±0.05ng/mL (cycle 6) and 0.866±0.05ng/mL (post-treatment) (Figure 3.20.A). No significant differences in serum NmU concentrations were found between patients over the course of their treatment overall or when grouped for response (Figure 3.20.B-D).

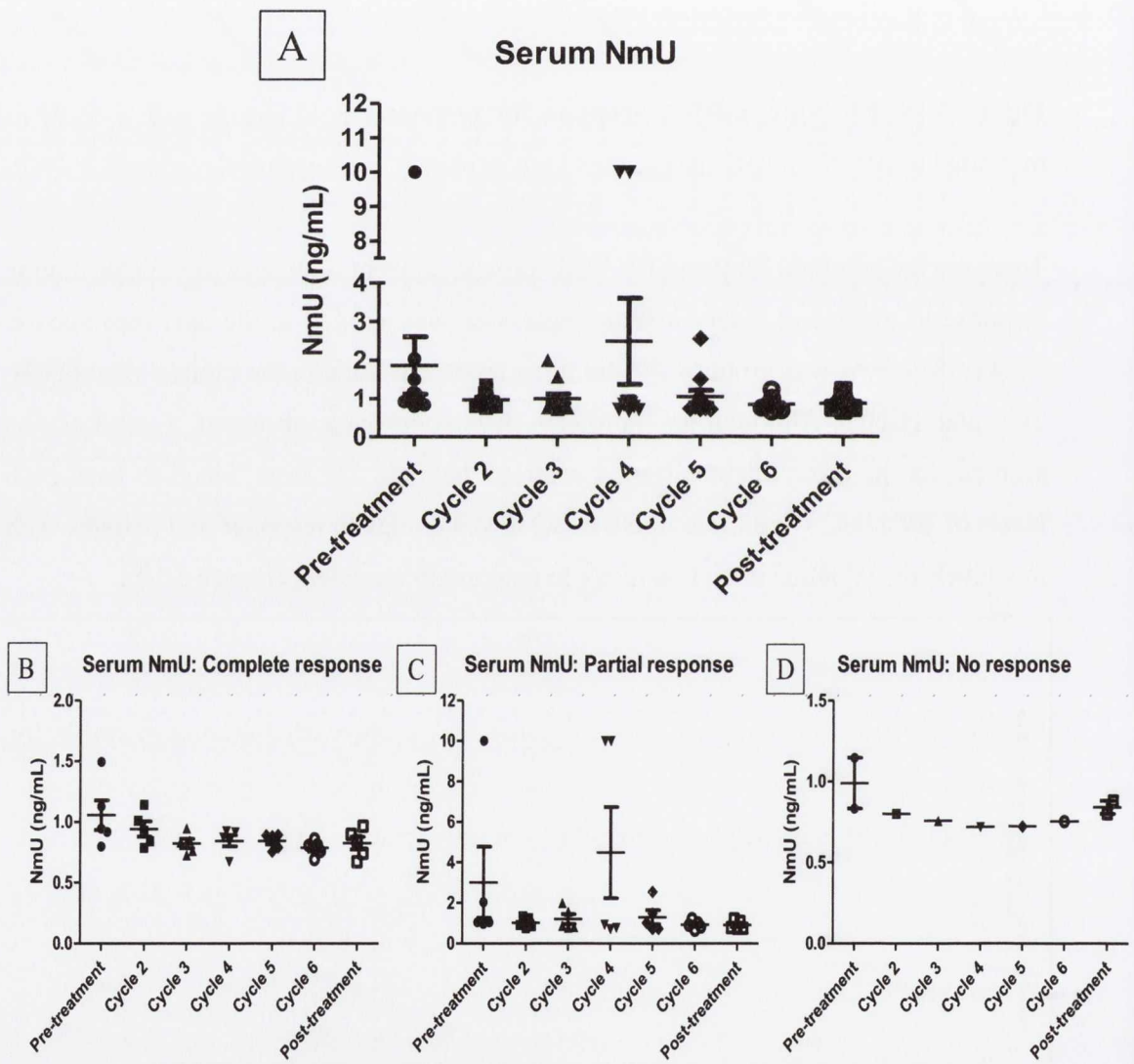

Figure 3.20. Serum NmU concentration during treatment. A. There was no significant differences in serum NmU concentration between patients when compared pre-, during and post-treatment. B-D. No significant variation in serum NmU levels between patients was detected during the course of treatment when patients were grouped as having CR, PR or NR.

Serum NmU concentrations were compared for patients who were grouped for response to treatment, both pre-treatment and post-treatment (Figure 3.21). At pre-treatment, average serum NmU was 1.056±0.12ng/mL, 3.017±1.76ng/mL and 0.990±0.16ng/mL for patients who achieved CR, PR and NR, respectively, where there was no significant difference between patients with CR and PR serum NmU concentrations (p=0.298). Similarly, at post-treatment, no significant differences were seen when comparing average serum NmU between CR and PR (p=0.431), where concentrations were 0.825±0.05ng/mL, 0.918±0.1ng/mL and 0.841±0.04ng/mL, for patients who achieved CR, PR and NR patients, respectively.

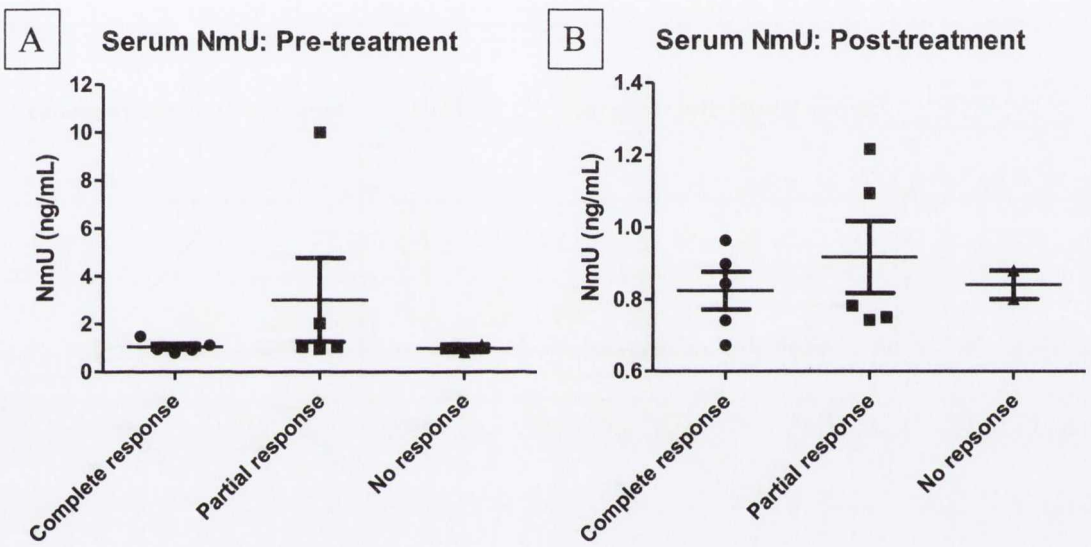

Figure 3.21. Serum NmU at pre- and post-treatment with patients grouped for response. Serum NmU concentrations did not differ significantly between patients who achieved CR, PR and NR pre-treatment (A) or post-treatment (B).

Serum NmU values for patients grouped for those who achieved CR, PR and NR were then compared at pre-treatment and post-treatment time points (Figure 3.22). Average concentrations of serum NmU for patients who achieved CR were 1.056±0.12ng/mL and 0.825±0.05ng/mL at pre- and post-treatment, respectively (p=0.119). Patients who achieved PR had 3.017±1.76ng/mL and 0.918±0.1ng/mL serum NmU at pre- and post-treatment, respectively (p=0.175); and patients with NR to treatment had 0.990±0.16ng/mL serum NmU at pre-treatment which reduced slightly to 0.841±0.04ng/mL by post-treatment.

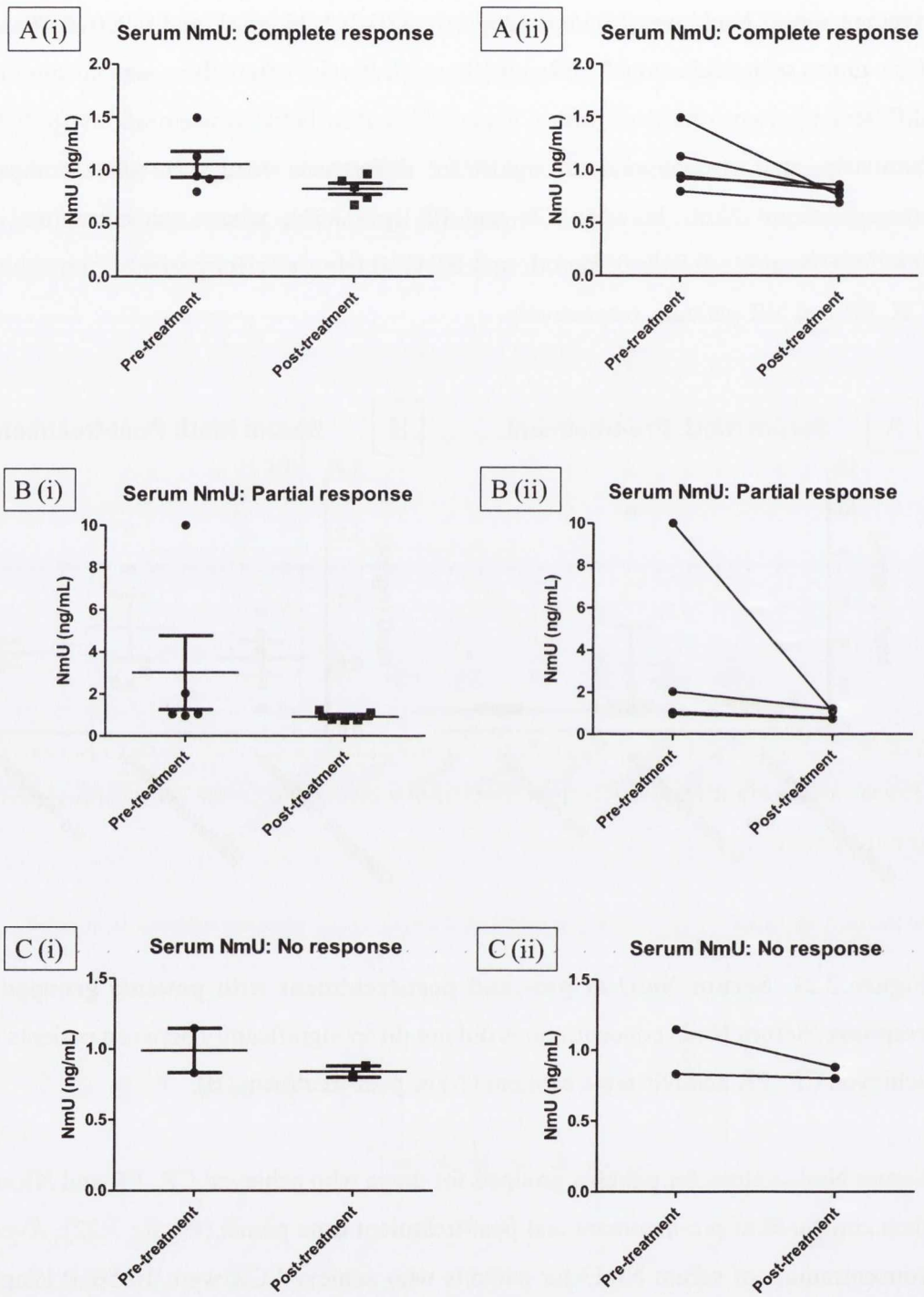

Figure 3.22. Serum NmU concentrations for patients grouped for CR, PR and NR. There was no significant difference in serum NmU in patients who achieved CR (A), PR (B) or NR (C) to treatment between pre-treatment and post-treatment.

Concentrations of NmU were measured both in EVs and directly from serum (Figure 3.23). While NmU was detectable in both specimen types, serum NmU had 1.32 fold higher NmU than EV ($p=0.555$), where EV NmU was 1.412±0.1ng/mL and serum NmU was 1.862±0.7ng/mL, at pre-treatment.

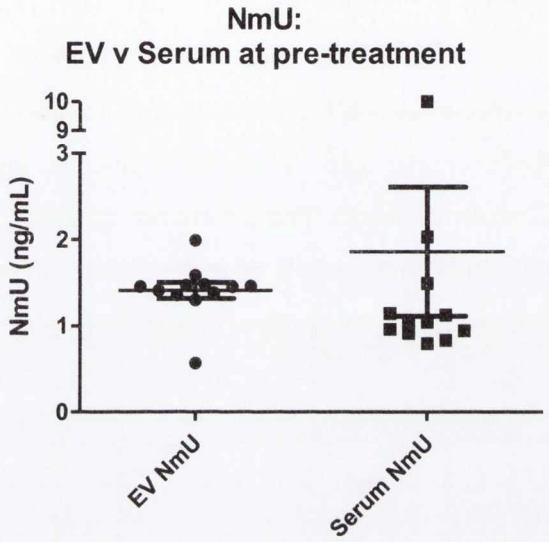

Figure 3.23. EV NmU compared to serum NmU concentrations pre-treatment. There was no significant difference between EV NmU and serum NmU concentrations pre-treatment.

3.3.6 Survivin

EV survivin content was measured by ELISA and amounts present in healthy control EVs were compared to that found in cancer patient EVs pre-treatment (Figure 3.24.A). EV survivin in healthy controls was found to be 18.5±3.8pg/mL, while cancer patient EV survivin was 25.9±4.5pg/mL. This 1.4 fold increase in survivin found in cancer patients compared to healthy controls did not reach significance ($p=0.213$). Additionally, EV survivin was measured for patients at all stages of treatment: 25.9±4.5pg/mL (pre-treatment), 20.9±4.0pg/mL (cycle 2), 14.0±3.6pg/mL (cycle 3), 26.2±4.4pg/mL (cycle 4), 17.9±4.0pg/mL (cycle 5), 38.2±4.6pg/mL (cycle 6) and 9.5±2.8pg/mL (post-treatment). There were no significant differences between patient EV survivin concentrations overall over the course of their treatment cycles (Figure 3.24.B), or when grouped for response (Figure 3.24.C-E).

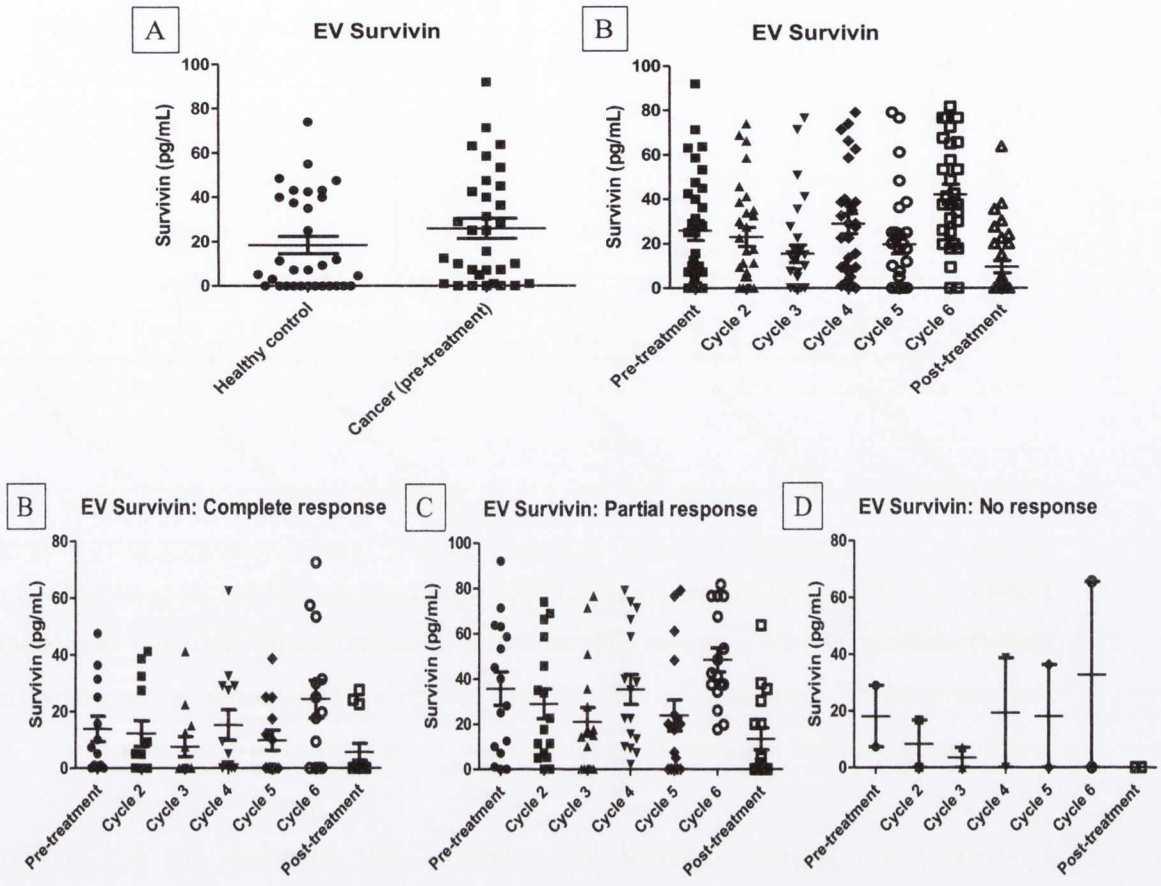

Figure 3.24. EV survivin concentrations during treatment. A. 1.4 fold more EV survivin was detected in cancer patients than in healthy controls. B. No significant difference in EV survivin concentrations between patients when compared pre-, during and post-treatment were detected. C-E. No significant variation in EV survivin concentrations were detected between patients during treatment, when patients are grouped as having CR, PR or NR.

Average EV survivin levels did not differ significantly when grouped for response (Figure 3.25). The average concentration of survivin pre-treatment was 13.9±4.5pg/mL, 35.7±7.3pg/mL and 18.1±10.9pg/mL, for patients who achieved CR, PR and NR, respectively. At post-treatment, survivin concentrations had decreased to 5.7±3.0pg/mL, 13.4±4.8pg/mL and 0±0pg/mL, for patients who achieved CR, PR and NR, respectively. At pre-treatment, EV survivin concentrations were significantly higher in patients who had achieved CR than PR ($p=0.032$). No significant differences in EV survivin were observed at post-treatment.

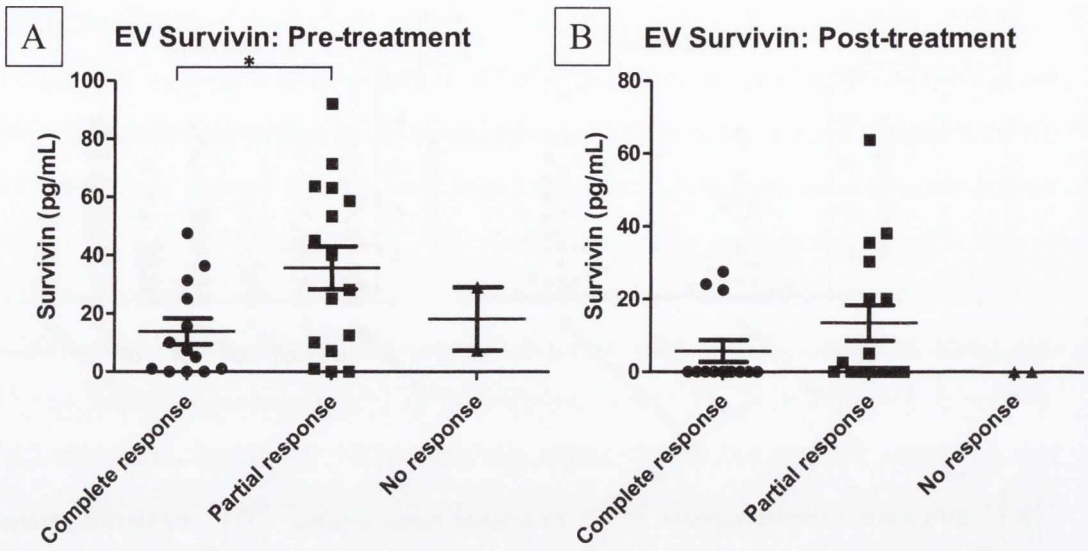

Figure 3.25. EV survivin concentrations for patients grouped for response pre- and post-treatment. (A) EV survivin concentrations increased significantly in patients who had achieved PR compared to CR. (B) EV surviving concentration did not differ significantly between patients who achieved CR, PR and NR post-treatment.

Following this, patients grouped for response were compared for EV survivin concentrations pre- and post-treatment (Figure 3.26). EV survivin values at pre-treatment and post-treatment were 13.9±4.5pg/mL and 5.7±3.0pg/mL, respectively, for patients who had achieved CR ($p=0.144$). For patients who achieved PR, pre-treatment EV survivin concentrations, 35.7±7.3pg/mL, were significantly ($p=0.017$) higher than post-treatment amounts, 13.44±4.8pg/mL. While pre-treatment values for non-responders were 18.1±10.9pg/mL at pre-treatment, which reduced to 0±0pg/mL by post-treatment.

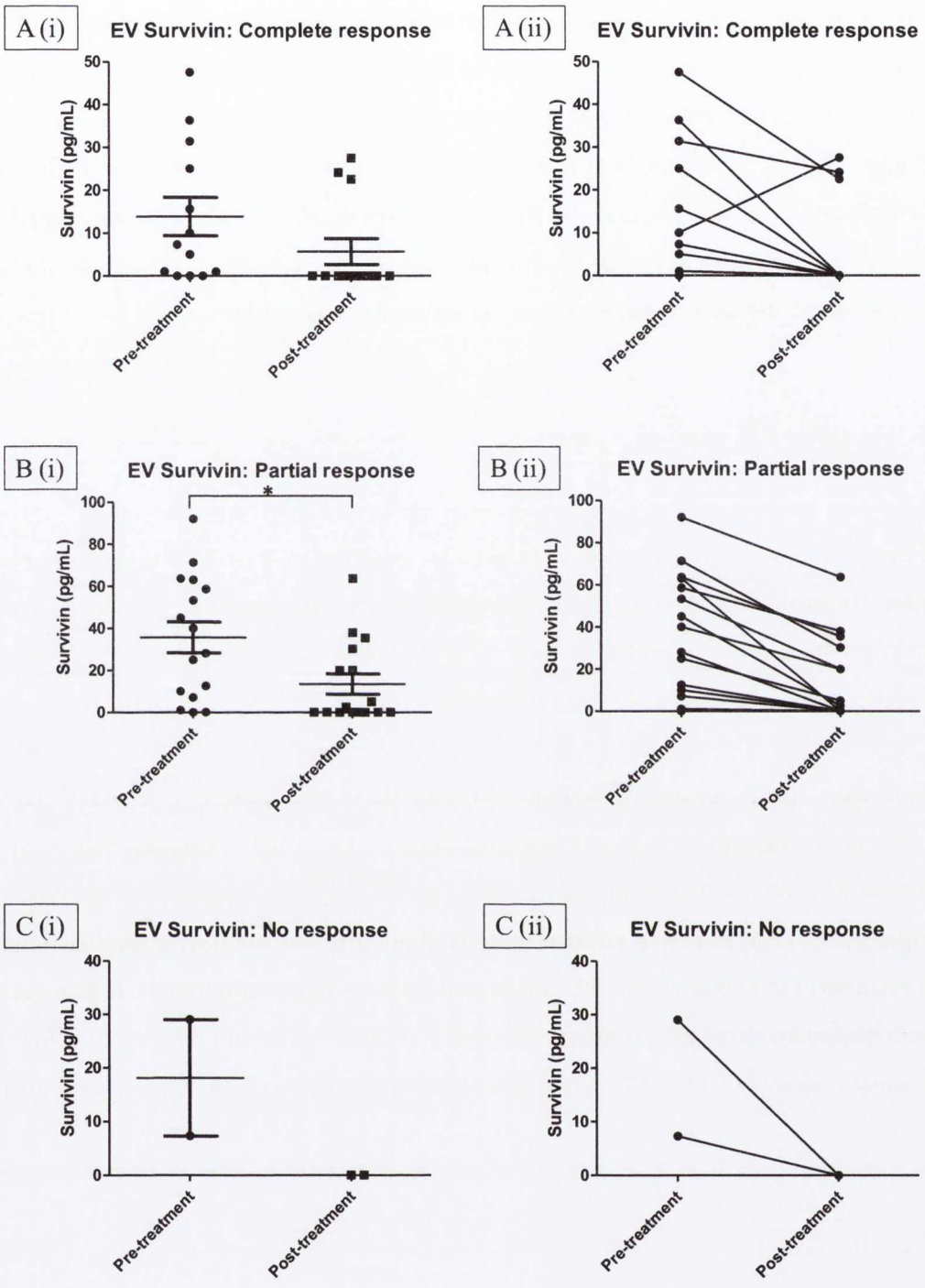

Figure 3.26. EV survivin concentrations for patients grouped for response. EV survivin concentrations when compared pre-treatment to post-treatment decreased in patients who achieved CR (A) (not significantly), PR (significantly) and NR (C) (not significantly), respectively.

To investigate the potential role of EV survivin as a biomarker for prediction of response to breast cancer therapy, data was grouped for the three treatment arms of the trial (TCH, TCL and TCHL) and analysed using binary logistic regression (see Section 3.2.11). Figure 3.27 demonstrated that low levels of survivin was associated the likelihood of achieving a complete response to treatment, whereas high levels were associated with being less likely to respond to therapy. While the data does not reach statistical significance, the same trend was seen across each treatment arm.

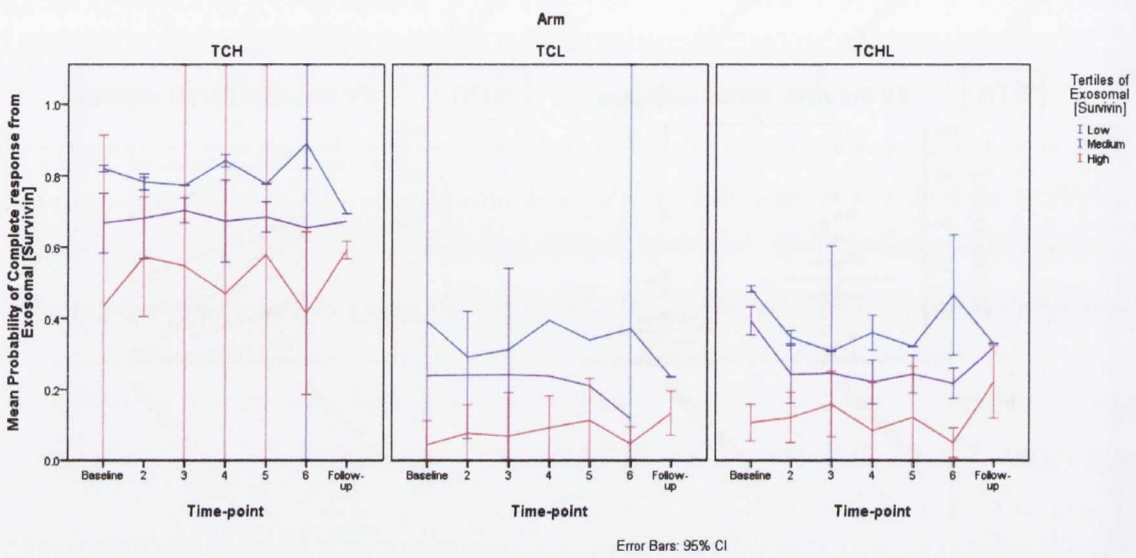

Figure 3.27. EV survivin concentrations show a trend for predicting response to treatment. Patients with low EV survivin were more likely to achieve CR than patients with higher levels of EV survivin.

3.3.7 miR-210

EV levels of miR-210 was measured using qPCR and results were grouped for response pre-treatment and post-treatment (Figure 3.28). C_T values for miR-210 at pre-treatment were 33.7±0.6, 34.3±0.2 and 36.4±0.2 for patients who had achieved CR, PR and NR, respectively, where there was no significant differences between patients who achieve CR and PR (p=0.384). At post-treatment, C_T values were 33.6±0.8, 34.7±0.3 and 35.6±0.4, respectively. Again, there was no significant difference observed between patients who achieved CR and PR (p=0.243). Additionally, levels of miR-210 in EVs were measured and compared at pre-treatment and post-treatment for who achieved CR, PR and NR (Figure 3.29). For patients who achieved CR, EV miR-210 was increased by 1.1 fold, those who achieved PR was decreased by 1.25 and those who experienced NR to therapy was increased by 1.65 fold, on average at post-treatment compared to pre-treatment.

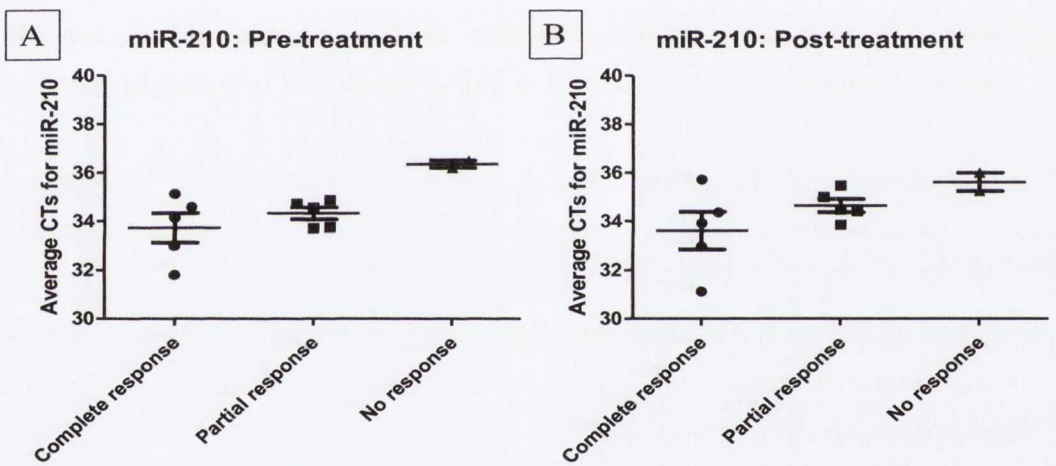

Figure 3.28. EV miR-210 CT values for patients grouped for complete response, partial response and NR.

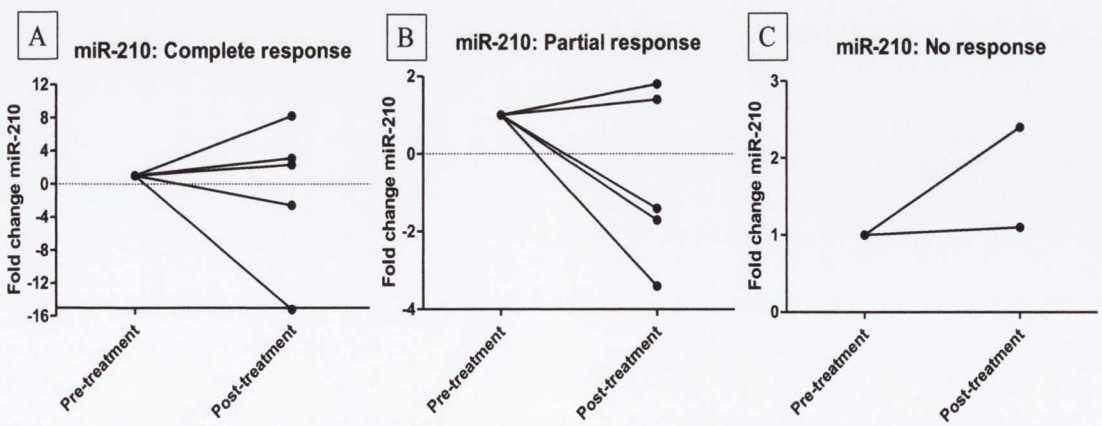

Figure 3.29. Fold change in EV miR-210 as measured by qPCR for patients grouped for complete response, partial response and NR.

EV Quantities	• EV quantities were higher in breast cancer patients compared to healthy controls
	• Patients with higher concentrations of EVs were less likely to achieve CR than those with lower EVs
EV HER2	• HER2 was not detected in serum-derived EVs
Serum soluble HER2	• A significant decrease in serum soluble HER2 concentration from pre- to post-treatment was predictive of response to therapy
EV NmU	• EV NmU concentrations were lower in breast cancer patients compared to healthy controls
	• EV NmU concentrations were not predictive of response to therapy
EV NmU mRNA	EV NmU mRNA levels were not predictive of response to therapy
Serum NmU	• Serum NmU concentrations were not predictive of response to therapy
EV survivin	• EV survivin concentrations were slightly but not significantly higher in cancer patients compared to healthy controls
	• EV survivin concentrations were higher in PR patients compared to CR patients pre-treatment
EV miR-210	miR-210 levels were not predictive of response to therapy

Table 3.8. Summary of the relevance of EVs as biomarkers for HER2-overexpressing breast cancer detection and prediction of response to therapy.

3.4 Discussion

3.4.1 ICORG trial 10-05

The ICORG 10-05 clinical trial aimed to investigate the efficacy of pre-operative combination therapy using docetaxel and carboplatin with trastuzumab and/or lapatinib in HER2-overexpressing breast cancer patients [219]. Overall, the rate of pathological complete remission in patients accrued for ICORG 10-05 clinical trial was high with 45% of patients achieving a CR with adjuvant treatment. Taking treatment into consideration, 29.7% of those with CR were part of the TCH treatment arm, 12.5% were from the TCHL arm and 3.1% were treated with TCL, which indicates that patients who received trastuzumab as part of their adjuvant therapy were most likely to achieve CR. This observation agrees with previous studies that have seen that the use of pre-operative trastuzumab as part of patient therapy increases the likelihood of complete response, for example a study by Bhargava *et al.*, reported that HER2-overexpressing patients who received neo-adjuvant therapy which included trastuzumab were 10-20% more likely to completely respond to treatment [220].

In addition to the efficacy of trastuzumab in the pre-operative therapy regimen, it is also possible that high levels of CR were achieved due to the fact that combination therapy was used. It is well established that using multiple drugs with different mechanisms of action to treat cancer is more effective than monotherapy at killing cancer cells and reduces the chance for drug resistance [221, 222]. In this case, the drugs used to treat patients were from different drug families where docetaxel is a mitotic inhibitor, carboplatin is an alkylating agent, trastuzumab is a monoclonal antibody and lapatinib is a small molecule inhibitor; and so combinations of these drugs are likely to be more successful in anti-cancer treatment compared to single drug therapy.

In this chapter, serum specimens acquired over the course of the clinical trial were blindly analysed for translational studies to investigate for potential biomarkers that are predictive of response to treatment. However, a limitation of this translational work was that, although the patient numbers accrued for the trial were appropriate for investigating patient response to drugs, there were not enough patient specimens in the three response groups (CR, PR and NR) for full analysis of our findings. This detail only became known after analysis had already been carried out, as the experimental part of this translational work was performed blind to patient response. As a result, statistical analysis was performed when comparing patients who achieved CR and PR but, as serum specimens were only available for 2 patients with NR to treatment, statistics were

not applicable to this response group. However, trends observed for the NR group were reported on, where appropriate. Due to the small NR group and that fact that the overall patient numbers that were available for testing were quite low, any trends observed using these specimens would have to be validated in a larger cohort of patients to see if they stand true for a larger population of breast cancer patients.

3.4.2. Successful EV isolation

Over the past number of years there has been a large increase in the number of publications that contain EV data. However, there are a number of different types of EVs, for example exosomes, microvesicles, apoptotic vesicles and ectosomes [223]. Of these vesicles, different types can have different biological functions and relevance. Accordingly, transparency towards which relative type of EV being investigated in a body of work is essential. Recently, a position paper was published by the International Society for Extracellular Vesicles [224], in which they highlight this issue and suggest that papers publishing data that reports on EVs should contain a certain set of criteria for EV characterisation if they are to claim that EVs are present in their work (see table 3.9). The aim of this position paper is to enable clearer identification of EVs from non-vesicular entities, which would enable more standardisation of this research area. These minimal requirements include that the potential EVs are isolated from extracellular fluids, that at least two separate technologies be used to look at the size and appearance of the vesicles (e.g., TEM, AFM & NanoSight size distribution analysis), and that an overview of the protein contents of the specimens investigated is provided.

1. Transmembrane or lipid-bound extracellular proteins	2. Cytosolic proteins	3. Intracellular proteins	4. Extracellular proteins
Argues presence of a membrane in the isolate	With membrane- or receptor-binding capacity	Associated with compartments other than plasma membrane or endosomes	Binding specifically or non-specifically to membranes, co-isolating with EVs
Present or enriched in EVs/ exosomes	Present or enriched in EVs/ exosomes	Absent or under-represented in EVs/exosomes, but present in other types of EVs	Variable association with EVs
Examples: Tetraspanins (*CD9*, *CD63*, *CD81*) Integrins (*ITG***) or cell adhesion molecules (*CAM**) Growth factor receptors Heterotrimeric G proteins (*GNA***) Phosphatidylserine-binding *MFGE8*/lactadherin	Examples: Endosome or membrane-binding proteins (*TSG101*, annexins = *ANXA**, Rabs = *RAB**) Signal transduction or scaffolding proteins (syntenin)	Examples: Endoplasmic reticulum (Grp94 = *HSP90B1*, calnexin = *CANX*) Golgi (*GM130*) Mitochondria (cytochrome C = *CYC1*) Nucleus (histones = *HIST*H**) Argonaute/RISC complex (*AGO**)	Examples: Acetylcholinesterase (*ACHE*) Serum albumin Extracellular matrix (fibronectin = *FN1*, collagen = *COL*A**) Soluble secreted proteins (cytokines, growth factors, matrix metalloproteinases = *MMP**)

Table 3.9. Different categories of proteins and their expected presence in EV isolates, including some examples (non-exclusive) [224].

The International Society for Extracellular Vesicles [224] suggest a panel of proteins that should be screened for (either to be present or absent from EV preparations), which is broken into three categories; and at least one protein from each section should be quantified. Category 1 is for the detection of transmembrane/lipid bound extracellular proteins, which is included as EVs should be membrane bound and so detection of a protein from this section implies the presence of a membrane in the specimen. These proteins are enriched in EVs and exosomes and examples of acceptable proteins in this group include tetraspanins, cell adhesion molecules and integrins. Proteins detected in category 2 are cytosolic proteins that have the ability to bind the membrane or receptors that are also enriched for in EVs and exosomes. Examples include endosome-binding proteins, membrane-binding proteins and Rabs. Category 3 from the published position paper represents other intracellular proteins that non-membrane and non-endosomal in nature; and tend not to be detected in exosomes, but can be found in isolates of other EVs. Examples include endoplasmic reticulum, mitochondrial and nuclear proteins.

With this in mind, the EVs isolated from patients' serum were analysed accordingly. NanoSight analysis that showed that vesicles isolated using the filtration and ultracentrifugation method yielded vesicles within the acceptable 30-130nm diameter exosomal size bracket typically reported. TEM imaging confirms that our isolates are of the correct shape commonly associated with the presence of EVs. Additionally, examination of the protein content of our EVs indicated the presence of CD81 (a tetraspanin) and ALIX/PDC6I (a cytosolic protein and ESCRT machinery component), which are components of categories 1 and 2, respectively. Category 3 was represented here as a negative control by Grp94 (an endoplasmic reticulum associated protein), and was not detected in our EV specimens. Overall this data indicated the successful isolation of EVs and also implies that at least a portion of these vesicles are exosomal in origin.

3.4.3. EV Quantities

Using the isolated EVs from healthy control and patient serum, we aimed to investigate the relevance of EV quantities to breast cancer diagnosis and prediction of patient response to drug treatment. A significantly higher level of EVs was detected in serum taken from breast cancer patients when compared healthy control serum, which indicates that measuring EV quantity may have potential for use as a non-invasive diagnostic tool for breast cancer detection. The increase in EVs as a result of cancer has also recently been reported by Melo *et al.*, [225] where they report that patients with

both breast and pancreatic cancer had higher concentrations of EVs compared to healthy controls.

An additional observation is that EV concentration may be useful as a predictor of response to therapy, as we found that there was a stepwise increase in EVs with decreasing response to therapy. Here, we found that prior to treatment the average EV quantity was higher in patients who achieved PR in comparison to CR, while patients with NR had even higher EV quantities, on average, than patients with PR. This indicates that EV concentration could potentially be used as a biomarker for drug resistance and a prediction of response marker, which has not been observed in breast cancer patients prior to this study. However, trends observed would need to be validated in a larger set of patients.

Furthermore, the trend of increasing EV quantities with poor response to therapy holds until post-treatment, where patients were assessed for the efficacy of treatment and were grouped as having completely or partially responded, or as having had NR to therapy. So at post-treatment, while patients who achieved CR showed complete absence of cancer cells in the breast or axillary lymph nodes, their EV levels have not yet reduced in comparison to pre-treatment levels. This indicates that while EV quantity may prove to be a useful biomarker for cancer and drug resistance, more research is needed into details like the half-life of the cancer EVs in serum, as it could be the case that EV quantity, in addition to being used to diagnose cancer, could be used to monitor patient progress, which would require long term monitoring of serum EVs. In the eventuality of knowing the half-life of serum EVs, long term patient surveillance could be performed to see when a patient has completely responded to therapy, or on the other hand, monitor if the patient has responded at all to therapy. Additionally, this type of patient monitoring could also be used as a non-invasive screen for patient relapse following successful anti-cancer therapy.

3.4.4. EV HER2 and serum soluble HER2

EVs were analysed for HER2 expression using ELISA, however HER2 was detected only at negligible amounts in these specimens. To ensure that this observation was not a technical error, western blotting was performed on the same specimens. No HER2 was detected when blots were probed. Serum soluble HER2 levels were also measured by ELISA, where soluble HER2 was found to be expressed in the serum of the HER2-overexpressing patients, which is to be expected. Here, soluble HER2 was measured using a volume of serum that was relative to the amount of serum from which EVs were

isolated. As the measurements of both EV and serum HER2 were performed on comparable specimen volumes, it would appear, at least from the data presented here, that HER2 present in serum is likely from soluble HER2 and is not specifically packaged into EVs, as we were unable to detect HER2 in our EVs either by ELISA or western blotting. However, this finding is in disagreement with another research group's work, in which they were able to detect HER2 in their serum EV specimens also isolated from HER2-overexpressing breast cancer patients [113]. A potential explanation for this conflicting data could be that a larger starting specimen serum volume was used in the Ciravolo *et al.*, paper, and in this manner, they potentially had more serum specimen to detect HER2 from compared to the 250μL starting volume available for testing for this project. However, as they do not disclose the volume of serum from which their EVs were isolated from, this cannot be determined for certain.

Serum levels for soluble HER2 were measured and comparisons were made between pre-treatment, cycles 2-6 and post-treatment HER2. Overall, HER2 decreased significantly from pre-treatment to cycle 2 and remained significantly reduced for all cycles until post-treatment. Once patients are grouped for response, HER2 levels for patients who achieved CR are significantly decreased at cycle 2 from pre-treatment levels and remain significantly reduced for all treatment cycles up to and including post-treatment. While this trend is also observed for patients who achieved PR and NR, the reduction in serum soluble HER2 is not significant, which demonstrates that a significant decrease in serum soluble HER2 for patients at cycle 2 compared to pre-treatment, is indicative only of patients who may obtain a complete response to treatment. A significant decrease in serum soluble HER2 between patients pre-treatment and post-treatment was also seen when grouped for response. While each response group shows a decrease in serum HER2 at post-treatment compared to pre-treatment, this reduction is only deemed significant for those who achieved CR. Additionally, when patients were grouped for response, there was no significant difference in serum soluble HER2 pre-treatment, however, at post-treatment there was a trend for increasing levels of soluble HER2 with decreased response to therapy, where average serum HER2 at post-treatment is highest for non-responders, lower for those who achieved PR and decreased stepwise again for those who achieved CR, implying that measuring soluble HER2 at post-treatment could be indicative of response to therapy. Altogether this data suggests that serum soluble HER2 levels may be useful as a biomarker for predicting response to therapy, where patients that have a significant decrease in serum HER2 by cycle 2 of their drug therapy are likely to achieve a CR to treatment. Similar observations

for the use of serum HER2 as a biomarker for predicting patient response to treatment were reported by Esteva *et al* [226]. They measured serum soluble HER2 in metastatic breast cancer patients who had received trastuzumab as part of their treatment regimen. It was found that progression-free survival was longer (587 days) in patients whose serum soluble HER2 was reduced by 77% 2-4 weeks after treatment was initiated, compared to patients whose serum soluble HER2 was above 77% relative to baseline amounts (217 days progression-free survival).

3.4.5. EV NmU and serum NmU

Levels of NmU were measured both in EVs and serum, where we aimed to use this data to investigate its potential as a biomarker for HER2-overexpressing cancer diagnosis or prediction of patient response to treatment. A significantly higher concentration of NmU was found in the EVs of healthy controls specimens compared to breast cancer patients. This is an unexpected result as we have previously published data indicating that an increase in NmU is associated with poor response and drug resistance [209], and in keeping with this we would have speculated that average NmU levels would have been higher in breast cancer patients than normal controls. However, there is conflicting evidence in multiple cancer types as to whether NmU is up- or down-regulated in association with cancer. While Ketterer *et al.*, [227] found that NmU mRNA was up-regulated in pancreatic cancer, there are reports that NmU is downregulated in oral cancer [228] and oesophageal squamous cell carcinoma [229] in comparison to normal tissue. As NmU has been found increased in cancer in most cases but decreased with the development in cancer in others, it is clear that further research is required to fully make clear the role NmU expression plays in cancer.

While differences in EV NmU levels were observed between healthy control and breast cancer patient specimens, no difference in EV NmU or serum NmU was seen over the course of patient therapy or in associated with patient response to treatment. Overall, no changes in EV or serum NmU was found between patients who achieve CR, PR or NR at pre- and post-treatment. This indicates that while NmU has previously been associated with drug-resistance and poor prognosis [209], our data does not indicate that NmU is useful as a biomarker to predict patient response to treatment.

In addition to EV NmU, whole serum NmU levels were also measured for patients over the course of their therapy. As there was no significant difference between the average values for patient EV and serum NmU, it would appear that most NmU

detected in serum is contained within EVs. As a result, serum EVs are a good biological source of NmU, if patient testing for the peptide were to be required.

3.4.6. Survivin

EV concentrations of survivin were also measured to investigate the relevance of this protein to breast cancer diagnosis and its potential as a predictive biomarker for breast cancer therapy. It was found that breast cancer patients had more EV survivin than healthy controls. Although this difference did not reach significance, the trend is in agreement with the literature. Survivin is a promotor of mitosis, an inhibitor of apoptosis and also has a role in facilitating angiogenesis [230], as such, it is not surprising that its overexpression has previously been associated with breast cancer compared to normal tissue [231, 232]. While EV survivin levels did not change over the course of treatment for patients who achieved CR, PR and NR, there was a significant increase in levels of survivin at pre-treatment for patients who achieved PR compared to CR, indicating that high base-levels of survivin may be indicative of poor prognosis. This trend has also been seen by Ryan et al., [233] who also found higher levels of survivin were associated with a poor prognosis.

3.4.7. miR-210

MicroRNAs (miRNA) are a type of non-coding RNA that have been associated with cell proliferation, differentiation and apoptosis [234] and their relative expression are being investigated for potential use as disease biomarkers. Here, levels of miR-210 in patient EVs were measured using qPCR at pre- and post-therapy, in order to investigate if there was any correlation in expression of this miRNA and response to therapy. We found no significant differences in miR-210 levels between patients who achieved CR, PR and NR either before or after therapy, however a slight trend was observed towards more miR-210 being present in patients who achieved PR and non-responders compared to those who achieved a CR. Similarly, but for patients diagnosed with acute lymphoblastic leukaemia, Mei *et al.*, [235] report that high levels of miR-210 are associated with disease-free survival and overall survival. However, in contrast to our observations, it has been reported by others that miR-210 is detected at higher levels in breast cancer patients serum compared to healthy controls. For example, Jung *et al.*, [205] report that patient base-line levels of miR-210 was significantly higher in breast cancer patients compared to healthy controls and also that high levels of miR-210 in

serum was associated with resistance to trastuzumab, suggesting that miR-210 may have potential as a biomarker for detecting breast cancer and may also serve as a predictor for response.

3.5 Conclusion

EVs were successfully isolated from patient and healthy control serum and from the characterisation of these EVs, it appears that at least a portion of these vesicles are EVs. The increase in breast cancer patient EV quantities in comparison with those of healthy controls observed here demonstrates the potential of EV quantity as a diagnostic biomarker for HER2-overexpressing breast cancer. Additionally, EV quantities displayed potential as a biomarker for prediction of patient response to therapy as patients with higher levels of EVs were less likely to respond to therapy. Similarly, the decrease in breast cancer EV NmU concentrations compared to healthy controls seen here may also prove to be useful in the detection of breast cancer. While HER2 was not detected in EVs here, serum soluble HER2 demonstrated its use as biomarker for the prediction of patients' response to treatment. Although we observed that EVs contain NmU and survivin, these proteins were not found to be of use for prediction of patient response to therapy.

Chapter 4: Innate levels of drug resistance differs between cells grown as monolayers compared to 3D cell cultures

4. Abstract

Introduction: Cells grow *in vivo* in a 3D environment where they interact with their surroundings. Cells grown using 3D cell culture methods form cell-cell interactions and 3D cell-structures. With this in mind, it has been proposed that 3D cell culture may mimic the natural *in vivo* setting better than traditional monolayer cell culture, where cells are grown flat on tissue culture plastic. Here, the effects of growing cells in monolayer/2D cell culture compared to cells grown in 3D were assessed in terms of cellular protein expression, enzyme activity, response to drug therapy, and EV release.

Methods: 2D cells were grown using the typical cell culture method, attached flat on cell culture plastic flasks, whereas 3D cells were grown using the forced-floating 3D method on poly-HEMA coated round-bottomed 96 well plates. Immunoblots were used to measure differences in protein expression between the two culture methods. ATP assays were used to measure cell viability and response to neratinib, trastuzumab and docetaxel. CYP3A4 activity of both 2D and 3D cells and their EVs was measured using a P450-Glo assay. EVs were isolated from both 2D and 3D cells using filtration and ultracentrifugation. Quantification of these EVs was performed by measuring their relative protein concentrations.

Results: The morphology of cells grown in 2D compared to 3D was substantially different, where 2D cells grow flat, while 3D cells bound to each other to form 3D structures. Expression of proteins involved in cell survival, drug transporters and drug targets were found to be up-regulated in 3D cells compared to their 2D counterparts. Cell viability in 3D cells was substantially lower than cells grown in 2D, while 3D cells were less sensitive to the effects of neratinib, trastuzumab and docetaxel compared to cells grown in 2D. We found that 3D cell cultures released more EVs compared to 2D cells. Finally, CYP3A4 activity was found to be increased in cells grown in 3D compared to 2D cultures.

Conclusion: The biological information represented by 2D and 3D cell cultures differ substantially. Results from this research suggest that 3D cell cultures demonstrate higher innate resistance to anti-cancer drugs compared to 2D cultures, which may be facilitated by the increase in protein expression and enzyme activity observed. The different cell culture methods also altered the rate of release of EVs from cells.

4.1 Introduction

In the drug development process, or indeed, any laboratory setting wishing to recapitulate the *in vivo* environment for their study analysis, it is important that the experimental model of the disease being used in testing is as true to life as possible. For breast cancer research, it is important that the cell model used to research and further our knowledge of the disease represents the disease state in terms of target receptor expression, drug transporter levels and expression of proteins essential to cell survival and growth.

The natural environment in which cells grow *in vivo* is a three-dimensional one in which the cells interact with their surroundings. The differences between how we grow cells in typical monolayer/2D cell culture in the laboratory and their natural *in vivo* setting has been discussed in Section 1.5. There is an assumption that growing cells in 3D mimics the *in vivo* environment better than traditional 2D cell culture due to the ability of 3D cells to form cell-cell interactions and develop into 3D structures, as opposed to growing flat and attached to cell culture plastic. This supposition that 3D culture is more *in vivo* like than 2D culturing is supported by the fact that cells grown in 2D cell culture lose some of their natural functional abilities; however these changes can be restored simply by growing cells in 3D again. For example, immortalised human hepatocyte HepG2 cells are routinely used as a liver model for drug toxicity testing *in vitro*. However, it is established that when these cells are grown in traditional 2D culture they lose substantial amounts of CYP450 enzyme mRNA and activity, that are critical to a liver cells ability to metabolise drugs [236, 237], thus limiting their ability to effectively mimic liver function and predict drug toxicity in humans. Ramaiahgari *et al.* [238] found that growing the HepG2 cells in 3D using an ECM hydrogel resulted in restored phenotypic characteristics of hepatocytes *in vivo* in terms of proliferation and formation of bile canaliculi and also in terms of increased levels of drug metabolising CYP450 enzyme mRNA and activity, and the nuclear transcription factors that induce them, which are, ultimately, the liver-like properties of the cells. Together this data suggests that 3D cell culture is more similar and relevant to the *in vivo* environment than 2D cell culture.

The field of 3D cell culture research is, however, still in its infancy in comparison to the knowledge behind 2D cell culture. More work is needed to fully characterise this method of growing cells *in vitro*. The aim of the research in this chapter was to grow cells using conventional 2D cell culture conditions and also using the

forced-floating poly-HEMA method of 3D cell culture and to characterise any differences observed between the two methods of cell culture. More specifically, we aimed to compare any differences in expression of cell survival proteins, drug targets and drug transporters between 2D and 3D cells. Additionally, cell viability, response to drug treatment and CYP3A4 activity were compared in both cell culture methods. Finally, we aimed to determine if growing cells in 2D or 3D effects EV secretion from these cells.

4.2 Methods

4.2.1 2D and 3D cell culture

BT474 (derived from ductal carcinoma), HCC1954 and EFM192A cells were obtained from ATCC, while neratinib-resistant variants, HCC1954-NR and EFM192A-NR cells were developed as detailed in Section 2.2.1. Cells were cultured in RPMI supplemented with 1% L-glutamine and 10% FBS and were maintained at 37°C/5% CO_2. In this chapter, cells described as 2D cells refer to those grown in the typical manner, attached to T25cm^2 (Corning; Cat. #: CLS430639) or T75cm^2 (Corning; Cat. #: CLS430641) plastic cell culture flasks. Cells referred to as 3D cells were grown under 'forced floating' conditions (see Section 1.5.3), where round-bottomed 96 well plates (Corning; Cat. #: CLS3799) were coated with poly-HEMA (Sigma-Aldrich; Cat. #: P3932). Poly-HEMA was prepared by dissolving 1.2mg poly-HEMA in 100mL 95% ethanol overnight while on a rocker. 50µL of this poly-HEMA solution was added to each well of the round-bottomed 96 well plate and allowed to evaporate overnight in a tissue culture hood. This coating process was repeated once more and plates were allowed to dry completely before addition of cells. BT474 and EFM192A cells were seeded at 5x10^3 cells/200µL/well, while HCC1954 cells were seeded at 3x10^3 cells/200µL/well. Once seeded, 3D cell plates were centrifuged at 146*g* for 5 minutes. 50µL of medium was removed and replaced with fresh medium every second day.

4.2.2 Optical microscopy

Phase contrast images of BT474, HCC1954 and EFM192A cells grown in 2D and 3D were taken at 5x and 10x magnification using an AxioVert 200M microscope (Zeiss) and AxioCam MRc (Zeiss).

4.2.3 Scanning electron microscopy (SEM) imaging

[SEM imaging was performed in the Centre for Microscopy and Analysis in Trinity College Dublin, with the help of Neal Leddy, Chief Technical Officer]

SEM imaging of 3D cell cultures that were grown as described in Section 4.2.1 was performed. SEM images were taken of HCC1954 2D and 3D cells. Glass coverslips (VWR; Cat. #: 631-1570) were coated with 29.4µg/mL poly-d-lysine (Sigma-Aldrich; Cat. #: P6407) diluted in dH_2O for 10 minutes, washed with deionised H_2O and allowed to air dry. For 2D SEM images, 3x10^3 cells in 200µL medium was placed on a sterile, poly-d-lysine coated coverslip and were allowed to attach overnight. The next day,

medium was removed and cells were washed with PBS prior to processing for SEM. 3D cultures were seeded and grown for 7 days as described in Section 4.2.1. Spheroids were collected in a 15mL tube and allowed to settle to the bottom of the tube, washed with PBS and allowed to settle to the bottom of the tube once again. Cells were not centrifuged to prevent distortion of 3D structure of spheroids. Using 1mL pipette tips that had been coated with 1% BSA (to prevent 3D culture from sticking to the pipette tip), almost all PBS was removed from the tube – approximately 100-200µL liquid was left in tube with the cells. This small amount of liquid was pipetted, with the 3D cells, onto the poly-d-lysine coated coverslip and placed at 4°C for 15 minutes or until cells had attached to the coverslip.

For both 2D and 3D cells that were attached to coverslip, cells were fixed for 60 minutes with 3% glutaraldehyde (Agar Scientific, Cat. #: 101504) and washed 3 times with 0.1M phosphate buffer for 10 minutes at 4°C. At this point Neal Leddy continued with cell processing for SEM imaging. A secondary fixation step was performed with 1% OsO_4 in buffer for 60 minutes and washed for 10 minutes at 4°C and again at room temperature for 10 minutes. Cells were then dehydrated in serial increasing ethanol concentrations (10%, 30%, 50%, 70%, 95% and 100%) for 5 minutes each at room temperature. Dehydration was completed with a 5 minute incubation with 50% hexamethyldisilazane (Sigma-Aldrich; Cat. #: 379212) in ethanol at room temperature and a final 5 minute incubation with 100% hexamethyldisilazane at room temperature. Spheroids were gold sputter-coated using an EMScope SC500 Sputter Coater at 25mA for 3 minutes (approximately 15nm coating) and examined at various magnifications in a Tescan Mira XMU Field Emission Scanning Electron Microscope at 5Kv using a secondary electron detector.

4.2.4 Immunoblotting

Protein was extracted from cells, quantified and prepared for immunoblotting as per Section 2.2.7. 30µg total cellular sample protein was used for Akt, pAkt, Erk, pErk EGFR, pEGFR, HER2, pHER2, herstatin, HER3, while 50µg total cellular sample protein was used for HER4, PGP and BCRP immunoblots. Akt, pAkt, Erk and pErk proteins were all resolved in 10% gels, while EGFR, pEGFR, HER2, pHER2, herstatin, HER3, HER4, PGP and BCRP were resolved in 7.5% gels. Protein was transferred to PVDF membrane and blocked as per Section 2.2.7. Blots were blocked in 5% bovine serum albumin (BSA) in PBS-tween (0.1%) for 1 hour at room temperature and washed 3 times for 5 minutes in PBS-tween (0.1%). Blots were incubated with primary

antibodies at 4°C overnight: HER2 (Calbiochem; Cat. #: OP15; 1:500), phosphorylated HER2 (pHER2) (Cell Signalling; Cat. #: 2247; 1:1000), EGFR (Cell Signalling; Cat. #: D38131; 1:1000), phosphorylated EGFR (pEGFR) (Cell Signalling; Cat. #: 2234; 1:1000), HER3 (Cell Signalling; Cat. #: 4754; 1:1000), HER4 (Cell Signalling; Cat. #: 4795; 1:1000), PGP (Santa Cruz; Cat. #: SC55510; 1:200), BCRP (Santa Cruz; Cat. #: sc-58224; 1:200), CD63 (AbCam; Cat. #: AB68418) and β-actin (Sigma-Aldrich; Cat. #: A5316; 1:1000). Blots were washed 3 times for 5 minutes in PBS tween (0.1%) following primary antibody incubation and were incubated for one hour at room temperature with the relevant horseradish peroxidase-conjugated secondary antibodies: anti-rabbit (Cell Signalling; Cat. #: 7076; 1:1000), anti-mouse (Cell Signalling; Cat. #: 7074; 1:1000) and anti-rat (Santa Cruz; Cat. #: sc-2006; 1:1000). Blots were washed again and protein bands were visualised by chemiluminescence (ThermoFisher; Cat. #: 34080) using a Chemidoc exposure system (BioRad laboratories). Densitometry was performed on the bands of protein detected by immunoblot using ImageJ software and normalised to β-actin which served as a loading control.

4.2.5 2D and 3D cell viability

BT474 and EFM192A cells were seeded at $5x10^3$ cells/200μL/well and HCC1954 cells were seeded at $3x10^3$ cells/200μL/well, for both 2D and 3D cultured cells. 6 days after seeding, cell viability was determined by measuring cellular ATP levels using CellTitre-Glo 3D (Promega; Cat. #: G9681). This assay was performed by incubating cells with 90μL serum-free medium and 90μL CellTitre-Glo solution and were pipetted to mix. Cells were incubated in this solution for 40 minutes at room temperature. To ensure 3D spheroids were lysed, the solution was vigorously pipetted up and down until spheroids were no longer visible and were dissolved by solution. The lysates were then transferred to opaque white 96-well plates (Brand; Cat. #: 781670) for luminescence reading. Plates were read using a Luminoskan luminescence plate reader (Thermo Scientific).

4.2.6 2D and 3D cell response to drug treatment

Cells were seeded as in Section 4.2.5. 24 hours after seeding, 2D and 3D cells were treated with the same fixed concentrations of neratinib, docetaxel and trastuzumab. Approximate IC_{50} concentrations of drugs were used as established previously in our lab by the acid phosphatase method. Concentrations of neratinib used were: 2.5nM – BT474 cells, 49nM – HCC1954 cells and 6.8nM – EFM192A cells. Concentrations of

docetaxel used were: 2.8nM – BT474 cells, 0.6nM – HCC1954 cells and 2.6nM – EFM192A cells. BT474 and EFM192A cells were both treated with 20μg/mL trastuzumab. 5 days after treatment, cell viability was determined by measuring cellular ATP levels using CellTitre-Glo 3D as per described in Section 4.2.5.

4.2.7 EV isolation

EVs were isolated from cells grown in 2D and 3D. BT474 and EFM192A (Par and NR) cells were seeded at $5x10^3$ cells/200μL/well and HCC1954 (Par and NR) cells were seeded at $3x10^3$ cells/200μL/well. 2D cells were seeded into 96 well plates, while 3D cells were seeded in poly-HEMA coated round bottomed 96 well plates. Cells were seeded in medium supplemented with 1% L-glutamine and 10% EV-depleted FBS. Of note, FBS was depleted of EVs by ultracentrifugation at 110,000g for 16 hours at 4°C. The supernatant was removed and used [239]. Cells were grown in 2D and 3D for 5 days. After this time, medium was removed from wells and was centrifuged at 2,000g for 10 minutes at 4°C to remove cells and debris. The supernatant was then processed for EV isolation as in Section 3.2, with the only adjustments being that 28mL polyallomer ultracentrifuge tubes (Beckman-coulter; Cat. #: 358651) were used to accommodate the larger sample volumes used here. EVs were lysed and quantified as described in Section 2.2.7, where equal volumes of EVs and lysis buffer were used to lyse the EVs.

4.2.8 CYP3A4 activity in 2D and 3D cells and their EVs

For cells, BT474 and EFM192A cells were seeded at $5x10^3$ cells/200μL/well and HCC1954 cells were seeded at $3x10^3$ cells/200μL/well, for both 2D and 3D cell cultures. 6 days after seeding, CYP3A4 activity was determined using P450-Glo CYP3A4 (Promega; Cat. #: V9001). This assay was performed by removing medium from wells (being particularly careful with 3D spheroids here) and adding 50μL of 3μM Luciferin-IPA solution (1:1000 dilution of Luciferin-IPA solution provided in kit, diluted in base RPMI) per well. Plate was returned to the incubator at 37°C/5% CO_2 for 60 minutes, and following, this 50μL of the Luciferin detection reagent was added and assay solution was allowed to incubate at room temperature for 20 minutes. To ensure 3D spheroids were lysed, solution was vigorously pipetted up and down until spheroids were entirely dissolved. The lysates were then transferred to opaque white 96-well plates for luminescence reading as in Section 4.2.5.

4.2.9. Statistical analysis

Statistical analysis of data was performed using Excel. *P*-values were generated using Student's t-tests, where $p<0.05$ was considered as statistically significant. Results are displayed as n=3± standard error of mean (SEM). Graphs were generated using GraphPad software.

4.3 Results

4.3.1 Different morphology of cells grown in 2D versus 3D

Phase contrast images of BT474, HCC1954 and EFM192A cells grown in 2D and 3D demonstrate the dramatic difference in cell morphology between the two different methods of cell culture (Figure 4.1). BT474 cells grow together in patches in 2D culture, but, when grown under forced floating conditions, they form uniform spheroids with relatively smooth surface. HCC1954 cells grow more independently as opposed to in groups/colonies and are more spread out than BT474 cells. HCC1954 3D cultures form a tight spheroid, but with a less smooth surface than BT474 3D cells. EFM192A cells grow similarly to BT474 cells in 2D in that they grow in patches; however, these cells have a more rounded shape. EFM192A cells grown in poly-HEMA coated 96 well plates form a 3D structure, however their 3D shape is not as tight or homogenous as either the BT474 or HCC1954 spheroids.

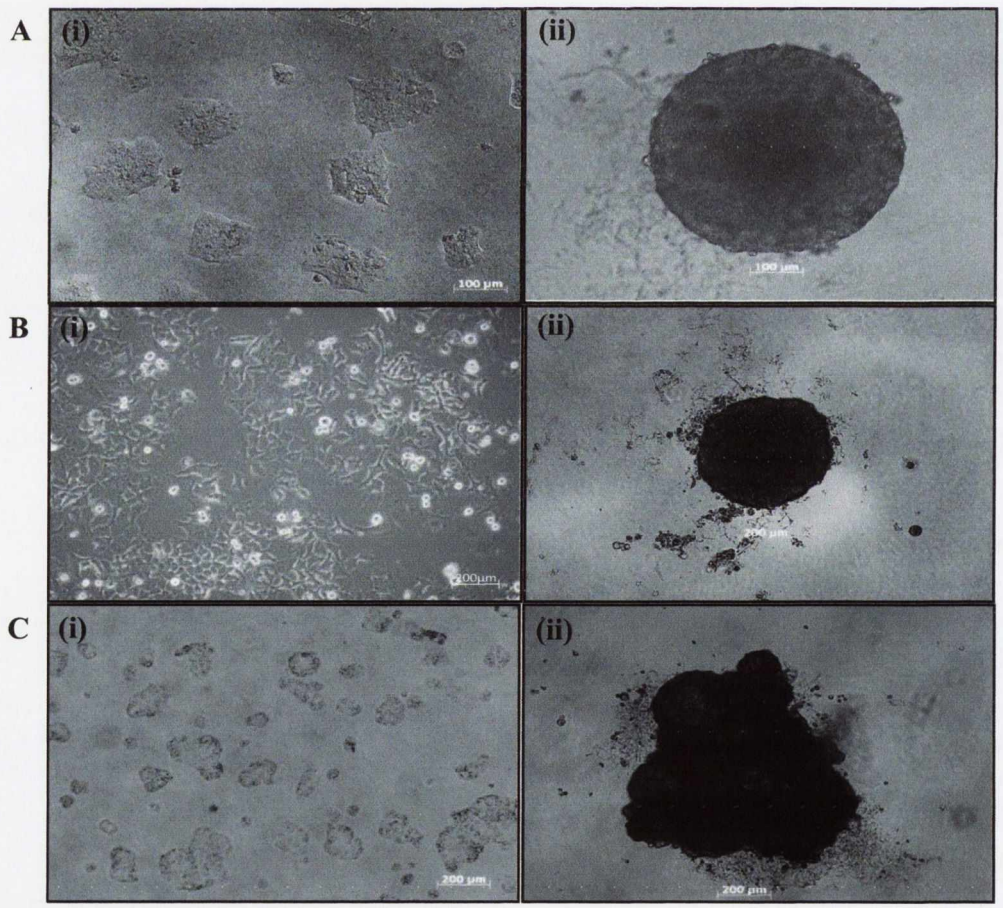

Figure 4.1. Phase contrast images of 2D (i) and 3D (ii) cell cultures. (A) BT474, (B) HCC1954 and (C) EFM192A cells.

SEM imaging of HCC1954 cells reveals a more in depth view of the difference in cell morphology of cells grown with the 2D and 3D culture methods (Figure 4.2). The cell body and projections are clear in these 2D images, and the stretched out formation of the cells are also clearly visible. SEM images of cells grown using the 3D poly-HEMA method reveal the spherical nature of the 3D HCC1954 cell structure. Furthermore, when these cells are grown in 3D they appear to secrete an ECM which smoothens the surface of the sphere and makes it difficult to distinguish individual cells. Additionally, pores appear to form in the surface of the spheroids.

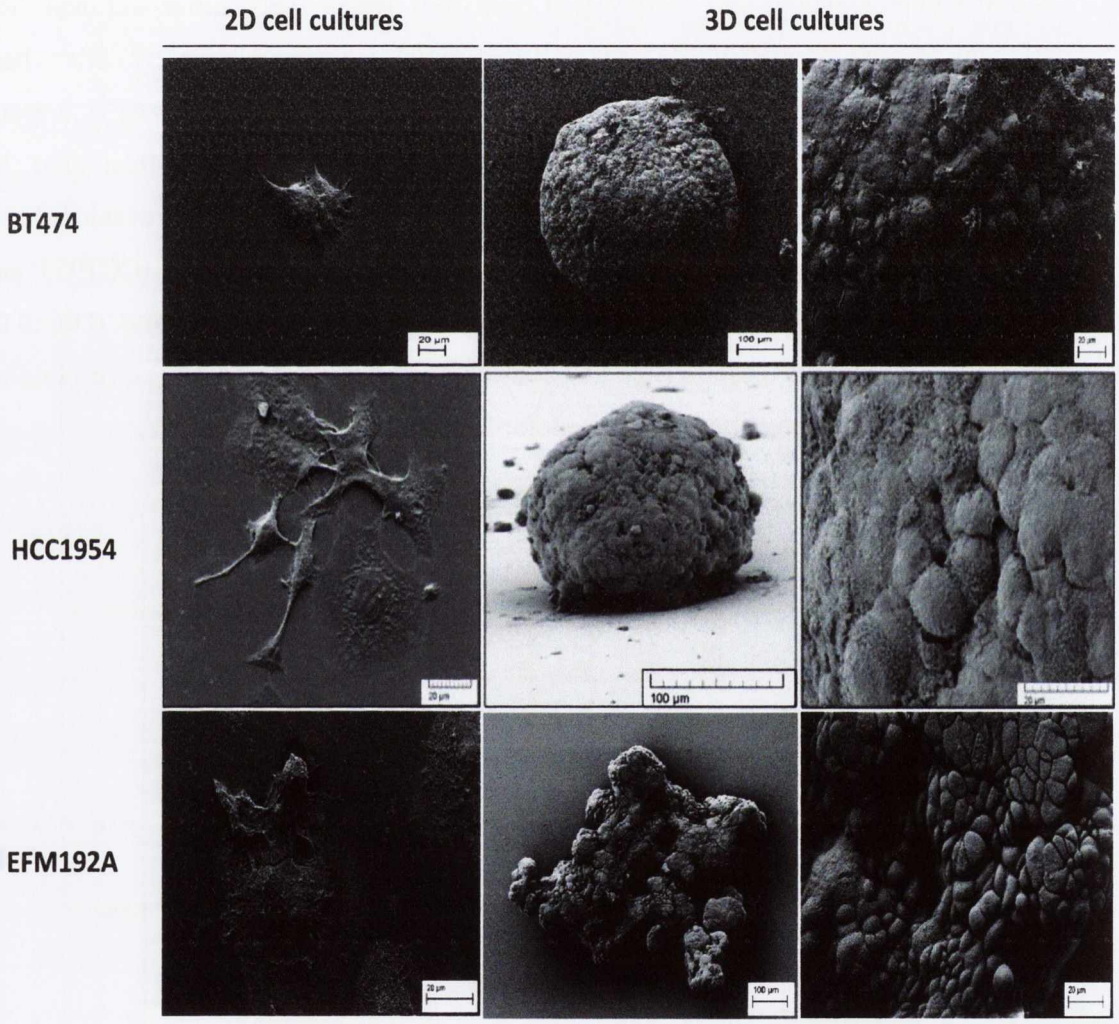

Figure 4.2. SEM images of HCC1954 cells grown in 2D and 3D cultures.

4.3.2 Cell survival pathways in 2D and 3D cell culture

The effects of different methods of cell culture on Akt and Erk, important components of cell survival pathways (see Section 1.3.6), were measured using immunoblots (Figure 4.3). It was found that pAkt was overexpressed in 3D cells where BT474 3D, HCC1954 3D and EFM192A 3D cells had 2.8±0.5 fold (p=0.025), 4.9±0.5 fold (p=0.001) and 1.7±0.2 fold (p=0.019), respectively, more pAkt than their corresponding 2D cells. It follows that Akt was upregulated in cells grown in 3D compared to cells grown in 2D, where BT474 3D, HCC1954 3D and EFM192A 3D cells had 2.1±0.2 fold (p=0.002), 4.6±0.8 fold (p=0.009) and 2.0±0.2 fold (p=0.004), respectively, more Akt than their 2D counterparts. Similarly, 3D cells had higher Erk expression than 2D cells where BT474 3D, HCC1954 3D and EFM192A 3D cells had 1.8±0.2 fold (p=0.013), 2.9±0.3 fold (p=0.002) and 1.7±0.1 fold (p=0.005), respectively, more Erk than their 2D counterparts. Conversely, levels of pErk measured by immunoblotting revealed that it is decreased in 3D cells in comparison to 2D cultures in BT474, HCC1954 and EFM192A cell lines to 0.65±0.1 (p=0.004), 0.84±0.05 (p=0.046) and 0.66±0.05 (p=0.002). β-actin was used as a loading control for all immunoblots. The corresponding densitometry graphs for these immunoblots are displayed in Appendix IV.

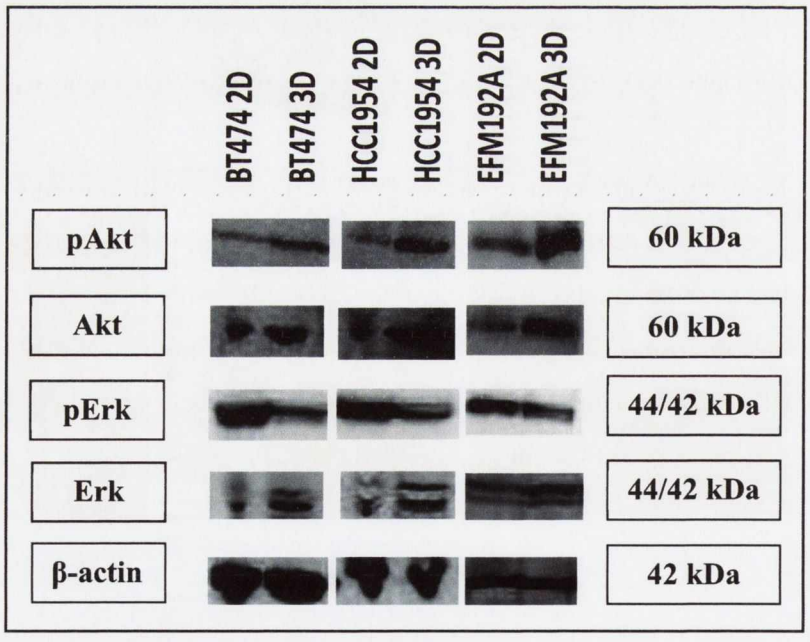

Figure 4.3. Immunoblots of 2D and 3D pAkt, Akt, pErk and Erk expression. Immunoblots show that cells grown in 3D display overexpression of Akt, pAkt and Erk compared to their expression in 2D counterparts. However, pErk expression was decreased in 3D cell cultures compared to 2D cells. Blots are representative images of n=3.

4.3.3. HER-family drug target expression in 2D and 3D cell culture

The effects of growing cells in 2D and 3D cultures on the expression of the EGFR family of receptors, which are often targeted by HER-targeted therapies, was investigated using immunoblots (Figure 4.4). We found that EGFR expression was increased in both BT474 3D and HCC1954 3D cells by 4.2±0.5 fold (p=0.003) and 3.3±0.8 fold (p=0.036), respectively, compared to their relative control cells. Similarly, pEGFR expression was increased in both BT474 3D and HCC1954 3D cells by 6.2±0.8 fold (p=0.003) and 3.2±0.6 fold (p=0.028), respectively, compared to their 2D control cells. EGFR and subsequently pEGFR were not found to be expressed by EFM192A cells, which were performed on the same blots as BT474 3D and HCC1954 3D cells, which serve here as positive controls for EFM192A EGFR and pEGFR blots.

HER2 expression was found to be increased in BT474 3D, HCC1954 3D and EFM192A 3D cells by 9.5±1.5 fold (p=0.005), 3.9±0.3 fold (p=0.001) and 1.8±0.2 fold (p=0.013), respectively, compared to their 2D cells. Likewise, pHER2 expression was increased in 3D compared to 2D cultures, where expression was increased in BT474 3D, HCC1954 3D and EFM192A 3D cells by 5.0±0.8 fold (p=0.008), 3.4±0.3 fold (p=0.008) and 3.2±0.3 fold (p=0.003), respectively, in comparison to cells grown in 2D.

Levels of herstatin (see Section 1.2.4.3) were measured and were increased in BT474 3D, HCC1954 3D and EFM192A 3D cells by 7.4±1.5 fold (p=0.012), 8.9±1.4 fold (p=0.005) and 5.9±1.0 fold (p=0.009), respectively, in comparison to 2D cell cultures.

HER3 expression was increased in BT474 3D, HCC1954 3D and EFM192A 3D cells was increased by 4.0±0.8 fold (p=0.018), 2.7±0.15 fold ($p=2.9x10^{-4}$) and 2.3±0.3 fold (p=0.011), respectively, in comparison to cells grown in 2D. While HER4 expression was only slightly increased in 3D cell cultures compared to 2D, where BT474 3D, HCC1954 3D and EFM192A 3D HER4 expression increased by 1.28±0.1 (p=0.112), 1.91±0.2 (p=0.005) and 1.31±0.1 (p=0.025).

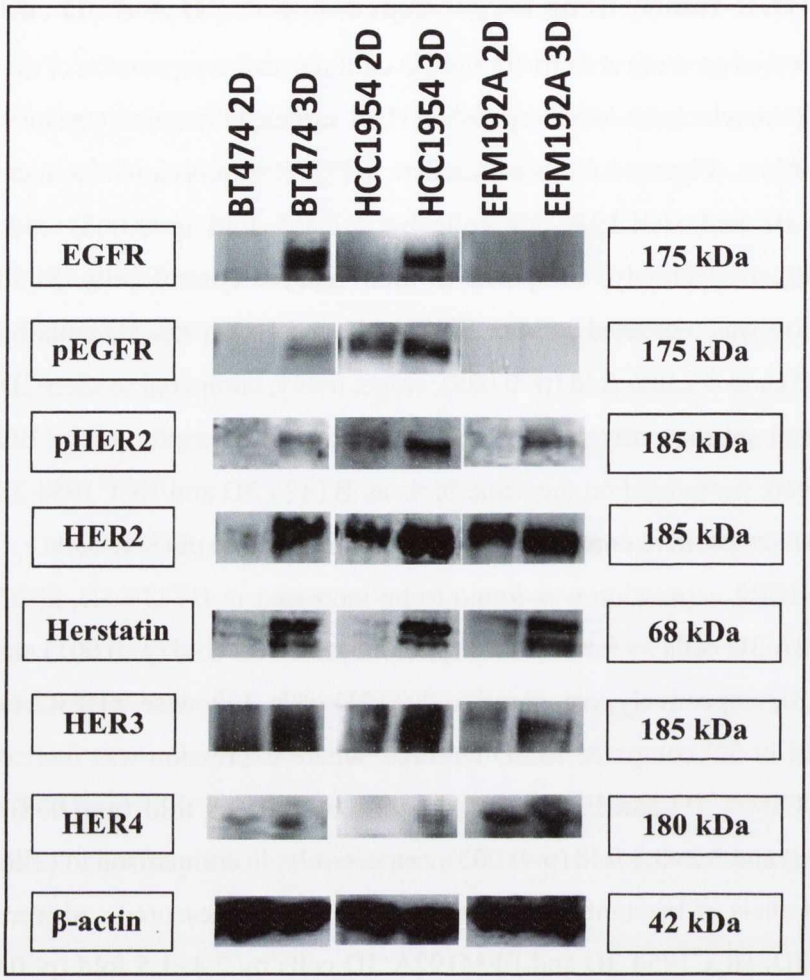

Figure 4.4. Expression of EGFR family receptors in cells grown in 3D compared to 2D cells. Expression of all the members of the EGFR family were increased in 3D compared to 2D cell cultures. Blots are representative images of n=3.

4.3.4. Drug efflux pump expression in cells grown using 2D and 3D culture methods

Expression of two different drug transporters, PGP and BCRP, was measured by immunoblotting and compared between cells grown in 2D and 3D cell culture methods (Figure 4.5). PGP expression was found to be increased by 11.1±1.3 fold (p=0.001), 3.6±0.7 fold (p=0.02) and 1.4±0.15 fold (p=0.049), in BT474 3D, HCC1954 3D and EFM192A 3D cells, respectively, compared to their relative expression measured in 2D cultures. The expression of drug efflux pump BCRP was also measured but was not found to be significantly (p=0.962) altered in 3D compared to 2D cells. BT474 3D cells had 1.01±0.2 fold more BCRP compared to BT474 2D cells, HCC1954 3D cells were found to have 0.9±0.1 less BCRP compared to HCC1954 2D cells (p=0.457), while EFM192A 3D cells had 1.5±0.5 fold more BCRP than their corresponding 2D cells (p=0.309). See Appendix IV for corresponding densitometry graphs.

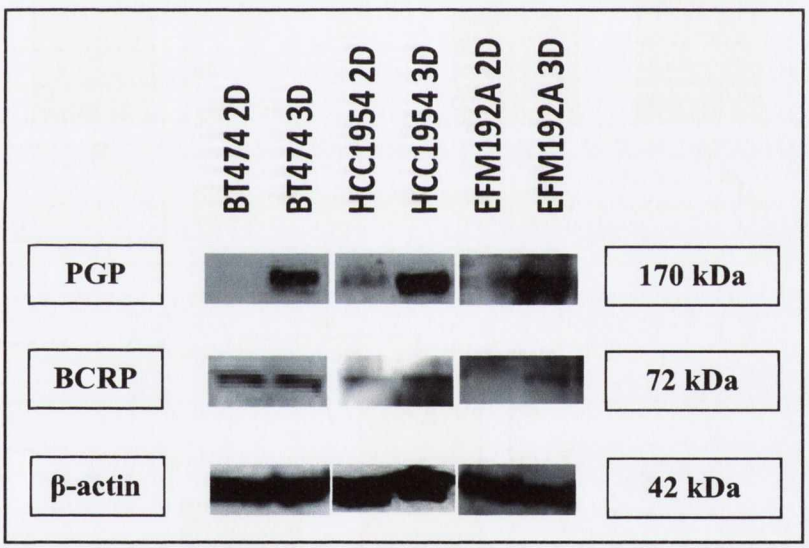

Figure 4.5. Expression of drug transporters in 3D compared to 2D cells. Cells grown in 3D show higher expression of drug efflux transporters PGP and BRCP compared to cells grown in 2D. Blots are representative images of n=3.

4.3.5 Altered cell viability in 2D and 3D cell culture

Cells were seeded at the same density in 2D and 3D (see Section 4.2.5) and, after 6 days in culture, cellular levels of ATP were measured in order to compare cell viability in 2D and 3D cell cultures (Figure 4.6). Results showed that BT474 3D cell viability was 41.6±5.9% of that measured in BT474 2D cells ($p=5.8x10^{-4}$). It was found that HCC1954 3D cell viability was 18.4±1.5% of that measured in HCC1954 2D cells ($p=6.3x10^{-7}$). Similarly, EFM192A 3D cell viability was 44±3.7% that of the EFM192A 2D cells ($p=1.1\ x10^{-4}$).

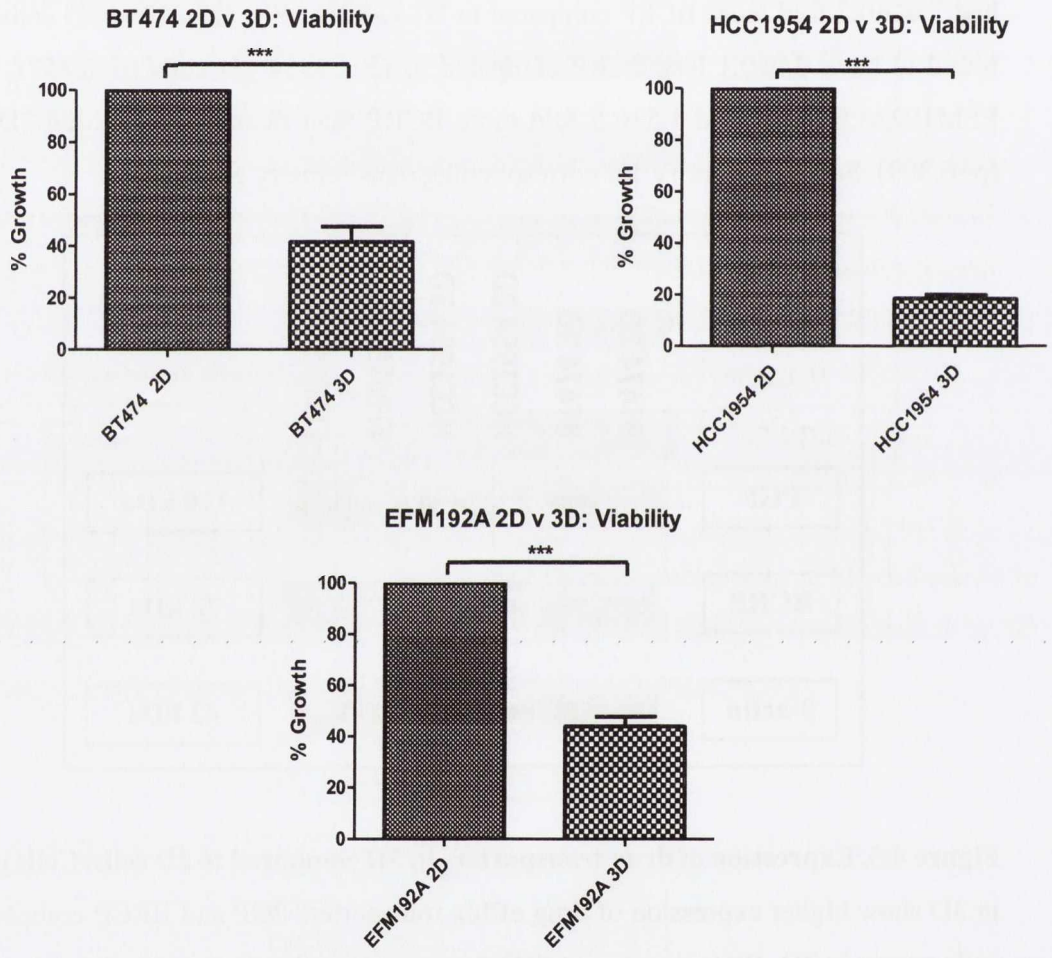

Figure 4.6. Viability of cells grown in 3D compared to 2D cultures. Viability of BT474, HCC1954 and EFM192A cells grown in 3D is substantially reduced in comparison to their corresponding 2D cell cultures (n=3±SEM), where ***$p<0.001$.

4.3.6 Altered drug toxicity in 2D and 3D cell culture

4.3.6.1 Reduced efficacy of neratinib in 3D compared to 2D cultures

Efficacy of neratinib was compared between cells grown in 2D and 3D cultures (Figure 4.7). For BT474 cells, results showed that 2D cells treated with neratinib (see Section 4.2.6) had 62.7±1.2% cell survival compared with untreated (NT) cells ($p=7.3x10^{-6}$), while BT474 3D cells treated with the same concentration of neratinib showed 90.8±4.5% cell survival compared to untreated 3D cells (p=0.107). The increased difference in cell survival between 2D and 3D cells following the same treatment was 28.1±5.4%, this difference in drug response between 2D and 3D cells is statistically significant (p=0.004). A similar trend was seen in both HCC1954 and EFM192A cells where 2D cells treated with fixed concentrations of neratinib (See Section 4.2.6) showed 64.7±3.9% ($p=8.0x10^{-4}$) and 59.7±2.1% ($p=4.2x10^{-5}$) cell survival, respectively, compared to untreated 2D cells, while neratinib treated 3D cells maintained a higher 77.3±6.9% (p=0.031) and 86.8±0.6% ($p=2.3x10^{-5}$) survival, respectively. In these cell lines the difference in 2D and 3D cell survival after neratinib treatment was 12.6±5.3% (p=0.188) and 27.1±2.7% ($p=2.3x10^{-4}$).

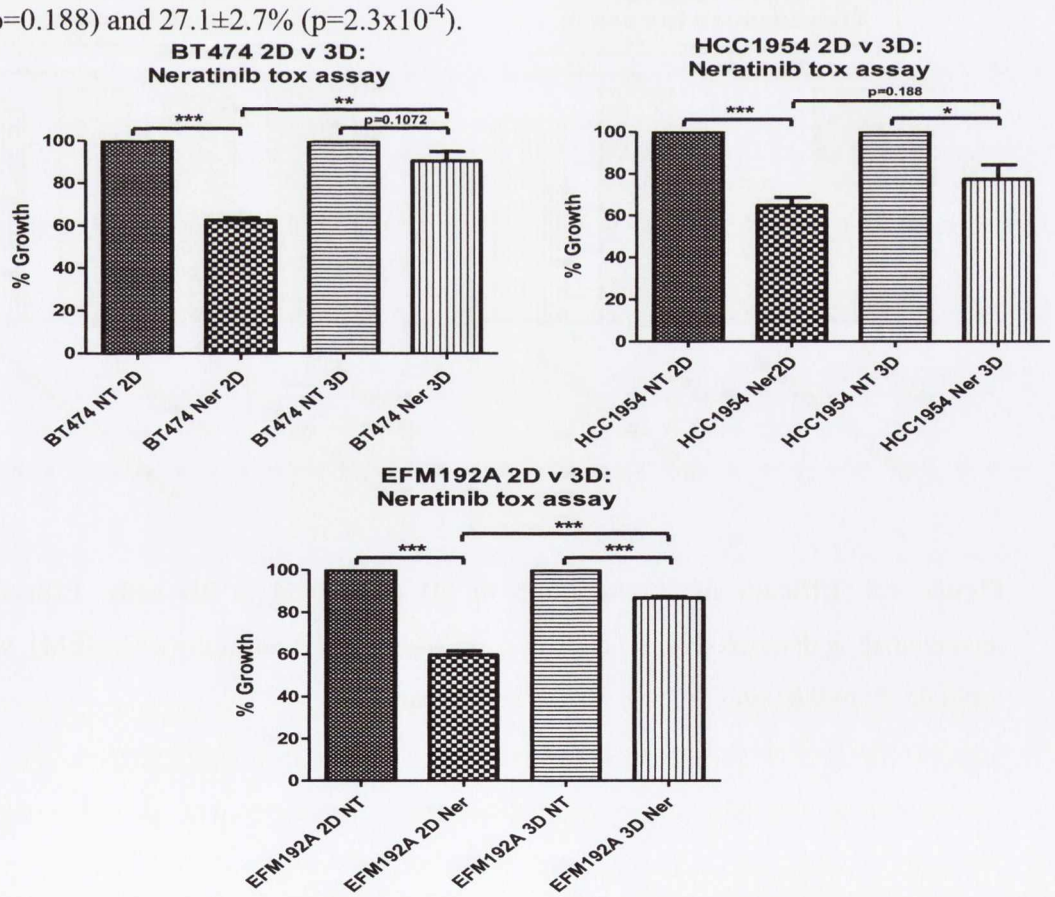

Figure 4.7. Efficacy of neratinib in 3D compared to 2D cells. Efficacy of neratinib is decreased in BT474, HCC1954 and EFM192A 3D compared to 2D cells (n=3±SEM), where *p<0.05, **p<0.01 and ***p<0.001. NT=untreated

4.3.6.2 Reduced efficacy of trastuzumab in BT474 3D cells compared to 2D cells

The efficacy of trastuzumab was compared between BT474 and EFM192A cells grown in 2D and 3D cultures (Figure 4.8). HCC1954 cells were not tested here as HCC1954 cells are innately resistant to trastuzumab [211]. Results showed that BT474 cells grown in 2D and treated with trastuzumab had 60.6±5.0% cell survival compared with untreated cells (p=0.001), while 3D cells treated with trastuzumab showed 86.3±0.2% cell survival compared to untreated 3D cells ($p=1.1x10^{-7}$). The difference in cell survival between 2D and 3D cells following the same treatment was 25.7±5.0%, this difference in drug response between 2D and 3D cells is statistically significant (p=0.007).

On the other hand, EFM192A cells grown in either 2D or 3D did not show a substantial response to trastuzumab treatment at 20μg/mL, where 2D cells maintained 95.4±0.9% cell growth (p=0.007) and 3D cells maintained 91±3.2% cell growth (p=0.049). This slight response to drug treatment in these cells is not significantly (p=0.254) different between 2D and 3D cell cultures.

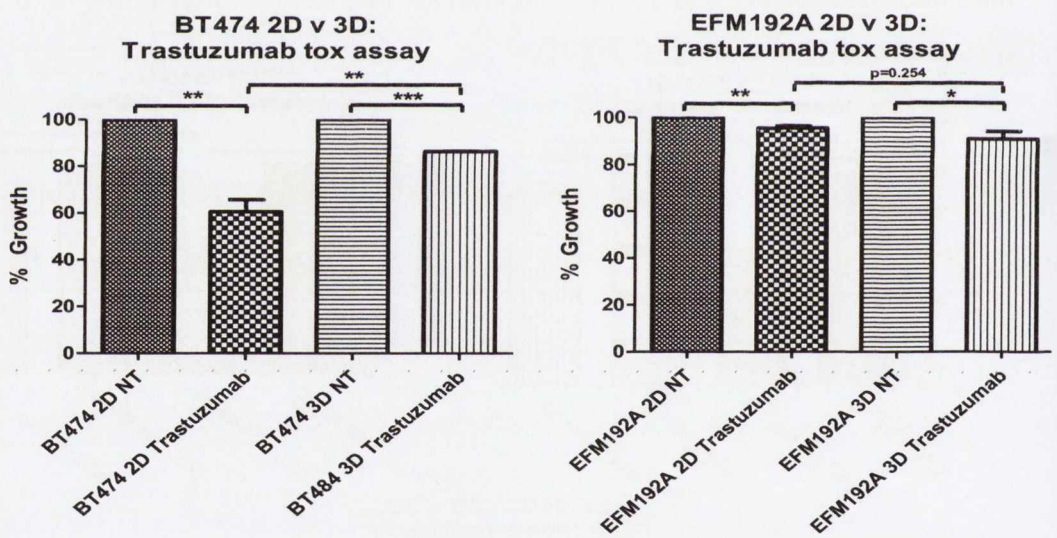

Figure 4.8. Efficacy of trastuzumab in 3D compared to 2D cells. Efficacy of trastuzumab is decreased in 3D cells in comparison to 2D cultures (n=3±SEM), where *p<0.05, **p<0.01 and ***p<0.001. NT= untreated.

4.3.6.3 Reduced efficacy of docetaxel in 3D cells compared to 2D cells

The efficacy of docetaxel was also reduced in 3D compared to 2D cultures. BT474 cells grown in 2D and treated with docetaxel had 60.3±8.7% cell survival compared with untreated cells (p=0.01), while 3D cells treated with the same concentration of docetaxel (See Section 4.2.6) maintained 91±5.9% cell survival compared to untreated 3D cells (p=0.203). The difference in cell survival between 2D and 3D cells following the same treatment was 30.7±2.8%, this difference in drug response between 2D and 3D cells is statistically significant (p=0.043). A similar trend was seen in both HCC1954 and EFM192A cells where 2D cells treated with fixed concentrations of docetaxel (See Section 4.2.6) showed 52.3±8.5% (p=0.005) and 46.2±2.6% ($p=4.2x10^{-5}$) cell survival, respectively, compared to untreated 2D cells, while 3D cells treated with docetaxel maintained a higher rate of survival at 101.6±5.7% (p=0.795) and 96.2±1.9% (p=0.118), respectively. For these cell lines, the increase in 3D cell survival compared to 2D cell survival after docetaxel treatment was 49±3.1% (p=0.009) and 50±2.5% ($p=1.0x10^{-4}$).

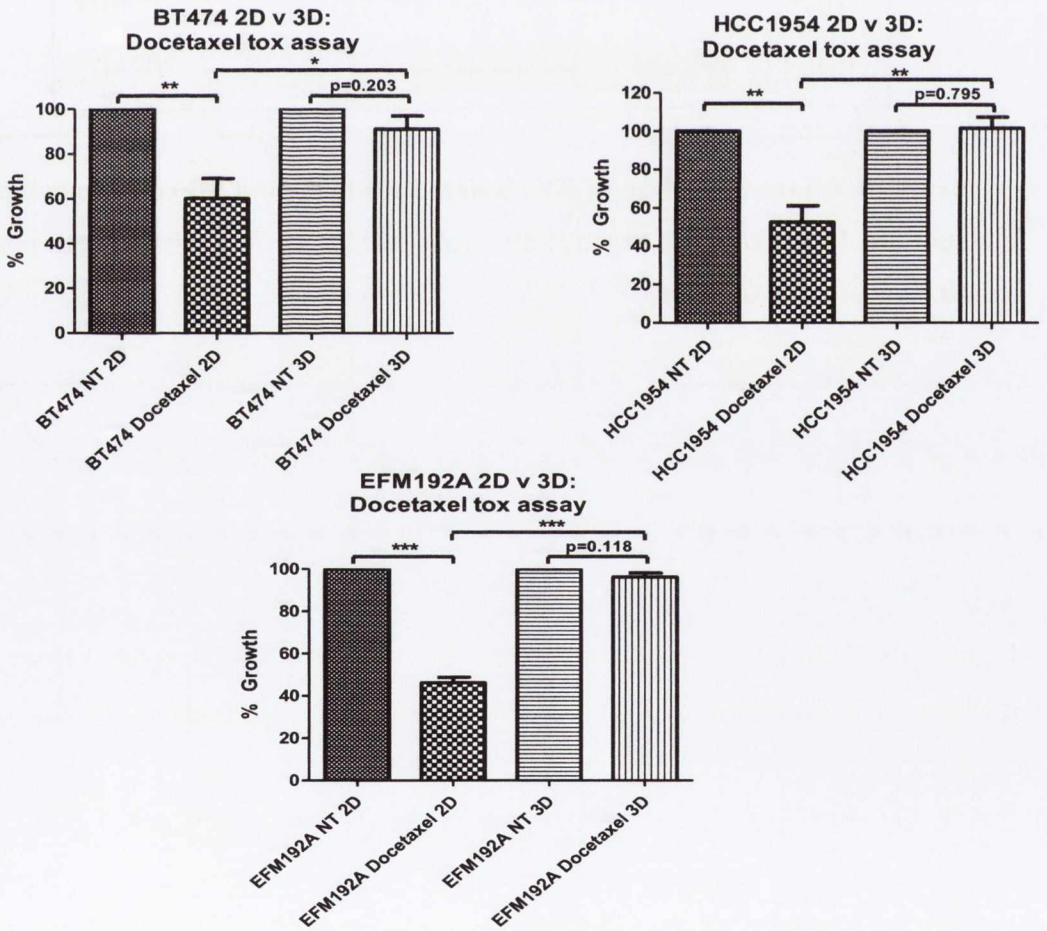

Figure 4.9. Efficacy of docetaxel in 3D compared to 2D cells. Efficacy of docetaxel is decreased in 3D cells in comparison to 2D cultures (n=3±SEM), where *p<0.05, **p<0.01 and ***p<0.001. NT=untreated.

4.3.7 Isolation of EVs from 2D and 3D cells

4.3.7.1 Characterisation of EVs isolated from 2D and 3D cultures

EVs were successfully isolated from 2D and 3D cell cultures using the filtration and ultracentrifugation method and were characterised by immunoblotting (Figure 4.3.10). Immunoblots of isolated EVs showed that these vesicles contain typical EV-markers including CD63 and Alix/PDC61 and were negative for the negative control protein, Grp94.

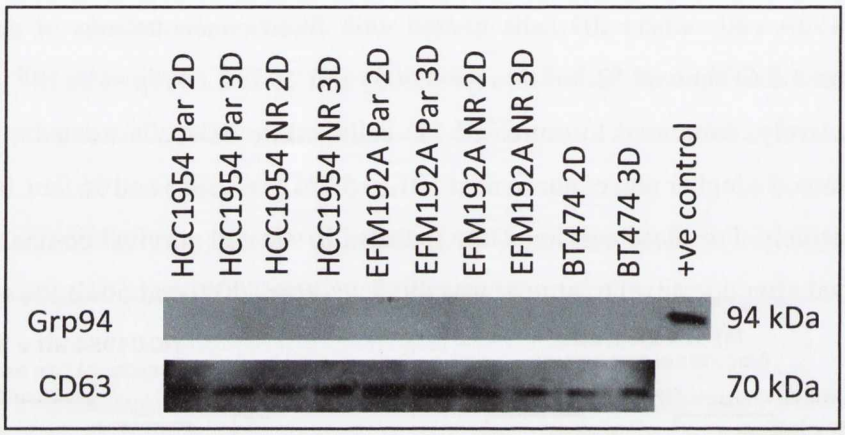

Figure 4.10. Characterisation of EVs isolated from 2D and 3D cells. Immunoblots indicate that EV isolated are negative for Grp94, where SKBR3 cells serve as positive control and positive for CD63.

4.3.7.2 Effect of 2D and 3D cell culture on EV secretion

EVs isolated from 2D and 3D cell cultures were quantified by measuring their relative protein quantities in order to investigate if growing cells in 2D or 3D affects the relative amounts of EVs secreted by cells (Figure 4.11). Overall, we found that EV quantities decreased slightly, but not significantly, when isolated from 3D compared to 2D cells (Figure 4.11.A(i)). More specifically, results showed that EV quantities decreased slightly from 104.4±2.7μg/mL when isolated from BT474 2D cells to 100.7±10.3μg/mL ($p=0.748$). Similarly, EV quantities decreased slightly from 96.1±5.8μg/mL in HCC1954 2D cells and 104.8±5.6μg/mL in EFM192A 2D cells to 82.0±3.9μg/mL in HCC1954 3D cells ($p=0.117$) and 94.0±4.8μg/mL in EFM192A 3D cells ($p=0.219$).

When normalised for viable cells, EV quantities were found to increase from 3D compared to 2D cells (Figure 4.11.A(ii)), where EV quantity increased 2.3±0.2 fold ($p=0.002$), 4.7±0.4 fold (7.6×10^{-4}) and 2.0±0.2 fold ($p=0.002$) for BT474 3D, HCC1954 3D and EFM192A 3D cells compared to 2D cells, respectively.

EVs released from HCC1954 and EFM192A parent and neratinib-resistant cells were also evaluated in 2D and 3D. Quantities of these EVs were compared for cells grown in 2D and 3D. Here, it was found that EV quantities from HCC1954-Par cells grown in 2D compared to HCC1954-NR cells grown in 2D decreased slightly from 96.1±5.8μg/mL to 95.6±5.7μg/mL ($p=0.958$) (Figure 4.11.B(i)). Similarly, EV quantities from EFM192A-Par cells grown in 2D compared to EFM192A-NR cells grown in 3D decreased slightly from 104.8±5.6μg/mL to 83.0±7.4μg/mL ($p=0.079$) (Figure 4.11.B(ii)). Conversely, EV quantities increased from 82.0±3.9μg/mL in HCC1954-Par 3D cells to 104.8±6.04μg/mL in HCC1954-NR 3D cells ($p=0.033$). While EFM192A-Par 3D cells decreased from 94.0±4.8μg/mL EVs compared to 84.6±2.28μg/mL in EFM192A-NR 3D cells ($p=0.15$).

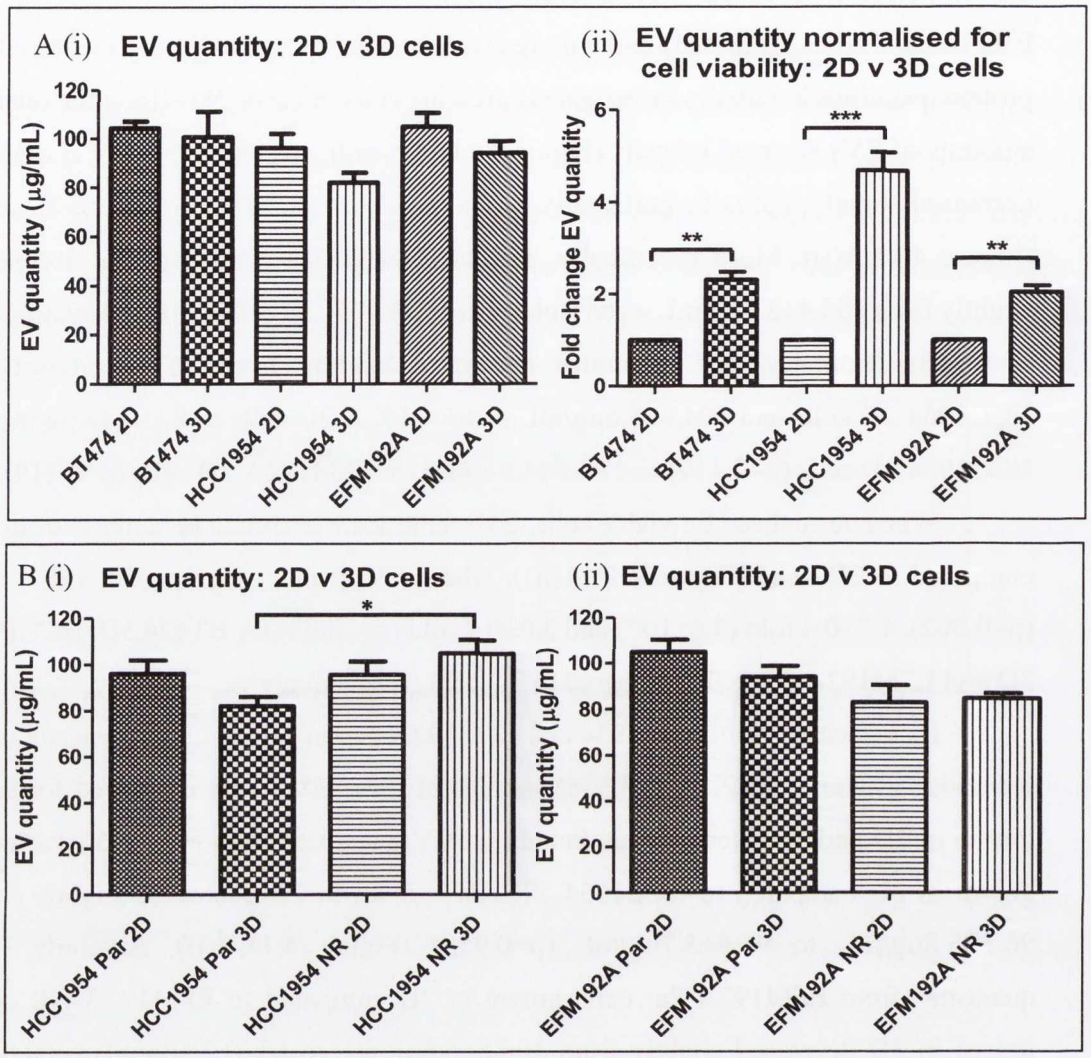

Figure 4.11. EV quantities released from 3D compared to 2D cells. A. (i) Quantification of EVs isolated from 2D and 3D cells; A (ii) Quantification of EVs isolated from 2D and 3D cells normalised for viable cells; B. Quantification of EVs isolated from HCC1954 (i) and EFM192A (ii) parent and neratinib-resistant cells grown in 2D and 3D (n=3±SEM), where *p<0.05, **p<0.01 and ***p<0.001.

4.3.8 CYP3A4 activity

4.3.8.1 CYP3A4 activity in 2D and 3D cultured cells

CYP3A4 activity was measured in 2D and 3D cells and normalised for cell viability in order to investigate if growing cells using the two different cell culture methods affects the activity of this drug metabolising enzyme (Figure 4.12). BT474 3D cells had 2.8±0.1 fold more CYP3A4 activity compared to that detected in BT474 2D cells ($p=1.5x10^{-4}$). Similarly, HCC1954 3D and EFM192A 3D cells had 5.3±0.7 fold (p=0.003) and 2.1±0.1 fold ($p=8.3x10^{-4}$) more CYP3A4 activity than their corresponding 2D cells, respectively.

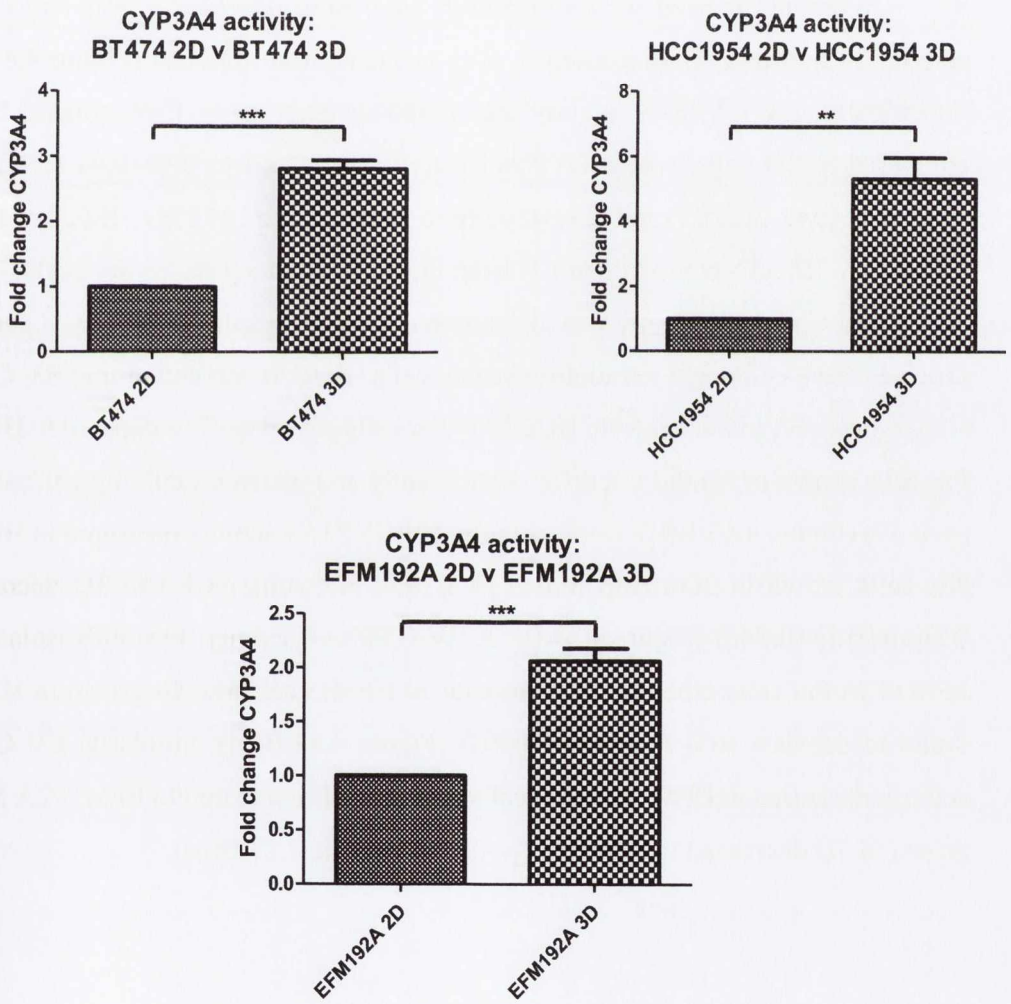

Figure 4.12. CYP3A4 activity in 3D compared to 2D cells. CYP3A4 activity is increased in 3D cells compared to 2D cells (n=3±SEM), where **p<0.01 and ***p<0.001.

4.3.8.2 CYP3A4 activity in EVs isolated from 2D and 3D cultured cells

CYP3A4 activity of EVs released from cells grown in 2D and 3D was measured (Figure 4.3.13). We found that EVs released from cells carry active CYP3A4. Specifically, results revealed that EV CYP3A4 activity did not differ significantly in EVs isolated from BT474 3D and HCC1954 3D cells where activity levels increased by only 1.1±0.03 fold (p=0.116) and 1.03±0.03 fold (p=0.39), respectively, compared to EV CYP3A4 activity detected from corresponding 2D cells (Figure 4.3.13.A(i)). Contrastingly, EV CYP3A4 activity decreased in EVs isolated from EFM192A 3D cells to 0.70±0.04 (p=0.002) compared to EV CYP3A4 activity detected from their corresponding 2D cells (Figure 4.13.A(i)).

When normalised for EV quantity, the overall observation was that CYP3A4 activity is significantly decreased in EVs isolated from 3D cells (Figure 4.13.A(ii)). Specifically, EV CYP3A4 activity was found to decrease in EVs isolated from 3D compared to 2D cells, where CYP3A4 activity decreased to 0.46±0.01 ($p=3.5x10^{-6}$), 0.22±0.01 ($p=2.01x10^{-8}$) and 0.34±0.02 ($p=6.9x10^{-6}$) for BT474 3D , HCC1954 3D and EFM192A 3D cells compared to EV from their 2D counterparts, respectively.

EV CYP3A4 activity was also measured for EVs isolated from aged parent (i.e. drug sensitive cells) and neratinib-resistant cells. Here, it was found that EV CYP3A4 activity from EVs isolated from HCC1954 Par cells grown in 2D compared to HCC1954 Par cells grown in 3D did not differ significantly and increased only by 1.02±0.03 fold (p=0.39) (Figure 4.13.B(i)). Contrastingly, EV CYP3A4 activity measured in HCC1954 NR cells grown in 2D compared to HCC1954 NR cells grown in 3D decreased to 0.86±0.05 (p=0.046) (Figure 4.13.B(i)). EV CYP3A4 activity from EVs isolated from EFM192A Par cells grown in 2D compared to EFM192A Par cells grown in 3D, it was found to decrease to 0.7±0.04 (p=0.002) (Figure 4.13.B(ii)). Similarly, EV CYP3A4 activity measured in EFM192A NR cells grown in 2D compared to EFM192A NR cells grown in 3D decreased to 0.84±0.1 (p=0.197) (Figure 4.13.B(ii)).

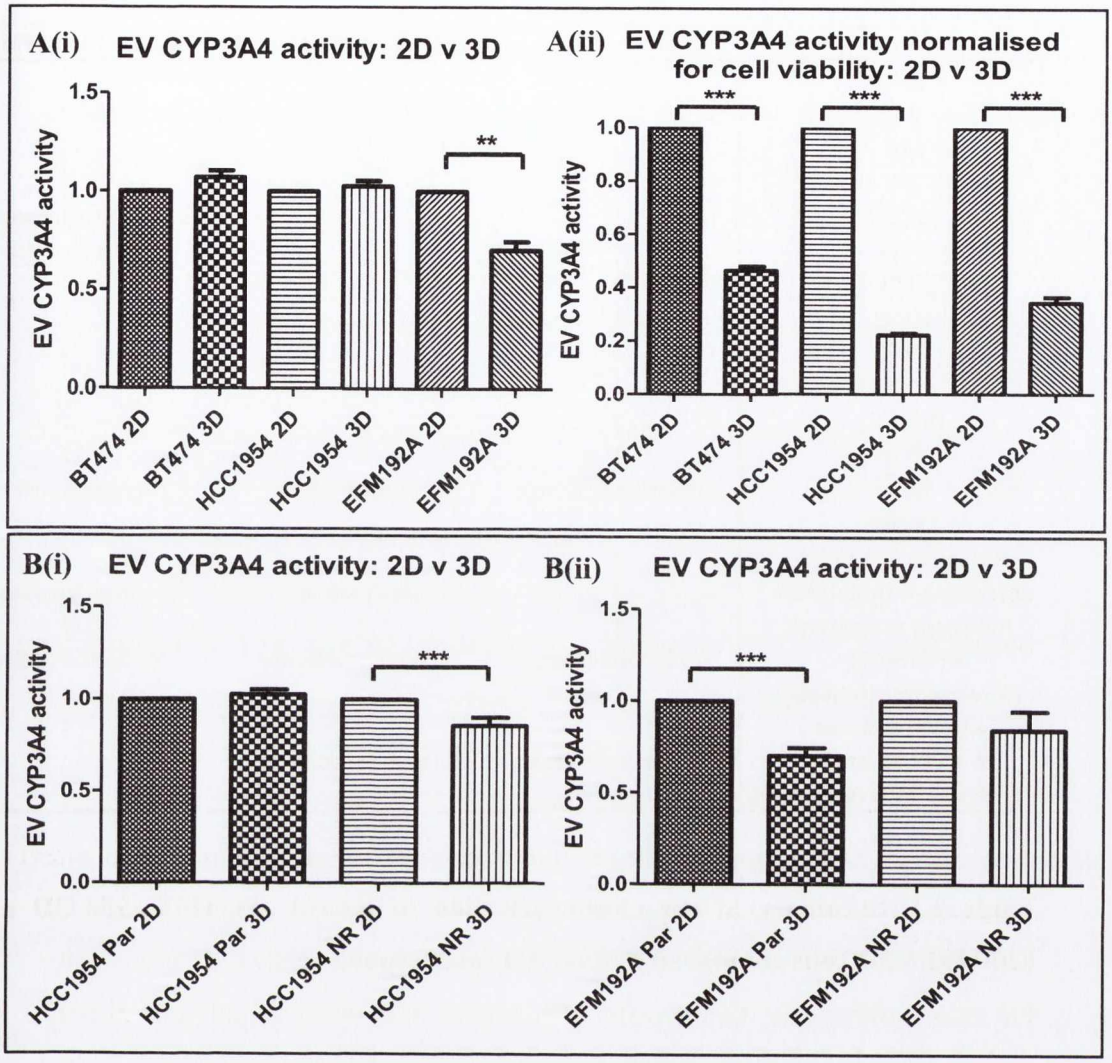

Figure 4.13. EV CYP3A4 activity from EVs released from 2D and 3D cells. A. (i) CYP3A4 activity in EVs isolated from BT474, HCC1954 and EFM192A cells in 2D and 3D; A (ii) CYP3A4 activity in EVs isolated from 2D and 3D cells normalised for cell viability; B. CYP3A4 activity in EVs isolated from parent and neratinib-resistant HCC1954 (i) and EFM192A (ii) cells, in 2D and 3D (n=3±SEM), where **$p<0.01$ and ***$p<0.001$.

Characteristic	BT474-3D vs BT474-2D	HCC1954-3D vs BT474-2D	EFM192A-3D vs EFM192A-2D
pAkt	↑	↑	↑
Akt	↑	↑	↑
pErk	↓	↓	↓
Erk	↑	↑	↑
pEGFR	↑	↑	Not expressed
EGFR	↑	↑	Not expressed
pHER2	↑	↑	↑
HER2	↑	↑	↑
HER3	↑	↑	↑
HER4			
Herstatin	↑	↑	↑
PGP	↑	↑	↑
BCRP	No significant difference	No significant difference	No significant difference
Viability	↓	↓	↓
Resistance to neratinib	↑	↑	↑
Resistance to trastuzumab	↑	Innately resistant	Innately resistant
Resistance to docetaxel	↑	↑	↑
EV secretion	No significant difference	No significant difference	No significant difference
EV secretion (normalised)	↑	↑	↑
Cell CYP3A4 activity	↑	↑	↑
EV CYP3A4 activity	No significant difference	No significant difference	↓
EV CYP3A4 activity (normalised)	↓	↓	↓

Table 4.1. Summary of the characterisation of BT474 3D, HCC1954 3D and EFM192A 3D cells compared to their 2D counterparts.

4.4 Discussion

4.4.1 Altered morphology of cells grown in 2D and 3D cultures

The poly-HEMA method of 3D cell culture involves coating round-bottomed 96 well plates with poly-HEMA, preventing cell attachment to culture plastic, which encourages the cells to adhere to each other instead and so, form 3D cell structures. This is a relatively simple method of 3D cell culture, albeit more labour intensive than traditional 2D culture, that allows for the generation of a single spheroid per well of the 96 well plate. The morphology of cells grown using this technique is substantially different in comparison to traditional methods. In 2D culture, cells grow flat and spread out on the cell culture plastic, whereas the 3D cells aggregate together and form 3D structures, formations which have also been reported by Sahin *et al.* [240] (ECM method), Ivascu and Kubbies [241] (poly-HEMA method) and Yao *et al.* (ECM method) [242] for HCC1954, BT474 and EFM192A cells, respectively. This ability to form 3D structures is not a characteristic of all cell lines, as MDA-MB-231, MDA-MB-468, SKBR3 and MDA-MB-361 cells have been shown to form only loosely bound, flat aggregates when grown using the poly-HEMA method [134]. Furthermore the SEM images of HCC1954 3D cells revealed that these 3D spheroids form what is apparently an ECM on their surface through which pores are formed. This characteristic has also been observed by Kelm *et al.*, [137] who grew HepG2 liver cells in 3D using the hanging-drop method and also found, using SEM, that pores formed in the surface of the spheroids produced.

4.4.2 Growing cells in 3D as opposed to 2D can alter protein expression

Growing cells using the poly-HEMA 3D cell culture method resulted in vastly different cell morphology and, in addition, revealed that 3D cultured cells have substantially altered protein expression in comparison to 2D cells. Proteins investigated here, and found to be significantly up- or down-regulated in association with 3D cell culture are those involved in cell growth and survival (Akt, Erk and EGFR family of receptors); are targets of drugs (certain EGFR family members); and are well known drug-transporters (PGP and BCRP).

While we found that expression of Akt, pAkt and Erk were all up-regulated and pErk was down-regulated in all 3D compared to 2D cell cultures, other groups have also seen that expression of these proteins can change with altered growth methods. Konishi *et al.* [243] found that ovarian cancer ES-2 cells, grown in 3D using the forced-floating

technique, had increased levels of Akt and pAkt, and while levels of both Erk and pErk decreased with 3D cell culture. Luca *et al.* [244] cultured Caco-2 cells, a colon cancer cell line, using Matrigel to form 3D spheroids and also found that these cell survival proteins altered in 3D cell culture. Specifically, in their case both Erk and pErk expression was increased in 3D compared to 2D cells, while Akt was increased but pAkt was decreased in 3D compared to 2D cells. In relation to this project, it is, perhaps, the case that the increased levels of Akt and pAkt observed in our 3D cells is, at least partially, responsible for the increased ability of cells grown in 3D to resist the effects of drug treatment in comparison to the treatment response of cells grown in 2D. It could be speculated that the observed decrease in 3D cell viability compared to cells grown in 2D may be due to the decrease in 3D levels of pErk. Collectively, however, the substantial differences in expression of these proteins by cells grown in 2D and 3D *in vitro* culture methods indicates that the separate methods do not represent the same basic biological information within the cells .

Similarly, expression of the EGFR family was found to differ between 2D and 3D cells. Specifically, EGFR, pEGFR, HER2, pHER2, HER3 and HER4 were all found to be expressed at higher levels in 3D cells in comparison to 2D cells. As an increase in EGFR and HER2 has previously been associated with resistance to lapatinib [85, 189], it is perhaps the case that the overexpression of these receptors in 3D cells mediates part of the resistance of the cells cultured in 3D to the effects of neratinib, docetaxel and trastuzumab. Other groups have also observed differential expression of these receptors between 2D and 3D cells. For example, Konishi *et al.* [243] also found that EGFR and pEGFR increase in ovarian ES-2 cells grown in 3D compared to 2D cells. Fong *et al.* [245] found HER2 was increased in Ewing sarcoma, EWS, cells grown in 3D using scaffolds compared to 2D cells. They also measured HER2 expression in *in vivo* Ewing sarcoma TC-71 xenographts and found that this increased expression of HER2 in 3D cells is more representative of HER2 levels seen in the *in vivo* xenographts than the lower HER2 expression levels detected in 2D cells. While Pickl and Reis [156] did not find any differences in HER2 expression between 2D and 3D cells, they did report that pHER2 levels in 3D cells were increased in SKBR3 cells grown in 3D compared to 2D cells. Weigelt *et al.* [246] demonstrated that HER3 expression differs between 2D and 3D cells. Specifically, they found that HER3 expression is increased in HCC1569 breast cancer cells grown in 3D using Matrigel compared to 2D cells; however, they also showed that HER3 expression is decreased in AU565, SKBR3 and BT549 cells grown in 3D compared to 2D cultures. Hua *et al.* [247] found that NBL neuroblastoma cells

grown in 3D using the poly-HEMA method have higher levels of HER4 compared to cells grown in 2D.

Interestingly, we found that in addition to the significantly increased levels of HER2 expression in 3D cultures, expression of herstatin, a splice variant of subdomains I and II of HER2, the extracellular domain [248], is also substantially increased in 3D cells compared to 2D cells. It has been shown that herstatin binds to both EGFR and HER2, and can interfere with receptor dimerisation [249]. The significance of the increase in herstatin levels in 3D cells has not yet been established and so requires further investigation.

The expression of PGP, but not BCRP, was found to be increased in 3D cells in comparison to 2D cells. Increased levels of this drug transporter could reduce the levels of substrate drugs within cells in 3D, therefore the increase in PGP in 3D cells may contribute to the decrease in drug efficacy observed in 3D cells in comparison to the effects of drugs tested in 2D cells. Doublier *et al.* [250] had similar observations and found that growing MCF7 cells in 3D resulted in higher PGP levels compared to cells grown in 2D. They also found that this increase in PGP levels in 3D cells corresponded to a decrease in doxorubicin accumulation within the cells, in comparison to cell cultured in 2D.

4.4.3 Cells grown in 3D have reduced viability compare to 2D cultures

The reduced level of viable cells seen in 3D cell cultures versus 2D cell cultures may be a result of reduced pErk in the 3D cells, as per discussed in Section 4.4.2. However, another factor that likely plays a role in the observed decrease in viable cells in 3D is the fact that while cells grow continuously in 2D, provided they have the space to do so in their cell culture container, 3D cells do not follow the same growth pattern. Due to the logistics of cells growing in a 3D structure, the cells at the centre do not receive oxygen (*i.e.* experience hypoxia) or nutrients to the same extent as outer cells and die as a consequence of this, resulting in the necrotic core commonly associated with 3D cell spheroids [133]. At the same time, the outermost layer of cells in a spheroid can proliferate, while the middle layer of cells are typically reported as being comprised of quiescent cells [133]. As a result, while the same number of cells can be seeded in 2D and 3D, each of the 2D cells is likely to continue to divide as are their daughter cells, while only the cells that form the outer layer of 3D cell cultures are able to proliferate. It is in this way that the viability of our 3D cells is likely to be substantially reduced compared to 2D cultured cells. The reduced viability in 3D compared to 2D cells has

also been widely reported by other groups, where MCF7 breast cancer cells grown in 3D using collagen gels had substantially reduced proliferation compared to cell grown in monolayer [251]. Similarly, Luca *et al.* [244] found that the proliferation of a range of colon cancer cell lines (Caco-2, DLD-1, HT-29, SW-480, LoVo, COLO-205 and COLO-206f) grown in 3D using Matrigel was decreased compared to growth observed in 2D cells.

4.4.4 Drugs have reduced efficacy in 3D cells compared to 2D cells

In vitro drug testing using 2D cell culture is commonplace to find which, out of a range of lead compounds are most effective. Consequently, we investigated the efficacy of neratinib, docetaxel and trastuzumab in both 2D and 3D cultured cells in order to monitor any differences that culture method may have on drug efficacy *in vitro*. We found that cells grown in 3D show a degree of resistance to the effects of all three drugs, in comparison to 2D cells. We also found that a number of proteins involved in cell growth and survival (Akt, pAkt, Erk and EGFR family of receptors), that are common drug targets (EGFR and HER2) and a well-known drug-transporter (PGP), are all up-regulated in cells grown in 3D. It is likely that the increases in these proteins are responsible for the increase in innate resistance of these cells to the drugs investigated here, as the overexpression of these proteins has previously been associated with facilitating drug-resistance.

The decrease in drug efficacy in 3D cells that was observed here has also been seen by other groups but not in breast cancer. Wen *et al.* [252] cultured two pancreatic cancer cell lines, MIAPaCa-2 and PANC-1, in 3D using Matrigel and found that 3D cells treated with gemcitabine and 5-FU had a higher resistance to the effects of these drugs in comparison to cells grown in 2D. Similarly, Ponce de León *et al.* [253] found that lung cancer INER-51 cells grown in 3D using agarose had an increase in resistance to the effects of doxorubicin, etoposide and methotrexate compared to the effects these drugs had on cells grown as monolayers. Together, this data indicates that cells cultured using 3D methods have a higher innate resistance to cytotoxic agents in comparison to cells grown in 2D.

While 3D cells demonstrate an increase in resistance to the effects of drugs, cell models of acquired-resistances to drugs are still a necessary tool for researchers. The increase in resistance to drugs seen here in 3D cells is an increase in innate-resistance, cell models that mimic the effects of chronic drug exposure on cells are still required, as innate and acquired-resistance don't always show the same trends. For example, here

we demonstrate that PGP expression in 3D cells is substantially increased compared to 2D cells, while neratinib-resistant cells have decreased PGP expression in comparison to drug-sensitive parent cell lines (see Section 2.3.7). The effects of growing cells with acquired neratinib-resistance in 3D have not yet been investigated in our lab but could reveal more information on this matter (see Section 5.3.9).

4.4.5 Growing cells in 3D alters secretion of EVs

EVs isolated from cells grown in 2D and 3D were characterised in accordance to some of the minimal requirements outlined in [224], which were also described here in Section 3.4.2. Analysis of protein content of the EVs isolated by immunoblotting showed that these vesicles contain CD63, a tetraspanin protein. Additionally, Grp94, an endoplasmic reticulum protein, serves as a negative control by Grp94 and was not detected in our EV samples. Further characterisation of these EVs is required and the factors to be addressed for completion of this characterisation are outlined in Section 5.3.8. Additionally, we looked at EV quantities secreted from cells cultured in 2D and 3D. We observed that, when normalised for viable cells, more EVs are released from cells grown in 3D compared to 2D, which suggests that the quantities of EVs released from cells grown *in vitro* is underrepresented in 2D cell cultures.

4.4.6 3D cell cultures have higher CYP3A4 activity than 2D cells

CYP3A4 is a cytochrome p450 enzyme that plays a role in the metabolism of approximately 50% of drugs being used in the clinical setting [210]. Also, it has been shown that elevated levels of this enzyme may contribute to drug resistance [82]. Due to the prominence of CYP3A4 in drug metabolism and drug resistance, the activity of this enzyme in both 2D and 3D cell cultures was measured and it was found that 3D cells have higher CYP3A4 activity than 2D cells. Neratinib [211] and docetaxel [254] are both substrates for CYP3A4 and, as these drugs exhibit decreased efficacy in 3D cells, it is likely that the increased CYP3A4 activity in 3D cells is at least partially responsible for the decreased drug efficacy observed in 3D cells compared to 2D cells. The increased enzyme activity in relation to 3D cell culture observed here has also been seen by others in liver cells, where Ramaiahgari *et al.* [238] found that HepG2 cells culture in 3D using Matrigel had higher CYP3A4 activity and genetic expression of CYP3A4. Additionally, Takahashi *et al.* [255] found that CYP3A4 mRNA levels were increased in HepG2 cells grown in 3D using the hanging drop method, in comparison

to 2D cells. However, to the best of our knowledge, this is the first report of this observation in breast cancer.

Additionally, we found that EVs contain active CYP3A4. As EVs have been shown to transfer active biomolecules and induce effects on secondary cells [111], the EVs maybe have the capacity to transfer their active CYP3A4 to secondary cells, which may affect the drug-resistant capabilities of these cells. We found that CYP3A4 activity is decreased in 3D EVs compared to 2D EVs which suggests that CYP3A4 activity may be over-represented by 2D cell EVs compared to 3D cell EVs.

4.4.7 Consistency of trends observed

Trends of alterations in protein expression, cell viability, response to drugs and enzyme activity between cells grown in 2D and 3D were all observed here. These differences are seen consistently across the three cell lines used in this project. The consistency in data trends supports the likelihood of the results as being meaningful and suggests that the observations of this study are not cell line specific.

4.5 Conclusion

In vitro cell culture is an essential method for biological sciences and the drug development process. Therefore, the methods used must be of the highest quality and relevance to the *in vivo* situation of the biological processes being investigated. The data presented here indicates that the biological information represented by both 2D and 3D cell cultures are fundamentally different, which may call into question the relevance of 2D culture in terms of representation of the *in vivo* setting. We showed that the expression of a number of proteins involved in cell survival, drug targeting and drug transporters, the activity of an enzyme that plays a major role in drug metabolism and EV quantities are all increased in 3D compared to 2D cell cultures. Additionally, we found that drug efficacy is reduced in cells grown in 3D as opposed to the effects observed in 2D cultures. Overall, this implies that 3D cells demonstrate a higher innate resistance to both targeted and classical chemotherapeutic drugs, compared to 2D cells and this increase in resistance is likely facilitated by the increased protein expression and enzyme activity observed.

Chapter 5: Discussion, conclusion and future work

5.1 Discussion

The aim of this project was to investigate both innate and acquired drug-resistance in HER2-overexpressing breast cancer and to also evaluate the potential of EVs as breast cancer biomarkers. Specifically, the objective was to investigate the effects and possible mechanism of acquired neratinib-resistance using 2 cell line models; to determine the relevance of EVs as biomarkers that are predictive of response to therapy; and to clarify the difference in innate drug-resistance of cells when grown using 2D and 3D cell culture methods, respectively.

The chronic exposure of HCC1954 and EFM192A HER2-overexpressing breast cancer cell lines to neratinib resulted in the generation of neratinib-resistant cell line variants, demonstrating that, like other HER2-targeting agents, long-term exposure to neratinib will result in acquired-resistance to the drug. Furthermore, these cell lines were then used to characterise the developed drug-resistance, producing information on the associated phenotypic changes in cells that develop resistance to neratinib. To date there is no published research describing the establishment or the use of similar models of neratinib-resistance, indicating the novelty of this research. We found that cells with resistance to neratinib were cross-resistant to other HER-targeting agents (lapatinib and afatinib tested) and also that cells resistant to other HER-targeting agents (lapatinib and trastuzumab tested), while neratinib-resistant cells maintained sensitivity to the toxic effects of docetaxel. This substantial cross-resistance in association with neratinib has not been investigated and so not seen previously and may have implications in patient therapy in the clinic. If the *in vitro* data presented here validates in the clinic it could be the case that breast cancer patients who progress on neratinib will not respond well to other HER-targeted therapies and similarly, patients who have progressed on other HER2-targeted therapies may not respond to neratinib therapy. Preliminary clinical trials suggest that this may be the case as breast cancer patients with previous exposure to trastuzumab [72] and lapatinib [171] do not respond as well to neratinib treatment as patients without previous exposure to neratinib.

The increased cell aggression in association with acquired neratinib-resistance is something that has also been in observed with resistance to other drugs [187, 188]. While this occurrence is not uncommon, it is another limiting factor associated with the problem that acquired drug-resistance poses to effective breast cancer management. This also shows that even the newest drugs in development are not free from some the issues and limitations that have plagued drugs that have already been approved for use.

Here, in addition to cross-resistance to other drugs, cells with neratinib-resistance are also more migratory, invasive (HCC1954-NR cells only) and more resistant to *anoikis* than drug-sensitive cells. As these assays mimic the metastatic potential of cell lines, this suggests that tumour cells with acquired neratinib-resistance are more likely to metastasise, should the same trends be observed in patients.

Finally, our work on neratinib-resistant cell lines revealed that these neratinib-resistant cells contained higher CYP3A4 enzyme activity than their age-matched parent cells. This mechanism of resistance has not previously been associated with breast cancer cell resistance to a tyrosine kinase inhibitor. It is important to elucidate the mechanism through which drug resistance is mediated in order to potentially circumvent this issue by either preventing the development if drug-resistance in the first place or reinstating activity of the drug. However, in the case of neratinib-resistance, this may cause complications as CYP3A4 is involved in the metabolism of almost half of all drugs [210] and so if a patient is also on other medication, the co-administration of a CYP3A4 inhibitor to prevent/reduce neratinib-resistance, may also effect the metabolism of any other drugs being taken. Of course many young patients may not be on many other drugs and so, potentially, this may be a useful approach to circumventing drug resistance in these cases.

Research for this thesis then moved on to investigating the relevance of EVs as biomarkers for response to therapy in breast cancer. It was found that relative EV quantity may be used to diagnose breast cancer, whereby the quantity of EVs isolated from cancer patients was significantly higher than that of healthy age-matched controls. Additionally, data revealed that, although not significantly, EV quantities may give an indication to patient response to treatment with docetaxel and carboplatin plus trastuzumab or lapatinib, where there was a trend for increased EV quantity and decreased response to therapy. This suggests that using this minimally-invasive, albeit relatively labour-intensive method for quantifying EVs may have an impact on breast cancer patient diagnosis and monitoring of effective therapy by identifying those less/more likely to respond to therapy.

In addition to evaluating at the relevance of EV quantities with regards to patient care, the content of these EVs was also investigated. However, when EV NmU was measured and compared to serum NmU, we found that in addition to NmU being detected in the EVs, the levels of EV NmU and serum NmU did not differ significantly, suggesting that the majority of NmU detected in serum is contained within the EVs. Together, this supports claims by others that some proteins are specifically packaged

into EVs [102] and that EV contents may have a role as biomarkers. Levels of EV NmU and EV survivin did not differ significantly between patients who did and did not response to treatment when compared pre- and post-treatment, suggesting that these proteins are not indicative of patients' response to therapy. We found, contrary to another groups findings [113], that EVs isolated in this project did not contain HER2. However, serum levels of HER2 were found to be significantly decreased between pre- and post-treatment only in patients who achieved a complete response, for patients with partial and no response HER2 decreased, but not significantly, which supports the findings of other groups [226] that monitoring of serum HER2 may prove to be an effective predictive biomarker of patient response to therapy.

Finally, we investigated and characterised the effects of growing cells in 2D compared to 3D on innate resistance to drugs. At a first assessment the most obvious alteration between the two methods of cell culture is the difference in morphology of cells, where cells grown as 2D models form in a single monolayer flat on cell culture plastic, while 3D cells attach to each other and not cell culture plastic, to form a 3D spherical structure. Growing cells in 2D compared to 3D also alters the expression of proteins involved in cell growth and survival, drug targets and drug transporters, indicating that there are substantial differences in the basic biological information represented by the two culture methods. The sensitivity to the effects of drugs (neratinib, docetaxel and trastuzumab tested) was significantly reduced in cells grown in 3D as opposed to 2D. This is likely a result of a combination of factors including increased protein expression of drug targets and transporters and proteins involved in growth and survival and also the increase in CYP3A4 activity observed in 3D cultured cells compared to cells grown using the traditional monolayer cell culture method. Considering this data and the fact that 3D cultures in HepG2 liver cancer cells have been previously shown to be more representative of *in vivo* [238], it is perhaps the case that the innate resistance of cells to the effects of anti-cancer drugs is under-represented by cells grown in 2D and so *in vitro* research may benefit substantially from enhanced inclusion of 3D cell culture as a more widely utilised research method.

5.2 Conclusion

The research presented here shows that acquired neratinib-resistance develops with long-term exposure of cells to neratinib. This neratinib-resistance is associated with cross-resistance to other HER-targeting drugs and increased cell aggression, while the mechanism of resistance is mediated, at least in part, by increased NmU and CYP3A4 activity. We also demonstrate the potential of EV quantity as a diagnostic and predictive biomarker for HER2-overexpressing breast cancer. While EVs contain NmU and survivin, these proteins were not found to be of use for prediction of response to therapy. It should be noted, however, that this work requires validation due to small patient specimen numbers available for testing. We observed substantial differences between cells grown in 2D and 3D cultures. Specifically, protein expression, drug sensitivity and enzyme activity were all found to differ between the two culture methods. The main observation here was that cells grown in 3D appear to have a higher innate resistance to anti-cancer drug treatment compared to cells grown in 2D and so this should perhaps be considered for future *in vitro* drug screenings.

5.3 Future work

Examples of how the work presented in this thesis can be further explored are described below:

5.3.1 Is CYP3A4 activity functionally involved in acquired neratinib-resistance?

Our studies in Chapter 2 show that CYP3A4 activity is increased in neratinib-resistant cells. However, whether this increase in CYP3A4 activity is functionally involved in mediating this resistance has not yet been investigated. To elucidate this, CYP3A4 activity should be inhibited (e.g. with ketoconazole) and the effects of this enzyme inhibition on the sensitivity of cells to the effects of neratinib should be measured. Similar experiments should be performed with CYP3A4 inducers (e.g. with rifampin) to validate these experiments.

5.3.2 Does the increase in CYP3A4 activity in NR cells increase the rate of neratinib metabolism in these cells?

Studies into the metabolism of neratinib, in parent and neratinib-resistant cells, by mass spectrometry would indicate if increased CYP3A4 activity facilitates neratinib-resistance by metabolising the drug faster in neratinib-resistant cells where enzyme activity levels are higher compared to parent cells that have significantly less CYP3A4 activity. This would further clarify the role of increased CYP3A4 activity in neratinib-resistant cells.

5.3.3 Does FGFR play a role in neratinib-resistance?

In Section 2.4.3 the similarities between acquired neratinib-resistance in our NR cells and acquired afatinib-resistance in lung cancer cells investigated by Azuma *et al* [191] are described. There are similarities between neratinib and afatinib mechanisms of action and also similarities in the consequences of acquired resistance to these drugs (both show decreased EGFR, HER2 and HER3 in association with drug-resistance). Azuma *et al* [191] show that resistance to afatinib in their lung cancer cells is mediated, at least in part, by FGFR. So, due to the similarities established here between the drugs, it should be investigated if FGFR also has a role in neratinib-resistance.

5.3.4 Are the trends associated with neratinib-resistance observed here also seen in patients?

We found that neratinib-resistance is associated with cross-resistance to other drugs, increased cell aggression, increased NmU expression and increased CYP3A4 activity. To investigate the clinical relevance of these findings these observations should be investigated to see if the same trends are seen in patients treated with neratinib who then go on to develop resistance to the drug in the clinic.

5.3.5 Do the trends for the association of EV quantity with cancer and patient response to therapy observed here validate when tested over a larger patient cohort?

Experiments on EVs and corresponding serum were performed blinded to patient outcome to ICORG clinical trial 10-05. Consequently, it was not until this work was completed that we were made aware of the small patient numbers in the no response group in the trial. Due to this small number (n=2), statistical analysis was not applicable to this patient group. So it in order to validate any trends seen using this patient group, experiments would have to be progressed to a larger cohort of patients.

5.3.6 Is NmU expression in HER2-overexpressing tumours indicative of patient response to therapy?

We found that NmU expression in EVs and serum is not indicative of patient response to therapy. The levels of NmU contained within cells from breast cancer tumours, however, was not investigated. NmU content of tumours should be measured to see if it correlates to patients' response to therapy in order to establish if this measurement has potential in the clinic as a predictive biomarker for patient response to therapy.

5.3.7 Longer term follow up of trends observed for EV quantities in relation to patient response

The trend was observed that EV quantities at both pre- and post-treatment were indicative of response to therapy. A longer term monitoring EV quantities with follow up of long-term response to therapy would indicate if EV quantity is indicative of short-term or long-term response to therapy.

5.3.8 Complete characterisation of EVs isolated from 2D and 3D cultured cells

EVs isolated from 2D and 3D cultured cells were isolated using the filtration and ultracentrifugation method. While we have shown that the EVs isolated are negative for Grp94 and positive for CD63, further characterisation of the vesicles is necessary. An assessment for TSG101 and/or Alix/PDC6I is needed to indicate that vesicles contain cytosolic proteins, NanoSight analysis is required to show the size of the vesicles and TEM is needed to provide images of the EVs isolated.

5.3.9 Expand 2D and 3D culture comparisons to include parent versus resistant cell comparisons

At present we have demonstrated that there is a difference in the innate resistance of cells grown in 2D compared to 3D. This was associated with differences expression of specific proteins and also differences in drug efficacy between to the two methods of cell culture. It would be interesting to look at the effects of growing cells with acquired-resistance to neratinib in 3D in order to see if the changes in culture conditions alters the response of these cells to drug treatment when compared to cells grown in 2D.

Chapter 6: References

1. Hanahan, D. and R.A. Weinberg, *The hallmarks of cancer.* Cell, 2000. **100**(1): p. 57-70.
2. Cuttitta, F., et al., *Bombesin-like peptides can function as autocrine growth factors in human small-cell lung cancer.* Nature, 1985. **316**(6031): p. 823-6.
3. Korc, M., et al., *Overexpression of the epidermal growth factor receptor in human pancreatic cancer is associated with concomitant increases in the levels of epidermal growth factor and transforming growth factor alpha.* J Clin Invest, 1992. **90**(4): p. 1352-60.
4. Lyons, L.S., et al., *Ligand-independent activation of androgen receptors by Rho GTPase signaling in prostate cancer.* Mol Endocrinol, 2008. **22**(3): p. 597-608.
5. Shaw, P.H., *The role of p53 in cell cycle regulation.* Pathol Res Pract, 1996. **192**(7): p. 669-75.
6. Ryan, K.M., A.C. Phillips, and K.H. Vousden, *Regulation and function of the p53 tumor suppressor protein.* Curr Opin Cell Biol, 2001. **13**(3): p. 332-7.
7. Kerr, J.F., A.H. Wyllie, and A.R. Currie, *Apoptosis: a basic biological phenomenon with wide-ranging implications in tissue kinetics.* Br J Cancer, 1972. **26**(4): p. 239-57.
8. Wong, R.S., *Apoptosis in cancer: from pathogenesis to treatment.* J Exp Clin Cancer Res, 2011. **30**: p. 87.
9. Wuilleme-Toumi, S., et al., *Mcl-1 is overexpressed in multiple myeloma and associated with relapse and shorter survival.* Leukemia, 2005. **19**(7): p. 1248-52.
10. Krajewski, S., et al., *Reduced expression of proapoptotic gene BAX is associated with poor response rates to combination chemotherapy and shorter survival in women with metastatic breast adenocarcinoma.* Cancer Res, 1995. **55**(19): p. 4471-8.
11. Shen, X.G., et al., *Downregulation of caspase-9 is a frequent event in patients with stage II colorectal cancer and correlates with poor clinical outcome.* Colorectal Dis, 2010. **12**(12): p. 1213-8.
12. Reesink-Peters, N., et al., *Death receptors and ligands in cervical carcinogenesis: an immunohistochemical study.* Gynecol Oncol, 2005. **96**(3): p. 705-13.
13. Kim, N.W., et al., *Specific association of human telomerase activity with immortal cells and cancer.* Science, 1994. **266**(5193): p. 2011-5.
14. Neumann, A.A. and R.R. Reddel, *Telomere maintenance and cancer -- look, no telomerase.* Nat Rev Cancer, 2002. **2**(11): p. 879-84.
15. Cesare, A.J. and R.R. Reddel, *Alternative lengthening of telomeres: models, mechanisms and implications.* Nat Rev Genet, 2010. **11**(5): p. 319-30.
16. Henson, J.D., et al., *DNA C-circles are specific and quantifiable markers of alternative-lengthening-of-telomeres activity.* Nat Biotechnol, 2009. **27**(12): p. 1181-5.
17. Carmeliet, P. and R.K. Jain, *Angiogenesis in cancer and other diseases.* Nature, 2000. **407**(6801): p. 249-57.
18. Nishida, N., et al., *Angiogenesis in cancer.* Vasc Health Risk Manag, 2006. **2**(3): p. 213-9.
19. Kim, K.J., et al., *Inhibition of vascular endothelial growth factor-induced angiogenesis suppresses tumour growth in vivo.* Nature, 1993. **362**(6423): p. 841-4.
20. Nguyen, D.X. and J. Massague, *Genetic determinants of cancer metastasis.* Nat Rev Genet, 2007. **8**(5): p. 341-52.
21. Fidler, I.J., *The pathogenesis of cancer metastasis: the 'seed and soil' hypothesis revisited.* Nat Rev Cancer, 2003. **3**(6): p. 453-8.
22. Nguyen, D.X., P.D. Bos, and J. Massague, *Metastasis: from dissemination to organ-specific colonization.* Nat Rev Cancer, 2009. **9**(4): p. 274-84.
23. Sorlie, T., et al., *Gene expression patterns of breast carcinomas distinguish tumor subclasses with clinical implications.* Proc Natl Acad Sci U S A, 2001. **98**(19): p. 10869-74.
24. Slamon, D.J., et al., *Studies of the HER-2/neu proto-oncogene in human breast and ovarian cancer.* Science, 1989. **244**(4905): p. 707-12.

25. Schnitt, S.J., et al., *The relationship between microscopic margins of resection and the risk of local recurrence in patients with breast cancer treated with breast-conserving surgery and radiation therapy.* Cancer, 1994. **74**(6): p. 1746-51.
26. Hartmann, L.C., et al., *Efficacy of bilateral prophylactic mastectomy in BRCA1 and BRCA2 gene mutation carriers.* J Natl Cancer Inst, 2001. **93**(21): p. 1633-7.
27. Donegan, W.L., *Prognostic factors. Stage and receptor status in breast cancer.* Cancer, 1992. **70**(6 Suppl): p. 1755-64.
28. Mauri, D., N. Pavlidis, and J.P. Ioannidis, *Neoadjuvant versus adjuvant systemic treatment in breast cancer: a meta-analysis.* J Natl Cancer Inst, 2005. **97**(3): p. 188-94.
29. King, T.A., et al., *Long-term results of wide-field brachytherapy as the sole method of radiation therapy after segmental mastectomy for T(is,1,2) breast cancer.* Am J Surg, 2000. **180**(4): p. 299-304.
30. Houghton, J., et al., *Radiotherapy and tamoxifen in women with completely excised ductal carcinoma in situ of the breast in the UK, Australia, and New Zealand: randomised controlled trial.* Lancet, 2003. **362**(9378): p. 95-102.
31. Singh, G., *Oophorectomy in breast cancer-controversies and current status.* Indian J Surg, 2012. **74**(3): p. 210-2.
32. Robertson, J.F. and R.W. Blamey, *The use of gonadotrophin-releasing hormone (GnRH) agonists in early and advanced breast cancer in pre- and perimenopausal women.* Eur J Cancer, 2003. **39**(7): p. 861-9.
33. Ellis, M.J., et al., *Randomized phase II neoadjuvant comparison between letrozole, anastrozole, and exemestane for postmenopausal women with estrogen receptor-rich stage 2 to 3 breast cancer: clinical and biomarker outcomes and predictive value of the baseline PAM50-based intrinsic subtype--ACOSOG Z1031.* J Clin Oncol, 2011. **29**(17): p. 2342-9.
34. Dutertre, M. and C.L. Smith, *Molecular mechanisms of selective estrogen receptor modulator (SERM) action.* J Pharmacol Exp Ther, 2000. **295**(2): p. 431-7.
35. Fu, D., J.A. Calvo, and L.D. Samson, *Balancing repair and tolerance of DNA damage caused by alkylating agents.* Nat Rev Cancer, 2012. **12**(2): p. 104-20.
36. Bordin, D.L., et al., *DNA alkylation damage and autophagy induction.* Mutat Res, 2013. **753**(2): p. 91-9.
37. Parker, W.B., *Enzymology of purine and pyrimidine antimetabolites used in the treatment of cancer.* Chem Rev, 2009. **109**(7): p. 2880-93.
38. Kaye, S.B., *New antimetabolites in cancer chemotherapy and their clinical impact.* Br J Cancer, 1998. **78 Suppl 3**: p. 1-7.
39. Gewirtz, D.A., *A critical evaluation of the mechanisms of action proposed for the antitumor effects of the anthracycline antibiotics adriamycin and daunorubicin.* Biochem Pharmacol, 1999. **57**(7): p. 727-41.
40. Minotti, G., et al., *Anthracyclines: molecular advances and pharmacologic developments in antitumor activity and cardiotoxicity.* Pharmacol Rev, 2004. **56**(2): p. 185-229.
41. Jordan, M.A., D. Thrower, and L. Wilson, *Mechanism of inhibition of cell proliferation by Vinca alkaloids.* Cancer Res, 1991. **51**(8): p. 2212-22.
42. Himes, R.H., et al., *Action of the vinca alkaloids vincristine, vinblastine, and desacetyl vinblastine amide on microtubules in vitro.* Cancer Res, 1976. **36**(10): p. 3798-802.
43. Snyder, J.P., et al., *The binding conformation of Taxol in beta-tubulin: a model based on electron crystallographic density.* Proc Natl Acad Sci U S A, 2001. **98**(9): p. 5312-6.
44. Morse, D.L., et al., *Docetaxel induces cell death through mitotic catastrophe in human breast cancer cells.* Mol Cancer Ther, 2005. **4**(10): p. 1495-504.
45. Crown, J. and M. O'Leary, *The taxanes: an update.* Lancet, 2000. **355**(9210): p. 1176-8.

46. Rodi, D.J., et al., *Screening of a library of phage-displayed peptides identifies human bcl-2 as a taxol-binding protein.* J Mol Biol, 1999. **285**(1): p. 197-203.
47. Derleth, C. and I.A. Mayer, *Antiangiogenic therapies in early-stage breast cancer.* Clin Breast Cancer, 2010. **10 Suppl 1**: p. E23-31.
48. Ferrara, N., K.J. Hillan, and W. Novotny, *Bevacizumab (Avastin), a humanized anti-VEGF monoclonal antibody for cancer therapy.* Biochem Biophys Res Commun, 2005. **333**(2): p. 328-35.
49. Kim, S., et al., *Clinical response to sunitinib as a multitargeted tyrosine-kinase inhibitor (TKI) in solid cancers: a review of clinical trials.* Onco Targets Ther, 2014. **7**: p. 719-28.
50. Wilhelm, S., et al., *Discovery and development of sorafenib: a multikinase inhibitor for treating cancer.* Nat Rev Drug Discov, 2006. **5**(10): p. 835-44.
51. Jain, R.K., et al., *Lessons from phase III clinical trials on anti-VEGF therapy for cancer.* Nat Clin Pract Oncol, 2006. **3**(1): p. 24-40.
52. Chari, R.V., *Targeted cancer therapy: conferring specificity to cytotoxic drugs.* Acc Chem Res, 2008. **41**(1): p. 98-107.
53. Hudis, C.A., *Trastuzumab--mechanism of action and use in clinical practice.* N Engl J Med, 2007. **357**(1): p. 39-51.
54. Tse, C., et al., *HER2 shedding and serum HER2 extracellular domain: biology and clinical utility in breast cancer.* Cancer Treat Rev, 2012. **38**(2): p. 133-42.
55. Agus, D.B., et al., *Phase I clinical study of pertuzumab, a novel HER dimerization inhibitor, in patients with advanced cancer.* J Clin Oncol, 2005. **23**(11): p. 2534-43.
56. Badache, A. and N.E. Hynes, *A new therapeutic antibody masks ErbB2 to its partners.* Cancer Cell, 2004. **5**(4): p. 299-301.
57. Nahta, R., M.C. Hung, and F.J. Esteva, *The HER-2-targeting antibodies trastuzumab and pertuzumab synergistically inhibit the survival of breast cancer cells.* Cancer Res, 2004. **64**(7): p. 2343-6.
58. Baselga, J., et al., *Phase II trial of pertuzumab and trastuzumab in patients with human epidermal growth factor receptor 2-positive metastatic breast cancer that progressed during prior trastuzumab therapy.* J Clin Oncol, 2010. **28**(7): p. 1138-44.
59. Lewis Phillips, G.D., et al., *Targeting HER2-positive breast cancer with trastuzumab-DM1, an antibody-cytotoxic drug conjugate.* Cancer Res, 2008. **68**(22): p. 9280-90.
60. Burris, H.A., 3rd, et al., *Trastuzumab emtansine (T-DM1): a novel agent for targeting HER2+ breast cancer.* Clin Breast Cancer, 2011. **11**(5): p. 275-82.
61. Junttila, T.T., et al., *Trastuzumab-DM1 (T-DM1) retains all the mechanisms of action of trastuzumab and efficiently inhibits growth of lapatinib insensitive breast cancer.* Breast Cancer Res Treat, 2011. **128**(2): p. 347-56.
62. Welslau, M., et al., *Patient-reported outcomes from EMILIA, a randomized phase 3 study of trastuzumab emtansine (T-DM1) versus capecitabine and lapatinib in human epidermal growth factor receptor 2-positive locally advanced or metastatic breast cancer.* Cancer, 2014. **120**(5): p. 642-51.
63. Krop, I.E., et al., *Trastuzumab emtansine versus treatment of physician's choice for pretreated HER2-positive advanced breast cancer (TH3RESA): a randomised, open-label, phase 3 trial.* Lancet Oncol, 2014. **15**(7): p. 689-99.
64. Moy, B. and P.E. Goss, *Lapatinib: current status and future directions in breast cancer.* Oncologist, 2006. **11**(10): p. 1047-57.
65. Untch, M. and H.J. Luck, *Lapatinib - Member of a New Generation of ErbB-Targeting Drugs.* Breast Care (Basel), 2010. **5**(s1): p. 8-12.
66. Geuna, E., et al., *Potential of afatinib in the treatment of patients with HER2-positive breast cancer.* Breast Cancer (Dove Med Press), 2012. **4**: p. 131-7.
67. Cortés, J., et al., *Abstract P5-19-07: Randomized Phase II trial of afatinib alone or with vinorelbine versus investigator's choice of treatment in patients with HER2-positive breast cancer with progressive brain metastases after trastuzumab and/or lapatinib-*

based therapy: LUX-Breast 3. Cancer Research, 2015. **75**(9 Supplement): p. P5-19-07-P5-19-07.

68. Rimawi, M.F., et al., *A Neoadjuvant, Randomized, Open-Label Phase II Trial of Afatinib Versus Trastuzumab Versus Lapatinib in Patients With Locally Advanced HER2-Positive Breast Cancer.* Clin Breast Cancer, 2014.
69. Chan, A., et al. *Neratinib after adjuvant chemotherapy and trastuzumab in HER2-positive early breast cancer: Primary analysis at 2 years of a phase 3, randomized, placebo-controlled trial (ExteNET).* in *ASCO Annual Meeting Proceedings*. 2015.
70. Saura, C., et al., *Safety and efficacy of neratinib in combination with capecitabine in patients with metastatic human epidermal growth factor receptor 2-positive breast cancer.* J Clin Oncol, 2014. **32**(32): p. 3626-33.
71. Bose, P. and H. Ozer, *Neratinib: an oral, irreversible dual EGFR/HER2 inhibitor for breast and non-small cell lung cancer.* Expert Opin Investig Drugs, 2009. **18**(11): p. 1735-51.
72. Burstein, H.J., et al., *Neratinib, an irreversible ErbB receptor tyrosine kinase inhibitor, in patients with advanced ErbB2-positive breast cancer.* J Clin Oncol, 2010. **28**(8): p. 1301-7.
73. Awada, A., et al., *Safety and efficacy of neratinib (HKI-272) plus vinorelbine in the treatment of patients with ErbB2-positive metastatic breast cancer pretreated with anti-HER2 therapy.* Annals of oncology, 2013. **24**(1): p. 109-116.
74. Syed, B.A., *The breast cancer market.* Nat Rev Drug Discov, 2015. **14**(4): p. 233-4.
75. Trock, B.J., F. Leonessa, and R. Clarke, *Multidrug resistance in breast cancer: a meta-analysis of MDR1/gp170 expression and its possible functional significance.* J Natl Cancer Inst, 1997. **89**(13): p. 917-31.
76. Gottesman, M.M., *Mechanisms of cancer drug resistance.* Annu Rev Med, 2002. **53**: p. 615-27.
77. Fletcher, J.I., et al., *ABC transporters in cancer: more than just drug efflux pumps.* Nat Rev Cancer, 2010. **10**(2): p. 147-56.
78. Mechetner, E., et al., *Levels of multidrug resistance (MDR1) P-glycoprotein expression by human breast cancer correlate with in vitro resistance to taxol and doxorubicin.* Clin Cancer Res, 1998. **4**(2): p. 389-98.
79. Volk, E.L., et al., *Methotrexate cross-resistance in a mitoxantrone-selected multidrug-resistant MCF7 breast cancer cell line is attributable to enhanced energy-dependent drug efflux.* Cancer Res, 2000. **60**(13): p. 3514-21.
80. Doyle, L. and D.D. Ross, *Multidrug resistance mediated by the breast cancer resistance protein BCRP (ABCG2).* Oncogene, 2003. **22**(47): p. 7340-58.
81. AbuHammad, S. and M. Zihlif, *Gene expression alterations in doxorubicin resistant MCF7 breast cancer cell line.* Genomics, 2013. **101**(4): p. 213-20.
82. Yao, D., et al., *Detoxication of vinca alkaloids by human P450 CYP3A4-mediated metabolism: implications for the development of drug resistance.* J Pharmacol Exp Ther, 2000. **294**(1): p. 387-95.
83. Harbottle, A., et al., *Role of glutathione S-transferase P1, P-glycoprotein and multidrug resistance-associated protein 1 in acquired doxorubicin resistance.* Int J Cancer, 2001. **92**(6): p. 777-83.
84. Holohan, C., et al., *Cancer drug resistance: an evolving paradigm.* Nat Rev Cancer, 2013. **13**(10): p. 714-26.
85. Corcoran, C., et al., *miR-630 targets IGF1R to regulate response to HER-targeting drugs and overall cancer cell progression in HER2 over-expressing breast cancer.* Mol Cancer, 2014. **13**: p. 71.
86. Nagy, P., et al., *Decreased accessibility and lack of activation of ErbB2 in JIMT-1, a herceptin-resistant, MUC4-expressing breast cancer cell line.* Cancer Res, 2005. **65**(2): p. 473-82.

87. Rodrigues, A.S., et al., *DNA repair and resistance to cancer therapy.* New Research Directions in DNA Repair, InTech, Rijeka, 2013: p. 489-528.
88. Fisher, A.E., et al., *Poly(ADP-ribose) polymerase 1 accelerates single-strand break repair in concert with poly(ADP-ribose) glycohydrolase.* Mol Cell Biol, 2007. **27**(15): p. 5597-605.
89. Pierceall, W.E., et al., *Cisplatin benefit is predicted by immunohistochemical analysis of DNA repair proteins in squamous cell carcinoma but not adenocarcinoma: theranostic modeling by NSCLC constituent histological subclasses.* Ann Oncol, 2012. **23**(9): p. 2245-52.
90. Ravizza, R., et al., *Role of the p53/p21 system in the response of human colon carcinoma cells to Doxorubicin.* BMC Cancer, 2004. **4**: p. 92.
91. Fulda, S. and K.M. Debatin, *Extrinsic versus intrinsic apoptosis pathways in anticancer chemotherapy.* Oncogene, 2006. **25**(34): p. 4798-811.
92. Debatin, K.M. and P.H. Krammer, *Death receptors in chemotherapy and cancer.* Oncogene, 2004. **23**(16): p. 2950-66.
93. De Luca, A., et al., *Src and CXCR4 are involved in the invasiveness of breast cancer cells with acquired resistance to lapatinib.* Cell Cycle, 2014. **13**(1): p. 148-56.
94. Wang, Y.C., et al., *Different mechanisms for resistance to trastuzumab versus lapatinib in HER2-positive breast cancers - role of estrogen receptor and HER2 reactivation.* Breast Cancer Research, 2011. **13**(6).
95. Ceballos-Cancino, G., et al., *Regulation of mitochondrial Smac/DIABLO-selective release by survivin.* Oncogene, 2007. **26**(54): p. 7569-7575.
96. McCubrey, J.A., et al., *Roles of the Raf/MEK/ERK pathway in cell growth, malignant transformation and drug resistance.* Biochim Biophys Acta, 2007. **1773**(8): p. 1263-84.
97. Courtney, K.D., R.B. Corcoran, and J.A. Engelman, *The PI3K pathway as drug target in human cancer.* J Clin Oncol, 2010. **28**(6): p. 1075-83.
98. Du, C., et al., *MTDH mediates trastuzumab resistance in HER2 positive breast cancer by decreasing PTEN expression through an NFkappaB-dependent pathway.* BMC Cancer, 2014. **14**: p. 869.
99. Lee, Y.Y., et al., *Phosphoproteomic analysis identifies activated MET-axis PI3K/AKT and MAPK/ERK in lapatinib-resistant cancer cell line.* Exp Mol Med, 2013. **45**: p. e64.
100. Gerlinger, M., et al., *Intratumor heterogeneity and branched evolution revealed by multiregion sequencing.* N Engl J Med, 2012. **366**(10): p. 883-92.
101. Dean, M., T. Fojo, and S. Bates, *Tumour stem cells and drug resistance.* Nat Rev Cancer, 2005. **5**(4): p. 275-84.
102. Colombo, M., G. Raposo, and C. Thery, *Biogenesis, secretion, and intercellular interactions of exosomes and other extracellular vesicles.* Annu Rev Cell Dev Biol, 2014. **30**: p. 255-89.
103. Cocucci, E., G. Racchetti, and J. Meldolesi, *Shedding microvesicles: artefacts no more.* Trends Cell Biol, 2009. **19**(2): p. 43-51.
104. de Jong, O.G., et al., *Cellular stress conditions are reflected in the protein and RNA content of endothelial cell-derived exosomes.* J Extracell Vesicles, 2012. **1**.
105. Parolini, I., et al., *Microenvironmental pH is a key factor for exosome traffic in tumor cells.* J Biol Chem, 2009. **284**(49): p. 34211-22.
106. Urbanelli, L., et al., *Signaling pathways in exosomes biogenesis, secretion and fate.* Genes (Basel), 2013. **4**(2): p. 152-70.
107. Camussi, G., et al., *Exosomes/microvesicles as a mechanism of cell-to-cell communication.* Kidney Int, 2010. **78**(9): p. 838-48.
108. Walker, J.D., C.L. Maier, and J.S. Pober, *Cytomegalovirus-infected human endothelial cells can stimulate allogeneic CD4+ memory T cells by releasing antigenic exosomes.* J Immunol, 2009. **182**(3): p. 1548-59.

109. Janowska-Wieczorek, A., et al., *Microvesicles derived from activated platelets induce metastasis and angiogenesis in lung cancer.* Int J Cancer, 2005. **113**(5): p. 752-60.
110. Harris, D.A., et al., *Exosomes released from breast cancer carcinomas stimulate cell movement.* PLoS One, 2015. **10**(3): p. e0117495.
111. O'Brien, K., et al., *Exosomes from triple-negative breast cancer cells can transfer phenotypic traits representing their cells of origin to secondary cells.* Eur J Cancer, 2013. **49**(8): p. 1845-59.
112. Singh, R., et al., *Exosome-mediated transfer of miR-10b promotes cell invasion in breast cancer.* Mol Cancer, 2014. **13**: p. 256.
113. Ciravolo, V., et al., *Potential role of HER2-overexpressing exosomes in countering trastuzumab-based therapy.* J Cell Physiol, 2012. **227**(2): p. 658-67.
114. Kim, H.K., et al., *Elevated levels of circulating platelet microparticles, VEGF, IL-6 and RANTES in patients with gastric cancer: possible role of a metastasis predictor.* Eur J Cancer, 2003. **39**(2): p. 184-91.
115. Nilsson, J., et al., *Prostate cancer-derived urine exosomes: a novel approach to biomarkers for prostate cancer.* Br J Cancer, 2009. **100**(10): p. 1603-7.
116. Skog, J., et al., *Glioblastoma microvesicles transport RNA and proteins that promote tumour growth and provide diagnostic biomarkers.* Nat Cell Biol, 2008. **10**(12): p. 1470-6.
117. Taylor, D.D. and C. Gercel-Taylor, *MicroRNA signatures of tumor-derived exosomes as diagnostic biomarkers of ovarian cancer.* Gynecol Oncol, 2008. **110**(1): p. 13-21.
118. Bissell, M.J., A. Rizki, and I.S. Mian, *Tissue architecture: the ultimate regulator of breast epithelial function.* Curr Opin Cell Biol, 2003. **15**(6): p. 753-62.
119. Weaver, V.M., et al., *Reversion of the malignant phenotype of human breast cells in three-dimensional culture and in vivo by integrin blocking antibodies.* J Cell Biol, 1997. **137**(1): p. 231-45.
120. Hait, W.N., *Anticancer drug development: the grand challenges.* Nat Rev Drug Discov, 2010. **9**(4): p. 253-4.
121. Hopkins, A.L., *Network pharmacology: the next paradigm in drug discovery.* Nat Chem Biol, 2008. **4**(11): p. 682-90.
122. Kola, I., *The state of innovation in drug development.* Clin Pharmacol Ther, 2008. **83**(2): p. 227-30.
123. DiMasi, J.A. and H.G. Grabowski, *Economics of new oncology drug development.* J Clin Oncol, 2007. **25**(2): p. 209-16.
124. Mazzoleni, G., D. Di Lorenzo, and N. Steimberg, *Modelling tissues in 3D: the next future of pharmaco-toxicology and food research?* Genes Nutr, 2009. **4**(1): p. 13-22.
125. Kunz-Schughart, L.A., et al., *The use of 3-D cultures for high-throughput screening: the multicellular spheroid model.* J Biomol Screen, 2004. **9**(4): p. 273-85.
126. Bhadriraju, K. and C.S. Chen, *Engineering cellular microenvironments to improve cell-based drug testing.* Drug Discov Today, 2002. **7**(11): p. 612-20.
127. Abbott, A., *Cell culture: biology's new dimension.* Nature, 2003. **424**(6951): p. 870-2.
128. Debnath, J. and J.S. Brugge, *Modelling glandular epithelial cancers in three-dimensional cultures.* Nat Rev Cancer, 2005. **5**(9): p. 675-88.
129. Yamada, K.M. and E. Cukierman, *Modeling tissue morphogenesis and cancer in 3D.* Cell, 2007. **130**(4): p. 601-10.
130. Harrison, R.G., et al., *Observations of the living developing nerve fiber.* The Anatomical Record, 1907. **1**(5): p. 116-128.
131. Harrison, R.G., *The outgrowth of the nerve fiber as a mode of protoplasmic movement.* J Exp Zool, 1959. **142**: p. 5-73.
132. Bissell, M.J., et al., *The organizing principle: microenvironmental influences in the normal and malignant breast.* Differentiation, 2002. **70**(9-10): p. 537-46.
133. Lin, R.Z. and H.Y. Chang, *Recent advances in three-dimensional multicellular spheroid culture for biomedical research.* Biotechnol J, 2008. **3**(9-10): p. 1172-84.

134. Ivascu, A. and M. Kubbies, *Rapid generation of single-tumor spheroids for high-throughput cell function and toxicity analysis.* J Biomol Screen, 2006. **11**(8): p. 922-32.
135. Hart, C., *Microplates, Assay Reagents, Screening Consumables, and Kits.* J Biomol Screen, 2014. **19**(8): p. 1227-1230.
136. Friedrich, J., et al., *Spheroid-based drug screen: considerations and practical approach.* Nat Protoc, 2009. **4**(3): p. 309-24.
137. Kelm, J.M., et al., *Method for generation of homogeneous multicellular tumor spheroids applicable to a wide variety of cell types.* Biotechnol Bioeng, 2003. **83**(2): p. 173-80.
138. Anastasov, N., et al., *A 3D-microtissue-based phenotypic screening of radiation resistant tumor cells with synchronized chemotherapeutic treatment.* BMC Cancer, 2015. **15**: p. 466.
139. Bruderer, R., et al., *Extending the limits of quantitative proteome profiling with data-independent acquisition and application to acetaminophen-treated three-dimensional liver microtissues.* Mol Cell Proteomics, 2015. **14**(5): p. 1400-10.
140. Rebelo, S.R.P., *Development of 3D in vitro models for prediction of hepatic metabolism and toxicity.* 2015.
141. Goodwin, T.J., et al., *Reduced shear stress: a major component in the ability of mammalian tissues to form three-dimensional assemblies in simulated microgravity.* J Cell Biochem, 1993. **51**(3): p. 301-11.
142. Zhang, S., et al., *The effects of spheroid formation of adipose-derived stem cells in a microgravity bioreactor on stemness properties and therapeutic potential.* Biomaterials, 2015. **41**: p. 15-25.
143. Alcaraz, J., C.M. Nelson, and M.J. Bissell, *Biomechanical approaches for studying integration of tissue structure and function in mammary epithelia.* J Mammary Gland Biol Neoplasia, 2004. **9**(4): p. 361-74.
144. Chandrasekaran, S., H. Deng, and Y. Fang, *PTEN deletion potentiates invasion of colorectal cancer spheroidal cells through 3D Matrigel.* Integr Biol (Camb), 2015. **7**(3): p. 324-34.
145. Kleinman, H.K. and G.R. Martin, *Matrigel: basement membrane matrix with biological activity.* Semin Cancer Biol, 2005. **15**(5): p. 378-86.
146. Lee, G.Y., et al., *Three-dimensional culture models of normal and malignant breast epithelial cells.* Nat Methods, 2007. **4**(4): p. 359-65.
147. Sourla, A., C. Doillon, and M. Koutsilieris, *Three-dimensional type I collagen gel system containing MG-63 osteoblasts-like cells as a model for studying local bone reaction caused by metastatic cancer cells.* Anticancer Res, 1996. **16**(5a): p. 2773-80.
148. Glicklis, R., et al., *Hepatocyte behavior within three-dimensional porous alginate scaffolds.* Biotechnol Bioeng, 2000. **67**(3): p. 344-53.
149. Tan, W., R. Krishnaraj, and T.A. Desai, *Evaluation of nanostructured composite collagen--chitosan matrices for tissue engineering.* Tissue Eng, 2001. **7**(2): p. 203-10.
150. Justice, B.A., N.A. Badr, and R.A. Felder, *3D cell culture opens new dimensions in cell-based assays.* Drug Discov Today, 2009. **14**(1-2): p. 102-7.
151. Schmidt, J.J., J. Rowley, and H.J. Kong, *Hydrogels used for cell-based drug delivery.* J Biomed Mater Res A, 2008. **87**(4): p. 1113-22.
152. Ji, C., A. Khademhosseini, and F. Dehghani, *Enhancing cell penetration and proliferation in chitosan hydrogels for tissue engineering applications.* Biomaterials, 2011. **32**(36): p. 9719-29.
153. Benson, K., H.J. Galla, and N.S. Kehr, *Cell adhesion behavior in 3D hydrogel scaffolds functionalized with D- or L-aminoacids.* Macromol Biosci, 2014. **14**(6): p. 793-8.
154. Toh, Y.C., et al., *A novel 3D mammalian cell perfusion-culture system in microfluidic channels.* Lab Chip, 2007. **7**(3): p. 302-9.

155. Lei, K.F., et al., *Real-time and non-invasive impedimetric monitoring of cell proliferation and chemosensitivity in a perfusion 3D cell culture microfluidic chip.* Biosens Bioelectron, 2014. **51**: p. 16-21.
156. Pickl, M. and C.H. Ries, *Comparison of 3D and 2D tumor models reveals enhanced HER2 activation in 3D associated with an increased response to trastuzumab.* Oncogene, 2009. **28**(3): p. 461-8.
157. Tung, Y.C., et al., *High-throughput 3D spheroid culture and drug testing using a 384 hanging drop array.* Analyst, 2011. **136**(3): p. 473-8.
158. Wilson, W.R. and M.P. Hay, *Targeting hypoxia in cancer therapy.* Nat Rev Cancer, 2011. **11**(6): p. 393-410.
159. Vaupel, P. and A. Mayer, *Hypoxia and anemia: effects on tumor biology and treatment resistance.* Transfus Clin Biol, 2005. **12**(1): p. 5-10.
160. Weaver, V.M., et al., *beta4 integrin-dependent formation of polarized three-dimensional architecture confers resistance to apoptosis in normal and malignant mammary epithelium.* Cancer Cell, 2002. **2**(3): p. 205-16.
161. Li, Q., A.B. Chow, and R.R. Mattingly, *Three-dimensional overlay culture models of human breast cancer reveal a critical sensitivity to mitogen-activated protein kinase kinase inhibitors.* J Pharmacol Exp Ther, 2010. **332**(3): p. 821-8.
162. David, L., et al., *Hyaluronan hydrogel: an appropriate three-dimensional model for evaluation of anticancer drug sensitivity.* Acta Biomater, 2008. **4**(2): p. 256-63.
163. Dhiman, H.K., A.R. Ray, and A.K. Panda, *Three-dimensional chitosan scaffold-based MCF-7 cell culture for the determination of the cytotoxicity of tamoxifen.* Biomaterials, 2005. **26**(9): p. 979-86.
164. Thurber, G.M. and K.D. Wittrup, *Quantitative spatiotemporal analysis of antibody fragment diffusion and endocytic consumption in tumor spheroids.* Cancer Res, 2008. **68**(9): p. 3334-41.
165. Lee, J., et al., *Engineering liver tissue spheroids with inverted colloidal crystal scaffolds.* Biomaterials, 2009. **30**(27): p. 4687-94.
166. Bose, P. and H. Ozer, *Neratinib: an oral, irreversible dual EGFR/HER2 inhibitor for breast and non-small cell lung cancer.* Expert opinion on investigational drugs, 2009. **18**(11): p. 1735-1751.
167. Wissner, A. and T.S. Mansour, *The Development of HKI-272 and Related Compounds for the Treatment of Cancer.* Archiv der Pharmazie, 2008. **341**(8): p. 465-477.
168. Wong, K.K., et al., *A phase I study with neratinib (HKI-272), an irreversible pan ErbB receptor tyrosine kinase inhibitor, in patients with solid tumors.* Clin Cancer Res, 2009. **15**(7): p. 2552-8.
169. Burstein, H.J., et al., *Neratinib, an Irreversible ErbB Receptor Tyrosine Kinase Inhibitor, in Patients With Advanced ErbB2-Positive Breast Cancer.* Journal of Clinical Oncology, 2010. **28**(8): p. 1301-1307.
170. Swaby, R., et al., *Neratinib in combination with trastuzumab for the treatment of advanced breast cancer: a phase I/II study.* J Clin Oncol, 2009. **27**(15 suppl): p. 1004.
171. Awada, A., et al., *Safety and efficacy of neratinib (HKI-272) plus vinorelbine in the treatment of patients with ErbB2-positive metastatic breast cancer pretreated with anti-HER2 therapy.* Ann Oncol, 2013. **24**(1): p. 109-16.
172. Jankowitz, R.C., et al., *Safety and efficacy of neratinib in combination with weekly paclitaxel and trastuzumab in women with metastatic HER2positive breast cancer: an NSABP Foundation Research Program phase I study.* Cancer Chemother Pharmacol, 2013. **72**(6): p. 1205-12.
173. Martin, M., et al., *A phase two randomised trial of neratinib monotherapy versus lapatinib plus capecitabine combination therapy in patients with HER2+ advanced breast cancer.* Eur J Cancer, 2013. **49**(18): p. 3763-72.

174. Chakraborty, A.K., C. Zerillo, and M.P. DiGiovanna, *In vitro and in vivo studies of the combination of IGF1R inhibitor figitumumab (CP-751,871) with HER2 inhibitors trastuzumab and neratinib.* Breast Cancer Res Treat, 2015. **152**(3): p. 533-44.
175. Seyhan, A.A., et al., *A genome-wide RNAi screen identifies novel targets of neratinib resistance leading to identification of potential drug resistant genetic markers.* Mol Biosyst, 2012. **8**(5): p. 1553-70.
176. Konecny, G.E., et al., *Activity of the dual kinase inhibitor lapatinib (GW572016) against HER-2-overexpressing and trastuzumab-treated breast cancer cells.* Cancer Research, 2006. **66**(3): p. 1630-1639.
177. O'Driscoll, L., et al., *Galectin-3 expression alters adhesion, motility and invasion in a lung cell line (DLKP), in vitro.* Anticancer Res, 2002. **22**(6a): p. 3117-25.
178. Corcoran, C., et al., *Docetaxel-resistance in prostate cancer: evaluating associated phenotypic changes and potential for resistance transfer via exosomes.* PLoS One, 2012. **7**(12): p. e50999.
179. Fichter, C.D., et al., *EGFR, HER2 and HER3 dimerization patterns guide targeted inhibition in two histotypes of esophageal cancer.* International Journal of Cancer, 2014. **135**(7): p. 1517-1530.
180. Wang, Q., et al., *RON confers lapatinib resistance in HER2-positive breast cancer cells.* Cancer Lett, 2013. **340**(1): p. 43-50.
181. Ryan, Q., et al., *FDA drug approval summary: lapatinib in combination with capecitabine for previously treated metastatic breast cancer that overexpresses HER-2.* Oncologist, 2008. **13**(10): p. 1114-9.
182. Nahta, R., et al., *Lapatinib induces apoptosis in trastuzumab-resistant breast cancer cells: effects on insulin-like growth factor I signaling.* Molecular Cancer Therapeutics, 2007. **6**(2): p. 667-674.
183. Yang, S., J.J. Zhang, and X.Y. Huang, *Orai1 and STIM1 are critical for breast tumor cell migration and metastasis.* Cancer Cell, 2009. **15**(2): p. 124-34.
184. Hulkower, K.I. and R.L. Herber, *Cell migration and invasion assays as tools for drug discovery.* Pharmaceutics, 2011. **3**(1): p. 107-24.
185. Taddei, M.L., et al., *Anoikis: an emerging hallmark in health and diseases.* J Pathol, 2012. **226**(2): p. 380-93.
186. Kim, Y.N., et al., *Anoikis resistance: an essential prerequisite for tumor metastasis.* Int J Cell Biol, 2012. **2012**: p. 306879.
187. Formisano, L., et al., *Epidermal growth factor-receptor activation modulates Src-dependent resistance to lapatinib in breast cancer models.* Breast Cancer Res, 2014. **16**(3): p. R45.
188. La Monica, S., et al., *Gefitinib inhibits invasive phenotype and epithelial-mesenchymal transition in drug-resistant NSCLC cells with MET amplification.* PLoS One, 2013. **8**(10): p. e78656.
189. McDermott, M.S., et al., *PP2A inhibition overcomes acquired resistance to HER2 targeted therapy.* Mol Cancer, 2014. **13**: p. 157.
190. Brown, B., *The role of receptor tyrosine kinase signalling in HER-2-positive cells and trastuzumab (Herceptin) resistance in breast cancer.* PhD thesis, Dublin City University., 2009.
191. Azuma, K., et al., *FGFR1 activation is an escape mechanism in human lung cancer cells resistant to afatinib, a pan-EGFR family kinase inhibitor.* Oncotarget, 2014. **5**(15): p. 5908-19.
192. Debenham, P.G., et al., *DNA-mediated transfer of multiple drug resistance and plasma membrane glycoprotein expression.* Mol Cell Biol, 1982. **2**(8): p. 881-9.
193. Calatozzolo, C., et al., *Expression of drug resistance proteins Pgp, MRP1, MRP3, MRP5 and GST-pi in human glioma.* J Neurooncol, 2005. **74**(2): p. 113-21.
194. Ross, D.D., *Novel mechanisms of drug resistance in leukemia.* Leukemia, 2000. **14**(3): p. 467-73.

195. Germano, S. and L. O'Driscoll, *Breast cancer: understanding sensitivity and resistance to chemotherapy and targeted therapies to aid in personalised medicine.* Curr Cancer Drug Targets, 2009. **9**(3): p. 398-418.
196. Zhao, X.Q., et al., *Neratinib reverses ATP-binding cassette B1-mediated chemotherapeutic drug resistance in vitro, in vivo, and ex vivo.* Mol Pharmacol, 2012. **82**(1): p. 47-58.
197. Dai, C.L., et al., *Lapatinib (Tykerb, GW572016) reverses multidrug resistance in cancer cells by inhibiting the activity of ATP-binding cassette subfamily B member 1 and G member 2.* Cancer Res, 2008. **68**(19): p. 7905-14.
198. Bartel, D.P., *MicroRNAs: genomics, biogenesis, mechanism, and function.* Cell, 2004. **116**(2): p. 281-97.
199. Roth, C., et al., *Circulating microRNAs as blood-based markers for patients with primary and metastatic breast cancer.* Breast Cancer Res, 2010. **12**(6): p. R90.
200. van Schooneveld, E., et al., *Expression profiling of cancerous and normal breast tissues identifies microRNAs that are differentially expressed in serum from patients with (metastatic) breast cancer and healthy volunteers.* Breast Cancer Res, 2012. **14**(1): p. R34.
201. Corcoran, C., et al., *Intracellular and extracellular microRNAs in breast cancer.* Clin Chem, 2011. **57**(1): p. 18-32.
202. Yu, S.L., et al., *MicroRNA signature predicts survival and relapse in lung cancer.* Cancer Cell, 2008. **13**(1): p. 48-57.
203. Dvinge, H., et al., *The shaping and functional consequences of the microRNA landscape in breast cancer.* Nature, 2013. **497**(7449): p. 378-82.
204. Schwarzenbach, H., et al., *Clinical relevance of circulating cell-free microRNAs in cancer.* Nat Rev Clin Oncol, 2014. **11**(3): p. 145-56.
205. Jung, E.J., et al., *Plasma microRNA 210 levels correlate with sensitivity to trastuzumab and tumor presence in breast cancer patients.* Cancer, 2012. **118**(10): p. 2603-14.
206. Hong, L., et al., *High expression of miR-210 predicts poor survival in patients with breast cancer: a meta-analysis.* Gene, 2012. **507**(2): p. 135-8.
207. Xu, X.D., et al., *Warburg effect or reverse Warburg effect? A review of cancer metabolism.* Oncol Res Treat, 2015. **38**(3): p. 117-22.
208. Zhou, Y., et al., *Intracellular ATP levels are a pivotal determinant of chemoresistance in colon cancer cells.* Cancer Res, 2012. **72**(1): p. 304-14.
209. Rani, S., et al., *Neuromedin U: a candidate biomarker and therapeutic target to predict and overcome resistance to HER-tyrosine kinase inhibitors.* Cancer Res, 2014. **74**(14): p. 3821-33.
210. Guengerich, F.P., *Cytochrome P-450 3A4: regulation and role in drug metabolism.* Annu Rev Pharmacol Toxicol, 1999. **39**: p. 1-17.
211. Abbas, R., et al., *Pharmacokinetics of oral neratinib during co-administration of ketoconazole in healthy subjects.* Br J Clin Pharmacol, 2011. **71**(4): p. 522-7.
212. Dresser, G.K., J.D. Spence, and D.G. Bailey, *Pharmacokinetic-pharmacodynamic consequences and clinical relevance of cytochrome P450 3A4 inhibition.* Clin Pharmacokinet, 2000. **38**(1): p. 41-57.
213. Kapucuoglu, N., et al., *Expression of CYP3A4 in human breast tumour and non-tumour tissues.* Cancer Lett, 2003. **202**(1): p. 17-23.
214. Piccart-Gebhart, M.J., et al., *Trastuzumab after adjuvant chemotherapy in HER2-positive breast cancer.* N Engl J Med, 2005. **353**(16): p. 1659-72.
215. Kudchadkar, R., K.H. Paraiso, and K.S. Smalley, *Targeting mutant BRAF in melanoma: current status and future development of combination therapy strategies.* Cancer J, 2012. **18**(2): p. 124-31.
216. van 't Veer, L.J., et al., *Gene expression profiling predicts clinical outcome of breast cancer.* Nature, 2002. **415**(6871): p. 530-6.

217. van de Vijver, M.J., et al., *A gene-expression signature as a predictor of survival in breast cancer.* N Engl J Med, 2002. **347**(25): p. 1999-2009.
218. Cronin, M., et al., *Analytical validation of the Oncotype DX genomic diagnostic test for recurrence prognosis and therapeutic response prediction in node-negative, estrogen receptor-positive breast cancer.* Clin Chem, 2007. **53**(6): p. 1084-91.
219. Crown, J., et al., *Abstract P4-12-25: Randomized phase II study of pre-operative docetaxel, carboplatin with trastuzumab (TCH) and/or/lapatinib (L) in HER-2 positive (H+) breast cancer patients (BC pts). ICORG 10-05.* Cancer Research, 2013. **73**(24 Supplement): p. P4-12-25.
220. Bhargava, R., et al., *Semiquantitative hormone receptor level influences response to trastuzumab-containing neoadjuvant chemotherapy in HER2-positive breast cancer.* Mod Pathol, 2011. **24**(3): p. 367-74.
221. Komarova, N.L. and C.R. Boland, *Cancer: calculated treatment.* Nature, 2013. **499**(7458): p. 291-2.
222. Bozic, I., et al., *Evolutionary dynamics of cancer in response to targeted combination therapy.* Elife, 2013. **2**: p. e00747.
223. van der Pol, E., et al., *Classification, functions, and clinical relevance of extracellular vesicles.* Pharmacol Rev, 2012. **64**(3): p. 676-705.
224. Lotvall, J., et al., *Minimal experimental requirements for definition of extracellular vesicles and their functions: a position statement from the International Society for Extracellular Vesicles.* J Extracell Vesicles, 2014. **3**: p. 26913.
225. Melo, S.A., et al., *Glypican-1 identifies cancer exosomes and detects early pancreatic cancer.* Nature, 2015. **523**(7559): p. 177-82.
226. Esteva, F.J., et al., *Clinical utility of serum HER2/neu in monitoring and prediction of progression-free survival in metastatic breast cancer patients treated with trastuzumab-based therapies.* Breast Cancer Res, 2005. **7**(4): p. R436-43.
227. Ketterer, K., et al., *Neuromedin U is overexpressed in pancreatic cancer and increases invasiveness via the hepatocyte growth factor c-Met pathway.* Cancer Lett, 2009. **277**(1): p. 72-81.
228. Alevizos, I., et al., *Oral cancer in vivo gene expression profiling assisted by laser capture microdissection and microarray analysis.* Oncogene, 2001. **20**(43): p. 6196-204.
229. Yamashita, K., et al., *Pharmacologic unmasking of epigenetically silenced tumor suppressor genes in esophageal squamous cell carcinoma.* Cancer Cell, 2002. **2**(6): p. 485-95.
230. Lv, Y.G., et al., *The role of survivin in diagnosis, prognosis and treatment of breast cancer.* J Thorac Dis, 2010. **2**(2): p. 100-10.
231. Jha, K., M. Shukla, and M. Pandey, *Survivin expression and targeting in breast cancer.* Surg Oncol, 2012. **21**(2): p. 125-31.
232. Kennedy, S.M., et al., *Prognostic importance of survivin in breast cancer.* Br J Cancer, 2003. **88**(7): p. 1077-83.
233. Ryan, B.M., et al., *Survivin expression in breast cancer predicts clinical outcome and is associated with HER2, VEGF, urokinase plasminogen activator and PAI-1.* Ann Oncol, 2006. **17**(4): p. 597-604.
234. Miska, E.A., *How microRNAs control cell division, differentiation and death.* Curr Opin Genet Dev, 2005. **15**(5): p. 563-8.
235. Mei, Y., et al., *Effect of microRNA-210 on prognosis and response to chemotherapeutic drugs in pediatric acute lymphoblastic leukemia.* Cancer Sci, 2014. **105**(4): p. 463-72.
236. Wilkening, S., F. Stahl, and A. Bader, *Comparison of primary human hepatocytes and hepatoma cell line Hepg2 with regard to their biotransformation properties.* Drug Metab Dispos, 2003. **31**(8): p. 1035-42.

237. Larson, B., et al., *The Effect of Cell Culture Method on Long-Term Primary Hepatocyte Cell Health.* 2014.
238. Ramaiahgari, S.C., et al., *A 3D in vitro model of differentiated HepG2 cell spheroids with improved liver-like properties for repeated dose high-throughput toxicity studies.* Arch Toxicol, 2014. **88**(5): p. 1083-95.
239. Rani, S., et al., *Isolation of exosomes for subsequent mRNA, MicroRNA, and protein profiling.* Methods Mol Biol, 2011. **784**: p. 181-95.
240. Sahin, O., et al., *Modeling ERBB receptor-regulated G1/S transition to find novel targets for de novo trastuzumab resistance.* BMC Syst Biol, 2009. **3**: p. 1.
241. Ivascu, A. and M. Kubbies, *Diversity of cell-mediated adhesions in breast cancer spheroids.* Int J Oncol, 2007. **31**(6): p. 1403-13.
242. Yao, E., et al., *Suppression of HER2/HER3-mediated growth of breast cancer cells with combinations of GDC-0941 PI3K inhibitor, trastuzumab, and pertuzumab.* Clin Cancer Res, 2009. **15**(12): p. 4147-56.
243. Konishi, H., et al., *PEGylated liposome IHL-305 markedly improved the survival of ovarian cancer peritoneal metastasis in mouse.* BMC Cancer, 2012. **12**: p. 462.
244. Luca, A.C., et al., *Impact of the 3D microenvironment on phenotype, gene expression, and EGFR inhibition of colorectal cancer cell lines.* PLoS One, 2013. **8**(3): p. e59689.
245. Fong, E.L., et al., *Modeling Ewing sarcoma tumors in vitro with 3D scaffolds.* Proc Natl Acad Sci U S A, 2013. **110**(16): p. 6500-5.
246. Weigelt, B., et al., *HER2 signaling pathway activation and response of breast cancer cells to HER2-targeting agents is dependent strongly on the 3D microenvironment.* Breast Cancer Res Treat, 2010. **122**(1): p. 35-43.
247. Hua, Y., et al., *Slow down to stay alive: HER4 protects against cellular stress and confers chemoresistance in neuroblastoma.* Cancer, 2012. **118**(20): p. 5140-54.
248. Doherty, J.K., et al., *The HER-2/neu receptor tyrosine kinase gene encodes a secreted autoinhibitor.* Proc Natl Acad Sci U S A, 1999. **96**(19): p. 10869-74.
249. Azios, N.G., et al., *Expression of herstatin, an autoinhibitor of HER-2/neu, inhibits transactivation of HER-3 by HER-2 and blocks EGF activation of the EGF receptor.* Oncogene, 2001. **20**(37): p. 5199-209.
250. Doublier, S., et al., *HIF-1 activation induces doxorubicin resistance in MCF7 3-D spheroids via P-glycoprotein expression: a potential model of the chemo-resistance of invasive micropapillary carcinoma of the breast.* BMC Cancer, 2012. **12**: p. 4.
251. Fallica, B., et al., *Alteration of cellular behavior and response to PI3K pathway inhibition by culture in 3D collagen gels.* PLoS One, 2012. **7**(10): p. e48024.
252. Wen, Z., et al., *A spheroid-based 3-D culture model for pancreatic cancer drug testing, using the acid phosphatase assay.* Braz J Med Biol Res, 2013. **46**(7): p. 634-42.
253. Ponce de Leon, V. and R. Barrera-Rodriguez, *Changes in P-glycoprotein activity are mediated by the growth of a tumour cell line as multicellular spheroids.* Cancer Cell Int, 2005. **5**(1): p. 20.
254. Hirth, J., et al., *The effect of an individual's cytochrome CYP3A4 activity on docetaxel clearance.* Clin Cancer Res, 2000. **6**(4): p. 1255-8.
255. Takahashi, Y., et al., *3D spheroid cultures improve the metabolic gene expression profiles of HepaRG cells.* Biosci Rep, 2015. **35**(3).

Appendix I:

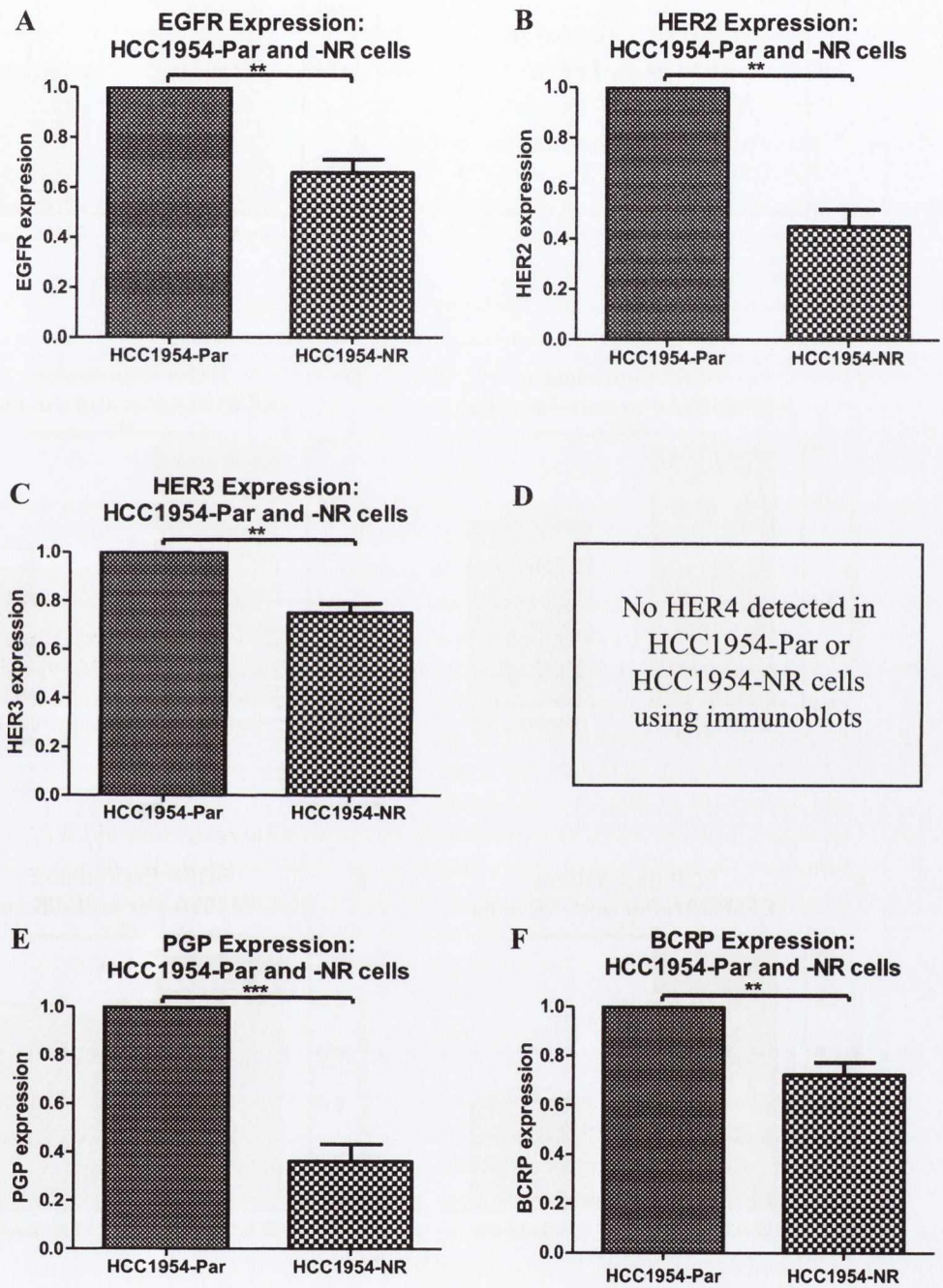

Appendix Figure 1. Densitometry for HCC1954-Par and HCC1954-NR immunoblots displayed in Figure 2.3.5. (A) EGFR; (B) HER2; (C) HER3; (D) HER4; (E) PGP and (F) BCRP.

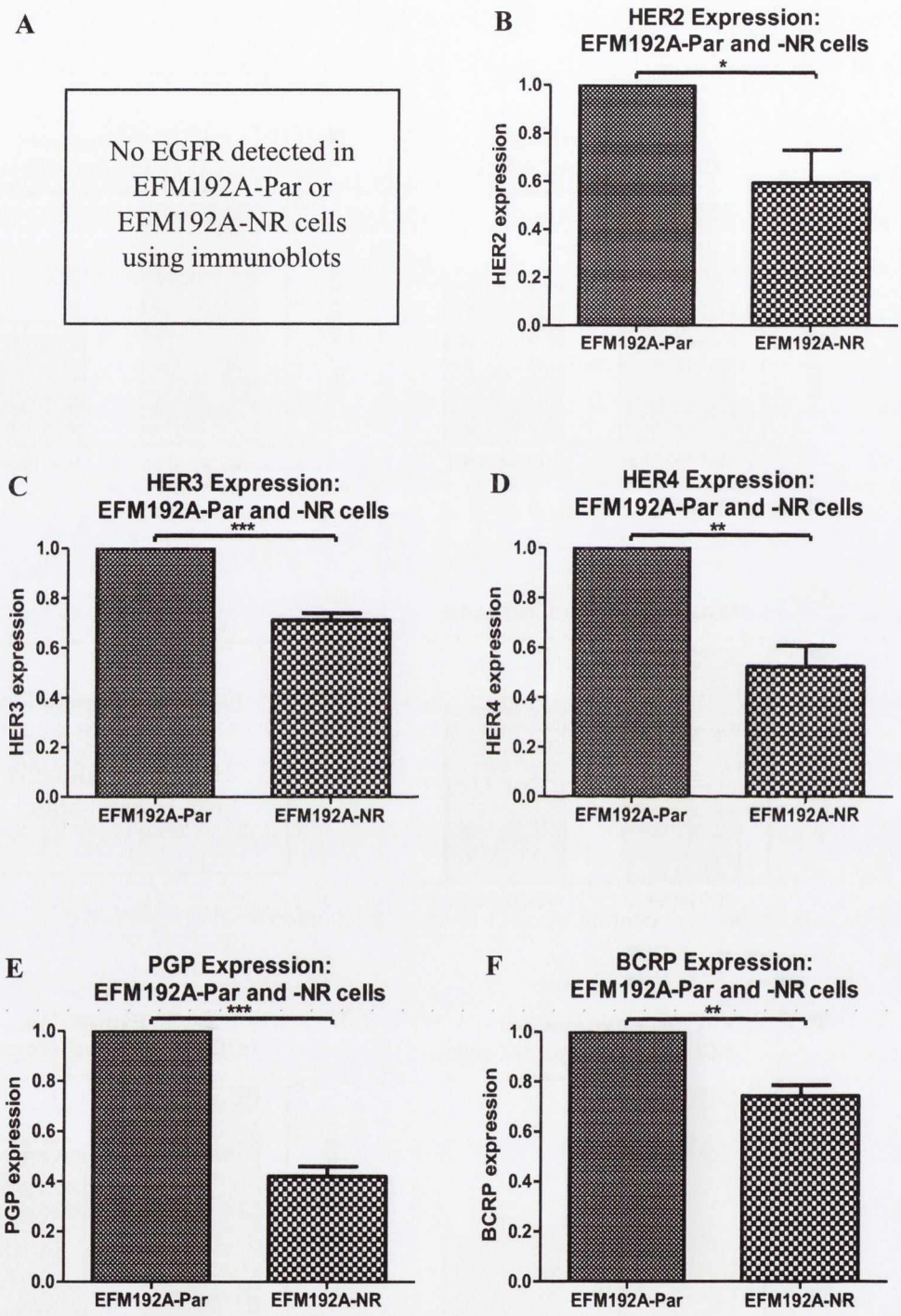

Appendix Figure 2. Densitometry for EFM192A-Par and EFM192A-NR immunoblots displayed in Figure 2.3.5. (A) EGFR; (B) HER2; (C) HER3; (D) HER4; (E) PGP and (F) BCRP.

Appendix II

ICORG instructions for serum specimen collection:

Serum samples were collected prior to commencement of treatment, at the start of each cycle of treatment and at the end of the 6 cycles of chemotherapy treatment.

Supplies required:

- Non-heparinised serum tube
- Cryovials
- Disposable single use pipettes
- Freezer-proof (permanent) marker

Procedure

- Blood specimen was collected (10mL) in labelled non-heparinised serum tube and allowed to clot for 30 minutes to 1 hour at room temperature.
- Centrifuged at 400*g* for 15 minutes at room temperature.
- Pipetted serum (top layer) into four labelled cryovials* (approx 0.5mL per cryovial).
- Specimens frozen immediately at -80°C and store at -80°C, until ready for shipping in batches.
- Shipping was coordinated by ICORG central office.
- *Cryovial tube label included: (a) patient identifier; (b) date.
- *Note:* Serum must be placed at -80°C within 3 hours of procurement.

Appendix III

RNA quantification data:

ICORG 10-05 patients									Healthy controls	
Patient	Pre-treatment	Cycle 2	Cycle 3	Cycle 4	Cycle 5	Cycle 6	Post-treatment	Response	Normal	ng/μL
	ng/μL									
53	20.5	13.4	24.0	22.5	19.6	19.8	23.0	N/A	B09 1592	22.1
9	15.0	N/A	N/A	N/A	N/A	N/A	25.6	CR	B08 0399	17.2
49	18.3	7.1	20.2	23.7	21.1	25.6	12.5	PR	B13 0223	10.7
61	22.1	50.8	16.9	18.4	38.1	24.5	20.5	CR	B14 1613	26.7
3	49.5	27.3	29.2	9.7	18.8	17.0	23.8	PR	B14 1621	9.7
6	13.2	23.0	13.3	29.0	103.6	28.7	27.6	PR	B06-0291	20.1
14	24.6	N/A	N/A	N/A	N/A	N/A	18.8	CR	B11 0262	29.9
7	19.8	22.7	23.4	9.2	38.8	28.1	17.4	PR	B13 0226	11.8
54	24.8	31.1	40.4	21.7	27.6	29.5	21.8	PR	B10 0753	0.0
45	20.5	14.5	15.6	22.8	16.4	15.3	29.5	CR	B14 1615	19.1
50	21.2	30.2	25.4	35.1	22.5	38.2	46.9	CR	B14 1659	13.5
46	10.4	34.6	22.1	14.6	16.8	12.2	33.6	CR	B11 0675	22.3
29	20.8	23.6	15.5	9.1	21.1	11.2	10.2	PR	B09 0667	36.3
84	53.4	101.5	74.1	20.8	55.1	33.1	51.3	PR	B07 1167	17.6
11	101.6	100.6	35.1	53.9	26.0	57.5	88.3	PR	B09 1278	14.5
34	14.5	20.2	8.7	20.8	33.3	18.7	17.6	CR	B09 1234	26.0
59	23.5	24.9	17.4	25.1	15.6	24.0	24.7	CR	B11 0864	5.7
42	12.7	19.2	33.8	19.9	25.8	19.6	50.7	PR	B09 1232	20.3
32	14.8	20.5	20.7	13.1	7.5	15.2	47.0	PR	B13 0262	23.5
18	16.3	38.2	47.8	12.0	29.4	15.4	37.1	PR	B06 0290	18.3
4	17.8	24.8	35.2	27.7	55.7	18.8	39.9	PR	B09 1276	22.1
26	12.8	16.1	18.6	18.1	21.9	15.9	13.6	CR	B10 0756	29.4
66	23.1	24.1	20.0	20.8	37.5	22.4	15.1	CR	B09 1275	29.0
15	16.2	13.8	30.1	20.2	18.8	47.9	19.6	CR	B14 2019	10.7
82	11.5	29.2	22.9	44.5	18.5	35.7	17.9	PR	B06 0347	11.2
64	21.4	N/A	N/A	N/A	N/A	N/A	25.8	CR	B09 1235	29.0
39	22.7	33.8	20.4	25.6	16.1	29.3	30.9	PR	B10 1668	27.9
88	97.2	57.2	71.6	66.8	41.9	41.1	133.3	PR	B14 2046	20.1
78	63.4	70.4	78.0	34.7	37.2	38.6	20.0	CR	B14 2040	12.2
20	18.8	29.9	38.2	28.7	40.9	36.6	41.2	CR	B06 0293	15.9
72	21.3	N/A	N/A	N/A	N/A	N/A	20.1	NR	B14 2043	7.8
12	47.3	54.6	102.5	66.7	42.9	39.7	35.2	NR	B14 2008	18.1
8	13.6	13.4	26.8	17.4	19.3	17.3	25.1	PR	B09 0743	15.8

Table A.1. RNA quantification of patient and healthy control EVs.

Appendix IV:

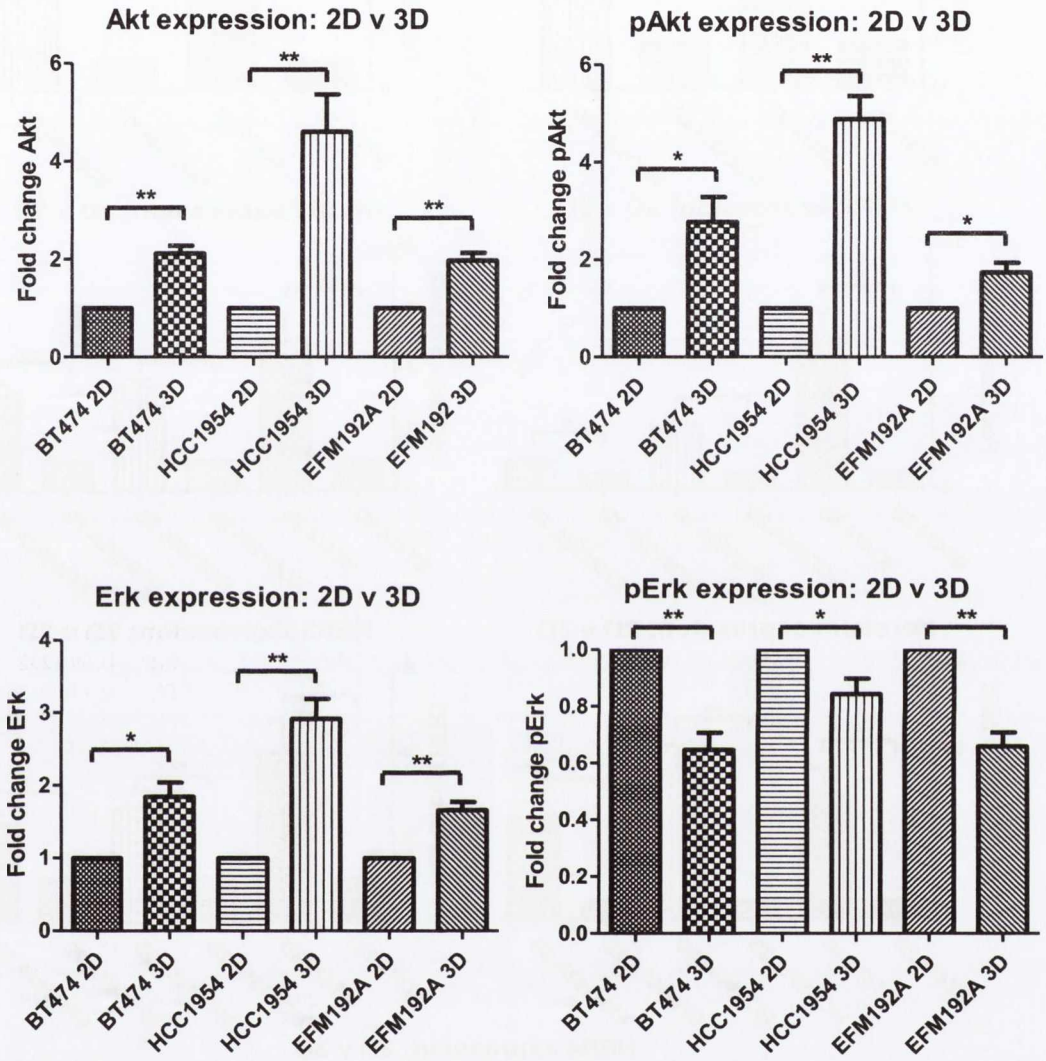

Appendix Figure 1. Densitometry for Akt, pAkt, Erk and pErk expression in BT474, HCC1954 and EFM192A cells grown in 2D and 3D, (n=3±SEM), where *$p<0.05$ and **$p<0.01$.

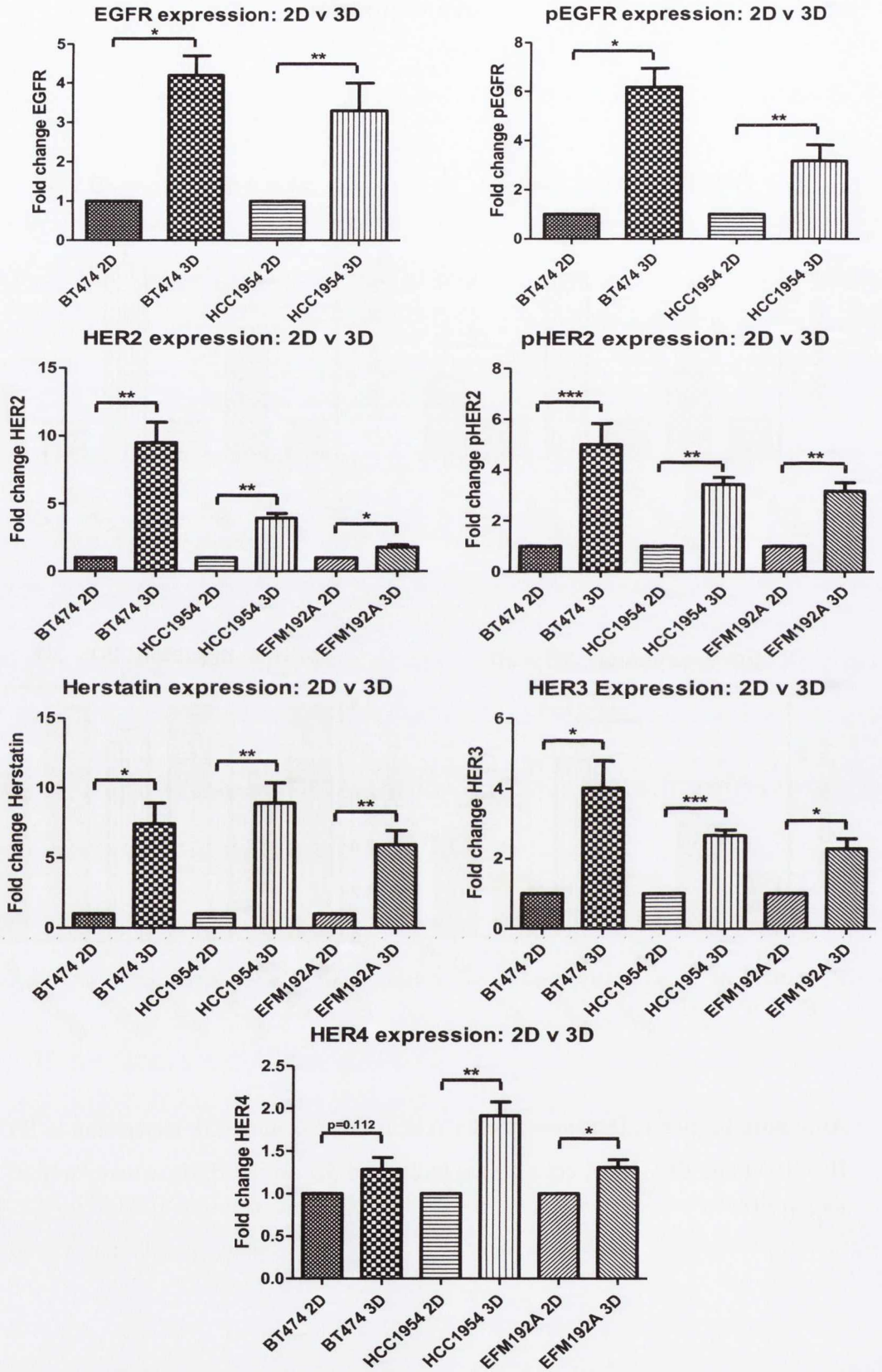

Appendix Figure 2. Densitometry for EGFR, pEGFR, HER2, pHER2, Herstatin, HER3 and HER4 expression in BT474, HCC1954 and EFM192A cells grown in 2D and 3D, (n=3±SEM), where *p<0.05, **p<0.01 and ***p<0.001.

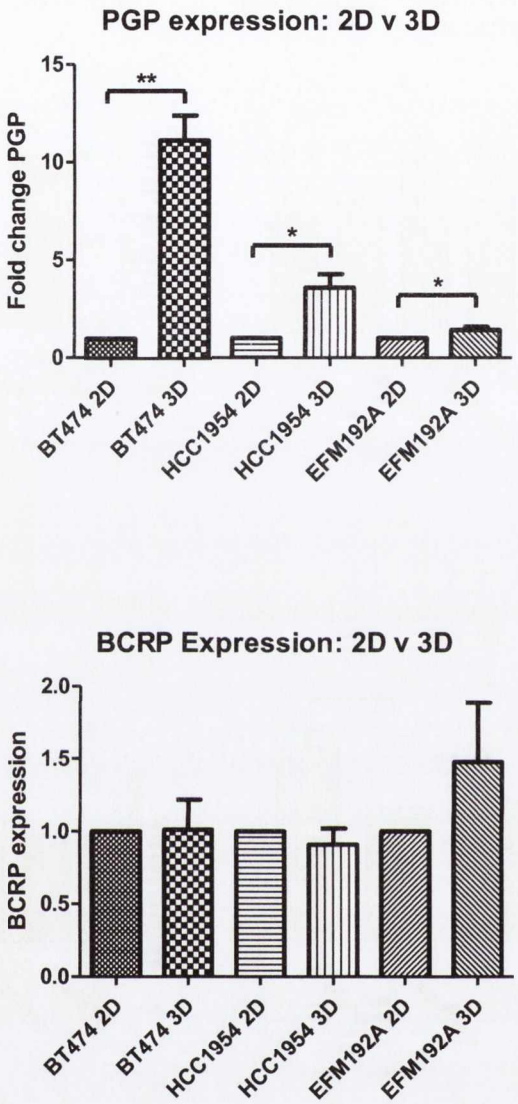

Appendix Figure 3. Densitometry for PGP and BCRP expression in BT474, HCC1954 and EFM192A cells grown in 2D and 3D, (n=3±SEM), where *$p<0.05$ and **$p<0.01$.

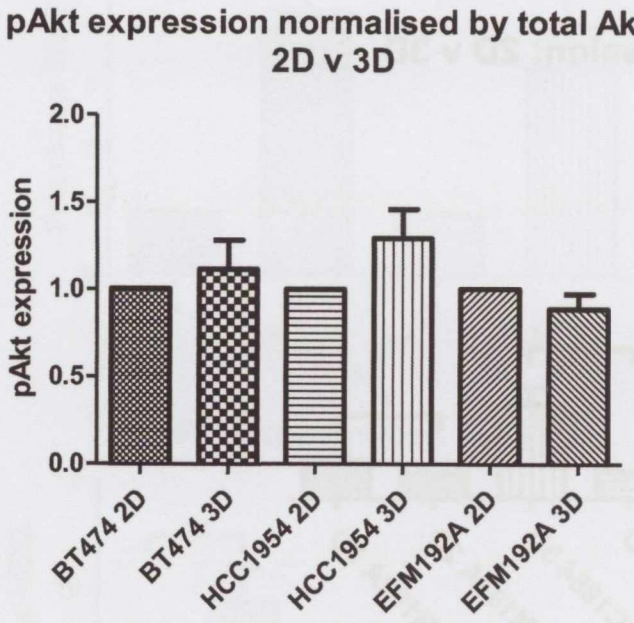

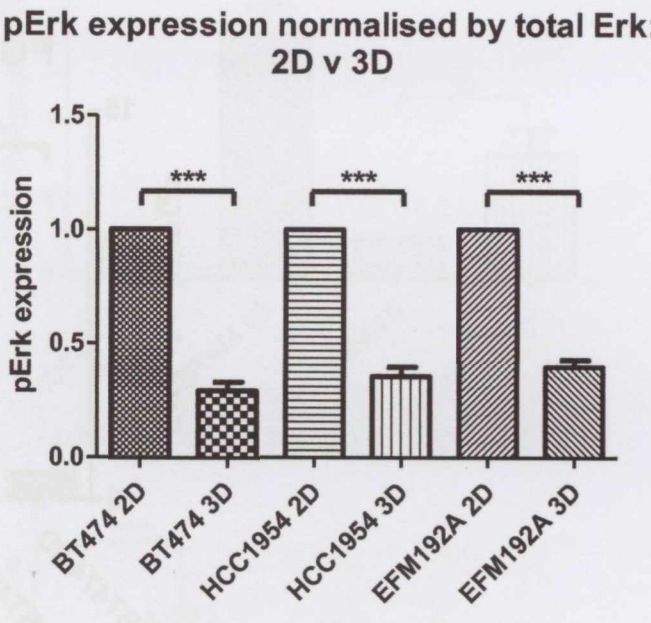

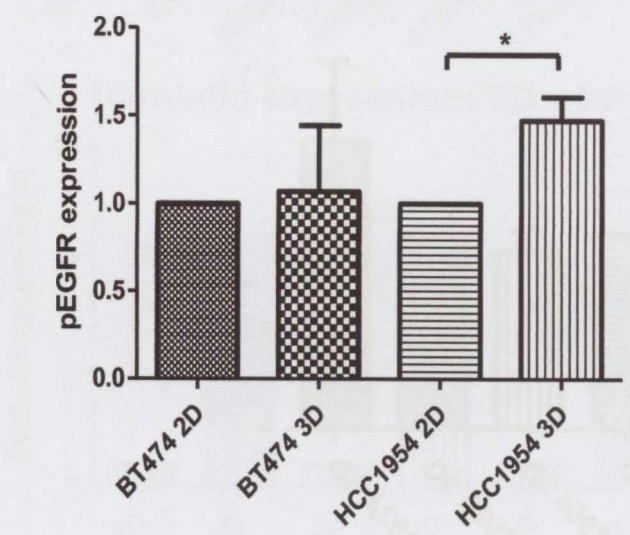

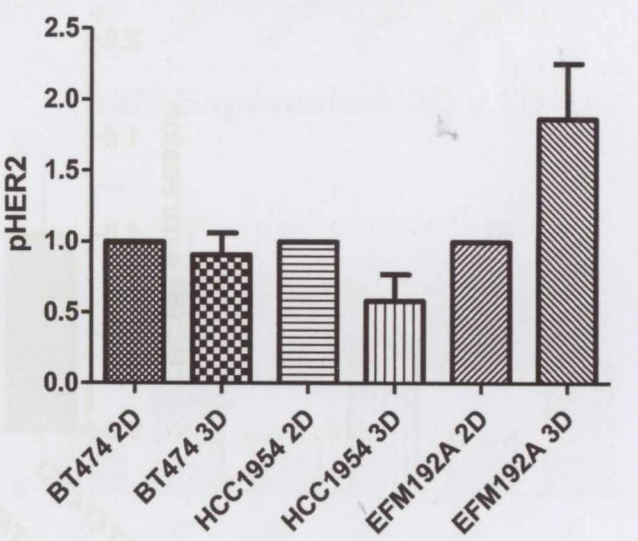

Appendix Figure 4. Phosphorlyated protein normalised for total protein for pAkt, pErk, pEGFR and pHER2, (n=3±SEM), where *$p<0.05$ and **$p<0.01$.

Appendix V

Poster presentations

'Better ways of assessing anti-cancer drugs in the laboratory to increase their success for breast cancer patients'
Susan Breslin, Sweta Rani, Claire Corcoran, Keith O Brien and Lorraine O' Driscoll.
All Ireland Schools of Pharmacy Conference 2012, University College Cork.

'Generation and characterisation of neratinib-resistant breast cancer cell line variants'
Susan Breslin, Sweta Rani, Claire Corcoran, Keith O Brien, Lorraine O' Driscoll.
EORTC-NCI-AACR Symposium, Dublin 2012

'Effects of acquired neratinib-resistance in breast cancer cell line variants'
Susan Breslin, Sweta Rani, Claire Corcoran, Keith O Brien, Lorraine O'Driscoll
Irish Association for Cancer Research Annual meeting, Dublin, 2013.

'Acquired neratinib-resistance in breast cancer cells induces cross-resistance to HER-targeting drugs through a mechanism mediated by Hsp90, IGF1R, Bcl2 and caspase-8'
Susamn Breslin, C. Corcoran, S. Rani, L. O' Driscoll.
Irish Association for Cancer Research Annual meeting, Galway, 2014.

'The potential of Neuromedin U as a prognostic biomarker in HER2-overexpressing breast cancer'
Susan Breslin, Melissa Daly, Norma O'Donovan, John Crown, Lorraine O'Driscoll.
Irish Association for Cancer Research Annual meeting, Limerick, 2015.

Oral presentations

'Investigating the development of neratinib-resistance in HER2-overexpressing breast cancer cells'
Susan Breslin and Lorraine O'Driscoll
All Ireland Schools of Pharmacy Conference 2013, Queen's University Belfast.

'Investigating the effects and putative mechanism of acquired resistance to neratinib in breast cancer'
Susan Breslin and Lorraine O'Driscoll
Annual meeting of the Biomedical Sciences section of RAMI 2013

'Investigating the role of neuronal calcium sensor-1 in acquired HER2 drug-resistance'
S. Breslin and L. O' Driscoll
TBSI Cancer Conference 2014.

'Potential use of extracellular vesicles as diagnostic or predictive biomarkers for breast cancer'
Susan Breslin and Lorraine O'Driscoll
EU COST BM1202 Microvesicles and Exosomes in Health and Disease (MEHAD), Helsinki, 2015.

Awards and other

Awarded prize for best post presentation:
'Effects of acquired neratinib-resistance in breast cancer cell line variants'

Shortlisted for the Donegan Medal at the annual meeting of the Biomedical Sciences section of the Royal Academy of Medicine in Ireland (RAMI) 2013 for oral presentation titled 'Investigating the effects and putative mechanism of acquired resistance to neratinib in breast cancer'